"NUMERICAL MODELLING OF WELD POOL CONVECTION IN GAS METAL ARC WELDING"

Mark H. Davies

B.E. Hons (Adelaide), 1992

Department of Mechanical Engineering

The University of Adelaide

South Australia 5005

Submitted for the degree of Doctor of Philosophy, 1st August 1995

CONTENTS

NUMERICAL MODELLING OF WELD POOL CONVECTION IN GAS METAL ARC WELDING

ABSTRACT

An investigation has been made into the development of numerical models of the Gas Metal Arc Welding (GMAW) process. Initial work focussed on furthering the understanding of fluid flow and convective heat transfer in GMA weld pools using theoretical, experimental and numerical techniques. Normalised scale analysis and simplified computational models have shown that the droplet impact forces are the dominant forces in driving weld pool flow. Induced electromagnetic forces are the next most significant, with forces due to surface tension gradients becoming unimportant at welding currents greater than 150 Amps. These results have been verified using flow visualisation experiments and parametric welding studies. The influence of droplet impact on turbulence within the pool has also been investigated and appropriate turbulence models and boundary conditions evaluated.

Further work concentrated on the development of weld pool convection models for the prediction of the weld pool shape and the near weld thermal history. This necessitated the development of 3 dimensional models that solve the Navier Stokes equations for the convection within the weld pool. These have been compared with traditional welding models which use empirically tuned heat source distributions and only consider heat transfer by conduction. This comparison demonstrated that numerical models must include the effects

of convective heat transfer within the pool if weld pool shapes and near weld thermal histories are to be accurately predicted.

Models that solve the full equations of motion within the pool are very computationally expensive and their accuracy is limited by the available turbulence and free surface models. An approximate heat-conduction only model has therefore been developed which uses enhanced thermal conductivity to simulate convection within the pool. The thermal conductivity enhancement is calculated from governing flow parameters using a semi-analytical technique, and the resulting model has been compared to traditional conduction solutions and to models which incorporate convection within the weld pool. This has shown that models using this enhanced thermal conductivity scheme predict weld pool shape and near weld thermal histories with the same level of accuracy as the full convection models and the best of the empirically tuned conduction models. However the enhanced thermal conductivity model requires several orders of magnitude less computational resources than full convection solutions and much less empirical tuning than the modified conduction solutions. As such it appears to be a valuable method for accurate practical prediction of near weld thermal behaviour.

STATEMENT OF ORIGINALITY

This thesis contains no material which has been accepted for the award of any other degree or diploma in any university or other tertiary institution, and to the best of my knowledge, contains no material previously published or written by another person, except where due reference has been made in the text.

I give consent to this copy of my thesis, when deposited in the University Library, being made available for loan and photocopying.

Mark H. Davies 31st July 1995

ACKNOWLEDGMENTS

This research has been undertaken with the support of the Co-operative Research Centre for Materials Welding and Joining.

The supervision of Dr M.A. Wahab and Dr M.J. Painter is gratefully acknowledged. The input and excellent technical support of Mr L. Jarvis and the workshop and materials technical staff at the CSIRO Division of Manufacturing Technology is also acknowledged. In particular the author would like to thank Dr Mike Painter for his many probing questions and ideas about the work and for his invaluable assistance with the preparation of this manuscript.

I like to thank Kym Burgemiester and Andrew Young with whom I shared an office for their friendship and constructive discussions throughout the course of my research. I would also like to thank my parents for their invaluable support and encouragement throughout my education endeavours.

Finally I would like to thank my wife, Fiona, for her assistance with this thesis and her invaluable love, support and friendship throughout the course of my research.

NOTATION

ε = Turbulent dissipation length

γ = Surface tension coefficient

$\acute{\eta}$ = Arc efficiency

ρ = Density

σ_e = Resistivity

σ_{ij} = Stress tensor

σ_n = Normal stress

σ_t = Tangential stress

μ = Viscocity

$\boldsymbol{B}$ = Magnetic flux density

B_x = X component of magnetic flux density

B_y = Y component of magnetic flux density

B_z = Z component of magnetic flux density

B_o = Reference magnetic flux density

C = Mean Gaussian curvature

c_p = Specific heat capacity

D_p = Plate thickness

E = Enthalpy

e = Emissivity

F_r = Froude number

f_x = partial derivative of the function f with respect to x

f_{yy} = the second partial derivative of the function f with respect to y and y

$\boldsymbol{g}$ = Gravity vector

g = Magnitude of gravity

H = Magnetic field vector

$\boldsymbol{J}$ = Current density

J_x = X component current density

J_y = Y component current density

J_z = Z component current density

h_c = Heat transfer coefficient

I = Arc current

k = Thermal conductivity

K = Turbulent kinetic energy

M = Hartman number

M_a = Marangoni number

n_j = Normal vector in the j direction

$\boldsymbol{n}$ = Normal vector

p = Pressure

p_a = Ambient pressure

q_g = Heat source generated per unit volume

Q = net heat energy of the source

Q_C = Convective heat flux

Q_R = Radiative heat flux

q_g = Heat generation per unit volume

r = Radial coordinate for coordinate system two

R = Radius

R_{arc} = Radius of arc

R_{drop} = Radius of drop

R_e = Reynolds number

R_m = Magnetic Reynolds number

R_i = Richardson number

S = Stefan Boltzmann constant

sp = Species concentration

t = Time

T = Temperature

T_m = Melting temprature

T_c = Convective reference temperature

t_j = Tangential vector

T_o = Ambient temperature

T_R = Radiation reference temperature

$T_{8/5}$ = 800-500°C cooling time

u = X component of velocity

$\boldsymbol{u}$ = Velocity vector

U_{drop} = Droplet impact velocity

U_o = Reference velocity

u_{weld} = Welding speed

v = Y component of velocity

V = Arc voltage

w = Z component of velocity

W_e = Weber number

x = X coordinate

y = Y coordinate

z = Z coordinate

Chapter 1

RELEVANCE AND MOTIVATION

1.1 INTRODUCTION

Gas metal arc welding (GMAW) is a common fusion welding process used for the joining of metal components. A large percentage of all welds carried out in industry are performed by the GMAW process. As the weld characteristics have a direct affect on the quality of the finished product, it would be very beneficial to be able to predict the characteristics of a particular weld before it is carried out.

Fusion welding is a complex process, controlled by a large number of interacting variables. These variables include work-piece and electrode composition, geometry, material type, weld sequence, weld power, welding speed and preheat. The properties affected include post weld residual stresses, distortions, microstructural features and mechanical characteristics of the finished weld. Therefore, establishing an appropriate combination of input parameters for a particular application is a significant task. The use of simulative mathematical models aims to replace or reduce the need to use costly experimental methods of achieving the optimum process parameters. In essence, models seek to predict process outcomes without the necessity or expense of carrying out the real process. As Goldak (1988) indicated,

welding engineers want a simple way of predicting the size and shape of a weld pool. However it is far from a simple problem, and most current methods rely on regression analysis of experimental data. At present there are about 100 commercial software packages directed at welding technology (Buchmayr, 1993). Many of these are for the interrogation and manipulation of experimental data bases, but some contain simple predictive calculations of thermal cycles. Increasingly, such software will become essential tools for welding engineers and, with the expected future increase in computer capacity and speed at a reduced cost, more sophisticated models will be available for shop-floor use.

Another important reason for developing numerical models is to provide an increased understanding of welding processes which are intrinsically difficult to study by conventional means. In turn, greater understanding should lead to improved processes, process control and productivity.

Hence, numerical models are broadly intended for process simulation or for process understanding. However, these two requirements place different demands on the model. The first requirement implies a need for rapid response and easy interactive use. There are practical demands which lead to further considerations such as, how accurate do we need the simulation to be, and what level of empiricism can be tolerated. The second requirement needs models which closely duplicate the physics of a process and almost inevitably lead to computationally intensive programs. Currently there has to be a compromise between these two, somewhat conflicting, requirements.

Within the solid work-piece heat is transported by conduction, i.e. the diffusion of heat from areas of high temperature to areas of low temperature. Within the molten pool heat is transported by conduction and by convection, in which the heat is transported by the motion of material. It is apparent from previous work within the literature that welding models must incorporate the effect of convection within the pool if accurate predictions of near weld temperature histories are to be made. It is the aim of this thesis to study and develop numerical models of fluid flow in a GMAW pool. This will enhance our understanding of the flow within the pool and its effect on the near weld thermal behaviour. The results of these complex simulations of the fluid flow within the weld pool will then be used to develop accurate and broadly applicable process simulation models. The physics of the welding process and the equations governing the process are briefly outlined in the next section to enable understanding of the flow and the development of numerical models.

1.2 BACKGROUND: THE GAS METAL ARC WELDING PROCESS

A schematic view of the gas metal arc welding (GMAW) process is shown in Figure 1.1.

An electric potential which is established between the electrode and the work piece causes current flow, which generates thermal energy and partially ionises the shielding gas forming an arc column. The arc current also creates a surrounding magnetic field. This interacts with the diverging current field to induce an electro-magnetic force which accelerates the plasma, generating a flow towards and across the work piece surface. Intense heat generation

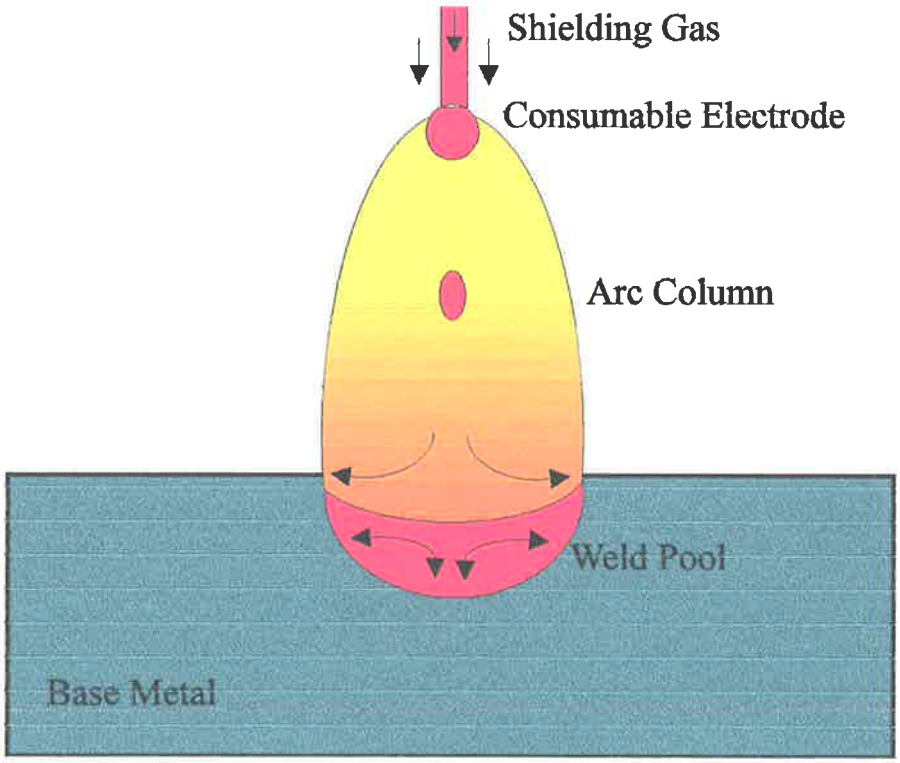

Figure 1.1 Gas Metal Arc Welding (GMAW)

and high plasma velocities are created with a rapid transfer of heat into a molten weld pool. In the consumable wire electrode of the GMAW process, heat is generated both by resistive heating and by heat transfer from the arc contact. The wire tip is melted and molten droplets are formed then driven into, and through, the plasma jet into the weld pool. Heat from the droplets and the arc is transferred through the pool mainly by convection within the molten metal into the base metal. The heat then diffuses throughout the base metal and is lost to the surroundings via conduction, convection and radiation.

Although the flow in GMAW pools is the primary topic of this thesis, the effects relating to the gas tungsten arc welding (GTAW) process are included in this literature review as the flow within a GTAW pool has been extensively modelled in the open literature. The GTAW process (Figure 1.2) is similar to GMAW, however instead of the arc being struck between a consumable electrode and the work piece, a non-consumable tungsten electrode is used. The electrode does not melt and consequently there is no metal transfer across the arc. It is essential to analyse the work that has been carried out for GTAW as the observations of pool behaviour, important driving forces and modelling techniques are an important starting point for the work on GMAW. In order to make full use of this significant existing knowledge base, the results of these investigations will be reviewed in some detail in Chapter 2.

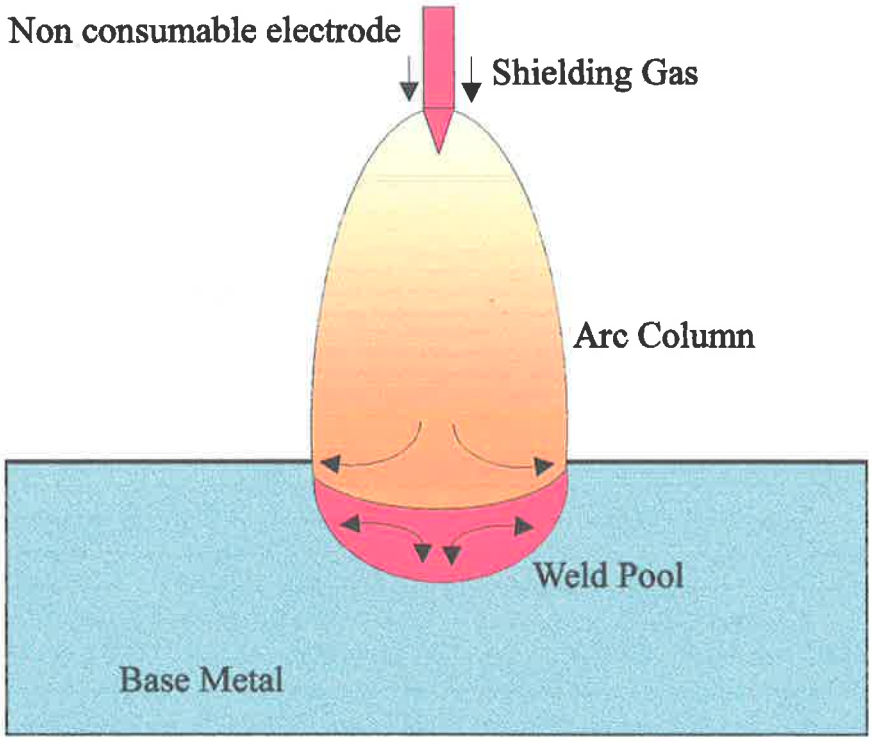

Figure 1.2 Gas Tungsten Arc Welding (GTAW)

The mathematical equations describing the physical processes taking place within these welding processes are those of mass and heat flow. The basic differential equations describe the conservation of mass, momentum and energy (Lancaster, 1984). An overview follows.

The following equation (equation 1.1) represents the conservation of mass for an incompressible fluid. Essentially this equation states that there can be no net gain or loss of mass.

$$\nabla \cdot \boldsymbol{u} = 0 \tag{1.1}$$

Equation 1.2 represents the conservation of momentum for an incompressible fluid. The first term on the left hand side represents the transient effects or the change in momentum with respect to time and the second term represents the convective effects, i.e. the transport of momentum due to fluid flow. On the right hand side are the force terms. The first term represents the pressure forces, the second: gravity body forces, the third: viscous forces, the fourth: buoyancy forces, and the final term represents electro-magnetic forces. Therefore, this equation states that the change in momentum with respect to time plus the change due to the flow of momentum in and out of the system is equal to the sum of the forces acting upon the fluid.

$$\rho\left(\frac{\partial \boldsymbol{u}}{\partial t} + \boldsymbol{u}\cdot\nabla\boldsymbol{u}\right) = -\nabla p + \rho \boldsymbol{g} + \mu \tau_{ij} - \boldsymbol{g}\Delta\rho + \boldsymbol{JxB} \tag{1.2}$$

Equation 1.3 represents the conservation of thermal energy. The first term on the left hand side again represents the transient effects or the change in energy with respect to time. The second term represents the transfer of thermal energy due to convection. The first term on the right hand side represents diffusion and the second is a generalised source term. In summary, the change in thermal energy with time plus the change due convection, is equal to diffusion plus internal generation.

$$\rho c_p\left(\frac{\partial T}{\partial t} + \boldsymbol{u}\cdot\nabla T\right) = \nabla\cdot(k\nabla T) + E \qquad (1.3)$$

Within the arc the driving force for plasma flow is the induced electro-magnetic force ($\boldsymbol{J}\boldsymbol{x}\ \boldsymbol{B}$, where $\boldsymbol{J}$ is the current density and $\boldsymbol{B}$ is the magnetic flux density), which can be solved from Maxwell's equations (Lancaster, 1980). The energy balance (equation 1.3) considers the convective transport of temperature, the heat generation from Joule heating and heat losses due to radiation or convection. A calculation of the flow velocity, pressures and temperatures within the plasma column requires the simultaneous solution of these equations (equations 1.1,1.2,1.3) under a given or assumed set of boundary conditions. Necessary boundary conditions include the geometry of surfaces, e.g. the electrode, the shape of the weld pool surface, and the current density distribution. A detailed presentation of these equations and a discussion of the necessary boundary conditions as they relate to arc modelling is given by Choo *et al.* (1990).

Similar equations also describe the heat and fluid flow within the weld pool and the work piece. Again, the Maxwell equations must be solved to determine the induced electro-magnetic driving forces. Buoyancy forces also occur, since in the molten metal the fluid density can vary with temperature (which is spatially varying). Surface tension forces form part of the boundary conditions, and these may also vary spatially with temperature or compositional gradients, causing fluid movement. A solution for the flow pattern and temperatures in the weld pool requires known or assumed boundary conditions relating to the boundary geometry, heat and current fluxes, and velocities at the surfaces. The surface of

the fluid is clearly able to change shape as is the molten interface, so the position of these boundaries must be part of the solution. All material properties are temperature dependent so solutions must be non-linear. This increases the complexity as there is a lack of knowledge of thermo - physical properties in the high temperature, plasma environment of an electric arc. The arc can reasonably be considered as axi-symmetric and the equations formulated in cylindrical coordinates. This gives some simplification, but the weld pool and the moving arc should be treated as a three dimensional problem.

The fusion welding process clearly links the physics and behaviour of the arc with the formation and maintenance of the weld-pool which is linked to the thermal history of the base material. It is an understatement to describe it as a complex system. The mathematical representation of the fully linked system, would require the coupling and simultaneous solution of equations formulated to describe the arc and plasma flow, the metal transfer and the fluid movement and energy dissipation in the weld pool. No models of this level of complexity have been attempted to date. All current work has sought to de-couple these linkages and solve only portions of the problem, accepting the need for some approximation and idealisation of boundary conditions. A statement made by Glickstein (1981) is still relevant;

"... interrelationships between the electrode, the arc and the weldment are complex and are yet to be incorporated into a complete analysis of the arc welding process. What is being done is to study the various component pieces of this complex puzzle and try to understand how the pieces fit together".

In GMAW variations in the welding process parameters can affect the way that the consumable electrode melts and how the molten drops are transferred across the arc plasma. These variations in the metal transfer behaviour can in turn affect the process outcomes, therefore they must be considered when developing numerical models of the welding process. The various metal transfer modes are discussed in the following section.

1.3 METAL TRANSFER

1.3.1 Introduction

In GMAW the mode of metal transfer has been shown to have a significant influence on the process outcomes (Bradstreet, 1967; Essers & Walter, 1981). The mode of metal transfer affects the stability of the process, the wetting of the base metal, weld quality and the available range of welding positions and parameters. The molten droplets contain a significant amount of heat; Essers and Walter (1979) and Watkins *et al.* (1990) estimate that 25-35% of the energy transferred to the work-piece is due to the droplet.

1.3.2 Droplet Transfer Modes

The formation of droplets and the way that they transfer to the pool has been the subject of extensive research, much of which has used high speed filming to observe variation in droplet shape, size, velocity and transfer frequency (Liu & Siewert, 1989). A wide range of droplet types and transfer modes exist and the International Institute of Welding (IIW) have produced an agreed terminology classifying transfer into three modes; bridging, slag protected and free flight. Short circuiting or "Dip" transfer occurs when the metal droplets are transferred to the pool whilst the electrode drop is in contact with the pool. Transfer involving large amounts of slag such as with flux cored wires is known as slag protected transfer. In free flight transfer the metal droplets detach from the electrode some distance above the pool and travel across the arc to the pool. See Figure 1.3.

In this thesis, work has focused on free flight GMAW with a direct current and electrode positive using solid steel wire and argon based shielding gases. These parameters have been chosen because they are commonly used, relatively simple, and a large body of experimental literature regarding the effect of process parameters exists. It should be noted that because the characteristics of a weld are strongly influenced by the mode of metal transfer, the results determined within this thesis will not necessarily be applicable to other transfer modes. However while the results of this thesis will not be directly applicable to variations in the transfer mode the form of analysis is broadly applicable and modifications to make the analysis suitable for other transfer modes should be relatively straightforward.

Under these broad welding conditions a major change in the free flight transfer behaviour occurs as the welding current is increased. At relatively low currents so-called globular transfer occurs. This is characterised by large elongated droplets, with radii larger than the wire and relatively low transfer frequencies of approximately 10 droplets per second. The initial acceleration of the droplet is approximately equal to gravity, i.e. it simply falls into the pool. For mild steel wires and argon rich gases this type of transfer occurs at currents of up to approximately 200 Amps. As the current increases globular transfer is replaced by a mode called spray transfer. In spray transfer mode smaller approximately spherical droplets are formed, droplet mass decreases and transfer rates continue to rise. The initial droplet acceleration is greater than gravity, i.e. the droplets are projected across the arc into the pool. As the current is progressively increased a conical tip develops on the wire and small droplets are generated at its tip. As the current increases further, a mode called streaming transfer occurs in which an almost continuous stream of molten metal is formed.

Droplet transfer modes are summarised in Figure 1.3.

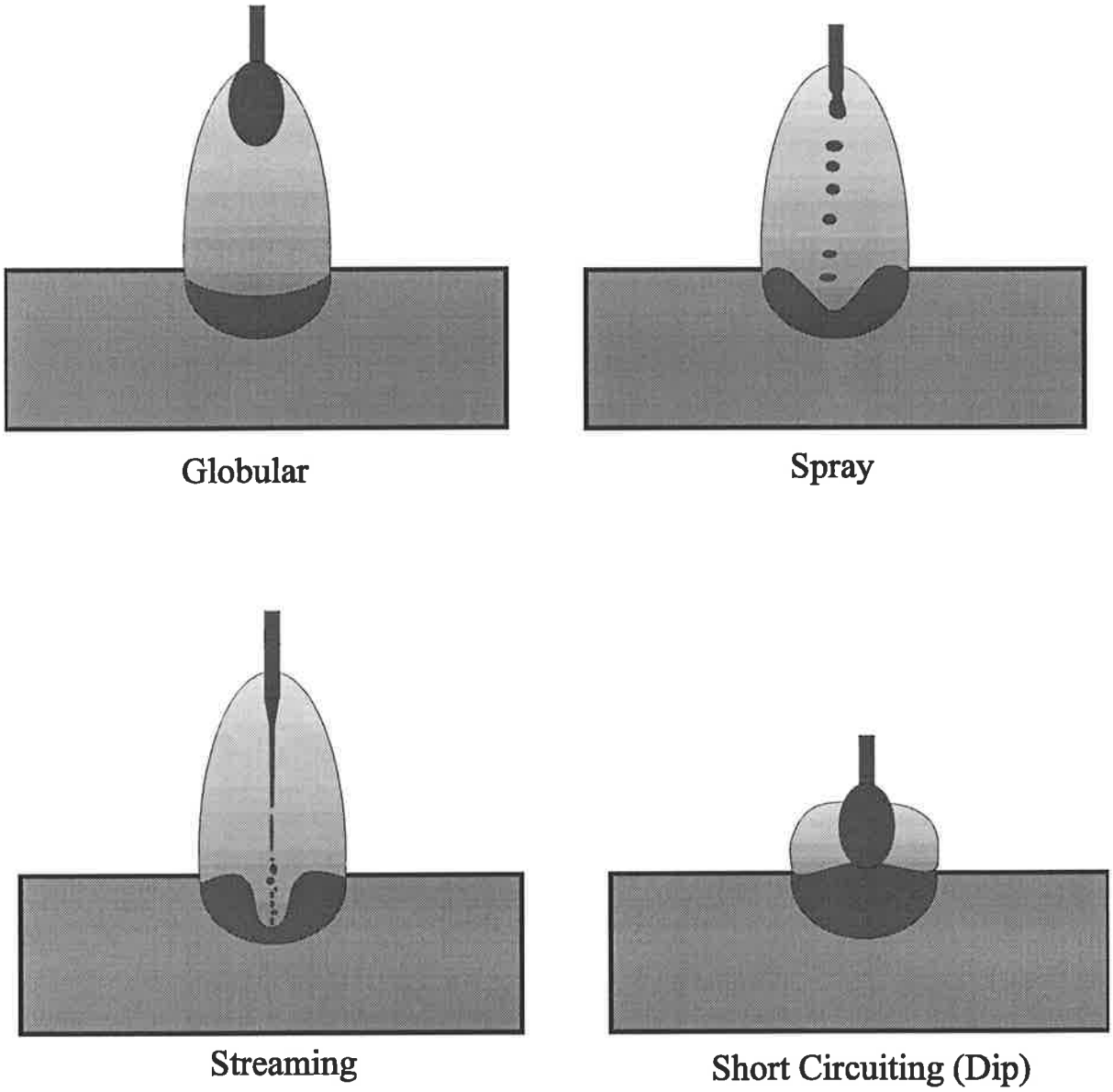

Figure 1.3 Metal Transfer modes.

1.7 OVERVIEW

The GMAW process is a highly complex process which cannot be modelled in its entirety given current and immediately foreseeable computational resources. This has necessitated the development of the following modelling approaches:

i) Process simulation : these models aim to interactively predict the effect of a variation in process parameters. They are often based on simple analytical and empirical modelling techniques and as such are often only applicable within the range of their empirical databases.

ii) Process understanding : these models are based on numerically solving the fundamental conservation laws. They provide insight into the physics of the process that can not be determined experimentally. Due to the complexity of the welding process individual components are considered separately, eg. the arc, the pool and the work-piece.

Thermal change is the key factor in modelling the welding process and predicting the suitability of a particular weld for its intended purpose. The thermal cycle strongly influences microstructural changes, post weld distortions and residual stress, and it can be used to provide information on weld penetration and heat affected zone (HAZ) geometry. Heat transfer within the pool is predominantly convective; a factor that must be considered if accurate predictions of near weld heat transfer is to be made. Therefore the aim of this thesis to investigate the flow within a GMAW pool. This will provide enhanced understanding of the mechanisms of near weld heat transfer which will then be used to

develop broadly applicable process simulation models. The scope of this thesis and exactly what needs to be done to achieve these aims will be presented in section 2.5 after a review of the literature which reveals the extent of the existing knowledge base.

Droplet transfer is a significant factor in determining the outcomes of the GMA welding process, this thesis will focus on direct current, electrode positive, argon rich GMAW because of its wide usage and the large pool of experimental data that exists for this form of welding. However with simple modifications the results of this work should be readily extendable to other transfer modes.

Chapter 2

MODELLING OF WELDING THERMAL BEHAVIOUR : HISTORICAL BACKGROUND

2.1 INTRODUCTION

As mentioned in Chapter 1 modelling thermal behaviour is the key to predicting welding process outcomes. There have been a variety of different approaches within the literature for predicting the thermal behaviour due to welding. The simplest ones effectively ignore convection within the weld pool and treat the problem as a purely conductive one. Within this approach both analytical and numerical techniques can be used for solving for the conduction equations. Modelling convection within the weld pool is a far more complex problem, however it has been extensively analysed in the literature for GTAW. Much less work has been carried in the case of GMAW pools and some of results within the literature are seemingly contradictory.

This literature review covers the development of conductive models as they are likely to be the only option for interactive process simulation in the immediately foreseeable future. Even with the rapid increase in computer power, it will be some time before a fully coupled convective solution, linking the pool and the arc, will be practical in a research environment let alone an everyday industrial environment. Furthermore, the conductive models provide

important information on the thermal modelling techniques and boundary conditions required for convective models. An extensive review of the literature relating to GTA weld pool convection will be made in order to provide insight and starting points for modelling GMA weld pool flow.

2.2 HEAT CONDUCTION SOLUTIONS

2.2.1 Introduction

A significant amount of weld process modelling has made the major simplifications of treating the arc as an arbitrarily defined heat source and ignoring convective flow within the weld pool. This approach effectively reduces the model to one of transient, conductive heat transfer, and the calculation of a solution to the energy balance equation (equation 1.3). The analysis then requires a solution of the following time dependent equation for conduction of heat in an isotropic material:

$$\rho C_p \frac{dT}{dt} = \frac{\partial}{\partial x}(k\frac{\partial T}{\partial x})+\frac{\partial}{\partial y}(k\frac{\partial T}{\partial y})+\frac{\partial}{\partial z}(k\frac{\partial T}{\partial z})+q_g \qquad (2.1)$$

under a known set of initial temperatures and boundary conditions. Here, ρ is the material density, C_p the materials specific heat, and k its thermal conductivity, while q_g is the heat generated per unit volume. The boundary conditions define the radiation and convective heat losses and the welding arc is considered as a moving heat load.

There are two possible methods of approach:

(a) The determination of a closed form analytic solution under certain specific simple boundary conditions.

(b) A solution by a numerical technique such as the finite difference or finite element method

(FEM).

Most researchers now use a numerical approach as it is less restrictive in the choice of boundary conditions and heat loads. However analytic solutions are still relevant since they are generally computationally faster, and for that reason they are often used in current commercial welding software.

2.2.2 Analytic Solutions

Rosenthal's (1941) solutions are the starting point for the majority of analytic solutions applied to welding. He developed equations for the temperature fields around idealised welding arcs which he treated as a point or line sources of heat. Other necessary assumptions were:

(1) A quasi-stationary state existed, i.e. the differential equation (2.1) was formulated relative to the position of the heat source using a moving coordinate system. The temperature field around it was then considered to be independent of time, i.e. $dT/dt = 0$, provided the heat source did not vary, ie. $q_g = Q/v$ = constant, (where Q is the net heat energy of the source, and v is its velocity).

(2) Thermal diffusivity and conductivity were constant and independent of temperature. No latent heat was considered.

Under these conditions, a solution of the general equation for a point heat source moving in the x-direction in a semi-infinite plate became,

$$T-T_o = \frac{Q}{4\pi kR} \exp-(\frac{v\xi}{2\alpha} + \frac{vR}{2\alpha}) \qquad (2.2)$$

where T_o is the initial temperature and T is the temperature at a point $R = (x^2+ y^2 + z^2)^{1/2}$ from a heat source Q. Where Q is the net heat source equivalent to the welding arc and is equal to ηVI, where η is an heat transfer factor often termed arc efficiency. The velocity of movement of the source is v and $\xi = x_o-vt$, where t is time and x_o is the x-distance from the source at $t=0$, k is the thermal conductivity and α is thermal diffusivity.

The initial solution referred to a point heat source on the surface of an infinite plate, neglecting any boundaries. In reality plates are often large in length and width and may consequentially be considered as infinite. However, they have a finite thickness and heat transfer through the bottom plate surface is considerably slower than that within the material. To produce a solution for a finite thickness material, where the top and bottom surfaces did not exchange heat with the surroundings, Rosenthal (1941) assumed a series of fictitious heat sources, placed so that they balanced out the effect of the real source. This gave rise to a series solution which was reduced to two closed form solutions, one for thick plate (infinite) and one for thin.

For example the solution for an infinite plate of finite thickness became,

$$T-T_O = \frac{Q}{2\pi k}\exp\frac{-v\xi}{2\alpha}\left[\frac{\exp\frac{-vR}{2\alpha}}{R} + \sum_{n=1}^{\infty}\left(\frac{\exp\frac{-vR_n}{2\alpha}}{R_n} + \frac{\exp\frac{-vR_n'}{2\alpha}}{R_n'}\right)\right] \qquad (2.3)$$

$$R_n = (\xi^2 + y^2 + (2nD_p + z)^2)^{1/2}$$
$$R'_n = (\xi^2 + y^2 + (2nD_p - z)^2)^{1/2} \qquad (2.4)$$

where n is a constant index indicating the number of the imaginary source, and D_p is the plate thickness.

This approach was widely used and investigated within the literature. Thermal cycles and cooling times could be calculated and bead parameters, such as pool depth and width could be determined by considering that their geometry was equivalent to that of the predicted melting point isotherm. Wells (1952), Wells & Roberts (1954), Adams (1958), Jhaveri *et al.* (1962) and Christensen *et al.* (1965) derived simplified equations from the Rosenthal solutions to predict fusion zone geometry, cooling times and cooling rates. McGlone & Grant (1992) have recently reviewed some of these and they are presented by Lancaster (1980), Masubushi (1980) and Easterling (1983).

Correlations between predictions and experimental behaviour were investigated by most of the above researchers as well as Paley (1964a,b) and Rykalin & Bekelov (1964 & 1971). Myers *et al.* (1967) reviewed publications prior to 1967. Generally investigators reported that the above theory correlated with experimental data except in regions close to the weld. The

difficulties encountered were mainly attributed to the restricted assumptions of; no heat loss from surfaces, constant thermal properties, and the assumption of point heat or line sources which had the obvious difficulty that the temperature tended to infinity as the distance from the source tended to zero. Some of these difficulties were overcome by introducing adjustable parameters to force correlation with experiment. Christensen *et al.* (1965) determined arc efficiency factors for a wide range of welding processes. These were essentially 'correction' factors required to get agreement between measured thermal histories and those calculated. He found reasonable agreement with predicted weld pool length and width, but penetration was not accurately predicted. Apps & Milner (1955) used the measured bead width to effectively fix the melting point isotherm and used the known temperature at that point to scale the calculated thermal cycle. Grosh *et al.* (1956) were the first to determine a solution using variable thermal properties. Conductivity and specific heat were taken to vary linearly with temperature, but their ratio, (the diffusivity) was constant. The effect was claimed to be small, however Malmuth *et al.* (1974) demonstrated that latent heat, which was effectively absorbed at the front of the weld pool and liberated at the rear, could influence the weld pool shape at high welding speed. Kohira *et al.* (1976) described a point source solution (originally referenced to Tanaka (1943)) which allowed for convective heat losses.

The next advance in the development of the thermal welding models was the introduction of a distributed heat source which was first considered by Pavelic *et al.* (1969). They considered the surface heat flux to be distributed as a Gaussian distribution,

$$q(r)=q_o\exp(-Cr^2) \tag{2.5}$$

where $q(r)$ is the heat flux at a radius, r, from the source centre, q_o is the maximum heat flux, and C is an adjustable constant.

Eagar & Tsai (1983) also modified the Rosenthal's theory (1941) to include a distributed heat source. Again in their approach, the net heat input was distributed in a Gaussian manner.

$$Q(x,y) = \frac{Q}{2\pi\sigma^2}\exp-\frac{r^2}{2\sigma^2} \tag{2.6}$$

The distribution parameter, σ, can be considered as an effective arc radius.

Heat input was now defined in magnitude via the arc efficiency factor, $Q = \eta VI$, and in distribution via the effective arc radius. With that scheme they found improved agreement between the predicted and observed pool geometry for GTAW. Tsai (1983) proposed the use of a Gaussian distributed source which lagged behind the electrode centre line, claiming an improved prediction of pool shape in GTAW with this technique. Nied (1986) also used this source model and obtained a good prediction of GTAW pool profiles in stainless steel.

Solomon & Levy (1982) published a Fortran program of the Rosenthal solution. Two programs were presented, one having a single point source and the other in which the heat source was represented by a conical distribution of mini-sources within the plate. A series solution was duplicated by effectively summing the temperature contributions from all mini-sources and their fictitious images. Heat loss was allowed for by reducing the efficiency of the auxiliary reflected sources. Generally, temperatures where overestimated at short times

(i.e. at distances near the source), and underestimated at long times (distances removed from the source). Although the thermal conductivity and diffusivity values were constant, pseudo-values were chosen at 600-800°C in order to obtain the best fit with experiment.

Nunes (1983) incorporated the effects of liquid metal flow in the weld pool and the latent heat from phase changes by introducing additional heat sources into the moving source model.

The problem with these models is that for a given welding process the arc efficiency factors, the distribution factor, the effective arc radius, or the spatial distribution of mini-sources, is not known a-priori and it will vary with process parameters. For the Gaussian distributions, commonly used for GTAW, the effective arc radius increases with increasing current and varies with gas composition. Ohija *et al.* (1986) have developed a two parameter optimisation method of determining the values of the effective arc radius and arc efficiency from a direct measurement of weld bead geometry in thin plate GTAW. Sudnik & Rybakov (1992) have also used a similar approach. In principle, any complex heat source can be represented as a spatial distribution of many point sources, and Kasuya & Yurioka (1993) have recently used this approach to represent a multi-arc submerged arc welding process.

Analytical solutions do have significant difficulties in dealing with real boundary conditions and complex non-linear material properties. However they are computationally efficient and are therefore, often used when interactive use is required. Analytical solutions also recognised that the welding process could be modelled using distributed heat sources to

represent the heat input from the arc. This shifts the focus of investigation towards determining the appropriate heat source distribution required to give the correct answer. Distributed heat sources have been used extensively in numerical solutions of the heat conduction equations. However numerical solutions can incorporate complex material properties and boundary conditions.

2.2.3 Heat Transfer : Numerical Solutions

Almost all of the constraining assumptions that were considered to limit the accuracy of the Rosenthal-type analytic solutions can be avoided by using direct numerical methods for solving the heat conduction equation. Non-linear temperature-dependent conductivity and diffusivity can be considered and the latent heat at phase changes allowed for. Distributed heat sources can be used to represent the welding arc, and radiative and convective heat losses can be included. Early numerical solutions by Westerby (1968), Pavelic *et al.* (1971), and Kou & Le (1983) used the finite difference approach, while Hibbett & Marcel (1973), Krutz & Segerlind (1978), Friedman (1975) and Paley & Hibbett (1975) used the finite element method. In general, most subsequent work has used the finite element approach since this method is more flexible in its treatment of variable part geometry (Zienkiewicz, 1977).

In such methods the governing equation of heat transfer becomes,

$$k\frac{\partial^2 T}{\partial x^2} + k\frac{\partial^2 T}{\partial y^2} + k\frac{\partial^2 T}{\partial z^2} + q_g = \rho C\frac{dT}{dt} \qquad (2.7)$$

with boundary conditions represented as,

$$k\frac{\partial T}{\partial n} + h(T-T_o) + S\epsilon(T^4-T_o^4) = 0 \qquad (2.8)$$

where $\boldsymbol{n}$ is the normal vector, h is the convection coefficient, ε is the emissivity, S the Stefan-Boltzmann constant and T_o is the ambient temperature.

Finite element discretisation (Zienkiewicz, 1977) leads to a matrix equation of the form,

$$\boldsymbol{KP(T)} + \boldsymbol{PM}(\frac{\partial T}{\partial t}) = \boldsymbol{Q} \qquad (2.9)$$

This set of first order differential equations is then solved. The simplest methods of solution linearise the time differential and integrate, through time, using a fixed time step.

In the period 1975 to 1985, solutions were limited to 2D approximations due to a lack of computer capabilities. The models developed by Friedman *et al.* (1976a, b, 1977, 1978, 1980, 1981) and applied to bead-on-plate GTA welding were typical. The 2D approximation is based on the assumption that the welding speed is so high that effectively no heat is conducted ahead of the welding arc. Accordingly, the heat flow through a planer 2D slice is considered to be negligible in comparison to the heat flow within the plane. The calculation then determines the temperature at each point within the plane as a time dependent heat source representing the welding arc acts on it, as illustrated in Figure 2.1. A quasi-stationary condition is assumed so the temperature at any plane in the plate (say, x_n,y,z,t) is simply determined from a displacement in the time scales, i.e.,

$$T(x_n,y,z,t) = T(0,y,z,t-\frac{x_n}{v}) \qquad (2.10)$$

Rectangular 4-noded elements were used and these were decreased in size towards the centre of the welding arc. Heat losses by radiation and convection were considered and temperature dependent physical properties were used.

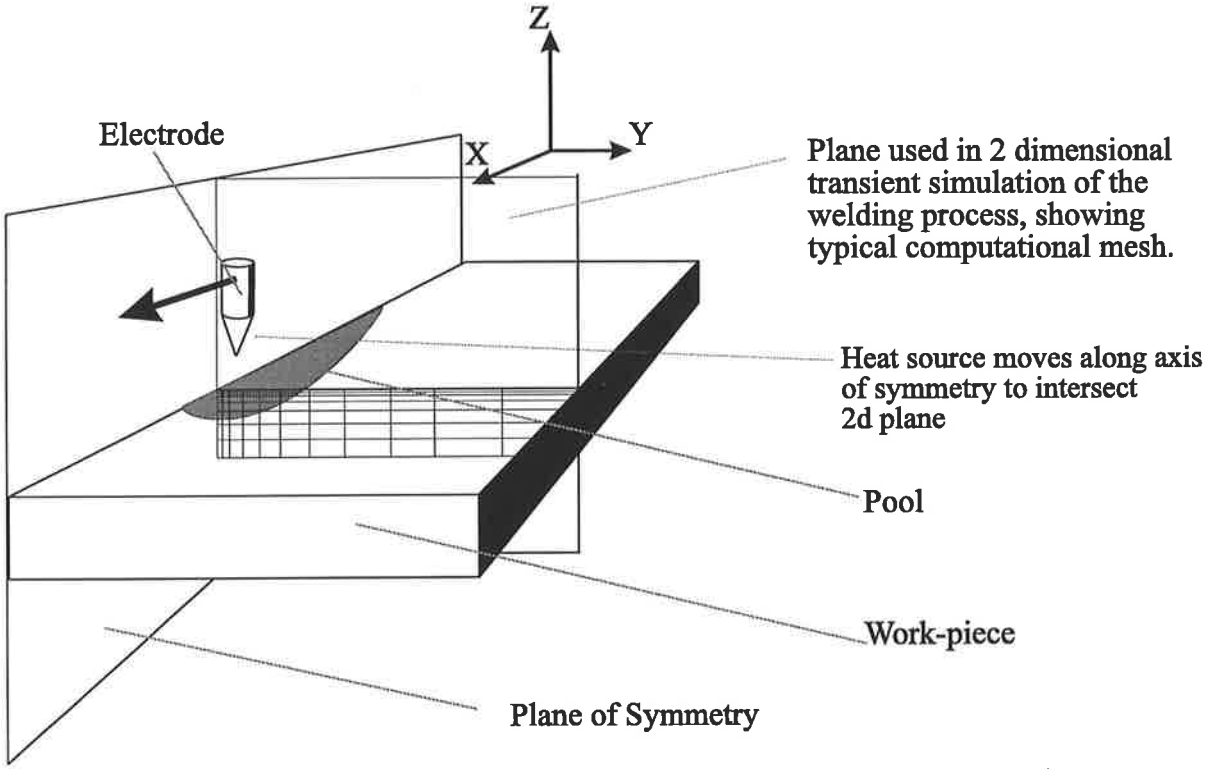

Figure 2.1 Two dimensional transient approximation showing computational plane.

Following the earlier work of Pavelic (1969), the welding arc was represented as a Gaussian distributed surface heat flux. The calculated results were compared with experimentally measured temperature cycles determined from thermocouples embedded within the work piece. Calculated values of weld pool size were found to be sensitive to the arc efficiency

η, the chosen arc radius, and to a lesser extent, the coefficient of convective heat loss. The arc radius was linearly increased in proportion to the arc current, consistent with observed GTAW arcs. One of the significant advantages claimed for this technique with respect to the use of Rosenthal's analytic solutions, was the elimination of the need to select either a 'thick' solution or a 'thin' analytic solution. The subsequent numerical summation of the series solution used by Solomon & Levy (1981) negates this criticism.

Andersson (1978) applied a similar analysis to Submerged Arc Welding (SAW). Planer 6-noded triangular elements were used and the latent heat allowed for by a modification of the thermally dependent heat capacity. Weld metal deposition was allowed for in a novel way by adding mesh during the transient solution. The welding arc was again considered as a planer surface heat flux, now distributed uniformly along the V-groove weld preparation. The total energy was uniformly distributed over the length (or time) taken for the joint to be filled. This is equivalent to an approximated weld pool length chosen in relationship to the weld speed and electrode configuration. No details of this relationship were given. Experimental thermal cycles for a 25mm thick SAW plate, welded with a 3-electrode configuration, (welding speed of 1500 mm/min, electrode heat input of 0.96,1.36 and 1.58 kJ/mm) were compared with calculated results. The comparison was good and the predicted weld penetration of 12.5mm also compared favourably with the measured value of 14.5mm.

The major concern in applying these numerical methods was the uncertainty in knowing which heat source, heat distribution factor or transfer efficiency to use. Applying the arc energy as a surface distribution tended to produce predicted weld pools with a half

cylindrical section, but in practice a wide range of pool shapes are obtained depending on welding conditions and process parameters. It was recognised that the force from the arc plasma and the convection of heat by fluid flow within the weld pool could generate an 'arc-digging' effect which could distribute the arc energy within the volume of the material, (Mills, 1979 and Essers & Walter, 1981). The 'Pavelic' surface heat source representation could be appropriate for some heat sources which did not cause melting, for example a pre-heat torch, but were too restrictive to simulate the welding arc.

In a series of publications Goldak *et al.* (1985), proposed a more general description of an arc heat source which they termed the 'double ellipsoidal' source. In the initial case the heat flux was distributed in a Gaussian manner throughout a semi-ellipsoidal volume. Their experience with this source showed that the predicted temperature gradients in front of the arc were less steep than experimentally observed ones, and gradients behind the arc were steeper than those measured. To overcome this difficulty, two ellipsoids were combined to give the final 'double ellipsoidal' source as illustrated in Figure 2.2. This source was described by six parameters: η the arc efficiency, such that $Q=\eta.VI$, ellipsoidal axis, a the width, b the depth, c_f & c_b length in front and behind the arc centre. In addition an apportionment of heat to the front and rear section of the source was made by factors r_f & r_b, where $r_f + r_b = 2$.

The heat flux at a point x,y,z within the ellipsoid in front of the arc centre, is then given by

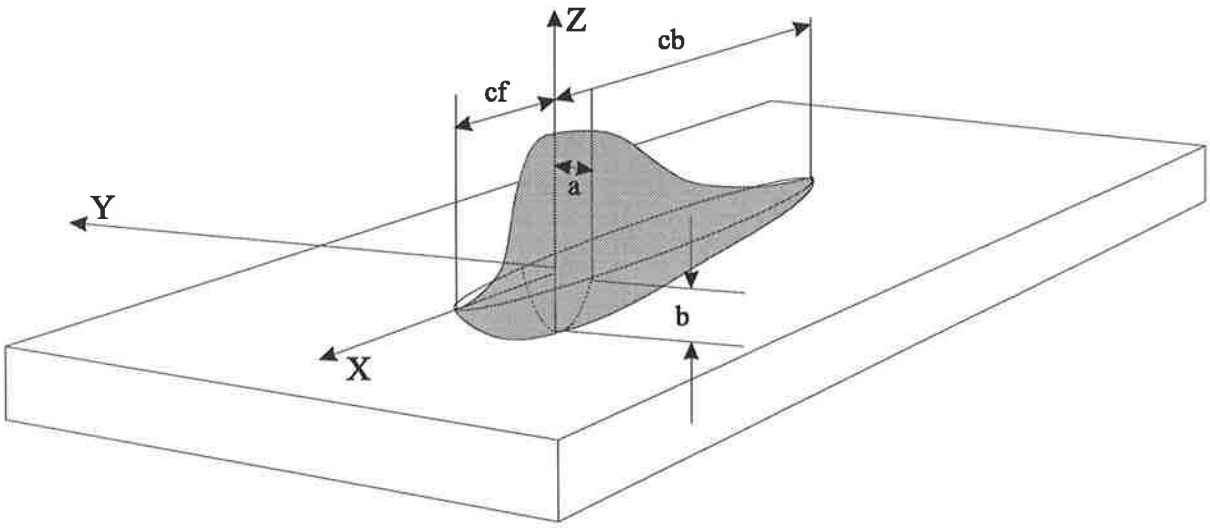

Figure 2.2. Double ellipsoidal heat source

the following equation,

$$q(x,y,z) = \frac{6\sqrt{3}r_f\eta VI}{abc_f\,\pi\sqrt{\pi}}\exp[\frac{-3x^2}{c_f^2}-\frac{3y^2}{a^2}-\frac{3z^2}{b^2}] \qquad (2.11)$$

A similar equation with the substitution of c_b, and r_b applies to points within the rear section of the ellipsoid.

Goldak *et al.* (1985) argued that this formulation provided a volume heat source, which reflected the concept that the weld pool motion would decrease towards the boundary of the weld pool. Additionally, the gradual reduction in heat flux avoided a sharp step change in heat load and reduced the need to use exceptionally small finite element mesh, which was computationally advantageous. Goldak *et al.* (1985) implied an equivalence between the source dimensions and those of the weld pool, and suggested that appropriate values for parameters a, b, c_f & c_b could be arrived at by direct measurement of a weld. It was suggested that reasonable values were; a: the width of weld, b: the depth, and c_f=a, c_b=$2a$.

If values were not available then estimations from Christensens non-dimensional method (1965) could be used. The credibility of the source was demonstrated by using it in a 2D FEM analysis of a submerged arc weld and an electron beam weld. The quoted results demonstrated good prediction of 800-500°C cooling times ($T_{8/5}$). They also demonstrated improved agreement between calculated and experimental temperature gradients, when using the double ellipsoidal source, compared to data from Krutz & Segerlind (1978) (who used a surface heat distribution).

In similar work Goldak *et al.* (1985) also compared the use of the finite element method with the point source method of Rosenthal. They set out to demonstrate the significance and the effects of the inherent assumptions within the Rosenthal model, by progressively incorporating them into the more general numerical technique. Comparisons were made on the basis of both $T_{8/5}$ and 1500-100°C cooling times. Somewhat surprisingly, in light of the benefits claimed for the double ellipsoidal source, its substitution for a point source achieved only small changes, i.e. 4.9 to 4.8 secs. The significant factors appeared to be the latent heat of fusion and phase transformation which increased the $T_{8/5}$ cooling time from 4.7 to 6.6 secs. Including the weld bead reinforcement in the calculation is also important, increasing $T_{8/5}$ from 6.6 to 7.2 seconds. The 1500-100°C cooling time was unaffected by the inclusion of latent heats or weld reinforcement. The final comparisons between the analytic solution, FEM and the experimental values, ie, $T_{8/5}$ of 8.5,7.2,8.1 seconds and 1500-100°C of 163,122,100 seconds respectively, are interesting and somewhat anomalous. With respect to the $T_{8/5}$ values, the analytic solution would appear to give better results than the finite element method. This highlights the difficulty in dealing with solutions in which there are

significant 'fitting' or 'tuning' parameters. In the analytic models pseudo thermal properties are used. In this particular case, they adequately compensate for the effects of model simplification. The FE method is not free of such factors since the source distribution is an arbitrary choice.

The fundamental problem in applying conduction models to welding is the arbitrary choice and formulation of the heat source through factors which are not known a-priori. Despite this difficulty, considerable effort has been made to improve such models.

Mahin *et al.* (1986) applied FEM to both static, axi-symmetric and 3D moving GTAW on 304 Stainless steel. A Gaussian heat source was used with a arc radius of 2mm, in line with measured heat flux distributions. Arc efficiency, η was measured by calorimetry to be 0.75. In order to simulate the more rapid transfer of heat due to fluid convection, the thermal conductivity of the liquid ($T > T_m$) was increased in a linear manner such that at 3000K it was 10 times greater than actual. They also introduced the idea of using an anisotropic thermal conductivity to control the calculated weld pool shape. With isotropic thermal conductivity, calculated weld pools had depth to width ratios $\geq$ 0.5. By enhancing the conductivity in the thickness direction relative to that in the plate the pool depth could be preferentially increased. Weckman, Mallory & Kerr (1988) used essentially the same approach and obtained good agreement with experimental pool shapes in GTAW. Mangonon & Mahimkar (1986) applied a 3D finite element analysis to SAW of steel. Using an essentially conventional approach, they documented the effect of using enhanced thermal conductivity. Two cases were considered: a constant liquid thermal conductivity of 45

W/m/°C, and a value which was linearly increased from 45 to 120 W/m/°C over the range of temperature from 1500-2500°C. On the basis of the results summarised they argued that as the heat input of the process increased, the need to account for convective flow by increasing the thermal conductivity also increased, the inference being that higher heat input weld pool had greater convective flow.

Tekriwal & Mazumder (1988a, 1988b & 1989), used a 3D commercial code (ABAQUS) to model single (1988a,b) and multiple (1989) pass GMA butt-welds. Temperature cycles were found to be close to experimental ones determined from embedded thermocouples, and predicted HAZ and fusion zone widths were within 5-15% of the experimental ones. In their models metal deposition was simulated by the periodic addition of mesh, and a radially symmetric Gaussian heat source was used.

Pardo & Weckman (1988) developed a 3D model for bead on plate GMAW with some novel features. A Gaussian heat source was used but the thermal conductivity of the liquid ($T > T_m$) material was artificially increased to twice the real value to reflect the increased heat transfer engendered by convective heat flow. The area of the weld reinforcement was determined from the known wire feed rate, wire diameter and welding speed, and a parabolic weld profile was assumed. An initial calculation was carried out using an estimated bead width and then compared with the predicted width of the melting point isotherm. The initial bead width was then adjusted, and further calculations carried out iteratively until the bead width and pool width converged. Agreement with experiment was good, although it was pointed out with some welding conditions that a characteristic 'finger' penetration was

obtained, and the model could not account for this situation. In discussing similar problems Easterling (1989), points out that models using Gaussian distributions predict smooth cylindrical penetrations which are only found with a limited number of weld conditions. To create weld pools of the 'finger and crater' type Ion (1984) used two separate input energies and distributions.

Various strategies to minimise total mesh size are generally necessary to increase the computational efficiency, particularly in 3D solutions. This is desirable because, as shown in Figure 2.3, to maintain solution accuracy and numerical stability a fine element mesh must be used near the welding arc (Oddy *et al.* 1989). However, using a fine mesh along the full length of a weld path has computational penalties. To avoid this Kannatey-Asibu *et al.* (1989) developed an adaptive meshing and re-meshing scheme. Kumar *et al.* (1992) have considered the problem of increasing computational efficiency and suggested a novel solution. They combined both the analytic and numerical solution schemes, using the efficient analytic solution to determine the boundary conditions on a restricted domain surrounding the welding arc, then used those boundary conditions for a numerical solution within the restricted zone. This unconventional technique effectively shrinks the size of the meshed zone and increases calculation speed.

Accepting that there are some computational strategies to be developed to improve efficiency, the major commercial FE codes, ANSYS, NASTRAN, ABAQUS etc can currently address non-linear heat transfer problems and can therefore be applied to the calculation of

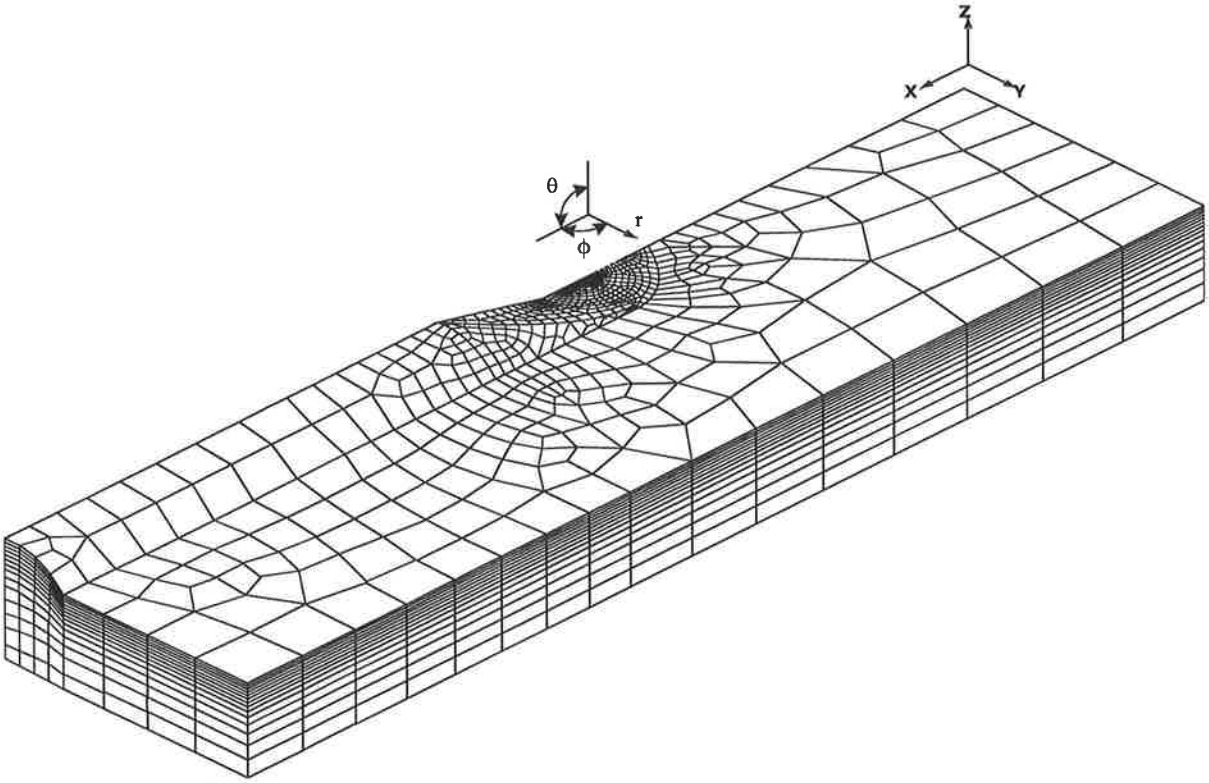

Figure 2.3 Typical meshing strategy

temperatures during welding. Current examples concern relatively simple structures, such as butt-joints in plates and pipes. Leung & Pick (1990) and Leung, Pick & Mok (1990) have applied ABAQUS code to both single and multi-pass semi-automatic submerged arc welding. Brown & Song (1992a,b) have also applied ABAQUS code to the determination of temperatures and residual stresses during pipe welding. The most complex models have generally been concerned with the prediction of residual stress patterns. The determination of residual stress, although again computationally demanding, is relatively straight forward if the mechanical properties of the material can be considered to be temperature dependent but independent of microstructure. Then, the thermal calculation can be de-coupled from the stress calculation so the calculation becomes a two part procedure. Firstly a calculation of the thermal history during welding and cooling is made, followed by a stress calculation

using the thermal data as a loading. The uncertainty in choice of heat source model is also of less concern here, since the heat source distribution tends to influence the near-weld temperatures to a greater extent than those in the bulk of the material. However, significant residual stresses are only generated in steels at temperatures below about 600°C, and are therefore more dependent on temperature changes away from the immediate weld site.

2.2.4 Summary

It is clear that the major failing of heat transfer models is that they inherently consider the heat input as the total arc energy. They do not directly recognise that the individual components of the arc energy can effect process outcomes, or that other process parameters such as shielding gas type, can have an influence. Experimentally, such effects have been extensively documented (Chakravarti *et al.*, 1985; Dillenbeck & Castagno, 1987 and Chandel, 1988). A clear result of such effects is that different cooling times, fusion zone and HAZ geometries can be obtained by changing process parameters such as voltage, current and speed, even though the net heat input is kept constant. Of course such effects are accounted for in models in a secondary way by the manipulation of variable factors, (often those defining the heat source distribution). In much of the published work, good agreement between experiment and model was reported but this was often a 'forced' agreement brought about by the appropriate choice of 'tuning'. A review by Goldak (1989) pointed out this basic difficulty stating that " a cynic may argue that these models require that the solution is known before the solution can be computed".

As a restricted set of welding conditions are often modelled, current published work has

failed to establish a general strategy for successful prediction, and the chosen factors have not been linked to process parameters. The following factors appear in most heat transfer models:

(a) arc efficiency : Arc efficiency is generally taken to be the ratio of heat energy used within a weldment to the heat equivalent of the total power output. GMAW values are quoted in the range 0.66-0.85 (Christensen *et al.* 1965). However, there have been different interpretations of this parameter which confuse and perhaps compromise these values. There have been two approaches:

(1) indirect methods where values are the correction factors necessary to obtain agreement between thermal histories from models and experimental measurement.

(2) direct measurement by calorimetry.

Giedt *et al.* (1989) considered that this resulted in two classes of 'arc efficiency'. They proposed that values determined from temperature field or fusion zone measurements were not a true measure of the fraction of arc energy transferred to the work-piece. They considered those values to be essentially the 'true arc efficiency' adjusted to obtain agreement between the solution of a particular model and experimental values. They suggested that as the model became more accurate the efficiency value would approach the true value as determined by calorimetry.

In most FEM models the arc efficiency used is of the 'best-fit' kind. Arc efficiency values are generally taken as constant i.e. no variation with changing welding parameters is

incorporated and $\eta = 0.7$ is a typical value for GMAW. Pardo & Weckman (1989) used the relationship, $\eta = 1.0 - (0.001 \times \text{arc current})$ in their work but gave no explanation of its derivation.

(b) heat source distribution : Gaussian distributions are favoured, usually justified by the evidence that current distributions in arcs have been measured to have similar distribution. This may not be completely acceptable however, since Choo *et al.* (1990) in modelling GTAW pools with distorted surfaces has predicted bi-modal current and heat flux distributions. Surface Gaussian distributions are most favoured for modelling GTA welding, and in those cases the arc radius is often chosen to proportionally increase with arc current. Double ellipsoidal sources have been generally related to the actual size of the weld pool, as originally proposed by Goldak (1985). However in subsequent work Goldak *et al.* (1986) used a completely variable distribution. In current work, Kamala & Goldak (1993) introduced the term 'power density distribution function' (pddf), which is a variable power or heat flux distribution equivalent to the welding arc. They considered the novel idea of taking a known 'correct' temperature field, (in their case, they used a field calculated from a 3D FEM) and derived the pddf that was required to calculate it, thereby providing in effect, a way of defining a heat source distribution. If, as in their work, a 2D FE model is used and compared with a 3D calculation, then a pddf could be derived. Then, when applied to a 2D model the pddf contained the appropriate compensation in distribution to account for the variation in the 2D to 3D approximation, such comparisons supported the concept of a double ellipsoidal heat source distribution for 2D models.

c) liquid thermal conductivity : To simulate the effect of convective heat transfer in a conductive model, the thermal conductivity of the molten material is artificially increased. However there is no prescribed method, and the level of increase in the thermal conductivity has been varied. Pseudo-conductivity values can be fixed at values of between 2-6 times the actual liquid conductivity, or they can be increased in proportion to temperature above the melting point, up to maximum values of 10 times the actual conductivity at the metals boiling point. The introduction of directional, anisotropic values of conductivity have also been used to simulate an assumed directional convective flow. The use of pseudo-conductivity values combined with volumetric heat sources is questionable. In reality heat is not added to a volume, it is added to the surface and then distributed within the pool by convection. Volumetric heat sources are supposedly used to incorporate the effect of convection. Within the volume of the heat source the conductivity is effectively infinite, as the heat is added directly to each point within the volume. These complex heat sources already have up to seven empirical tuning factors so the addition of one more would only seem to complicate the issue and require even more empirical tuning for little likely gain.

(d) joint configuration and metal deposition : The analytic solutions are not generally amenable to complex part geometry, whereas finite element models can be freely applied to any geometry. However, most work has currently focussed on relatively simple parts, such as bead-on-plate or bead-in-groove style single pass welds. Metal deposition, where it has been included, has generally been approached by dynamic meshing, ie. creating additional mesh during the solution, or by the "birth-and-death" scheme of activating pre-meshed elements during the solution.

Even though there are some problems associated with weld modelling approaches, numerical solutions based on conductive heat transfer are the closest to practical application. For the calculation of near weld temperature the status of conduction models is less satisfactory. The choice of heat source distribution is more problematic and the resulting temperatures are more sensitive to that choice. It is considered that progress can come through:

(a) the use of more empirical controls over the choice and formulation of heat source distribution, where possible linking these to welding process parameters;

and/or

(b) the development of more complex models which begin to include convective fluid flow within the weld pool, and a physically realistic energy distribution from the arc and transferred metal. The latter area has been focussed on in this thesis. It will be shown that the development of convective flow models, while not directly applicable to practical problems because of their significant computational cost, can be used to provide improved representations of the heat source for use in heat transfer solutions. In order to develop these models efficiently the following section will examine the literature regarding physical and numerical investigations of weld pool fluid flow.

2.3 WELD POOL FLUID FLOW

2.3.1 Introduction

As discussed in section 1.3, the convective dissipation of heat by fluid flow within the weld pool is effectively ignored, or at best crudely simulated, by conduction based weld models. In recent years this has been recognised as a major omission and a barrier to the development of a truly predictive process model. The flow within the weld pool affects the pool shape through the convective heat and mass transfer it generates, and in doing this it must strongly influence the near weld thermal cycles within the fusion and heat affected zones. In addition, the fluid movement may influence the uniformity of the material composition within the weld and the occurrence of solidification defects.

It is difficult to experimentally determine the flow within a weld pool because of the unfriendly local environment and the material concerned. Liquid metal is not transparent so at best only surface flow can be observed. This prevents a simple study of the crucial recirculating regions within the pool and the flow conditions at the solid-liquid interface. Hence there is a great practical need for numerical flow models in order to further our understanding of weld pool behaviour. With the significant advances in computer hardware and software over recent years such models are increasingly feasible and provide a previously unobtainable insight into weld pool flow.

Most attempts at modelling weld pool convective flow have concentrated on the gas tungsten

arc welding (GTAW) process, with relatively little work attempting to model the behaviour of gas metal arc (GMA) weld pools. In GTA weld pools, movement of the pool is driven by electromagnetic, buoyancy, arc pressure, plasma drag and surface tension forces. In the GMAW process such forces are also combined with an additional driving force from the impingement of molten metal droplets into the weld pool. Experimental investigations have shown that the weld pool shape can be dramatically altered by changing the characteristics of the droplet impact, position and momentum etc. So, it is apparent that droplet transfer has a significant influence on pool flow (Bradstreet, 1968; Essers & Walter, 1981 & 1989).

In this document we are primarily concerned with the GMAW process, although work related to the modelling of GTAW will also be considered in the following sections; since it is the research area that has currently received most attention.

2.3.2 Empirical Correlations and Experimental Investigations of Weld Pool Behaviour

There has been a large amount of experimental work done to investigate weld pool behaviour. However, it has been primarily aimed at understanding the physics of the weld-pool and determining empirical relationships between process parameters and pool shape, rather than on detailed studies of the flow characteristics. The experimental investigation of weld pool physics has been of interest to researchers for many years before computers were powerful enough to solve flow models. However the harsh welding environment makes experimental work very difficult. The weld pool in steel consists of molten metal at

temperatures of about 2700K, and it is covered in an intense plasma with temperatures in the order of 20,000K. At best the surface flow can be observed by placing particles on the surface of the pool and tracking their motion. Clearly this does not allow the investigation of sub-surface flow, and the flow observed may even be misleading because at such high temperatures the tracing materials may affect the surface tension of the pool and influence the flow. This is a significant problem in GTAW since surface tension induced flow is a dominant driving force. The majority of experimental investigations have determined the shape of the solidified weld metal and inferred how the flow within the weld metal has been altered by a change in the process parameters. Results from such work are obviously limited to qualitative observations, however, they have indicated the flow pattern beneath the surface of the pool and when used in combination with numerical models, they have provided evidence of several recirculation zones which were not detected by surface observations. Measurements of weld pool surface temperatures and temperatures within the base metal have also been used to study the relationships between process parameters and weld pool behaviour.

2.3.2.1 Gas Tungsten Arc Weld Pools: Related Experimental work

Lancaster (1987) produced a comprehensive review of work carried out prior to 1987. Much of the early experimental work sought to explain the wide variability in weld pool penetration experienced during the GTAW of stainless steel. Initial explanations, Ludwig (1968), attributed the variability to changed arc conditions due to the variation in the vaporised species from easily ionised impurities in the base material. Experimental measured anode spot sizes were observed to change in size in the presence of different alkaline metal

contamination on 304 stainless steel. This explanation was never pursued, and over the intervening years an alternative approach, based on the influence of surface tension on weld pool flow, has dominated. Subsequently Dunn & Eager (1986), using a numerical analysis of a tungsten arc, showed evidence that minor variations in the amount of aluminium or calcium vapour within an argon plasma (which already contained iron or manganese) was unlikely to cause big changes in the arc's thermal or electrical conductivity in the region of the weld pool. Recently Ohji *et al.* (1990) have again suggested that the popular explanation based on surface tension may not be the total view, and presented evidence of changes in anode spot size due to the presence of sulphur, oxygen and chlorine, using these changes to explain the observed changes in weld pool penetration.

Heiple & Roper (1979) are perhaps the most recognised for their work in considering the influence of minor alloy additions of aluminium, sulphur, selenium, tellurium, cerium and oxygen on the shape of GTA welds in stainless steels. They explained the effect of these elements in terms of their influence on the variation of surface tension with temperature. A variation in surface tension across a liquid surface causes flow, with a region of low tension flowing towards a high tension. Since the central region of a weld pool is likely to be at a higher temperature than the edge, and accepting that the surface tension of a metal is normally reduced as its temperature increases, the result would be a radially outward flow, (see Figure 2.4). With the hotter material at the centre flowing outwards a wide shallow weld pool would be produced. However, small concentrations of surface active elements can reverse the variation of surface tension with temperature, leading to a positive $d\gamma/dT$. This would encourage radially inward flow, setting up a circulation pattern which moves the

central hotter material downwards in the pool giving deep, narrow welds, (see Figure 2.4). Mills (1979), also considered GTA welding of stainless steel and concluded that the liquid flow patterns in the weld pool were of prime importance in determining pool shape, while arc current density and base metal characteristics were of secondary influence.

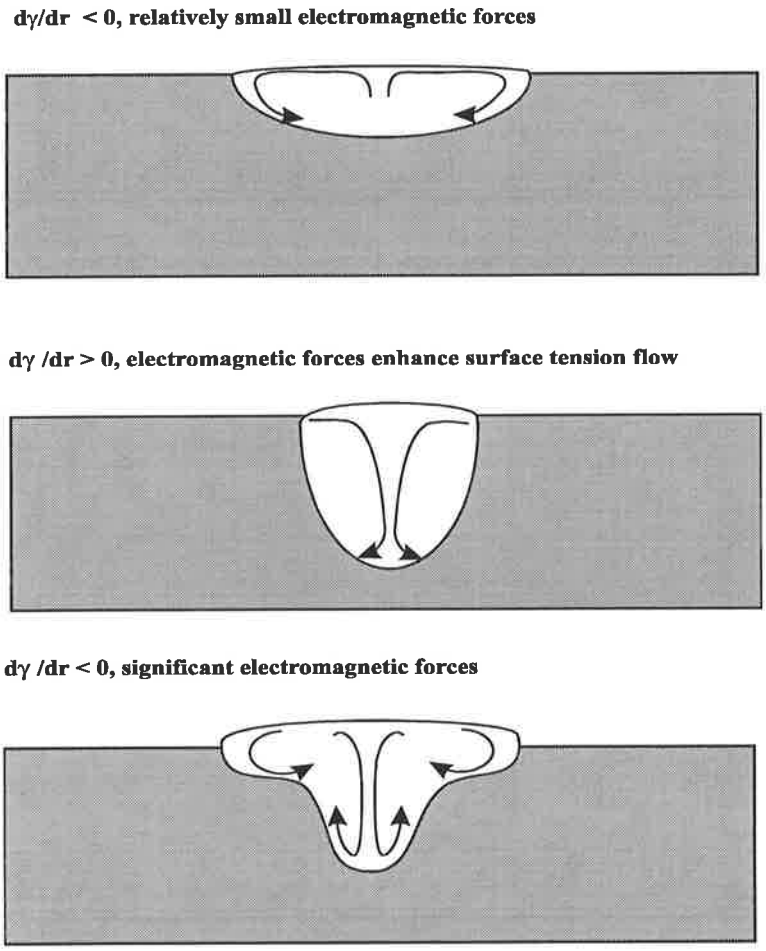

Figure 2.4. Surface tension driven flow in GTAW

Following Mills (1979) and Heiple & Roper (1982), an extensive amount of work has used similar arguments to relate process changes to fusion zone shapes by considering the

connection between surface tension and the alteration of pool flow. In many of these investigations welds were carried out within the presence of various surface active elements. These may have been in the base material, added by doping the work-piece surface, or included in the shielding gas. Such experiments as well as many numerical investigations in GTA welds have shown that the addition of a surface active agent can reverse the flow direction, turning a pool with radially inward flow to one with radially outward flow. This change in flow direction can, in turn, lead to a significant change in the weld pool shape, with inward flow creating a significantly deeper pool than that generated by outward flow. In stainless steel the effect can be significant, the bead depth to width ratio changing by 200% for a variation of 100 ppm of sulphur. In other alloys, however, as Spicer *et al.* (1990) found in 718, Ni-based superalloy, the effects where not so marked due to the presence of other numerous alloying additions.

Heiple & Burgardt (1985) have considered the effects of shielding gas composition and the influence of this on surface composition and subsequent weld geometry. Lienonen *et al.* (1990), again for 304 stainless steel, noted a changed penetration profile when welding with Ar, Ar+0.15%CO_2 and Ar+0.30%CO_2, and attempted to explain the differences in terms of the influence of oxygen on the pool's surface tension.

Surface tension changes are not however, the sole influence on the pool. Giedt *et al.* (1987) investigated the effect of varied process parameters on thermal cycles and pool shape, and concluded that welding current was a significant factor responsible for the characteristics of the final weld. High resolution surface temperature maps of stationary GTA weld pools on

304, 316 stainless steel and 8630 steel have been made using a optical spectral radiometric/laser reflectance method developed by Kraus (1987) & (1989). Other researchers have sought to develop methods of adaptive process control. Govardhan & Chin (1990) and Chen *et al.* (1990) have used thermography to dynamically measure the surface temperature of a weld pool during GTAW, and attempted to monitor changes in pool profile. Xiao *et al.* (1990) and Deam (1990) have related the natural frequency of oscillation of the weld pool surface to weld pool depth, with the objective of developing an adaptive controller for the process. This may be of use in gaining a fuller understanding of pool behaviour.

Other work in this area was contributed by Lambert (1991) and Shirali (1992). Heiple & Burgardt (1990) have reviewed many of the factors influencing penetration in GTA welding of stainless steels, and Ushio (1991) gives a good historic perspective.

2.3.2.2 Gas Metal Arc Welding: related experimental work

Experimental investigations of weld pool flow within GMAW has lagged the work for GTAW; for a review prior to 1987 see Lancaster (1987). Since then there has been some investigation of how the various process parameters affect the weld pool characteristics, e.g. Persson & Stenbacka (1989), Chandel (1988). Such work has focussed on the effect of current, shielding gas, etc on the form of the finished weld, in particular on the sectional form of the weld bead. There have not been many attempts to relate these findings to the potential flow pattern within the weld pool. This work has demonstrated that the arc current is the process variable most responsible for variation in the final geometry. Spencer (1984) has examined the penetration effects associated with the formation of a 'compound' vortex

within the weld pool, concluding that both convective flow and penetration increase with an increase in current. Shindoa *et al.* (1990) examined the effect of different filler wire surface tensions on the finished weld.

The direct investigation of weld pool flow is difficult, tending towards impossible. Investigators have therefore turned to the study of analog fluid models; Walsh & Dickinson (1989) have used a paraffin/wax model to study GTA weld pool forms, and Choo *et al.* (1992) have used a water/alcohol model to study the flow patterns set up during droplet interaction. In this latter work Choo *et al.* (1992) concluded that the flow within the pool was affected by the relative surface tension between the droplet and the pool, and that this force was of a similar magnitude to other forces in the pool. However the role of surface tension driven flow in a GMA weld pool is not clear. During the fusion welding of high strength steel, Makara *et al.* (1977) reported that weld penetration was influenced by small quantities of oxygen and sulphur for GTAW, but this effect was not seen in consumable electrode or electron beam welding.

Essers & Walters (1989) have shown that the impact of liquid droplets on the pool surface is a significant force in GMAW pool flow. However only Choo *et al.* (1992) have currently made attempts to experimentally study droplet impact in welding. Therefore for consideration of the phenomena and the factors inlvoved, examination of previous investigations into droplet/liquid interactions in other systems is required. The impact of a droplet onto a liquid surface has been extensively investigated in the open literature for fluids other than molten steel and the results of these investigations will be highlighted in the

following paragraphs. Since the results have been non-dimensionalised and so they should be directly applicable to molten steel.

When a liquid drop impinges on a free liquid surface two types of behaviour can occur. In the first case the drop may deform the pool surface producing a cavity in the pool, which then fills rapidly producing a rebound column (Figure 2.5). Alternatively the drop may enter into the pool with negligible splashing and produce a vortex ring within the pool which then travels down through the pool (Figure 2.6).

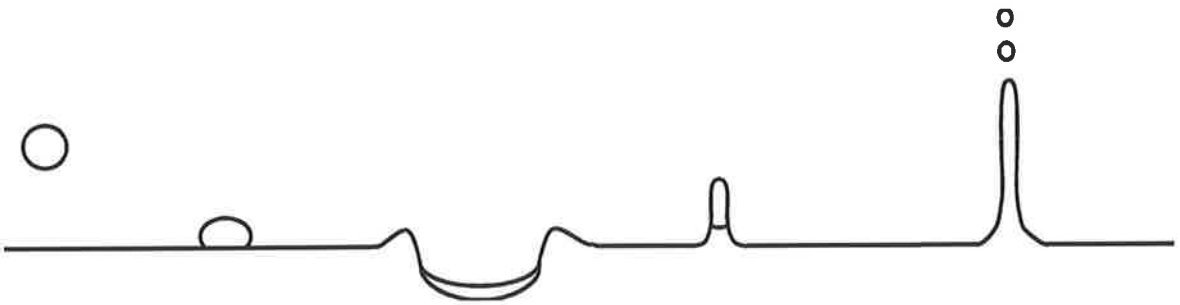

Figure 2.5 Droplet impact - rebound column formation

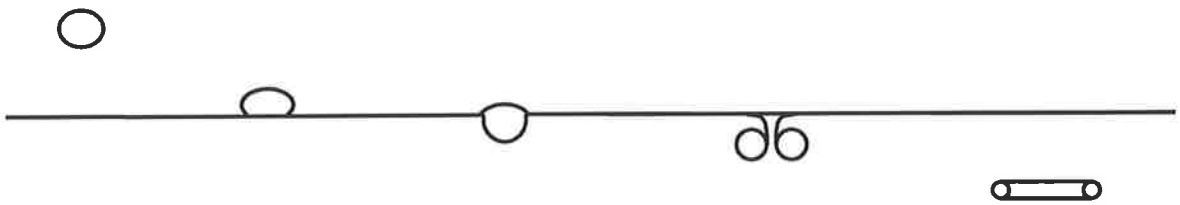

Figure 2.6 Droplet impact - vortex ring formation

Of particular interest in the case of GMAW is the modelling of the flow induced within the liquid pool. The vortex rings formed by droplet impact are likely to have a significant effect

on the thermal and compositional mixing that occurs within the pool (Shariff & Lenord, 1992). They may also affect the penetration profile of the pool (Chanine & Geboux, 1983).

Thomson & Newell (1885) were the first to report experimental investigations into the formation of vortex rings from droplets impacting on a liquid surface. They found that the vortex penetration varies cyclically with the height of fall, and therefore linked the droplet oscillation with the depth of penetration. Chapman & Critchlow (1967) also related drop fall height to depth of penetration and deduced that maximum penetration was achieved if the droplet was spherical and oscillating from oblate to prolate.

Rodrigeuz & Mesler (1988) presented a collection of experiments for water drops, in which they conclude that the maximum penetration occurs when the oscillating drop is prolate on impact, a contrary view to that of Chapman & Critchlow (1967). Hsiao *et al.* (1988) determined the limit for vortex ring formation in terms of the ratios of free surface energy and kinetic energy. They concentrated on determining the conditions for which the droplet will form a vortex ring rather than investigating why some droplets produce far more energetic vortex rings than others. They determined from their own experiments with mercury, and previously published results for water (Rodriguez & Mesler, 1988) that the critical Weber number is approximately equal to 8.

Morton & Cresswell (1992) have carried out a theoretical and experimental investigation into the formation of the vortex ring. They concluded that the explanations proposed by Thomson & Newell (1885) and Chapman & Critchlow (1967) for the generation of vorticity

were incorrect. Instead they stated that the vorticity is generated by the action of a finite force acting at the intersection between the drop and the pool, causing its acceleration relative to the underlying fluid.

It is apparent that the flow induced by the droplet surface interactions is a complex phenomena which must be investigated. Furthermore, these interactions should be incorporated into weld pool flow models if successful predictions of weld pool shape and heat transfer are to be made.

2.4 NUMERICAL MODELLING OF WELD POOL FLOW

2.4.1 Introduction

The development of a numerical model of a weld pool is a complicated task for two major reasons:

(1) the process is physically complex. Numerical representation requires the simultaneous solution of continuum equations for conservation of mass, energy and momentum. Although much of the basic mathematics exists, translating this into an efficient numerical solution procedure is a major task.

(2) it is a highly non-linear system, with material properties strongly dependent on temperature. In addition, our knowledge of material behaviour and thermo-physical properties under the environment of high temperature and plasma flow is limited.

Most initial efforts at modelling convective flow within weld pools have concentrated on the GTAW process. Here there is no transfer of molten material through the arc, and the process is therefore significantly less complex than GMAW. To date, the most complex numerical models have considered 3D moving non-autogenous GTA welds with non-linear thermo-physical properties, (Zacharia *et al.* 1988, & 1989). Currently these models are only qualitative, and no significant comparison has been made with experimental results. The most complex models to be clearly validated against experimental data are models of 2D stationary autogenous GTA weld pools (Zacharia *et al.* 1989, 1989, & 1991). These models

have been shown to predict weld pool sectional shapes and surface temperature profiles similar to those experimentally determined. However they do require the introduction of an empirical constant, the arc efficiency, which is a flexible parameter used to obtain the best fit with experimental data.

The development of convective flow within a GTA and GMA weld pools is a highly complex physical process which is controlled by a large number of parameters. The flow is driven by the following major forces in GTAW and GMAW:

(a)Electromagnetic force :

The current flow through the electrode, the arc-plasma and the work-piece generates a circumferential magnetic field. The diverging current and the self induced magnetic field interact to produce a force known as the Lorentz force. This acts towards the centre of the magnetic field, hence in the pool it generates a radially inward flow.

(b)Buoyancy force :

The temperature gradients within the pool can cause strong density variations. These induce flow, with the hotter, less-dense metal rising and cooler more dense metal sinking.

(c)Surface tension force :

The surface tension is a thermo-physical property of the fluid which generates a shear stress at fluid interfaces. The surface tension and hence the surface shear force, is a function of temperature, and so if the temperature varies across the surface so does the

surface tension and the shear stress. The variation in stress induces flow within the pool. Low tension regions tending to flow towards high tension ones. For molten steel the surface tension is also strongly influenced by the presence of surface active elements such as sulphur or oxygen, and the presence of these or their variation across the liquid surface can also affect the induced flow.

(d)Plasma induced flow :

The arc plasma impinging on the surface of the weld pool contributes to weld pool flow in two ways, firstly there is a downward pressure which can distort the pool surface, and then there are outward radial surface shear forces generated by the deflected plasma jet.

In GMAW there is the additional driving force of:

(e) Droplet impact :

The molten droplets transfer across the arc plasma have significant kinetic and free surface energy. Upon striking the pool the momentum of the drop induces flow within the pool. Furthermore, surface tension forces, due to region of high curvature during the droplets coalescence, can induce flow within the pool.

The above driving forces can combine in different ways to produce different weld pool flow patterns which will lead to various weld pool geometries, as illustrated previously in Figure 2.4. For example, when the surface tension at the edge of the weld pool is less than that at the centre ($d\gamma/dr<0$), then the surface tension driven flow and the electromagnetic flow combine to create a deep weld pool. When the surface tension gradient across the pool is positive ($d\gamma/dr>0$), then

surface tension forces oppose electromagnetic movement. Hence, for low arc current the pool flow would be predominantly outward, whereas for higher current there may be a central region in which the flow is inward and shoulder regions of outward flow. This creates a finger penetration. Experimental evidence supports this qualitative picture. Lambert (1991) suggested that to overcome the low penetration resulting from outward surface tension driven flow, the arc parameters should be chosen to give a smaller concentrated central anode spot. This would increase the inward driving electromagnetic forces and act to increase penetration.

Although these driving forces can interact, in computations it is often necessary to treat them separately in order to achieve a stable numerical solution. For example many models have studied the effect of surface tension with models that did not include electromagnetic forces. However this approach has to be viewed with caution, since there can be complex interactions between some of these forces. For example, when the plasma force deforms the weld pool surface it can change the current path. This affects the electro-magnetic force which in turn affects the plasma.

2.4.2 Modelling The GTA Weld Pool

Before 1980 the basic mathematics describing the physics of fluid flow were established. However their solution was computationally intractable. Atthey (1980) made the first attempt, calculating the flow induced by electro-magnetic force in a predefined isothermal hemispherical pool. He determined that convection was the dominant mode of heat-transfer within the pool. He also discussed the validity of the assumption of laminar flow, stating that in his case, since the Reynold's Number was less than the critical value for turbulent flow, the assumption was

valid.

Much of the initial work was carried out in the USA at MIT, and jointly between MIT and the University of Toronto by G.M.Oreper, J.Skezely, T.W.Eager, R.T.C.Choo and R.C.Westhoff. Oreper, Szekely & Eagar (1983), and Oreper & Szekely (1984) developed the first models of a GTA weld pool, which included the effects of surface tension, electro-magnetic forces and buoyancy forces on the flow pattern, again within a predefined pool shape. This initial work was for a static arc, effectively a 2D axi-symmetric weld pool, and it did not include a free surface, assuming that at low arc current the pool surface remained flat. They concluded that surface tension forces had a significant influence on the pool flow and that the assumed heat and current distributions also influenced the flow calculated. This demonstration of the relative magnitude of the surface tension force supported the experimental observations of Heiple & Roper (1982). The predictions qualitatively agreed with experiment and gave surface flow velocities of the same order as that measured.

At the University of Wisconson, S.Kou, Y.Le, Y.H.Wang & M.C.Tsai also produced models of GTA weld pools. The initial work of Kou & Le (1983) and Kou & Wang (1986a,b,c), produced models of moving arcs, and 3D convection for GTA and laser weld pools. They considered the effects of electro-magnetic, buoyancy and surface tension forces using a 'SIMPLE' based code after Patankar (1980). The first model did not consider a free surface and adopted constant thermo-physical properties. They again demonstrated that the variation of surface tension with temperature was the important factor in determining inward or outward flow within the pool. A significant advance was the inclusion of free surface movement by Lin & Eager (1985), who

determined that the arc pressure for arc currents above 300A caused significant distortion of the weld pool surface. However, the calculated depth of depression in the centre of a stationary GTA weld pool was a significant underestimate of that observed experimentally, i.e. 1.28 mm compared to 4.5 mm. They explained this difference by introducing a simple vortex flow, which at 2-3 rotations/sec could explain the increased surface distortion.

McLay *et al.* (1989), used the finite element method to calculate the heat and fluid flow within a weld pool, using fixed but non-flat weld pool surfaces and solid/liquid boundaries. Tsai & Kou (1990) developed a 2D finite difference model with a deformable pool surface fitted using orthogonal curvilinear coordinates. They used this to predict surface movement due to the arc pressure, electro-magnetically induced and surface tension flow.

In recent years T.Zacharia, S.A.David, J.M.Vitek, H.G.Kraus, A.H.Eraslan, D.K.Aidun, K.Mundra & T.Debroy at Oak Ridge National Labs & Oak Ridge in collaboration with Clarkson University, have concentrated on the development of the "WELDER" code based on the discrete element method (Zacharia *et al.* 1988 & 1989). Their work has concentrated on the application of this code to the GTA welding process including stationary and moving autogenous and non-autogenous welds. These models allow free surface movement but do not include the effect of plasma shear forces.

There are currently four areas of model refinement being addressed:

(1)the interaction between the arc and the weld pool surface shape.

(2)the significance of plasma shear forces on the surface of the weld pool, particularly if the pool surface is distorted.

(3)the significance of evaporation at the pool surface.

(4)the significance of thermo-physical properties.

2.4.2.1 Interaction between the arc and the weld pool

Much of the work to date has treated the arc and the weld pool separately. This generally takes the form of arc models, assuming that the surface of the weld pool is flat and of constant electric potential. Weld pool models on the other hand, take an assumed Gaussian distribution of current density and heat flux, this being the normal output from arc models with their assumed flat weld pool boundary. Using the commercial fluids code 'PHOENICS' based on the "SIMPLE" algorithm by Pankatar (1980), Choo, Szekely & Westhoff (1990) have addressed the difficulties and consequences of modelling the arc and the weld pool separately. In very interesting work they took the calculated deformed weld pool surface and used this as a boundary condition for an arc model, then did the reverse. They then calculated heat flux and current distribution on the distorted weld pool surface and examined the effect this may have on the flow within the weld pool.

The distorted weld pool surface had a marked effect on the calculated distribution of heat flux, turning the generally accepted Gaussian distribution into a bi-modal distribution at arc current levels of 200-300A when the surface distortion became significant. The bi-modal heat flux

distribution was then shown to effect the temperature distribution across the weld pool surface, with the obvious effect that the surface tension distribution was changed and the flow pattern was affected. The clear implication of this work is that there is an interdependence of the arc and weld pool and there are dangers in modelling these separately. In recent work Choo, Skezely & Westhoff (1992) have continued this theme and developed a linked arc and weld pool model, in which the arc heat flux and current distribution is calculated and applied to the pool, although at this stage the pool has an assumed flat surface. Vaporisation of elements from the pool and their influence on arc properties is considered, following Ludwig (1968) and Dunn & Eagar (1986).

2.4.2.2 The influence of plasma shear

The effect of plasma shear across the surface of the pool has often been ignored because it was considered that since the argon gas viscosity was small relative to that of the liquid, the transferred momentum would be negligible. Choo & Szekely (1991) calculated the plasma shear from an arc model and applied it to a weld pool model using stainless steel and arc currents of 100,200 & 300A. Their conclusion was that the effect of plasma shear was small in comparison to the influence of surface tension. However this work was applied to assumed planer weld pools, and as the authors pointed out, this conclusion could not be applied to non-planer pools. Kim & Na (1992) have considered this by modelling the effect of plasma flow across the surface of both flat and distorted pools. In their case the pool surface was calculated from the arc pressure, convective shape changes being ignored. For an arc current of 100A the surface distortion and plasma flow effects were small. At 200-300A the pool distortion increased penetration relative to a flat pool. At 300A the plasma drag forces became significant, slowed

the pool flow and reduced pool depth .

2.4.2.3 The effect of evaporation at the pool surface

Although it is recognised that evaporation of the liquid metal occurs during welding, the effect of this process has not been fully quantified. Zacharia *et al.* (1991 & 1993) concluded that it was important to include the effect of evaporation when modelling the pool, since without this the pool rapidly reached its boiling point, in line with an analysis by Block-Bolten & Eagar (1984) and Eagar (1990). However the work of Choo *et al.* (1992a,b) demonstrated that although evaporation played a role in limiting the weld pool temperature, thermo-capillary convection was the primary mechanism. Various ways of including the evaporation effect have been used by different researchers including Langmuir vaporisation (Zacharia *et al.* 1991 and Choo *et al.* 1992), limiting peak temperature (Choo *et al.* 1990) and mixed control techniques (Choo *et al.* 1992).

2.4.2.4 The role of thermo-physical properties.

A significant problem in modelling the flow within the weld pool is the accurate modelling of the thermo-physical properties of the materials. Very little data exists for molten steel at the temperatures found within the weld pool, and in several recent publications, Zacharia *et al.* (1993) and Mundra *et al.* (1992), the importance of accurate thermo-physical properties has been emphasised. Whilst all properties are significant, the viscosity and surface tension models appear to have the most dramatic effect on the computed results. Where possible all properties such as density, specific heat and conductivity should be treated as temperature dependent, however this can lead to problems in obtaining robust numerical solutions.

Viscosity

Investigations by Mundra *et al.* (1992) have demonstrated that accurate viscosity models are essential if accurate predictions of weld pool form are to be made. The measurement of the viscosity of molten metals at high temperatures is very difficult and little information exists (Zacharia *et al.* 1991). The appropriate viscosity for modelling weld pool flow is complicated because the eddy viscosity concept is commonly used in applied computational fluid dynamics (CFD) to account for turbulence. In the eddy viscosity concept the energy dissipation due to turbulence is accounted for by locally increasing the viscosity according to various schemes, i.e. the effective viscosity is the sum of the molecular viscosity and the eddy viscosity where the molecular viscosity is a physical property of the fluid and the eddy viscosity is a function of the turbulence and is derived from some form of turbulence model. Therefore, a suitable viscosity model cannot be determined without knowing the nature of the flow.

There has been some conflict in the literature as to whether the weld pools are laminar or turbulent. The size of the weld pool indicates that the flow should be laminar particularly for small GTA weld pools. However, the irregular nature of the driving forces, strong streamline curvature and shear effects would imply that the flow is most likely turbulent. For simplicity many existing weld pool models have assumed laminar flow, but the predicted pool is often larger than that measured experimentally unless "tuned" to give the correct answers using arc efficiency and distribution. The implication is that more energy is dissipated by the action of viscous forces than can be accounted for by the laminar model. Choo *et el.* (1994) and Malinowski & Bronicka *et al.* (1990) have questioned the assumption of laminar flow, with Choo *et al.* showing significantly improved prediction if turbulence is included. Of those models which

have considered turbulence, Choo *et al.* (1992) have used an enhanced viscosity/thermal conductivity scheme and a two equation K-ε model. Neither of these approaches have been fully investigated and further evaluation of various turbulence models is required. There is currently no consensus on the most appropriate turbulent viscosity model.

It is apparent that for GTA welding the flow should be modelled as turbulent. Therefore it is almost certain that GMA weld pools should be considered turbulent. Firstly the pool is generally larger, with larger velocities. Secondly, additional driving forces are due to the impinging droplet stream which is likely to lead to turbulence generation via irregular shear forces (due to droplet impact) and normal forces (due to surface tension). Furthermore the very high shear rates associated with surface velocities of the order of 0.5 to 1.0 ms^{-1} are likely to lead to turbulent fluctuations. If accurate predictions of heat transfer are to be made, accurate modelling of the turbulence transport is essential (Leschziner, 1994). Therefore it is likely that turbulence must be accounted for, in modelling the flow within a GMAW pool. (For a more detailed analysis please see Chapter 5) This dilemma has led to the investigation of various viscosity/turbulence models and their applicability to weld pool modelling. This information is summarised in the following section.

Turbulence Models

Turbulence models allow for energy dissipation caused by eddying at a scale smaller than the nodal mesh used in the flow calculations, by locally increasing the viscosity according to various schemes, (Rodi, 1980). A brief summary of the readily available and commonly used turbulence models are listed below, (Landahl, 1987; Lesiur, 1990).

(a) Zero Equation Models, mixed length models :

These models do not involve solving transport equations for turbulent quantities. They use a specified local eddy viscosity either directly, taking a value determined by trial and error, or indirectly, by determining a value from an empirical formula. This type of model is only useful for developed flow where large amounts of empirical data exist. It is therefore not well suited for modelling weld pool convection where little information on weld pool flow exists. However this technique has been the most widely used within the literature (Choo at al. 1992 & 1994) because of its low computational cost. Although little is known about weld pool flow, the pool profile can be easily measured and the viscosity modified until the predictions match experiment. In this way the viscosity can be used as "tuning factor" to enable the prediction of the required answers.

(b) One Equation Models :

These models solve a transport equation for a turbulence quantity. This approach overcomes some of the failings of the zero equation method, since it takes into account the movement and transport of turbulence. However, it is mainly suitable for shear layers where the length scale distribution can be empirically defined, and so it is not suitable for weld pool flow modelling. It has not been used to model weld pool flow because it offers no real benefit over zero equation models in the pool environment, where turbulence is generated from a wide variety of sources (not just shear layers).

(c)Two equation Models, eg K-ε models :

These models solve two transport equations; firstly for the turbulent velocity scale, and then for

the turbulent length scale. They are, therefore, the simplest models available in which the length scale is not prescribed in an empirical way. The K-ε model is the most commonly used turbulence model. It solves for the distribution of the turbulent kinetic energy, and for a length scale to determine the eddy viscosity. The K-ε approach is the most common method of modelling engineering flows, because of relatively low computational cost when compared to the more complex models, and much broader applicability than the simpler models.

In its standard form the K-ε model does not account for turbulence, induced by streamline curvature, buoyancy, or low Reynolds numbers and therefore in its standard form, it is not applicable to regions of transition. This may be a problem if it is to be used within a weld pool model, since all of these characteristics are present. If this type of model is to be used for weld pool modelling it may be necessary to use one of the modified (Leschinzer & Rodi, 1981) versions of the K-ε model. These modified models contain extra terms and modified empirical constants in order to account for streamline curvature and low Reynolds numbers. The choice of an appropriate turbulence model and the boundary conditions for K and ε is an area in need of more investigation.

It is envisaged that "two equation" turbulence models are the most complex that could be used in a weld pool environment for the immediate future, because of the significant computational demands and boundary condition limitations of the more complex schemes.

(d) Stress/Flux Models, (Differential Second Moment Closure and Algebraic Second Momentum Closure) :

i) Differential Second Moment Closure: These models solve for a large number of transport equations for the turbulent fluxes, as well as a length scale, rather than assuming that the stresses can be approximated by relating them to the transport of a velocity value. Stress/flux models inherently take into account the effect of buoyancy and curvature induced shear, and in this they are superior to "two equation" models. The large number of equations that must be solved for leads to significantly increased computational cost. There are several limitations that prevent these models from being used in applied computations. Firstly, they require specification of the boundary conditions for the turbulent fluxes, which is rarely available in practice. As a result, assumptions need to be made which inherently influence the solution. Secondly, in order to model the level of turbulence anisotropy, knowledge of the distance to the wall is required. Whilst this is relatively easy with simple geometry, it is almost impossible in the complex shape of a weld pool. Furthermore the effect of the free surface on the turbulent fluxes is not readily quantified.

ii) Algebraic Second Momentum Closure: These are simplified versions of the differential second moment closure schemes, where the differential equations governing the transport of the turbulent fluxes are converted to algebraic equations by making assumptions about the nature of the transport of the turbulent fluxes. This results in a significant computational saving. However, the simplifications on which these models are based are fundamentally flawed and lead to erratic predictions (Huang, 1986; Fu *et al.* 1988). These errors are unpredictable and so these schemes are best avoided (Haroutunian & Englemann, 1993) .

It should be noted that where the length scale equation is responsible for the poor performance of the K-ε model (e.g. axi-symmetric jets), then a stress/flux model with similar length scales

is no better (Rodi, 1980). Stress/flux models are likely to be more accurate at modelling weld pool flow than the previously listed schemes, however the K-ε approach is generally easier to implement and is less computationally expensive. Given the other significant demands present when modelling weld pool flow such as electro-magnetic forces, free surfaces and melt interfaces, the extra computational power needed for these schemes is not available. Furthermore, the difficulties encountered when specifying boundary conditions mean that these schemes are not applicable for weld pool modelling in their present form.

(e)Large Eddy Simulation :

Large eddy simulations with various sub-grid modelling schemes, such as re-normalisation group theory, are an improvement but these techniques require considerable computer resources. In the field of weld pool modelling where little experimental data exists, these techniques may be useful since they could be used to calibrate and provide boundary conditions for the more traditional methods. Due to their substantial computational cost and the complexities of weld pool flow, as well as uncertain boundary conditions, these schemes are not yet applicable to weld pool modelling.

(f)Direct Simulation of Turbulence:

It is also possible to obtain direct simulation of turbulence using the Navier Stokes equations provided the finite element grid is small enough to resolve down to the Kolmorgorov scale. In practice this requires vast computer resources, and the use of such a technique for practical purposes in the near future is unforeseeable.

Surface tension

The temperature distribution across the weld pool is only one of the factors influencing the strength of the surface tension driven flow. Many of the early models simply took $d\gamma/dT$ as a fixed value. Then since they also used a Gaussian distribution of heat flux, which gave the resulting pool a higher central temperature, a positive or negative $d\gamma/dr$ followed. However as Zacharia & David (1993) indicate, γ & $d\gamma/dT$ are both temperature and compositionally dependent. So depending on the temperature, the $d\gamma/dT$ can vary from positive to negative (see Figure 2.7). Accurate information on the variation of the surface tension of steels at high temperature is rare. It is even more difficult to obtain an accurate representation of the variation of surface tension with temperature and material composition. In weld pool models this is generally achieved through the implementation of theoretical relationships, such as that proposed by McNallen & Debroy (1991). This is based on a combination of the Gibbs & Langmuir absorption isotherms, and the interfacial tension is given by,

$$\gamma = \gamma^{o}_{m} - A(T-T_m) - RT\,\Gamma_s \ln(1 + k_l\, a_i\, e^{-\Delta H^{o}/RT}) \qquad (2.12)$$

where γ is the interfacial tension as a function of composition and temperature, γ^{o}_{m} is the interfacial tension of the pure metal at its melting point, R is the gas constant, T is the absolute temperature, Γ_s is the surface excess of the solute at saturation solubility, k_l is an entropy factor, a_i is the activity of the solute and ΔH^{o} is the enthalpy of segregation.

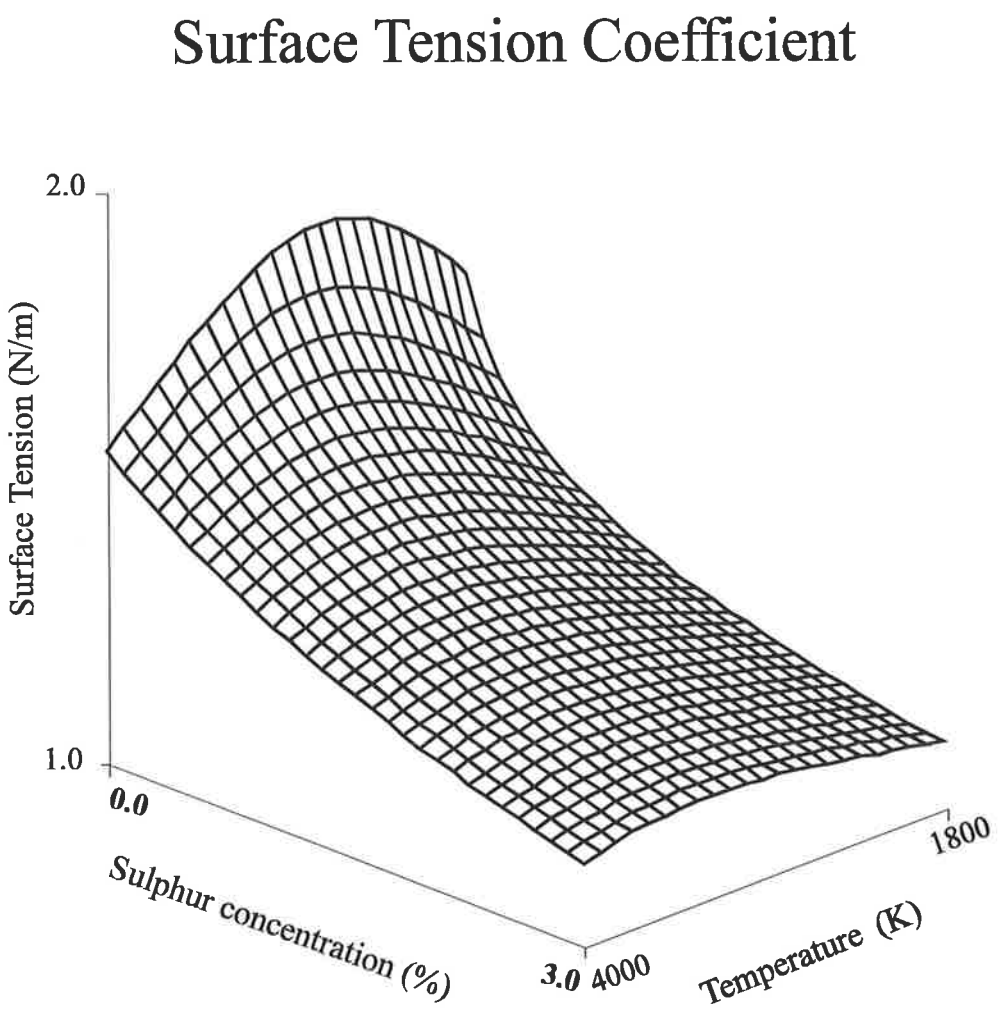

Figure 2.7 Surface tension coefficient as a Function of Temperature and Sulphur content using analysis of McNallen & Debroy (1991)

Additional complicating factors to the modelling of both vaporisation and surface tension, is the unknown influence of plasma on vaporisation rates or surface tension values. Debroy (1993) has demonstrated that under a low energy argon plasma the surface tension of copper reduces by about 20%, although the gradient of surface tension with temperature is essentially unaffected. He has also determined that the plasma can act to reduce the rate of vaporisation, however the

role of sub-species is not understood. Based on thermodynamic theory the presence of sulphur or oxygen should reduce vaporisation but the reverse has been observed. Sudo *et al.* (1989) report that presence of electro-magnetic fields also affects the surface tension although under welding conditions this variation is likely to be less than 10%. From this evidence it is clear that we cannot be confident in the exact values of surface tension or evaporation rate for the weld pool or droplet.

Specific heat & conductivity.

Whilst not as important as viscosity or surface tension, accurate temperature dependent values should be used for specific heat and conductivity. These can be obtained by the extrapolation of experimental results and the application of thermodynamic principles. Again, for simplicity some models have used constant values, but this can lead to significant differences in predicted values as shown by Mundra *et al.* (1992).

2.4.3 Modelling the GMA Weld Pool

The development of flow within a gas metal arc weld pool is even more complex than that in a GTA weld pool, due to the effects of a consumable electrode and metal transfer directly into the pool. All of the previously mentioned driving forces for pool flow, (electro-magnetic, surface tension, buoyancy and plasma forces) are present plus additional ones from the transferred droplets impacting into the pool. The molten droplets from the consumable electrode are transferred across the arc plasma at a high temperature 2400°C, velocity 0.5-1.5 m/s and frequency 10-300 drops/s. When these droplets impact on to the pool, the heat and momentum of the droplet is added to the pool. The experimental evidence is that the momentum of the

droplet has a major, perhaps a dominant influence, on the shape of the resulting weld pool (Essers & Walter, 1989).

There have been relatively few attempts to numerically model the convective flow within a GMA weld pool. Tsao & Wu (1988) have treated the droplets as a source of heat and solved the streamline and vorticity equations using a finite difference technique. Their model was limited to a 2D plane with a fixed horizontal upper surface, essentially a static arc, and it did not consider the effects of droplet shape, impact frequency or physical properties. They did not include the effect of droplet momentum and report that the characteristic finger penetration was caused by the heat from the droplets. Kim & Na (1994) have modelled a GMA weld pool using a three dimensional boundary finite difference model with boundary fitted co-ordinates. However they did not include the droplet momentum as a driving force, considering only electro-magnetic, surface tension and buoyancy forces. Not surprisingly, given their neglect of this, they had to modify the heat source distributions to get the finger penetration so typical of GMAW. Furthermore they did not consider latent heat, and therefore could not make accurate predictions of the thermal history. Both papers ignore the effect of droplet impact which appears to be a significant limitation; as the previous experimental work of Bradstreet (1968) and Essers & Walter (1981, 1989) implies that the droplet momentum has a significant effect on weld pool shape.

Choo *et al.* (1992) have used an analog fluid model to study the flow pattern in a liquid pool under droplet impact, and they concluded that the relative surface tensions between the droplet and the pool had a significant effect on the flow patterns generated. A schematic representation

of their findings is shown in Figure 2.8. A droplet with a high surface tension relative to that in the pool draws the pool surface towards it, resulting in a deeply penetrating droplet. Choo's picture of the relationship between weld pool flow and droplet impact is clearly different to that of Tsao's, as he presents a scene in which the droplets physical properties, shape and temperature, will influence the flow pattern. Tsao on the other hand views the droplet transfer to be a simple heat source, while Kim & Na ignore the droplets altogether. It is apparent that the relative importance of different driving forces on the weld pool flow in GMAW is an area in need of significant attention.

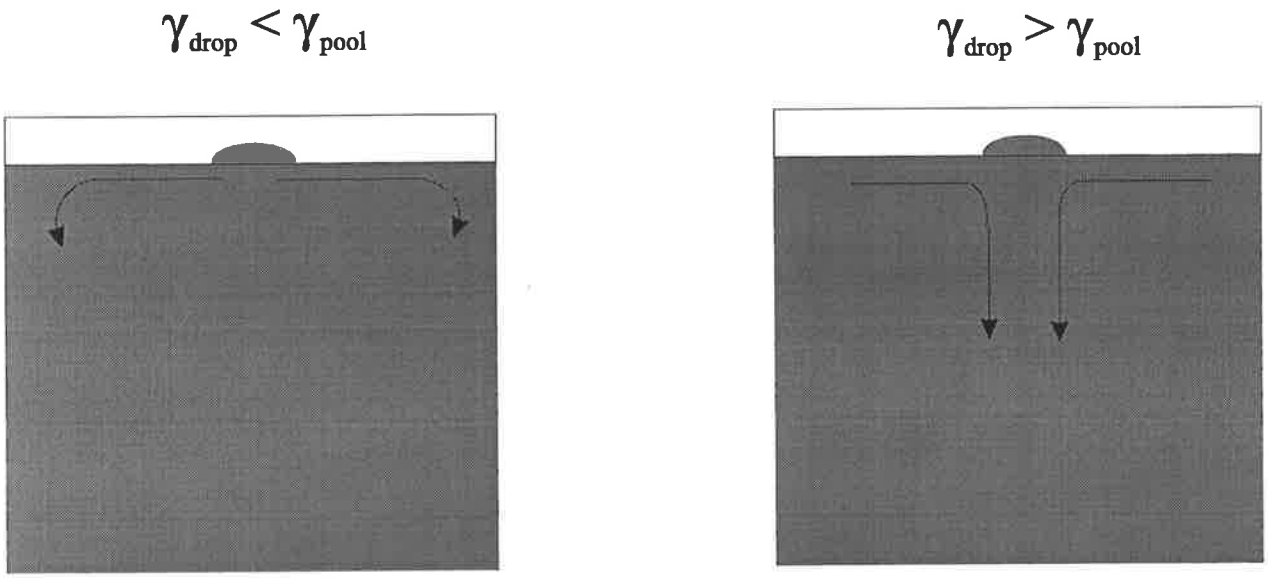

Figure 2.8 Flow visualisation results of Choo *et al.* (1992)

Attempts have been made to model the interaction of a droplet with a liquid surface in a non welding environment. Harlow & Shannon (1967) produced a model based on the Marker and Cell method (MAC) (Harlow & Welch, 1963) which did not consider surface tension, and hence did not model the formation of a vortex ring. However the results appear reasonable, showing

the formation of a rebound column. Experimental investigations carried out by Carroll and Mesler (1981) showed this model to be in error in predicting the formation of a liquid jet at Froude numbers $F_r = \frac{U}{\sqrt{gl}}$ that should produce a vortex ring. Furthermore, they suggested that the Weber number $W_e = \frac{\rho L U^2}{2\gamma}$ should be considered when predicting the limit of vortex ring formation.

Prospetti & Oguz (1993) used a boundary element method which included surface tension, to model the formation of bubbles caused by the collapse of the crater. This model assumed potential flow beneath the surface and hence could not model the vortex ring formation. If the formation of vortex rings is to be accurately modelled both surface tension and viscosity must be included. Nystrum (1986) has performed a simulation that includes surface tension and viscosity using the volume of fluid (VOF) approach (Hirt & Nichols, 1981). He does not mention any vortex ring formation (probably due to the mesh which appears too coarse to accurately capture the surface tension forces, and impact velocities which were generally too high). Because the curvature is related to the second derivative of the VOF function, any model which uses VOF method must use a very fine mesh if surface tension forces are to be accurately captured in regions of high curvature (Brackbill *et al.*, 1992). This is impractical for engineering computations because of the significant computational cost.

2.4.4 Summary

The basic procedures for modelling the GTA weld pool are established, and such models have significantly increased our understanding of the factors controlling weld pool geometry.

There are difficulties and challenges in dealing with the free surface movement of the pool, the solid/liquid interface, the effects of plasma flow, and the interaction between the pool and the welding arc. More investigation is needed into the effect of turbulence and the techniques used to model it. It must also be recognised that there is a lack of thermo-physical data on the behaviour of materials in a high temperature plasma field and this is a limiting factor in modelling the weld pool environment.

There is a danger in simply viewing the metal transfer forces as being additional to those present in GTAW, because now the relative magnitude of those forces may be altered. For example, on a relatively 'flat' weld pool surface, the plasma shear forces may be considered relatively minor. However, on a distorted pool the radially outward plasma flow may interact with the surface wave caused by droplet impact and induce complex flow behaviour.

The role of surface tension may not be so significant in the more dynamic environment of a GMA weld pool. Experimentally, Makara *et al.* (1977) have shown that during GTAW high tensile steels, small amounts of oxygen and sulphur affect the weld penetration, but this effect was not shown for GMA or electron beam welding. Zacharia *et al.*'s (1988 & 1989) models of non-autogenous welding have also showed that the introduction of filler wire to some extent reduced the effect of surface tension driven flow; they suggested that this was due to the evening out of the pool temperature due to filler addition.

The effect of distortion of the pool surface is a subject of some conjecture. Choo *et al.* (1992c) identified that a significant change from a single peak Gaussian to a bi-modal heat flux

distribution, occurred with a arc current of 250A in a GTA pool with a surface depression of about 4 mm. From a simple analysis of the expected pool depressions in GMAW, Lancaster (1984) estimated a depression of 3.1 mm at 200A. Clearly this is enough to suggest that some distortion of the heat flux distribution across the arc may also occur in GMAW. A further complication may be the dynamic nature of the surface in GMAW; again Lancaster(1984) estimated that at a current of 170A, droplet frequencies were sufficiently high that a cavity persisted during welding. Below that current the surface 'washed' back and filled up between individual drop transfers. Such effects would seem to imply a complex fluctuation in the arc heat and current distribution.

The role of plasma shear flow may also be considerably more complex in a GMA weld pool since waves and surface ripples are more likely and these may interact with the deflected plasma. Finally, with the droplet impact and the significant disturbances present in the welding environment, it is expected the assumption of laminar flow will be even less valid than in GTA weld pools.

Modelling a GMA weld pool, with the additional complication of molten droplet transfer, is a significant but stimulating challenge. Firstly, the seeming contradictions within the literature and the relative importance of the different driving forces need to be investigated.

2.5 OVERVIEW

If accurate predictions of near weld thermal histories are to be made, it is evident that the effect of convective heat transfer within the weld pool must be incorporated into the modelling process. However due to the significant computational cost of a full solution of the fluid flow within a weld pool, it is evident that heat conduction solutions are the only option for the solution of industrial problems in the immediate future. Heat transfer from an arc to the upper surface of the work-piece has been shown experimentally to be Gaussian. Therefore, it is intuitive to apply a surface Gaussian heat source to the upper surface of the work-piece when applying thermal boundary conditions to welding models. However, analytical and numerical models using this representation of the arc as a heat source do not predict accurate near weld thermal histories. In particular the weld pool depth and length as well as the $T_{8/5}$ cooling times are generally under-predicted. This is primarily due to the failure of these models to incorporate convection within the pool. The flow within the pool transfers the heat from the surface of the pool to the base metal much more efficiently than conduction alone. Therefore far more heat is transferred deeper into the work-piece than would occur if there was no flow within the pool. Modifications must be made to traditional heat transfer solutions to incorporate this effect. Traditionally, this has been done by modification of the heat source with the most popular approach being to use an arbitrarily defined volumetric heat source such as a double ellipsoidal Gaussian heat source. In these sources the heat is not applied to the surface as happens physically, but is distributed within a volume of the base metal, i.e. the heat is applied directly to the base metal at some depth below the surface. This effectively simulates the enhanced heat transfer due to convection

within the pool. However this modified heat source requires a significant amount of empirical tuning, via the form of the heat distribution and the volume to which it is applied. These tuning factors effectively force agreement with experiment. These factors do not reflect the effect of different welding conditions on the weld. They do not directly recognise that the individual components of the arc energy can affect process outcomes, or that other process parameters, such as shielding gas type, can have an influence. Such effects have been extensively documented, i.e. different cooling times, fusion zone and HAZ geometries can be obtained by changing process parameters such as voltage, current and speed, even though the net heat input is kept constant. Of course such effects are accounted for in models in a secondary way by the manipulation of variable factors, (often those defining the heat source distribution). Therefore, these models are not able to be used with confidence in situations that have not been tested and "tuned" for.

In order to avoid the limitations of existing conduction models, this thesis has concentrated on developing an understanding of the fluid dynamics within a weld pool, and using this knowledge to develop modifications to heat conduction solutions based on the physical changes that occur within the system. A heat source based on physical behaviour should result in a more broadly applicable, accurate and efficient model. In order to develop such a model the fluid dynamics of the pool must be investigated. This is not readily achievable experimentally hence the need for computational fluid dynamics models.

Modelling of the GTAW pool has been extensively carried out in the literature and has been very useful in developing our understanding of the flow behaviour. Modelling the GMAW process

lags behind that of GTAW with several obvious anomalies in the attempts reported in the literature. The first stage of modelling and understanding weld pool flow is to determine the relative importance of the different driving forces on the flow, and this is the focus of Chapters 3 and 4. The driving forces in GTAW pool flow have been determined within the literature. It has been shown that surface tension and electro-magnetic effects are the main forces driving flow within the pool, with buoyancy forces being negligible and arc pressure forces negligible for currents of less than 250 Amps. These forces have not been investigated in the literature for GMAW. Furthermore, in GMAW the metal transfer is an additional important driving force, and the effect of droplet momentum and droplet surface interactions have been investigated and compared to the other forces within the pool. In Chapter 3 a scale analysis has been carried out to indicate the expected magnitudes of the different driving forces and provide information on the modelling strategies required. The results of this analysis have then been verified using simple axi-symmetric numerical models, to further investigate the relative importance of the different driving forces. This is presented in Chapter 4.

Work within the literature has raised question about turbulence within the weld pool and its effect on the pool behaviour. Turbulence can have a significant effect on the heat transfer within a convective flow and must therefore be investigated. In GMAW the effect of droplet impact on the pool and the effect that this has on the turbulence within the pool must also be investigated. Chapter 5 focuses on the role of turbulence and droplet impact within the pool and how best to incorporate these effects into the numerical models.

A full 3 dimensional solution to the fluid flow and heat transfer within the pool using finite

element computational fluid dynamics has been developed using the knowledge of important driving forces and turbulence as developed in Chapters 3, 4 and 5. This is discussed and compared to the results of experiment and various solutions using heat conduction only Chapter 6. This has shown that incorporating convection within the pool does improve the prediction of weld pool shapes and near weld thermal histories. Based on these results, modifications to conduction solutions have been developed using a semi-analytical technique. This approach is compared to experiment, and traditional conduction and convection only solutions in Chapter 7. Conclusions and recommendations for future work are discussed in Chapter 8.

Chapter 3

NORMALISED SCALE ANALYSIS OF CONVECTIVE DRIVING FORCES IN GMAW POOLS

3.1 INTRODUCTION

In order to understand any flow behaviour it is often useful to look at the ratios between the different forces responsible for driving the flow. For the weld pool this facilitates a broad understanding of the effect of variations in the weld operating parameters have on process outcomes. Efficient numerical modelling of convective flow also requires ranking of the relative importance of different driving forces. This enables the model to include all important forces and ignore relatively unimportant ones, thus simplifying the model and promoting numerical stability. It also allows for efficient mesh development by providing insight into the regions where the flow will be undergoing the most significant changes. Furthermore if one is trying to modify the flow in the weld pool to provide different process outcomes, e.g. more or less penetration, one needs to know which force dominates. Whilst the literature contains information on the relative importance of different driving forces in GTA weld pools, the important driving forces in GMA weld pools have not been studied. Effects can only be inferred from these GTA results and some experimental work on the effect of different parameters on the penetration profile (for example see Essers *et al.* 1989). A detailed analysis has not been made. In this Chapter a normalised scale analysis has been

carried out in order to quantify the relative importance of the different driving forces. In this analysis the governing equations are normalised using the given boundary conditions and the force ratios determined from the resulting non-dimensionless equations. This technique is discussed in detail in the following sections.

3.2 FRACTIONAL ANALYSIS

3.2.1 Introduction

As discussed in Chapter 1 weld pool flow is very complex precluding a complete analytical solution. It is therefore necessary to perform some form of fractional analysis in which one obtains as much information as possible about the solution to the problem. The most common technique of fractional analysis used in engineering is dimensional analysis based on the Buckingham Pi theorem. Dimensional analysis is traditionally used for:

i) Conversion and checking of units.

ii) Reduction of the number of independent parameters.

iii) Generalisation and correlation of results.

iv) Construction of physical models and similitude laws.

v) Determining the ratios of the driving forces, if the dimensionless parameters are formed correctly.

In order to clarify the following discussion some definitions are required. In this thesis dimensionless variables (represented by *) are the non-dimensional form of the independent variables. e.g. x^*, y^*, z^*, T^*, t^*. Changing the value of the dimensionless parameters implies moving through the domain of a given problem, that is changing x* from 0 to 1 means moving from one side of the domain to the other in the x direction. Furthermore, dimensionless parameters are enclosed by brackets () or represented by their traditional abbreviation or title. e.g. $(\rho UL/\mu) = R_e$ = Reynolds Number. Dimensionless parameters are

formed from the boundary conditions, the characteristic scales of the body; and from the physical parameters of the governing equations. Dimensionless parameters are often interpreted as force ratios, e.g. R_e is the ratio of inertia force to viscous force. This is particularly useful when one wants to know the relative importance of the different forces, and it can be used to develop approximate solutions if some forces are negligible when compared to others. However unless the dimensionless parameter is properly formed it will not accurately represent the ratio of the appropriate forces. As Prandtl (1934) states " The Reynolds number does not always equal the ratio of inertia to viscous stress, hence to say only that when two systems are geometrically similar and have the same Reynolds number, the ratio of inertia to viscous stress is the same in both flows" (attributed to Prandtl (1934) by Kline (1965).) This means that one cannot simply take a traditional dimensionless parameter, feed in some arbitrary scales, and also define it as the ratio of the appropriate forces without checking that these definitions agree for the problem at hand. In practice they often disagree. Using the ratio of inertia force to viscous force as an example, it does not always follow that this ratio will be small because some arbitrary form of the Reynolds number is large. For example in the case of a flow through pipe, using the length of the pipe as the length scale for the formation of the Reynolds number yields a dimensionless parameter which is several orders of magnitude different to one based on the diameter of the pipe. Obviously they cannot both represent the ratio of viscous to inertia forces. So which, if either, is right? However if the dimensionless parameter is correctly formed it will represent a force ratio. For example, if we bring the terms in the governing equations to approximately unit magnitude and divide by the coefficient of one term, then the parameters must represent the ratios of the important effects, whether they are forces, energies or other

quantities. This follows from the fact that the governing equations must express the magnitude of these terms by their very nature. A process for the normalisation of the governing equations is outlined in the following section.

3.2.2 Procedure for Normalisation

Normalisation is the process of making the governing equations dimensionless in terms of non-dimensional variables of standard magnitude. To carry out a normalisation, several steps are required as outlined below:

1) Make all the variables non-dimensional in terms of the appropriate scales of the problem. This is done by:

   i) Defining all dependent variables so that they are approximately unity over a finite distance and do not exceed approximately unity in the domain of interest.

   ii) Defining all independent variables so that their increment is approximately unity over the same domain.

2) Divide through the equation by the coefficient of one term to make the equation non-dimensional.

The normalised equations can then be analysed using approximation theory to estimate the relative importance of the different terms within the governing equations. The dimensionless parameters can also be used in the development of numerical models. There is significant advantage in developing non-dimensional numerical models, because the non-dimensionalisation reduces the difference in magnitude between solution variables and

therefore enhances numerical stability.

3.2.3 Approximation Theory

If the governing equations can be reformulated in non-dimensional coordinates so that all the variables in the governing equations and boundary conditions are of order unity, and if the domain of interest be made of order unity, then the magnitudes of each term will be the product of the non-dimensional parameters and the non-dimensional partial differentials in that term. Approximation theory can then be applied by estimating the magnitude of the non-dimensional partial differentials and examining the magnitudes of the parameters in the normalised governing equations.

In order to determine the importance of the parameters within the governing equations an estimate of the magnitude of the partial differential terms is required. As the dependent and the independent terms have been normalised it is possible to estimate the order of these terms if we know an approximate form of the solution. For example, to estimate the derivative of velocity in respect to time, we know that in our normalised set of variables, time ranges form 0 to 1, and the velocity is approximately unity over a finite distance and does not exceed approximately unity within the domain. Therefore if the solution looks more or less like figure 3.1a the derivative will be of the order 1. If the solution looks like figure 3.1b then the derivative is likely to be of the order $1/\varepsilon$. Once the magnitude of the differential terms has been determined the importance of each term in the equation can be determined by inspection.

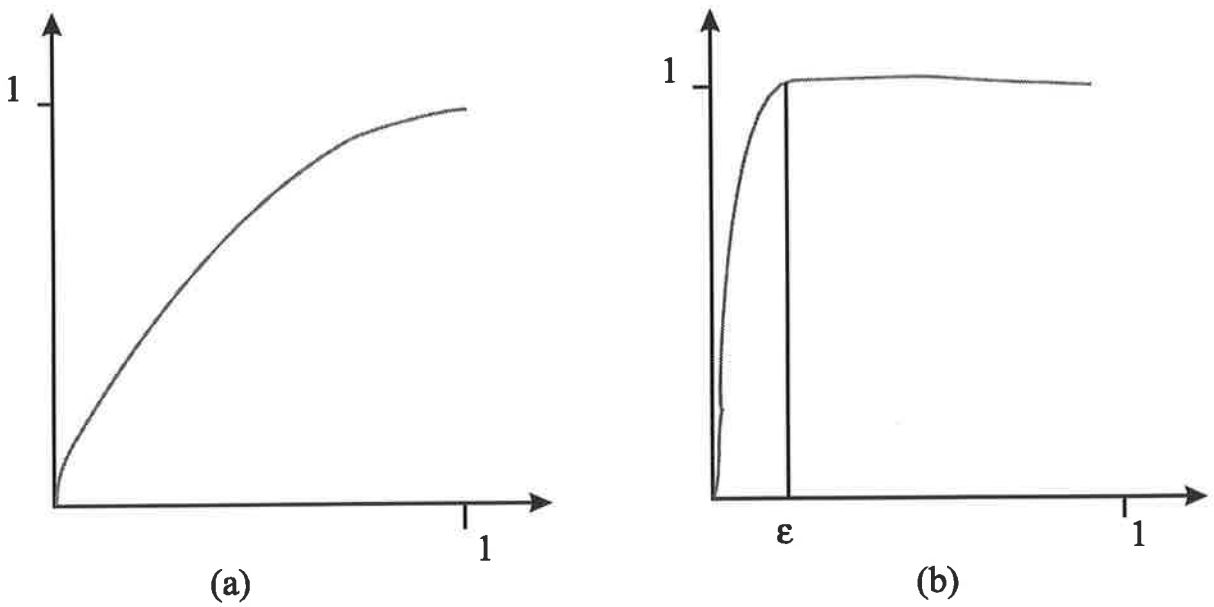

Figure 3.1 Expected form of solution:
a) smooth form of solution.
b) non smooth form solution.

In the following section the equations governing weld pool flow are normalised, then approximation theory is applied to these normalised equations to estimate the relative magnitudes of the driving forces within the pool.

3.3 DERIVATION OF NORMALISED DIMENSIONLESS COEFFICIENTS

In vector form the governing equations for convective fluid flow are as follows (Batchelor, 1967 & Cramer, 1973)

1) Continuity:

$$\nabla \cdot \boldsymbol{u} = 0 \tag{3.1}$$

2) Navier Stokes assuming the Boussinesq approximation for variable density,

$$\rho\left(\frac{\partial \boldsymbol{u}}{\partial t} + \boldsymbol{u}\cdot\nabla\boldsymbol{u}\right) = -\nabla p + \rho \boldsymbol{g} + \mu \tau_{ij} - \boldsymbol{g}\Delta\rho + \boldsymbol{JxB} \tag{3.2}$$

with surface tension stresses on the free upper surface, given by,

$$\sigma = (2\gamma C - p_a)\boldsymbol{n} + \nabla_s \gamma \tag{3.3}$$

where γ is the surface tension coefficient, C is the mean Gaussian curvature, p_a is the ambient pressure and $\boldsymbol{n}$ the normal vector. The first term in equation 3.3 represents the forces due to suface curvature less those due to the external pressure, whilst the second term represents the forces due to tangential surface tension gradients.

3) Energy Equation:

$$\rho c_p\left(\frac{\partial T}{\partial t} + \boldsymbol{u}\cdot\nabla T\right) = \nabla\cdot(k\nabla T) + \boldsymbol{E} \tag{3.4}$$

where equations 3.1, 3.2 and 3.4 are the same as equations and 1.1, 1.2 and 1.3 and the variables and terms are described in that section.

Normalising with the following transformations,

$$u_i^* = \frac{u_i}{U_d} \tag{3.5}$$

where * indicates a dimensionless quantity and where u_i is the dimensional velocity and U_d is the velocity scale.

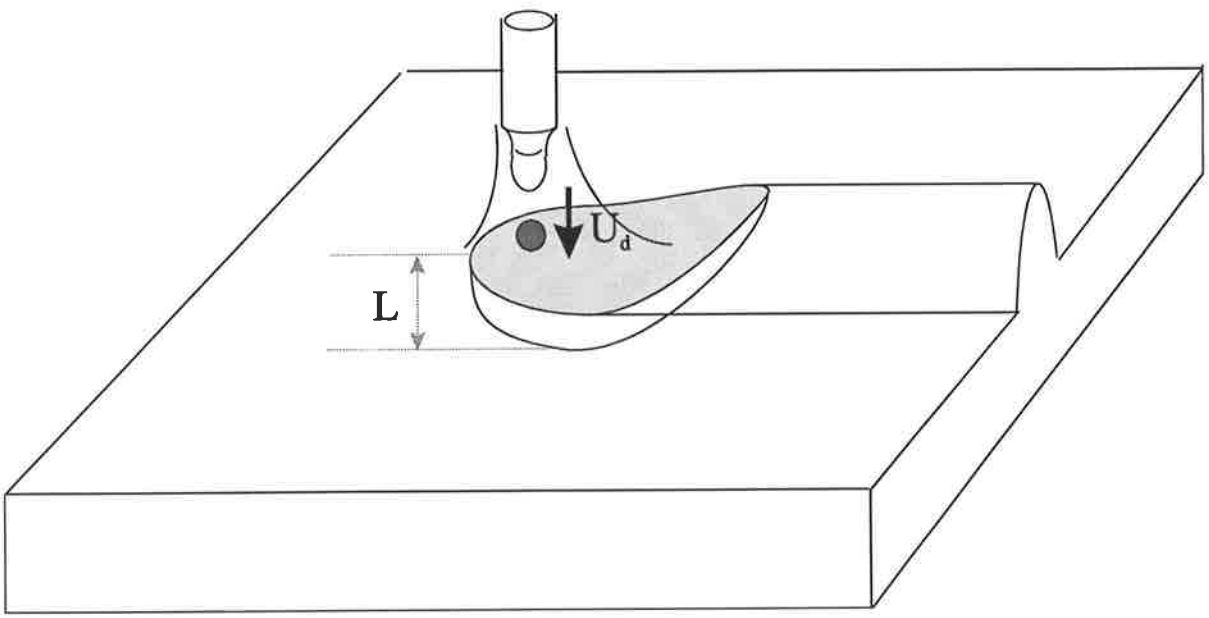

Figure 3.2 Characteristic Length and Velocity Scales

The characteristic length scale, L, and velocity scales, U_d, are detailed in Figure 3.2 where characteristic velocity U_d is the droplet impact velocity. The droplet impact velocity has been chosen to normalise the velocity because it is most probably the largest in the system and the only one that can be accurately measured.

Lengths are non-dimensionalised using the following equation

$$x_i^* = \frac{x_i}{L} \tag{3.6}$$

where x_i is the dimensional length and L is the depth of the weld pool. The pool depth has been chosen as the characteristic length because it is the dimension of most interest and it is of the same order as the largest dimension in the system. Therefore the dimensionless length scale, whilst not necessarily being between zero and one, will be of order one and will still be applicable for a normalised scale analysis.

The dimensionless shear stress is defined as:

$$\tau_{ij}^* = \tau_{ij} \frac{L}{\mu U_d} \tag{3.7}$$

where τ_{ij} is the shear stress tensor and μ is the viscosity of steel at the average weld pool temperature.

The dimsionless time scale is represented as:

$$t^* = \frac{tU_d}{L} \tag{3.8}$$

where t is time.

Pressure is non-dimensionalised using the following equation:

$$p^* = \frac{p}{\rho U_d^2} \tag{3.9}$$

where p is pressure and ρ is the density of steel at the average weld pool temperature.

Temperature is non-dimensionalised as follows:

$$T^* = \frac{T - T_o}{\Delta T} \tag{3.10}$$

where T is Temperature and T_o is some appropriate reference temperature and ΔT is the expected temperature variation.

Gravity is normalised using the following approach:

$$\boldsymbol{g}_i = g\boldsymbol{g}_i^* \tag{3.11}$$

where g is the magnitude of gravity and $\boldsymbol{g}$ is a unit vector in the direction of gravity.

Enthalpy is normalised below:

$$E^* = \left(\frac{L}{\rho c_p U_d \Delta T}\right) E \tag{3.12}$$

where E is enthalpy and c_p is the is the specific heat capacity of steel at the average weld pool temperature.

Substituting the above transformations into equations (2.1) to (2.4) gives the following normalised equations.

1) Continuity Equation:

$$\nabla \cdot (\boldsymbol{u}^* U_d) = 0 \tag{3.13}$$

dividing by U gives,

$$\nabla \cdot \boldsymbol{u}^* = 0 \tag{3.14}$$

2) Navier Stokes:

$$\rho\left(\frac{\partial \boldsymbol{u}^* U_d^2}{\partial t^* L} + \frac{U_d^2}{L}\boldsymbol{u}^* \cdot \nabla \boldsymbol{u}^*\right) =$$
$$-\nabla p* \frac{\rho U_d^2}{L} + \rho \boldsymbol{g}\boldsymbol{g}^* + \frac{\mu U_d}{L^2}\nabla^2 \boldsymbol{u} - \boldsymbol{g}\boldsymbol{g}^* \Delta\rho + \sigma_o U_d \mu_e^2 H_o^2 \boldsymbol{J}^* x \boldsymbol{B}^* \tag{3.15}$$

dividing by $\frac{\rho U_d^2}{L}$ gives,

which is equivalent to,

$$\left(\frac{\partial \boldsymbol{u}^*}{\partial t^*} + \boldsymbol{u}^* \cdot \nabla \boldsymbol{u}^*\right) =$$

$$-\nabla p^* + \frac{gL}{U_d^2}\boldsymbol{g}^* + \frac{\mu}{\rho U_d L}\nabla^2 \boldsymbol{u}^* - \frac{\Delta \rho g L}{\rho U_d^2}\boldsymbol{g}^* + \frac{L\sigma_o \mu_e^2 H_o^2}{\rho U_d}\boldsymbol{J}^* x \boldsymbol{B}^* \qquad (3.16)$$

$$\left(\frac{\partial \boldsymbol{u}^*}{\partial t^*} + \boldsymbol{u}^* \cdot \nabla \boldsymbol{u}^*\right) = -\nabla p^* + F_r^{-1}\boldsymbol{g}^* + \frac{1}{R_e}\nabla^2 \boldsymbol{u}^* - R_i \boldsymbol{g}^* + R_m^2 JxB \qquad (3.17)$$

where the dimensionless parameter $R_e = \frac{\rho UL}{\mu}$ is called the Reynolds number and is a measure of the relative importance of inertial forces to viscous forces. When the Reynolds number is small viscous forces dominate, and when it is large inertial forces dominate, boundary layers form and the flow may become turbulent. The parameter $F_r = \frac{U^2}{gL}$ is the Froude number and is a measure of the relative importance of inertial forces to gravitational forces. It is of importance in determining the effect of gravity on the free surface. The non-dimensional group $R_i = \frac{\Delta \rho g L}{\rho U_d^2}$ is the Richardson Number, which is the ratio of buoyancy forces to inertial forces and

$R_m = \mu_e H_o \left(\frac{\sigma L}{\rho u_d}\right)^{\frac{1}{2}}$ is the magnetic Reynold's number this is the ratio of the magnetic force to the inertial force.

Considering the boundary conditions at the upper free surface and using the following scales,

$$\sigma_{ij}^* = \frac{\sigma_{ij}}{\rho U_d^2} \qquad (3.18)$$

where σij is the stress tensor,

$$C^* = CL \tag{3.19}$$

and C is the mean gaussian curvature. The surface stresses due to surface tension can be given by:

$$\sigma_{ij}^* \rho U_d^2 = (2\gamma \frac{C^*}{L} - p_a^* \rho U_d^2)\boldsymbol{n} + \frac{\gamma_t \Delta T}{L} \phi(T^*) T_{,i}^* t_i \tag{3.20}$$

dividing by ρU_d^2 gives

$$\sigma_{ij}^* = (\frac{2\gamma}{\rho U_d^2 L} C^* - p_a^*)\boldsymbol{n} + \frac{\gamma_t \Delta T}{L \rho U_d^2} \phi(T^*) T_{,i}^* t_i \tag{3.21}$$

which is equivalent to

$$\sigma_{ij}^* = (W_e^{-1} C^* - p_a^*)\boldsymbol{n} + \frac{M_a}{R_e} \phi(T^*) T_{,i}^* t_i \tag{3.22}$$

where

$$W_e = \frac{\rho L U_d^2}{2\gamma} \tag{3.23}$$

is the Weber number and is the ratio of inertia forces to the normal component of the surface tension forces. Therefore W_e^{-1} as in equation 3.22 is the ratio of surface tension forces due to curvature effects to inertia forces. The Marangoni number;

$$M_a = \frac{\gamma_T \Delta t}{\mu U_d} \tag{3.24}$$

is the ratio of surface tension gradient forces or the tangential component of surface tension to inertia forces.

$$\frac{M_a}{R_e} = \frac{\gamma_T \Delta T}{L\rho U_d^2} \tag{3.25}$$

is the ratio of surface tension gradient forces to inertia forces, and;

3) Energy Equation:

$$\rho c_p\left(\frac{\partial T}{\partial t} + \boldsymbol{u}\cdot\nabla T\right) = \nabla\cdot(k\nabla T) + H \tag{3.26}$$

gives

$$R_e.P_r\left(\frac{\partial T^*}{\partial t^*} + \boldsymbol{u}^*\cdot\nabla T^*\right) = \nabla\cdot(k^*\nabla T^*) + H^* \tag{3.27}$$

where $Pr = \frac{\mu c_p}{k}$ is the Prandtl number which is a dimensionless measure of the ratio of molecular diffusion to thermal diffusion.

$R_e.P_r = P_e = \frac{\rho c_p U_d L}{k}$ is called the Peclet Number and is the ratio of convection to conduction.

Estimates of the importance of each individual driving force can now be carried out from equations 2.17, 2.26 and 2.31 using approximation theory. This will be the focus of the next section.

3.4 ANALYSIS USING APPROXIMATION THEORY

The analysis the preceeding section gives the following dimensionless parameters for the normalised Navier Stokes equations with a free surface boundary:

R_e-1 : Ratio of viscous forces to inertia forces.

F_r : Ratio of gravity forces to inertia forces.

R_i : Ratio of buoyancy forces to inertia forces.

R_m : Ratio of electro-magnetic forces to inertia forces.

W_e^{-1} : Ratio of surface tension forces due to curvature affects to inertia forces.

M_d/R_e : Ratio of surface tension gradient forces to inertia forces.

Assuming that the solutions for the dependent variables are all relatively smooth functions as shown in Figure 3.1a, all differential terms in the normalised Navier Stokes equations should be of order one. Given the low viscosity and high thermal conductivity of molten steel and that the flow within the pool is likely to be turbulent, it is probable that velocity and thermal distributions within the pool will be relatively smooth due to the enhanced turbulent mixing. This seems to be the best available approximation given our knowledge of the weld pool. If the variation of dependent parameters within the pool are not smooth (similar to the form of figure 3.1b) this may affect the accuracy of the analysis of by approximately 1 order of magnitude. However this is acceptable given the nature of the analysis. This technique never attempts to do more than estimate the order of magnitude of a given force, therefore an accuracy of 1 order of magnitude is acceptable. However this level of accuracy should be taken into account when analysing the results.

Given these assumptions the magnitude of the appropriate dimensionless parameter

determines the importance of that particular driving force. Furthermore as all of these dimensionless groups are ratios of the relevant force to the inertia force they can be directly compared to one another. The variation of these parameters can be calculated for the appropriate welding current by the substitution of the appropriate scale dimensions into these dimensionless numbers. Scales have been taken from the available experimental literature, (Essers 7 Walter, 1989 for the droplet impact velocity and Gunter & Sparrow, 1993 for the weld pool dimensions) and are outlined in Table 3.1. The material properties used for steel are taken from Zacharia *et al.* (1991) and are given in Table 3.2.

Arc Current (Amps)	Velocity (ms^{-1})	Pool Depth (m)
100	0.43	0.00125
125	0.5	0.00195
150	0.76	0.0025
175	1.18	0.0032
200	1.58	0.0037
225	1.94	0.0042

Table 3.1 The variation of length scale (weld pool depth) and velocity scale (droplet impact velocity) with arc current (Gunter & Sparrow, 1993; Essers, 1989)

Properties	Values
Density	6750 kg/m^3
Viscosity	4x10^{-3} kg/ms
Specific Heat	790 J/kgK
Thermal Conductivity	20 W/mK

Table 3.2 Material properties of steel at 2000K (Zacharia *et al.* 1991)

The variation in the dimensionless parameters with welding conditions is shown in Table 3.3 to facilitate an understanding of the flow conditions within the pool. Note that the dimensionless groups are shown in their standard form, not in the from derived in the normalised analysis, i.e. R_e not R_e^{-1}. This is done to assist the reader comprehend the magnitudes of the various force ratios, as the dimensionless groups are in their traditional rather than inverse form.

Arc Current (Amps)	Reynolds No. R_e	Weber No. W_e	Marangoni No. M_a	Richard-son No. R_i	Magnetic Reynolds No. R_m	Peclet No. P_e
100	645	1.6	42.6	0.00175	0.111	69.3
125	1170	3.5	36.6	0.00273	0.161	125.
150	2280	10	24.1	0.00350	0.178	245.
175	4531	32	15.5	0.00448	0.188	487.
200	7015	66	11.6	0.00518	0.200	754.
225	9777	113	9.4	0.00588	0.216	1051.

Table 3.3 Variation of dimensionless parameters with welding current.

The variation of the parameters as determined in the scale analysis, and hence an estimate of the relative importance of the individual driving forces is plotted in Figure 3.3. Both Table 3.3 and the plot presented in Figure 3.3 demonstrate that inertia forces are the largest in the system, with the importance of surface tension forces decreasing with current and the electro-magnetic forces of the order 10 % of inertia forces throughout the investigated range. This implies that the droplet impact force is likely to have the most significant effect on the

flow within the pool and hence on the weld pool shape and near weld thermal histories. It appears that if surface tension forces are to have an effect then they will only do so at relatively low currents. Futhermore it appears that bouyancy forces are negligable through the current range.

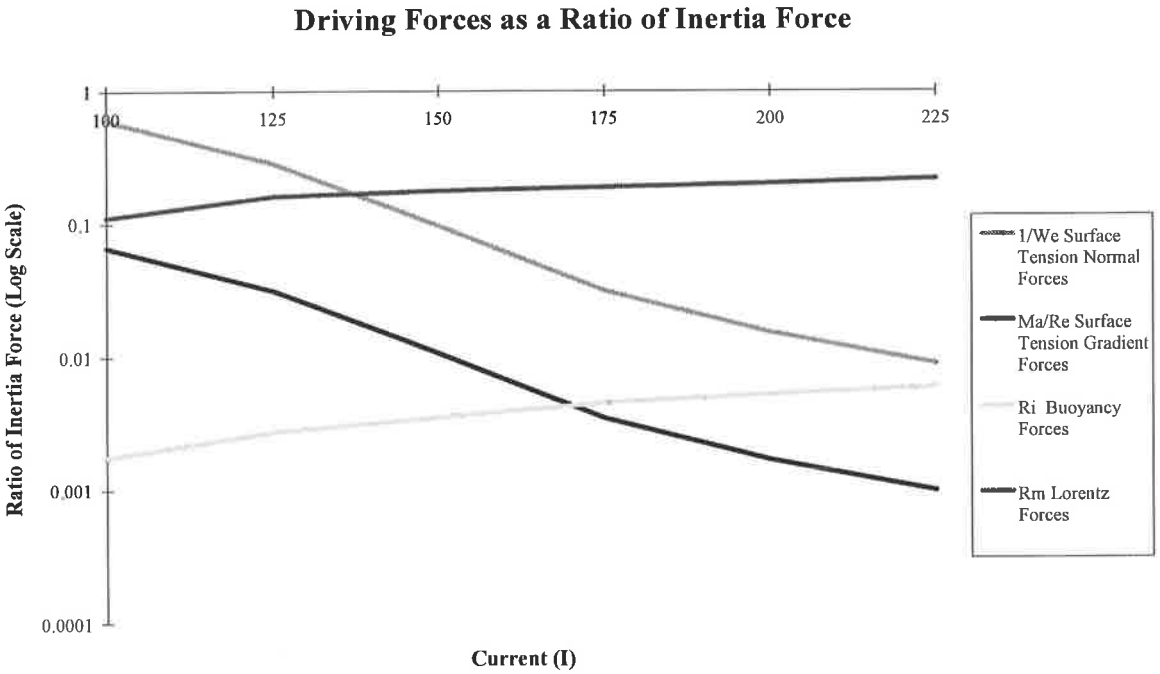

Figure 3.3 Ratio of driving forces to droplet inertia force.

The non-dimensional group derived from the energy equation is the Peclet number which is a measure of the ratio of convection to conduction within the weld pool. For the above conditions the Peclet number ranges from 69 at 100A to 1052 at 225A. This implies that convection is the dominant mode of heat transfer within the weld pool for all welding currents considered.

3.5 CONCLUSIONS

Based on this analysis the droplet momentum force is the dominate force in driving the weld pool flow. This is supported by the experimental results of Bradstreet (1968) and Essers & Walter (1981) & (1989), linking the penetration profile can be linked to the droplet momentum. It would appear that surface tension gradient forces, as investigated by Choo *et al.* (1992), may have an effect of similar magnitude to that of electromagnetic forces at low currents, but this effect rapidly decreases with increasing current to the point that it is the least important force by 170A.

The electro-magnetic force is second in importance throughout most of the welding range, although approximately one order of magnitude smaller than droplet inertia forces.

Buoyancy forces appear to be negligible across the entire current range although they do have more effect at higher currents. This is in agreement with the results of numerical studies of GTA weld pool flow by Mclay *et al.* (1989).

These results indicate that the investigation of Tsao *et al.* (1988) and Kim & Na (1992) who ignored the effect of droplet momentum in their analysis must be called into question.

It should also be noted that the Peclet number, which is the ratio of convection to conduction, is very much greater than 1 throughout the entire range of welding currents.

This means that convection is the dominant mode of heat transfer within the weld-pool. Therefore any attempt to model heat transfer in the near weld region, which does not consider convection in some form is incomplete

Scale analyses, whilst being a useful tool, is limited in that it provides a relatively global picture and may not accurately describe the ratio of important forces in the vicinity of singularities such as boundaries. This is because there is some uncertainty introduced by estimating the order of the differential terms in the governing equations in these areas. However this analysis clearly demonstrates that droplet impact forces cannot be ignored in any numerical model of GMAW pool flow. The level of detail of droplet impact that needs to be included is not certain. For this reason further investigation of the relative importance of the driving forces are required. In the following Chapter a series of numerical models has been developed to further investigate these force ratios.

Chapter 4

THE RELATIVE IMPORTANCE OF CONVECTIVE DRIVING FORCES IN GMAW POOLS

4.1 INTRODUCTION

In the previous chapter, a normalised scale analysis has been used to investigate the relative significance of the different driving forces in a GMA weld pool. Whilst this technique is useful to gain a general indication of the importance of relative forces, it can only be an approximate solution. Whenever a solution varies rapidly over a small distance, (e.g. boundary layers), it is very difficult to estimate the importance of the various terms. Therefore further work is required in order to verify the results of the scale analysis. As discussed in Chapter 1 experimental verification is very difficult, therefore mathematical modelling of the flow has been carried out in an attempt to further clarify the effect of these individual forces.

Although the flow within GMA weld pool is inherently three dimensional, in this section two dimensional approximations are used. Whilst such approximate flow models cannot accurately predict weld pool shape and near weld thermal history (see section 6.1), they are suitable for comparing the relative magnitudes of the different driving forces. This approach reduces the size and computational cost of the models without significantly reducing the

effectiveness of the comparison.

Highly coupled problems such as those with free and/or melt surfaces (as found in a weld pool) are inherently difficult to solve because the flow and the interface position are closely interrelated, ie. changing one changes the other. Therefore it takes many iterations of robust numerical schemes to obtain a suitable solution. Furthermore, the addition of surface tension and buoyancy forces (which are highly coupled to the temperature and hence the flow fields), as well as electro-magnetic forces (which depend upon the current distribution), gives a highly coupled and complex problem which is difficult to solve. These problems require vast computer resources which are not available at the present time. It is for these reasons that the problem has been split up by comparing the individual forces to some reference force, and by assuming that as a first approximation all forces can be considered additive.

Normalised scale analysis, as presented in Chapter 3 and previously published experimental results (Essers *et al.* 1981), indicate that the inertia forces resulting from droplet impact are the most significant forces driving weld pool flow. Therefore in this section, as in Chapter 3, all the other forces will be compared to inertia forces.

Numerical models have been generated using FIDAP finite element computational fluid dynamics code. A description of the general modelling strategy and solution techniques adopted is presented in Appendix 1.

In the following sections surface tension gradient, electro-magnetic and buoyancy forces are

compared to the droplet inertia forces. The effects due to curvature induced surface tension forces are discussed in Chapter 5.

4.2 MARANGONI (SURFACE TENSION GRADIENT) FORCES

4.2.1 Introduction

In a weld pool the gradients in surface tension caused by temperature and compositional variation generate a shear stress along the pool surface and induce flow within the pool. In this section a computational model has been used to study flow patterns driven by droplet induced Marangoni forces. It concentrates on examining the effect of the relative surface tension between the droplet and the pool, and on the influence of droplet momentum. It is intended that this section will identify the role that Marangoni forces play in driving the weld pool flow, and provide further direction for future models of welding processes involving non-autogenous metal transfer. This section only investigates the effect of surface tension gradients; curvature induced surface tension effects are discussed in Chapter 5.

As mentioned in Chapter 1, Choo *et al.* (April 1992) have investigated droplet and pool interactions with a flow visualisation technique, and have shown that significant flow is introduced by the relative surface tension differences between the droplet and the pool. These results contrast with an early model of a GMA weld pool, which treated the droplets purely as heat sources, ignoring droplet induced flow.

In addition the scale analysis presented in the previous Chapter indicates that Marangoni forces may play a role at lower welding currents. However this result relied on an estimated surface tension gradient (normally based on maximum temperature or concentration differences over the characteristic pool length), the actual surface tension gradient may be

much higher due to the significant temperature and/or concentration gradients near the point of droplet impact. It is clear that further quantification of the role of Marangoni forces is required.

4.2.2 Computational Model

The model was developed using "FIDAP"(1991,1993) finite element computational fluid dynamics code. The model considers a molten pool and determines the flow induced by droplets impinging on to its surface. It has been tested against the results from flow visualisation experiments published by Choo *et al.* (April 1992) by modelling a water/alcohol pool and droplet, and has shown good agreement in predicted flow patterns (see Figure 4.1 and Figure 4.2). The computational model predicted surface velocities of 0.02 to 0.15ms^{-1} which compare favourably to the experimentally measured velocities of 0.04 to 0.2 ms^{-1}. Following this verification the model was applied to a molten steel weld pool under impact from steel droplets.

The inherent assumptions, necessary simplifications and details of the model are as follows:

(1) It is considered that the droplet strikes the centre of a liquid pool, and that the induced flow is axis-symmetric. This is an approximation to a droplet transferring into a developed, stationary GMA weld pool.

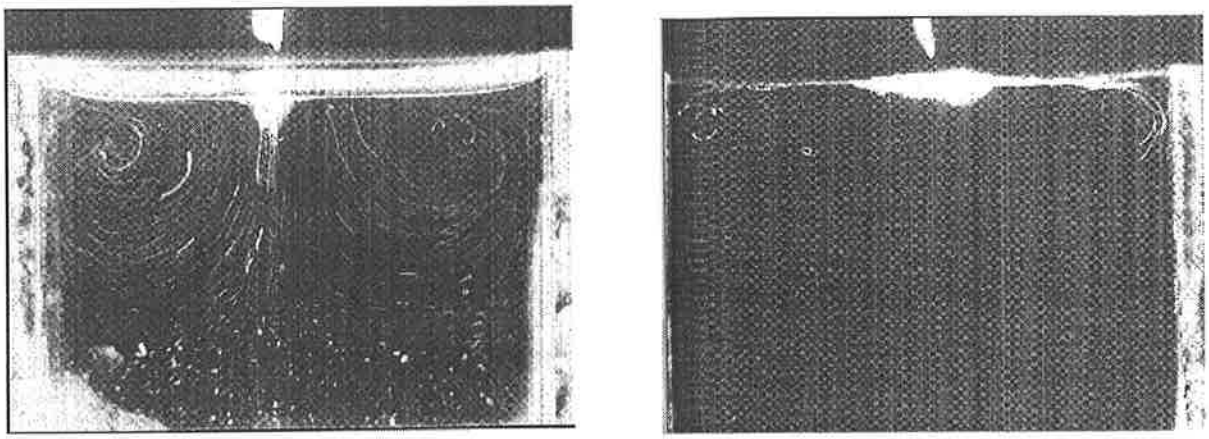

Figure 4.1 Flow visualisation studies of Choo *et al.*. Low surface tension drop on right, high surface tension drop on left.

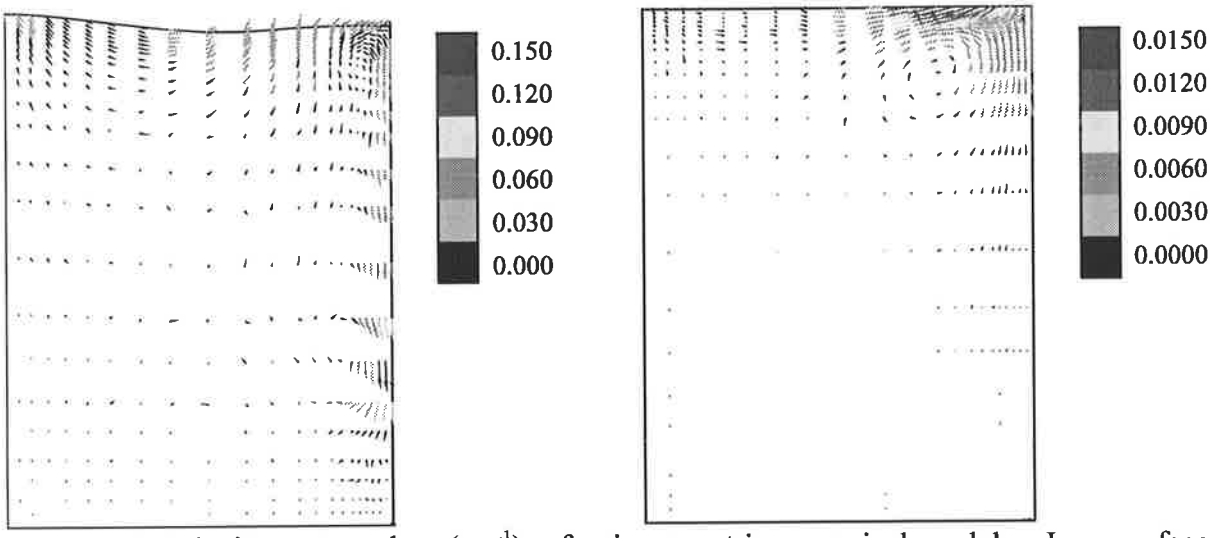

Figure 4.2 Velocity vector plots (ms^{-1}), of axi-symmetric numerical models. Low surface tension drop on right, high surface tension drop on left.

(2) The model is taken to be isothermal and both droplet and pool were assumed to be at a constant temperature of 2700K, as indicated by experimental measurements (Jelmorini *et al.*). Temperature gradients would normally occur within the pool and contribute to the spatial variation in surface tension and to the induced surface tension forces. However, surface tension is dependent on both composition and temperature and spatial variation in either will induce surface forces. The process has been extensively demonstrated for GTA weld pools (Zacharia, April 1991, & Mundra, 1992). In the current work, the influence of a differential in the surface tension of the droplet and the pool has been simulated by forcing a variation in their sulphur content. Using a compositional variation rather than simply ascribing a fixed surface tension value to droplet and pool, allows a changing surface tension as the droplet dissipates into the pool. Mathematically, the diffusion of sulphur is equivalent to temperature dissipation. Here, temperature is not used as an active variable in order to isolate the surface tension effect from the effects of buoyancy, and to enable parametric validation.

It is realised that the sulphur content of steel is controlled, however in this work it is introduced as a convenient means of adjusting the surface tensions of the droplet and the pool. Sulphur was chosen as the surface active agent since this could be varied to form drops with higher or lower relative surface tension. In practice, it is expected that the droplet would have a higher temperature than the pool and consequently would always have a lower surface tension.

(3) The model only considers the flow induced by the droplet and its surface interaction with the pool. Arc pressure and plasma shear forces, heat flux from the arc, electromagnetic effects and buoyancy forces are not included. It is recognised that all of these factors combine to influence weld pool flow, but the aim in this initial work was to isolate the relative effect of surface tension forces and momentum forces.

(4) A large pool size of 20 mm radius by 30 mm deep has been modelled. This relatively large volume was used since this is the case most sensitive to surface tension effects. In a shallow pool, an impacting drop would strike the bottom of the pool irrespective of the drop's surface tension. If surface tension gradients have a small effect on a large weld pool, they will definitely have a negligible effect on small pools. The assumed pool size also allowed direct comparison of the model with the water analogue of Choo *et al.* (April 1992).

(5) The size, impact velocity and transfer frequency of weld droplets has been taken from previously published experimental work (Lancaster, 1984), and these are detailed in Table 4.2.

(6) The top surface of the pool was free to deform.

(7) Along the edges of the pool 'no-slip' conditions for a viscous fluid were assumed.

(8) The flow was taken to be Newtonian. This assumption has been experimentally verified by a previous researcher (Atthey, 1981).

(9) There is no consensus on the choice of a laminar or turbulent model as both have been questioned in the literature (Choo *et al.* 1992). In this work numerical investigations have shown that a laminar model would be inappropriate at high droplet impact velocities. However, the common turbulence models are also ineffective in areas of low Reynold's number, high temperature gradients or high streamline curvature, all of which are present in the weld pool. As a compromise, the flow was considered as laminar when checking the model against Choo *et al*'s flow visualisation data as the observed flow appeared to be laminar. However when modelling the flow within a molten steel weld pool, an enhanced viscosity model was used to account for the effect of turbulent dissipation and to encourage numerical stability, as used by Choo *et al.* (1992b, 1994) At worst this approximation could lead to a 20% error in the predicted weld pool size (Mundra *et al.* 1992). However since the 'enhanced viscosity' will have no effect on the relative magnitude of the driving forces and only influence the damping of the flow, this particular assumption should have no effect on the results of this investigation.

(10) The previous work in modelling flow in GTA weld pools (Zacharia *et al.* April 1992), has shown that it is important to consider the effect of temperature-dependent thermo-physical properties. In the present isothermal model all properties were taken at a temperature of 2700K. These values are given in Table 4.1.

Table 4.1 Thermo-physical properties of pool material.

Property	Value
Viscosity	6×10^{-3} $kgm^{-1}s^{-1}$
Diffusivity	5×10^{-5} $m^{-2}s^{-1}$
Density	7.2×10^{3} kgm^{-3}

A fundamental difficulty in any calculation of the flow within the weld pool is the lack of dynamic fluid physical properties for molten steel at high temperatures. In this study, where sulphur content has been used to change the surface tension of the pool and the droplet, the data of McNallan & Debroy (1991) for a Fe-S binary alloy have been used. Other researchers (Zacharia *et al.* April 1991) have shown this to be the best available approximation.

4.2.3 Numerical Experiment

Using the computational model a series of numerical experiments were carried out. Droplets whose size and velocity were representative of three different welding currents (100, 150 & 200 Amp as indicated in Table 4.2) were simulated.

Table 4.2 Experimental Droplet Characteristics (Lancaster 1984)

Arc current (Amps)	Droplet radius (x 10^{-3} m)	Droplet velocity (ms^{-1})	Droplet frequency (s^{-1})
100	1.48	0.43	11
150	1.19	0.76	74
200	0.62	1.58	320

Process: Direct current, electrode positive
Shielding Gas: 80% Argon / 20% CO_2 at 18 litres/min.
Wire: 1.2 mm diameter solid C-Mn steel wire.

Surface tension differences between the droplet and the pool were produced by varying their respective sulphur contents. Three different conditions were taken for each current level; a standard case where the droplet and the pool had the same composition (both 0.0%S), and two additional conditions where the droplet had a surface tension lower and higher than the pool (+0.03%S in the drop and the pool respectively).

The model was used to predict the transient flow pattern during successive droplet strikes. Up to 400 hours of computer time (Sun Sparcstation 4/40) was required to develop a quasi-

steady state. Consequently, to reduce calculation time the investigation compared flow patterns after single droplet impacts. The characteristic flow pattern was taken to be that after impact from a single droplet at a time immediately prior to the next droplet strike. This approach was justified by a comparison of the flow after single and multiple droplets which established that the flow induced by a single impact was characteristic of the flow induced by successive droplets. Essentially, if a single drop produced a radially outward flow, then the quasi-steady state produced by multiple droplet impacts was also a radially outward flow. For example with a high surface tension drop at 200 Amp, the depth-to-width ratio of the $0.01 ms^{-1}$ speed contour was 4.23 and after 20 drops this falls to 4.11. In fact, this ratio remains approximately constant until the flow pattern is ultimately affected by the container walls. On this basis a comparison of changes in flow pattern after single droplet impacts seemed acceptable.

4.2.4 Results

The speed contours produced by the numerical model for a current of 100, 150 and 200 Amps are shown in Figures 4.4, 4.4 and 4.5 respectively, and vector and 0.06ms^{-1} contour line plots in Figures 4.6, 4.7 and 4.8.

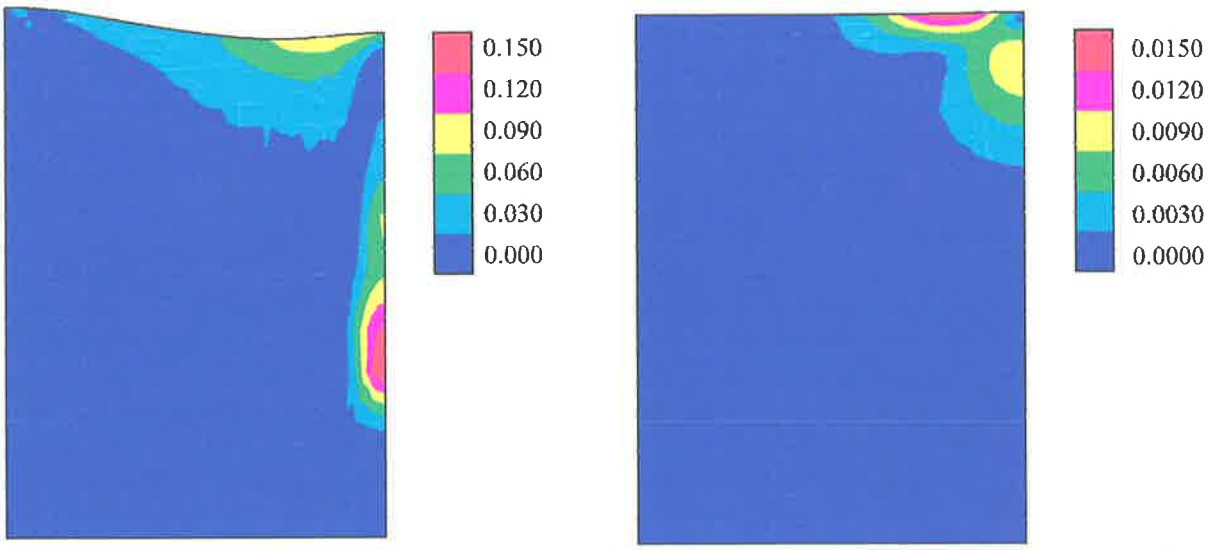

Figure 4.3 Speed contour plot (ms^{-1}) for droplet impact equivalent to I=100 Amps, high surface tension drop on left, low surface tension drop on right. Note an order of magnitude difference in the scales

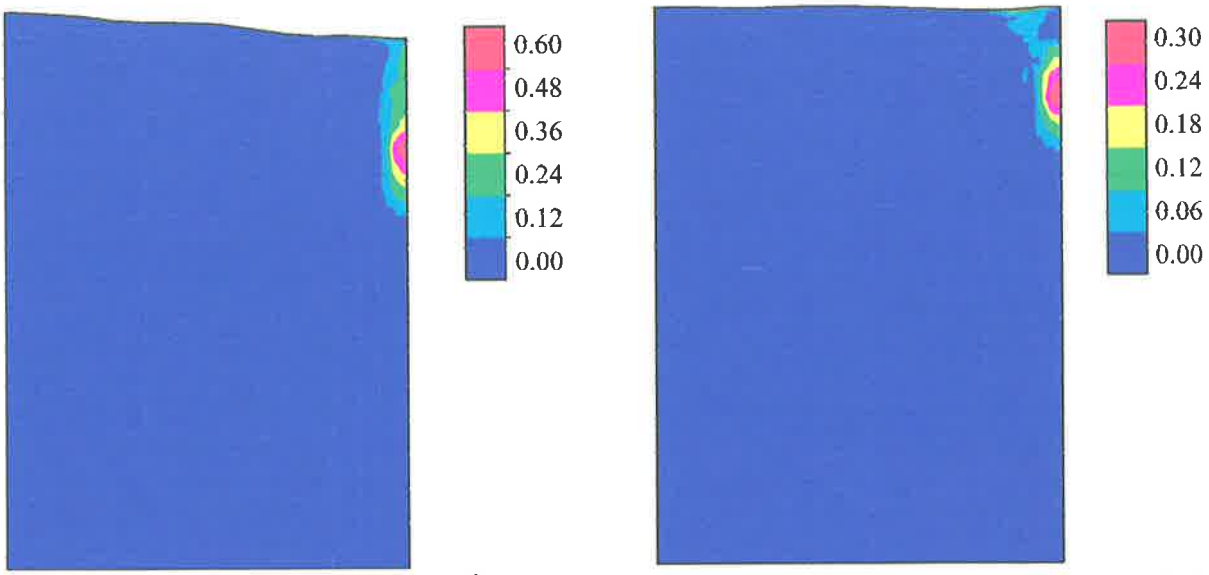

Figure 4.4 Speed contour plot (ms^{-1}) for droplet impact equivalent to I=150 Amps, high surface tension drop on left, low surface tension drop on right. Note the difference in the scales.

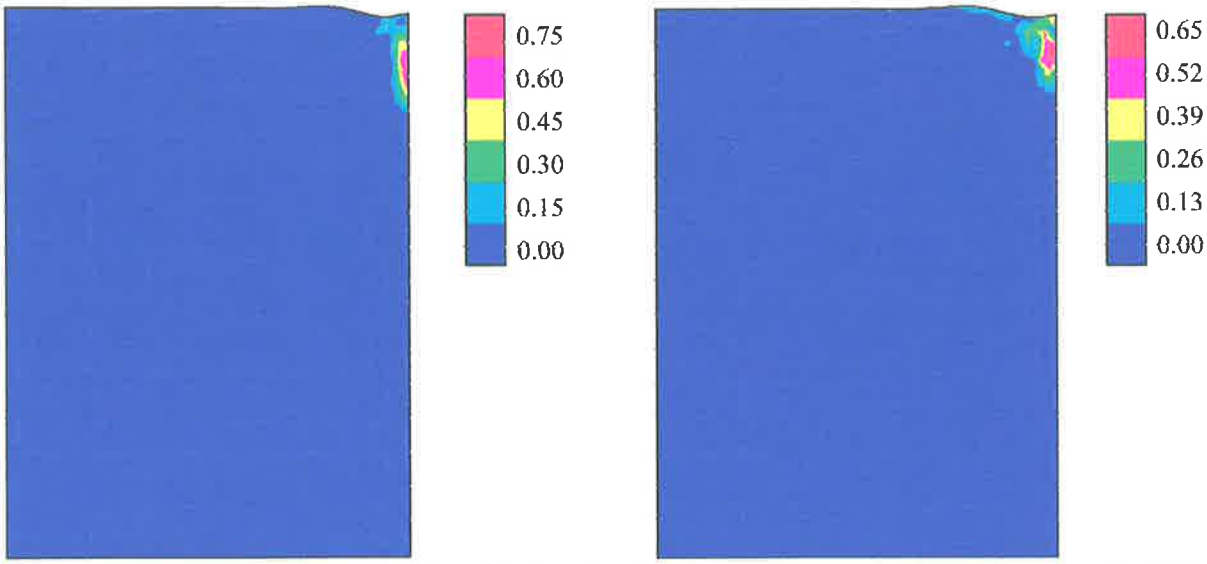

Figure 4.5 Speed contour plot (ms^{-1}) for droplet impact equivalent to I=200 Amps, high surface tension drop on left, low surface tension drop on right. Note: the difference in the scales.

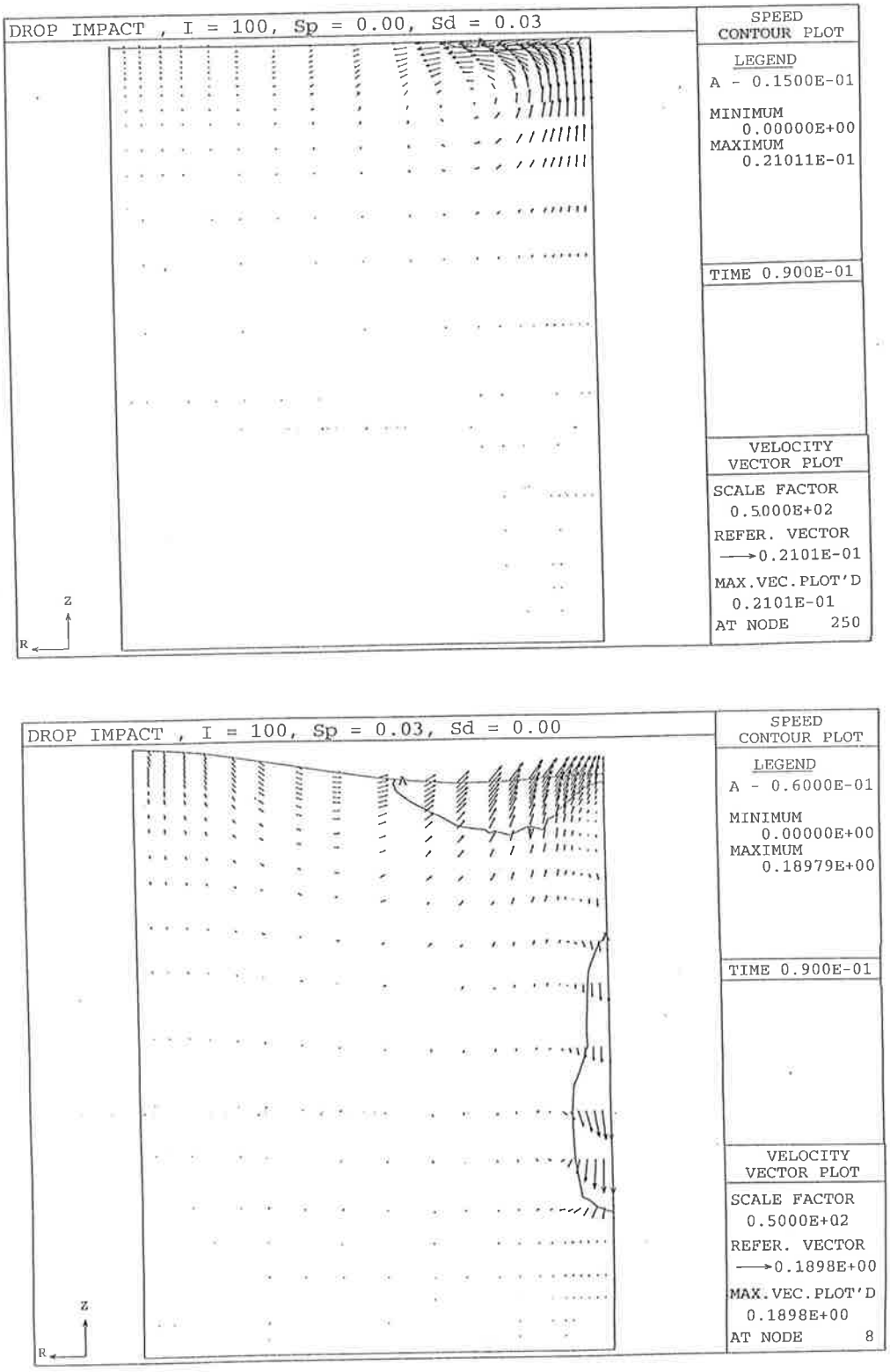

Figure 4.6 Vector and 0.06ms^{-1} speed contour plots I = 100 Amps, Low surface tension drop top, high surface tension drop bottom.

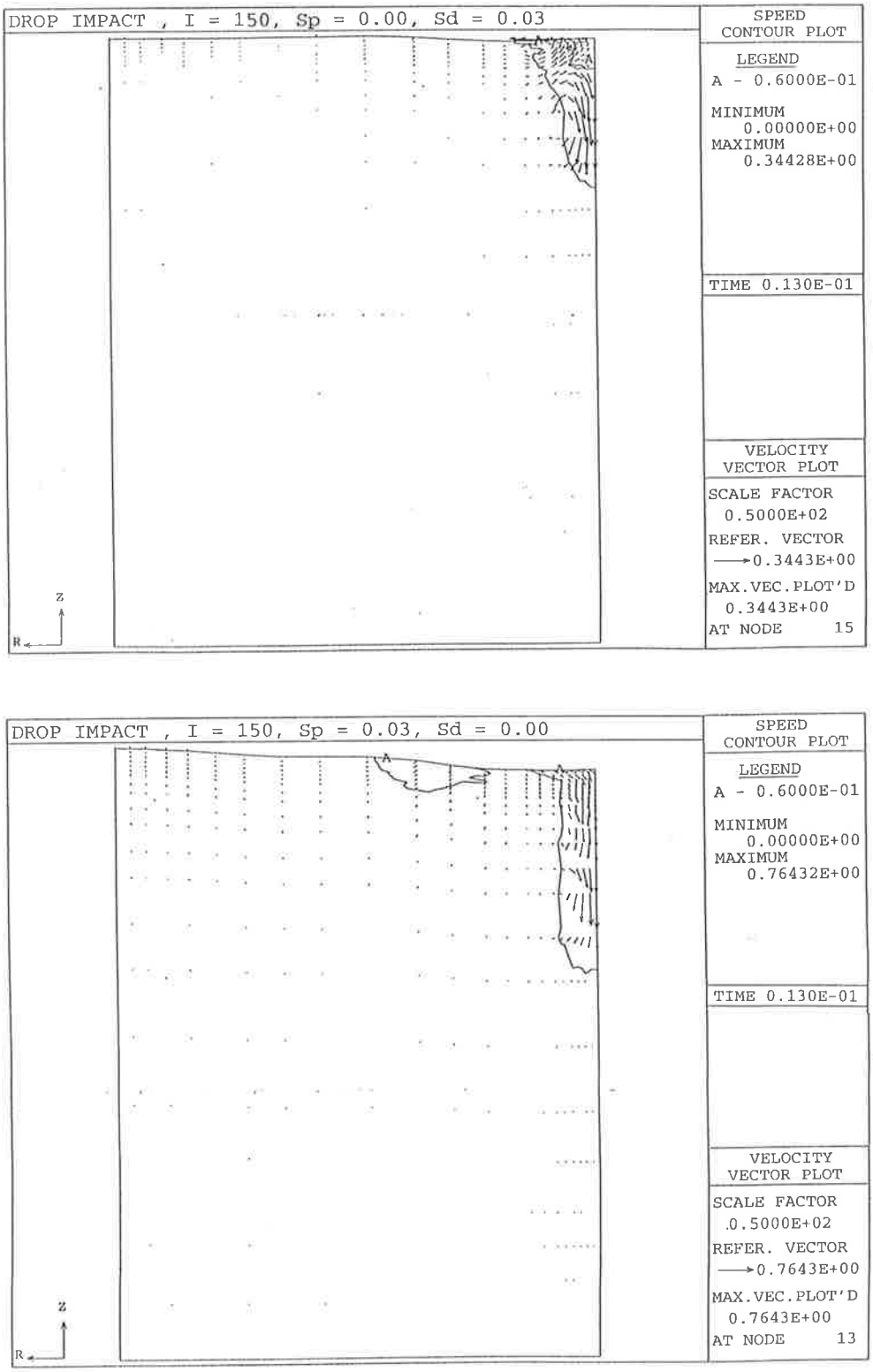

Figure 4.7 Vector and 0.06ms^{-1} speed contour plots I = 150 Amps, Low surface tension drop top, high surface tension drop bottom

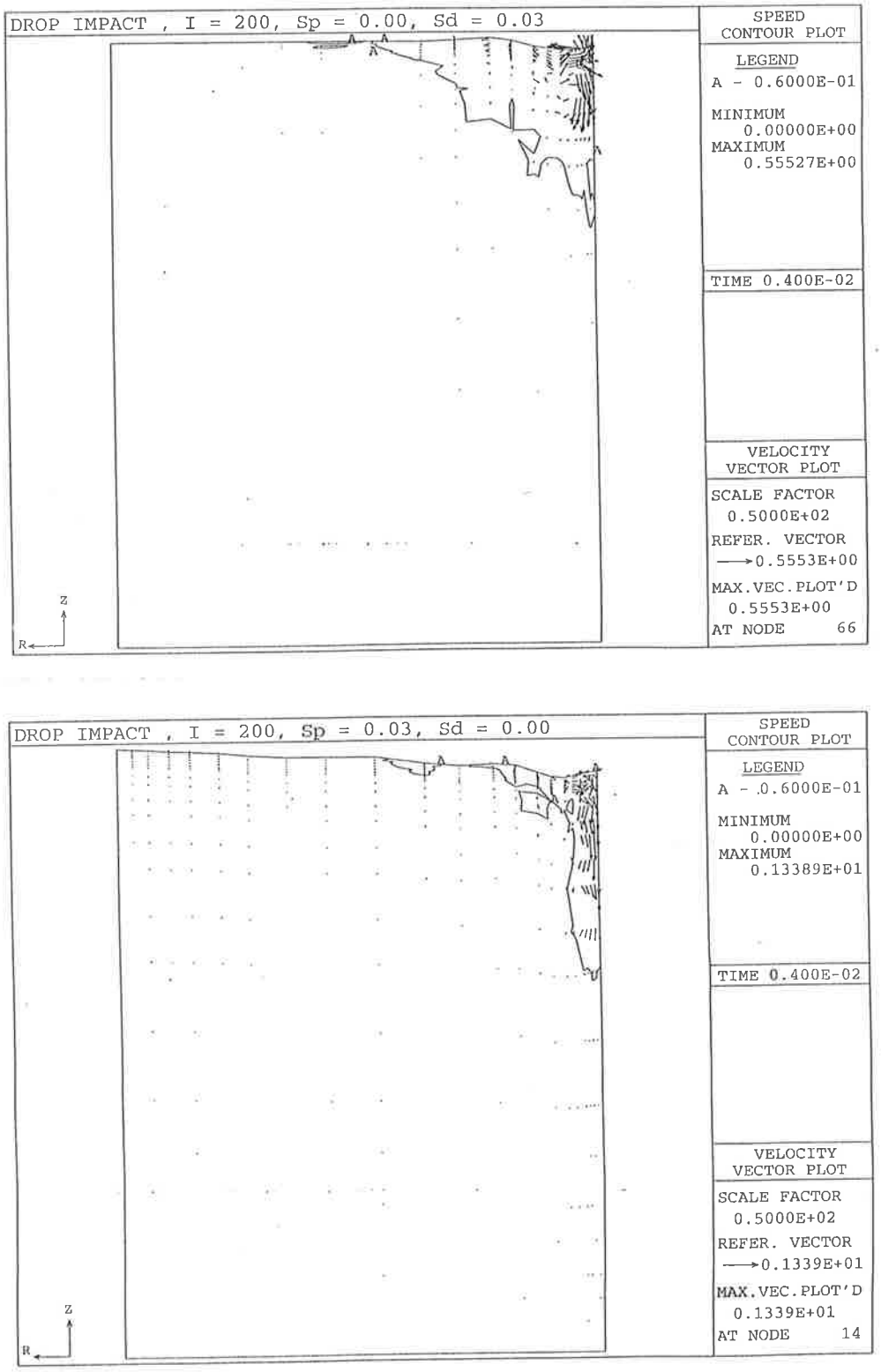

Figure 4.8 Vector and 0.06ms^{-1} Speed contour plots I = 200 Amps, Low surface tension drop top, high surface tension drop bottom

4.2.5 Discussion

At a welding current of 100 Amp (Figures 4.3 and 4.6), the variation of surface tension between the droplet and pool has a significant influence on the vector and speed contour plots. A droplet with a surface tension lower than the pool tends to produce a diffuse, radially outward flow, with the droplet essentially spreading across the surface of the pool. For a droplet with higher surface tension than the pool, the flow is reversed with the droplet producing a radially inward, penetrating flow pattern. These patterns are essentially similar to those observed and discussed by Choo *et al.* (1992) However at higher welding currents these effects are reduced (see Figures 4.5 and 4.8), with flow patterns becoming effectively the same for all surface tension conditions at a welding current of 200 Amp, (see Figure 4.8).

In order to discuss the differences between these results, some simple quantitative measure of the flow pattern was needed. The speed contours in Figures 4.3, 4.4 and 4.5, are a simple measure of the kinetic energy distribution within the pool, which is related to the energy available for weld pool formation and growth (Brown 1981). Changes in the shape of speed contours should therefore reflect the factors determining weld pool shape. The depth-to-width ratio is a common way of representing the weld pool shape, so using a similar approach to represent the flow pattern via the depth-to-width ratio of its speed contours seemed appropriate. Accordingly, the depth-to-width ratios of the 0.0625 m/sec speed contour were determined for all conditions, and these are presented relative to the standard case where the drop and the pool have the same surface tension in Figure 4.7. The 0.0625

m/s speed contour was chosen as it was the largest contour found on all plots, examination of other contour showed similar depth to width ratios. The 0.0625 m/s speed contours are plotted on the vector plots of Figures 4.4, 4.5 and 4.6.

For the conditions at a welding current of 100 Amp, the depth-to-width ratio for the relatively high surface tension drop was 400% greater than the ratio when the surface tension of the pool and drop were the same. For the same surface tension differences, this variation was only 3% at a welding current of 200 Amp. Similar results also apply in the case of a relatively low surface tension drop, the results are presented graphically and compared to experiment in Figure 4.10. The experimental validation is discussed in the following section.

4.2.5 Experimental Appraisal

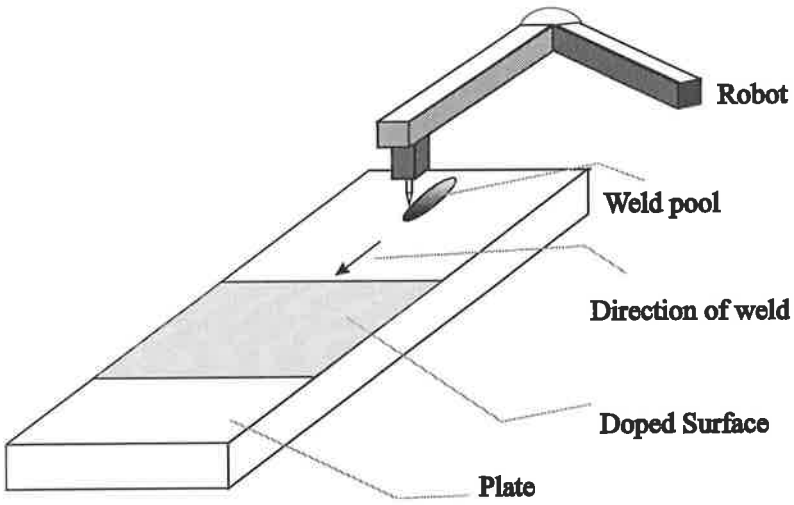

Figure 4.9 Experimental apparatus for the investigation of the influence of surface tension differences between the droplet and the pool.

Although it is expected that the effects predicted in the previous section may not be of the same magnitude as changes in weld pool shape, they are indicative of the expected trends. To test these trends an experimental appraisal of the influence of surface tension on weld pool geometry was carried out (Figure 4.9). The experiment consisted of producing a central bead-on-plate weld on a 10 mm thick mild-steel plate, under the conditions given in Table 4.3. One section of the plate was coated with FeS and one left in its 'natural' state. The plate surface was doped rather than the welding wire to avoid possible effects from the alteration of metal transfer behaviour. The resulting welds were then cross sectioned and the pool geometry determined for both the 'doped' and 'natural' regions. Chemical analysis of the weld metal in the 'doped' region showed a 0.02% increase in sulphur compared to the 'natural' region, giving an estimated 10% reduction in surface tension. Figure 4.10 includes the measured weld bead, depth-to-width ratio for the doped surface, expressed relative to that for the un-doped one at two welding current levels. The influence of the reduced surface tension is much greater at the low welding current, hence the experimental values show the same trend as the computed results.

Arc Current (amp)	Voltage (volts)	Speed (mm/min)
100.0	21.0	150.0
200.0	23.0	300.0

Table 4.3 Welding conditions for bead-on-plate tests.
Process: Direct current, electrode positive.
Shielding Gas: 82%Ar / 18% CO_2 at 15 litres/min.
Wire: C-Mn solid wire, 1.2 mm diameter.

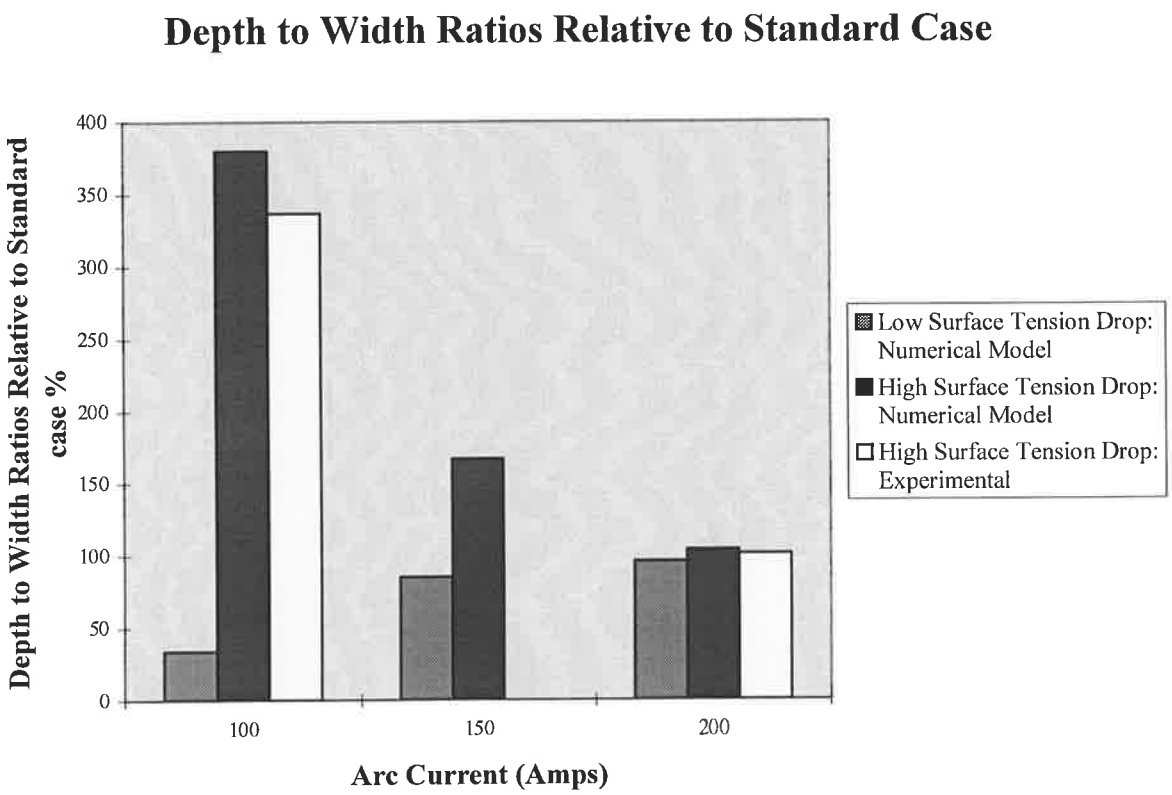

Figure 4.10 Comparison of numerical models to parametric experiment: Note that the standard case is the non-doped case, i.e. when there is no difference in surface tension between the drop and the pool.

It seems clear that the variation in the surface tension effect is due to the relative magnitude of the surface tension and momentum flux. At a welding current of 100 Amp the momentum of the droplet stream is significantly lower than that at 200 Amp, and it appears that as the welding current increases, the contribution from higher momentum forces completely swamps the contribution due to the concentration-gradient-driven surface tension flow. There are two main reasons for this: firstly, the impact velocity at low current is lower than that at a high one, and secondly, the frequency of impact at low current is significantly lower than that at high current. These changes indicate an increase in the total momentum transferred as the welding current is increased. A simple calculation shows that the momentum transfer in 1

second at 100 Amp is only 12% of that transferred at 200 Amp, whereas the surface tension effect would remain approximately the same. This relatively small contribution from surface-tension-driven flow at high welding current is also supported by the experimentally measured values of impact velocity ($\approx$1.5ms^{-1}) (Lancaster, 1981), and surface tension induced flow ($\approx$0.06-0.20 ms^{-1}) (Choo, 1992d).

4.2.7 Multiple Droplet Strikes

Based on the above results, it seems reasonable to ignore the influence of a difference in droplet and pool surface tension when modelling weld-pools for welding currents above about 150 Amps. This finding has implications for the type of computer model needed to represent a GMA weld pool. In any practical model of the weld pool the tracking of temperature is of crucial importance and the effect of temperature-dependent surface tension can be easily incorporated. However, to track the local concentration of surface active elements in the pool means solving another set of transport equations, making the computation significantly more expensive and numerically less stable.

It is recognised that surface active elements have a significant role in GTA weld pool flow where their presence can reverse the flow direction and radically change the weld profile. However, as there is no metal transfer in most GTA weld pool models, the surface tension is simply determined as a function of the overall pool composition and the local temperature. This situation will also hold in a GMA weld pool if the relative surface tensions between the droplet and the pool do not produce significant effects on the flow. In that case it would not be necessary to track the local variation of composition within the pool, no matter what the

difference in composition between the pool and drop and the task of modelling a GMA weld pool would be simplified. However the most important simplification would come from avoiding the need to treat metal transfer as individual droplets. Due to the dominance of the droplet momentum at welding currents greater than 150 Amps, one option is to represent the transferred droplets as a heat and momentum source. For this approach to be valid, a model treating them as such should predict the same flow pattern as one treating them as individual droplets. Two such models were developed and used to predict the weld pool flow pattern at a quasi-steady state. A weld at a current of 200 Amp was modelled, providing conditions under which the relative droplet/pool surface tension effects should be negligible.

The predicted flow profiles and velocities are similar for both models. Figure 4.11 compares the predicted streamline contour plots at an effective steady state. However, there are significant differences in computational efficiency. The momentum source model does not track local compositional variations, and used surface tension values based on average pool composition and local temperature. Since it does not treat individual droplets it can use significantly larger time steps. The momentum source model took approximately 10 hours of CPU time on a Sun workstation while the individual droplet model took 240 hours. This indicates that by treating transferred droplets as a heat and momentum source, significant savings in computational time and cost can be made, without sacrificing accuracy.

Whilst running these models for a longer periods of time (approx 1.5 second of real time in the momentum source case and 0.2 seconds in the individual droplet case), it was found that the pool had a natural frequency of oscillation. This natural frequency is related to the weld

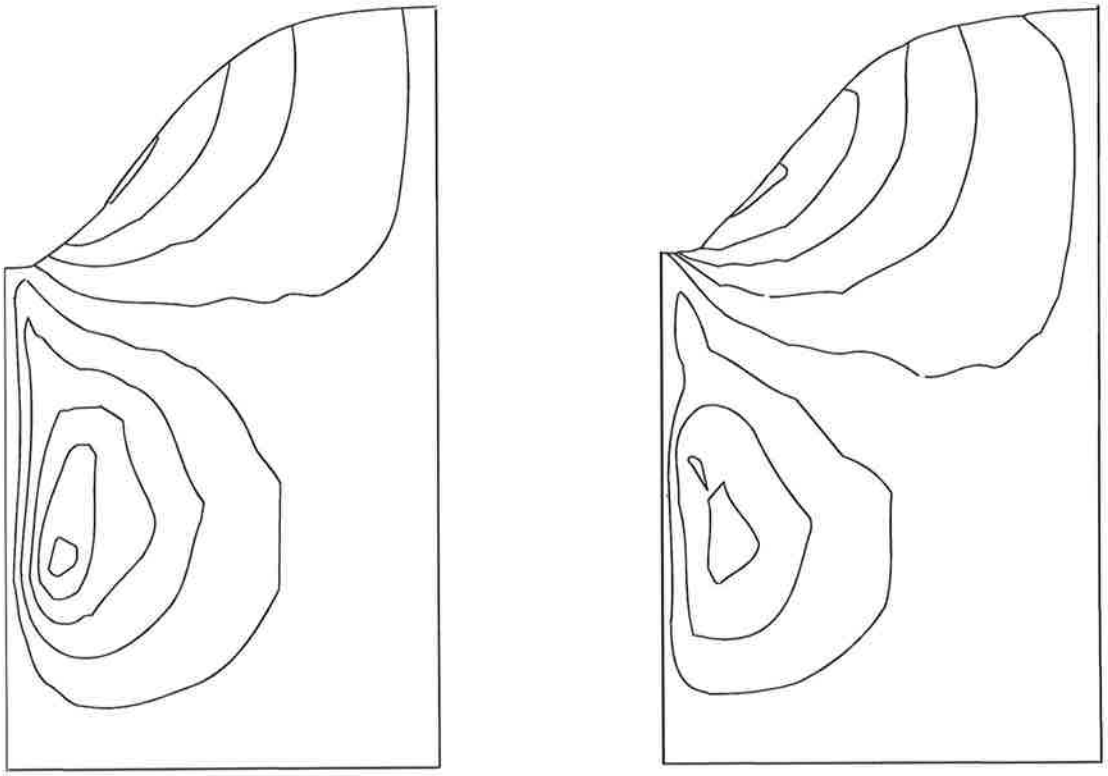

Momentum source term
10 hours CPU time.

Individual droplets
240 hours CPU time.

Figure 4.11 Comparison of streamline contours for individual droplet and momentum source models.

pool size and appears to be caused by the interaction of gravity and the mass flow into the pool. The predicted value is also of the same value as the frequency ripples which appear on the surface of the cooled weld bead, indicating that they might be formed by this behaviour. In GTAW the natural frequency can be used to calculate the weld pool size and may therefore be useful for the development of an active welding controller, (Xiao 1990); although in GTAW it is necessary to artificially disturb the pool in order to determine the natural frequency. While this result is interesting and potentially rewarding it is outside of the scope of this research at the moment, but could be investigated further at a later date.

4.2.8 Conclusions

A computational model of the interaction between a droplet and a liquid pool, has demonstrated that the flow induced by the relative surface tensions of the droplet and the pool is small compared to the flow produced by droplet impact. This result has been supported by experimental investigations. This study demonstrated that with direct-current GMA weld pools and welding currents of 150-200 Amp, it is not necessary to model the local variation in surface active elements. This reduces the number of transport equations that need to be solved, and decreases the complexity and running times. In addition it is shown that for such cases it is possible to model the droplet transfer as a heat and momentum source, significantly simplifying the task and increasing the efficiency of modelling flow within a GMA weld pool.

Having established the relative importance of surface tension gradient forces in relation to droplet inertia forces, electro-magnetic forces will be investigated in the following section.

4.3 ELECTRO-MAGNETIC FORCES

4.3.1 Introduction

Previous investigators such as McLay & Carey (1989) have shown that the electromagnetic forces are significant in driving flow in a GTA weld pool. The order of magnitude analysis presented in Chapter 2, indicates that electro-magnetic forces are likely to be the second most important force in GMAW pool flow although approximately an order of magnitude less than the droplet impact forces. Obviously further investigation is required regarding the importance of electro-magnetic forces in weld pool flow, as well as the most accurate method of modelling it.

The first consideration is how to include electro-magnetic forces in a computationally efficient way. Traditionally, calculating electromagnetic body forces has required the numerical solution of Maxwells equations. This requires the solution of several more transport equations to define the electric and magnetic fields. However in the case of modelling weld pool flow, where there are already seven or eight unknowns (u, v, w, p, t, K, ε, sp) at each node, the addition of more (J_x, J_y, J_z, B_x, B_y, B_z) makes the problem more complex and numerically unstable. Furthermore it requires dramatically more memory, reducing the number of computational nodes that can be modelled and hence the complexity of problems that can be tackled. Therefore it would be beneficial if the electro-magnetic force could be included in a more computationally effective manner.

Kou & Wang (1986) have developed an analytical solution for the distribution of the magnetic field in a plate with a Gaussian current distribution acting on a flat surface. Kim & Na (1992) used this solution in the modelling of GTA weld pool flows and showed it to be a valid approach. Kim & Na (1994) also used this approach in modelling GMAW and have demonstrated its validity for surface deformations of less than 3-4mm. The derivation of Kou and Wang's analytical solution is outlined below.

Since the welding speed is very low in comparison to the speed of electrical conduction, the arc can be considered quasi static. Therefore using the steady state version of Maxwells equations with the Magneto-Hydro-Dynamics (MHD) approximation (Szekely, 1979 and Hughes & Young 1966) the following equations define the electro-magnetic field in the work piece:

$$\nabla \times \boldsymbol{H} = \boldsymbol{J} \tag{4.1}$$

$$\nabla \times \boldsymbol{E} = 0 \tag{4.2}$$

$$\nabla \cdot \boldsymbol{J} = 0 \tag{4.3}$$

$$\nabla \cdot \boldsymbol{B} = 0 \tag{4.4}$$

where $\boldsymbol{E}$ is the electric field vector and $\boldsymbol{H}$ the magnetic field vector. Furthermore:

$$\boldsymbol{J} = \sigma_e \boldsymbol{E} \tag{4.5}$$

$$\boldsymbol{B} = \mu_m \boldsymbol{H} \tag{4.6}$$

where σ_e and μ_m are the electrical conductivity and magnetic permeability respectively. The above equations are good approximations when the current induced by the convective motion of the liquid metal is not very high (Szekely, 1979) and therefore it is applicable for weld pool modelling (Kou & Wang, 1986). The current distribution at the pool surface is assumed to be Gaussian following Oreper *et al.* (1983), and therefore the current distribution on the pool surface is given by:

$$J_z = \frac{3I}{\pi b^2} e^{\left(\frac{-3r^2}{b^2}\right)} \quad at\ z = 0 \tag{4.7}$$

where J_z is the Z component of $\boldsymbol{J}$ at radius r, I is the welding current, b is the effective radius of the current distribution and r is the radius. Equation 4.7 gives the boundary condition for $\boldsymbol{J}$ on the top surface. The bottom surface can be assumed to be electrically insulated by a ceramic backing or air gap, i.e.

$$J_z = 0 \quad At\ z = z_t \tag{4.8}$$

where z_t is the work piece thickness. From equations 4.2 to 4.8 the electro-magnetic force can then be expressed as follows:

$$\boldsymbol{J} \times \boldsymbol{B} = B_\theta (J_r \boldsymbol{z} - J_z \boldsymbol{r}) \tag{4.9}$$

$$J_z = \frac{1}{2\pi}\int_0^{\infty}\lambda J_0(\lambda r)\, e^{\left(\frac{-\lambda^2 b^2}{12}\right)}\, \frac{\sinh\lambda(z_t - z)}{\sinh\lambda z_t}\, d\lambda \qquad (4.10)$$

$$J_r = \frac{1}{2\pi}\int_0^{\infty}\lambda J_1(\lambda r)\, e^{\left(\frac{-\lambda^2 b^2}{12}\right)}\, \frac{\cosh\lambda(z_t - z)}{\sinh\lambda z_t}\, d\lambda \qquad (4.11)$$

$$B_\theta = \frac{\mu_m I}{2\pi}\int_0^{\infty} J_1(\lambda r)\, e^{\left(\frac{-\lambda^2 b^2}{12}\right)}\, \frac{\sinh\lambda(z_t - z)}{\sinh\lambda z_t}\, d\lambda \qquad (4.12)$$

J_r is the radial component of $\boldsymbol{J}$ and B_θ is the θ component of $\boldsymbol{B}$. J_0 and J_1 are the Bessel functions of zero and first order respectively.

4.3.2 Computational Model

The situation modelled to investigate electro-magnetic forces was an axi-symmetric model of a stationary GMAW pool. This was chosen because of its computational efficiency even though stationary GMAW is not generally carried out in practice. Again it is expected that the driving forces in a stationary pool will still have the same relative magnitudes as those in a moving one. Therefore the relative importance of electromagnetic forces to inertia forces can be determined by comparing the results from models including electro-magnetic forces, to those from models which don't include electro-magnetic forces within the weld pool. The model is fundamentally different to that used in the previous section (which modelled an effectively infinite weld pool) and therefore requires very different boundary and initial conditions. This was necessary so as to enable verification of the previous model by the previously published work of Choo *et al.* (1992). In this present case, there is no

published work against which the model can be verified, so a more realistic situation was modelled. This will enable direct measurement of change in penetration, rather than measurement of the change in speed contours.

As the model is similar to that presented in the previous section the inherent details of the model are the same except for the following points:

(1) The size, impact velocity and transfer frequency of weld droplets has been taken from previously published experimental work (Lancaster, 1984) and these are detailed in Table 4.2. The total momentum of the droplet stream is accounted for by including a momentum source term equivalent to the momentum flux transferred. This momentum source is applied to a semi-spherical volume with a radius equivalent to that of the impacting droplet. This volume is located with its upper surface flush with the top surface of the pool and its centre on the axis of symmetry.

(2) The top surface of the pool was not free to deform and was assumed to be horizontal. Whilst this is not accurate at higher arc current and would be unlikely to allow accurate modelling of weld pool shape, it is satisfactory for investigating the relative magnitude of electro-magnetic and inertia forces. Free slip velocity boundary conditions i.e. free tangential velocity and zero normal velocity, were assumed on the top surface of the pool.

(3) Along the melt interface of the pool 'no-slip' conditions for a viscous fluid were assumed.

(4) Previous work in modelling flow in GTA weld pools (Zacharia, April 1992) has

shown that it is important to consider the effect of temperature-dependent, thermo-physical properties. A fundamental difficulty in any calculation of the flow within the weld pool is the lack of dynamic fluid physical properties for molten steel at high temperatures. In the present model the material properties are taken from Zacharia *et al.* (1991). The solution was performed in non-dimensional form so as to enable easy modification and encourage numerical stability. Making the problem non-dimensional before solving numerically encourages stability, because the large differences in the magnitude of terms are reduced, thus minimising numerical errors. This is particularly true in problems involving melting and solidification. The latent heat of fusion is incorporated by calculating the specific heat capacity from the slope of the enthalpy temperature curve. As this does not involve a step in the specific heat temperature curve, this also improves the stability and accuracy of the solution.

The material properties were non-dimensionalised using the procedure detailed in Chapter 3, resulting in the scales, given in Table 4.4.

Physical Quantity	Dimensional Input	Dimensionless Input
Density	ρ	$R_e = \frac{\rho V L}{\mu}$
Viscosity	μ	1
Specific Heat Capacity	c_p	$P_r = \frac{\mu c_{po}}{k_o}$
Conductivity	k	1
Dissipation	1	$B_r = \frac{\mu U^2}{k_o \Delta T}$

Table 4.4 Non-dimensional material properties.

The variation in the material properties with temperature is accounted for by defining the above non-dimensional parameters at a fixed reference temperature , and then defining the material property temperature curve as the appropriate dimensionless parameter multiplied by its respective dimensionless property at the temperature in question. So, the material property temperature curve for the specific heat capacity is entered as $Pr.c_p^*$ and conductivity is entered as $1.k^*$.

5) Along the top surface of the pool there is a Gaussian heat and current distribution of the form of equation 4.7. The electro-magnetic force is then calculated using equations 4.9 to 4.12.

6) Within the droplet the temperature is constrained to 2400°C in line with the experimental work from Jelmorinio *et al.* (1977).

7) Convective losses from all external surfaces are included and symmetry about the axis is assumed.

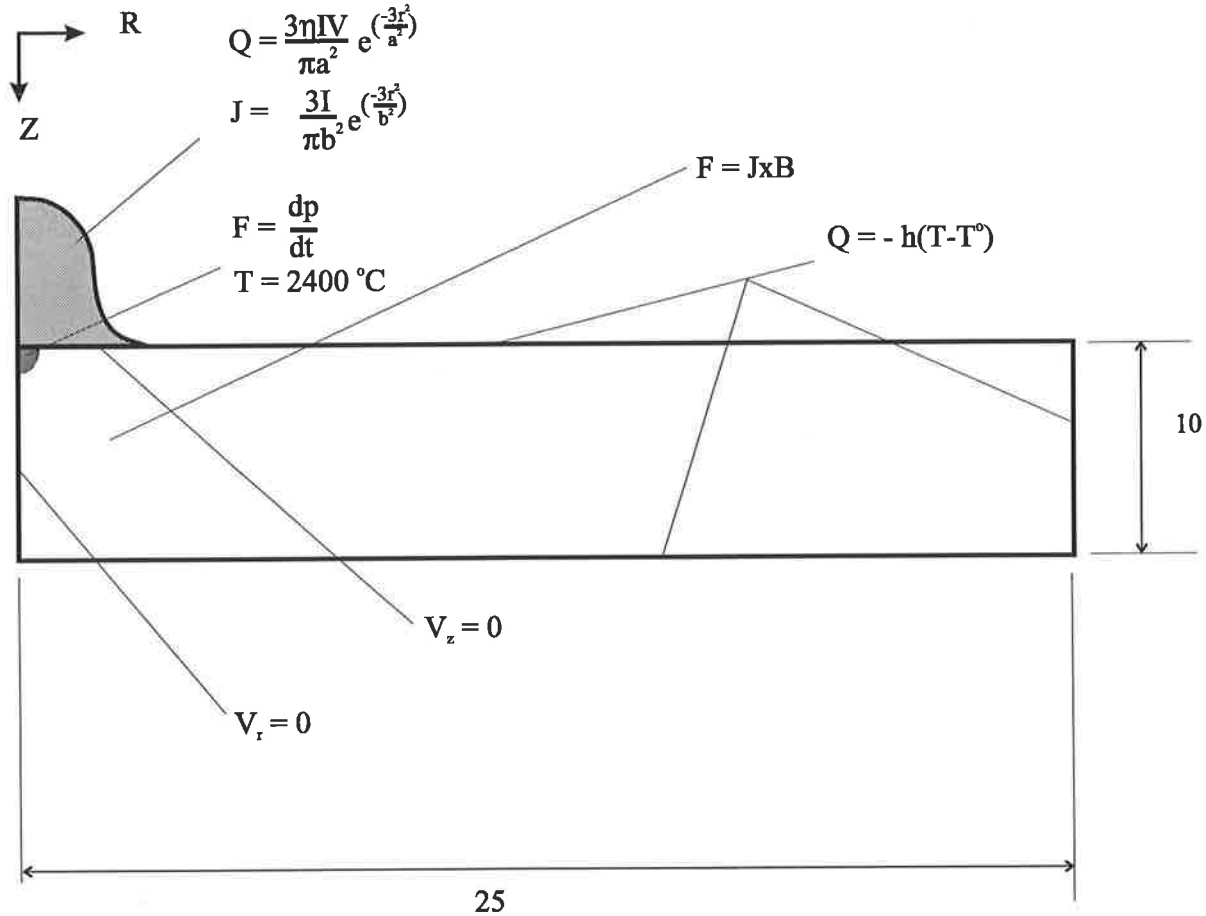

Figure 4.12 Boundary conditions on axi-symmetric electro-magnetic force model.

The boundary conditions for the model are shown schematically in Figure 4.12, and the computational mesh in Figure 4.13.

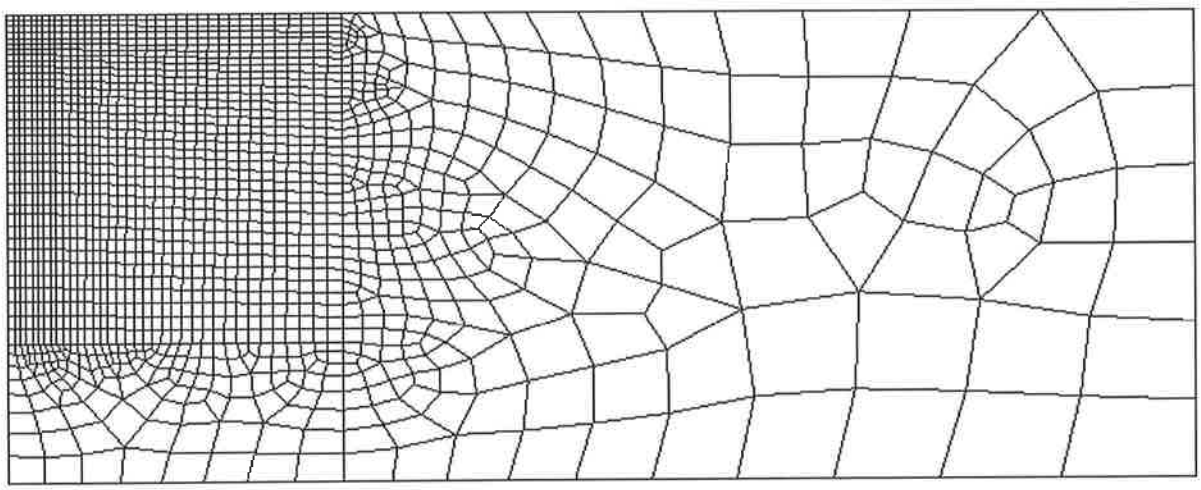

Figure 4.13 Computational mesh for electro-magnetic force (EMF) and buoyancy models.

This model has used linear elements for the velocities and temperature, with piece-wise constant pressure and a Newton-Raphson non linear equation solver. The mesh was examined for suitability using simple mesh refinement tests.

4.3.3 Results and Discussion

The predicted pool shapes after 1.2 seconds welding time are compared in Figure 4.14. This figure shows that the electro-magnetic forces do have an effect, particularly at higher currents. The depth to width ratio is increased by approximately 10% at 200 Amps and 4% at 100 Amps. A typical flow pattern with and without the electro-magnetic force is shown in Figure 4.13 and 4.14. The effect on weld pool depth to width ratio is detailed in Figure 4.15.

Figure 4.14 Weld pool temperature profiles for I = 200 Amps predicted with and without electro-magnetic forces. Note: Normalised temperature scale, melting point equivalent to 0.37.

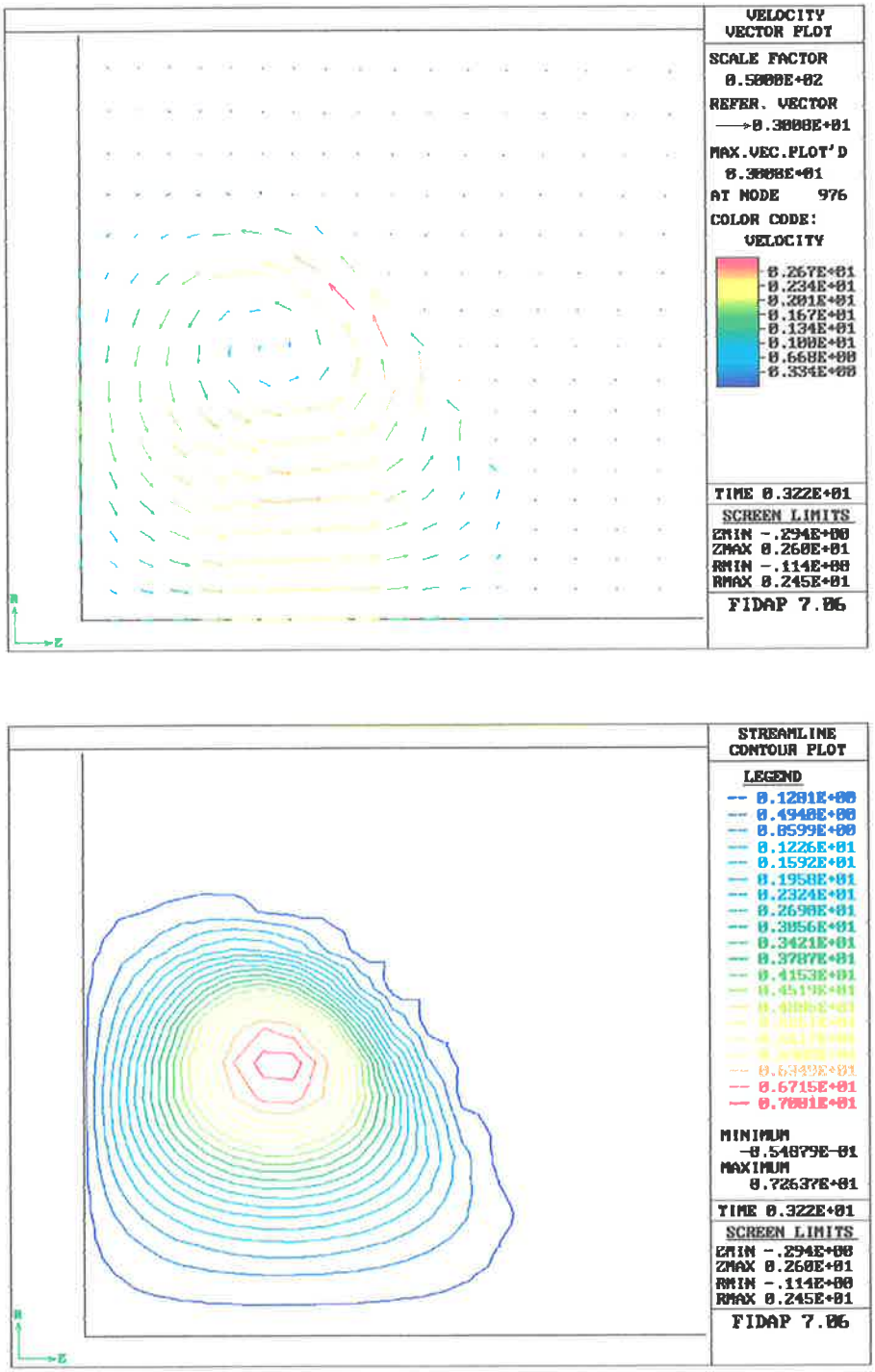

Figure 4.15 Vector velocity and streamline contour plots for I =200 Amps, including EMF.

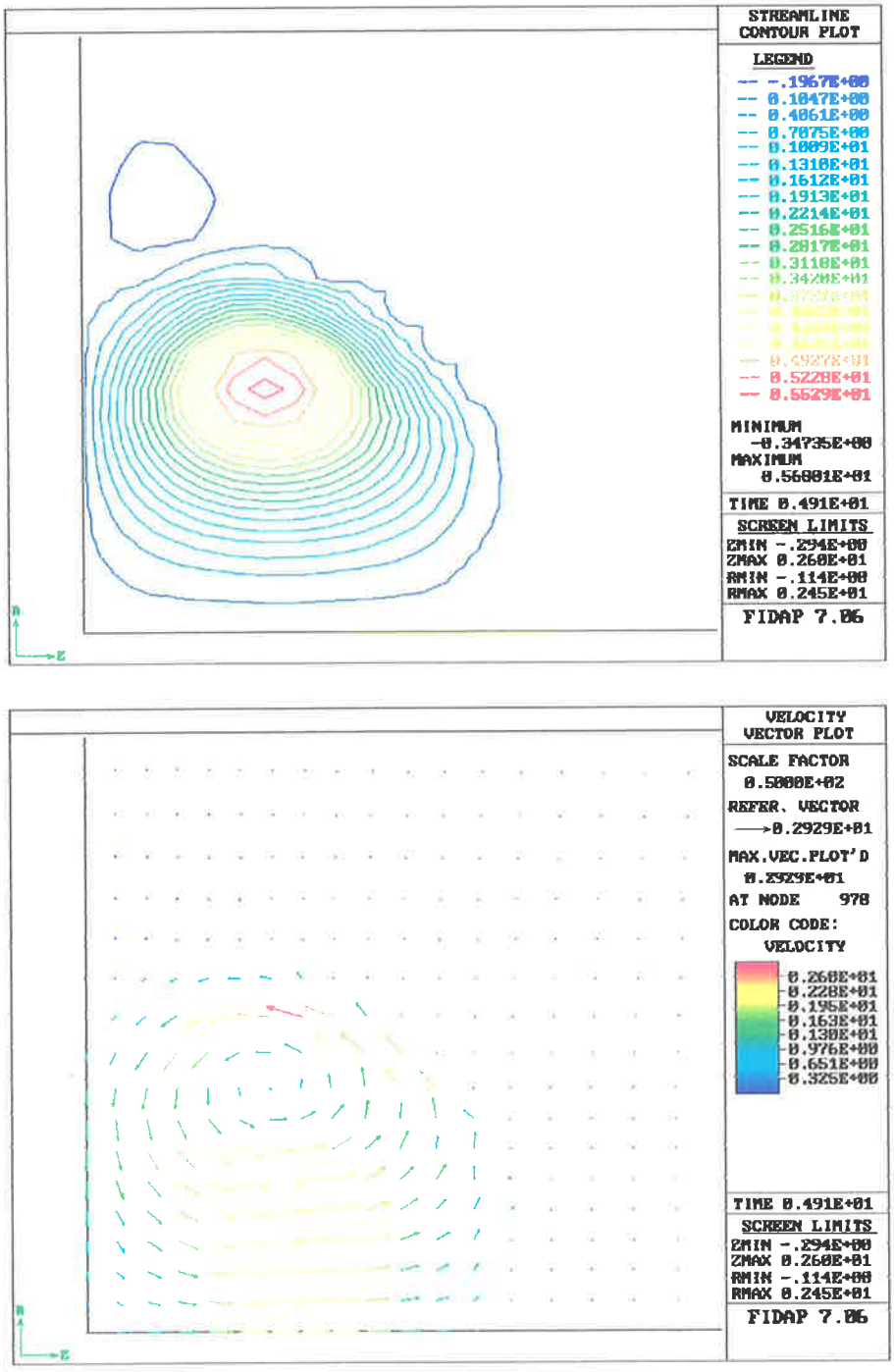

Figure 4.16 Vector velocity and streamline contour plots for I =200 Amps, excluding EMF.

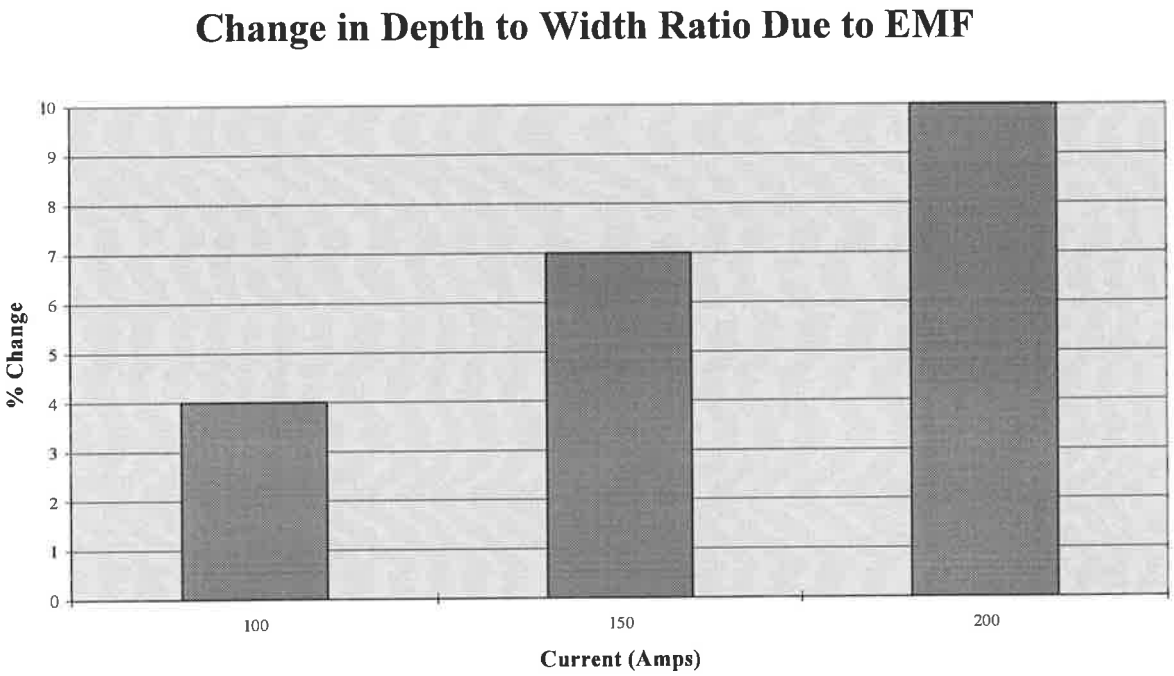

Figure 4.17 Change in depth to width ratio due to inclusion of EMF

4.4.4 Conclusions

It is apparent that the electromagnetic force can affect the weld pool shape particularly at high currents. However the effect is relatively small, being only 4% at 100 Amps and 10% at 200 Amps. Therefore one can still conclude that for spray transfer, droplet impact forces are by far the most important forces and the weld pool shape is effectively controlled by the total droplet momentum.

4.5 BUOYANCY FORCES

4.5.1 Introduction

Investigations of GTA weld pools by McLay & Carey (1989) and Ramanan & Korpela (1990), have shown that buoyancy forces are insignificant in driving GTA weld pool flow. The normalised scale analysis of Chapter 1 has also implied that the buoyancy forces are several orders of magnitude less than inertia forces. Therefore it is likely that buoyancy forces can be ignored when modelling GMA weld pool flows. To verify this assumption, weld pool profiles predicted by computational models incorporating buoyancy forces have been compared to those without buoyancy forces. 225 Amp welding conditions were the only ones modelled, as dimensional analysis had shown that buoyancy forces are at a maximum at high currents. If buoyancy forces are negligible at high currents it is safe to assume that they are negligible at low current.

4.5.2 Computational Model

The computational model used in this section is essentially the same as the one used in section 4.4 with the exclusion of electro-magnetic forces, and the inclusion of buoyancy forces. Buoyancy forces have been included using the Boussinesq approximation. In this approximation the variable density is included only in the gravity body force term. The details of the boundary conditions are shown in Figure 4.18. The computational mesh is the same as that used in the previous section and is shown in Figure 4.13.

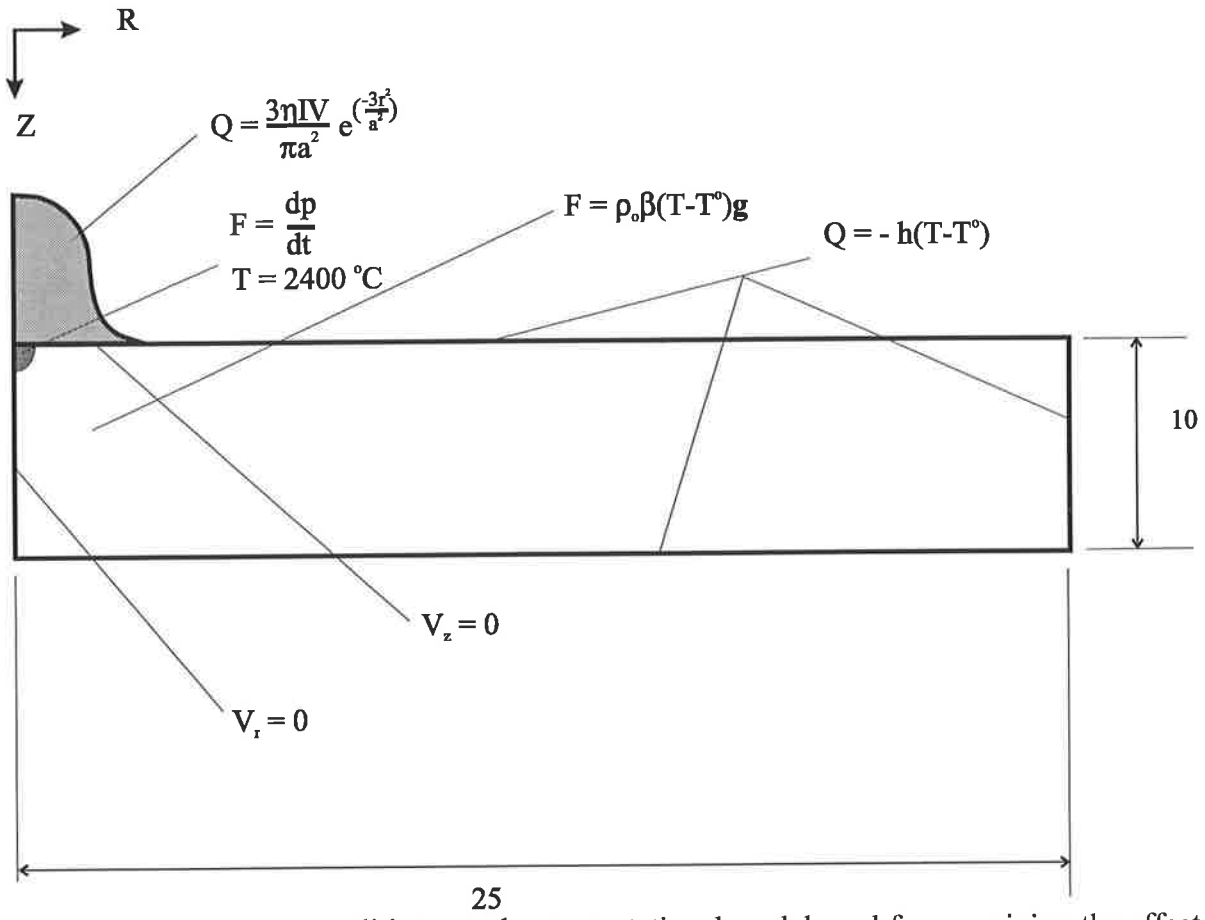

Figure 4.18 Boundary conditions on the computational model used for examining the effect of buoyancy.

This model has used linear elements for the velocities and temperature, with piece-wise constant pressure and a Newton-Raphson solver. As the mesh is the same as that used in the previous section no mesh refinement tests were required.

4.5.3 Results

Figure 4.19 shows the predicted weld pool shape with and without the effect of buoyancy.As can be seen there is very little difference in the predicted weld pool shapes. The depth to width ratio of the predicted pool shape without buoyancy forces is essentially the same as

that predicted without incorporating the buoyancy force. It is apparent that the inclusion of this term has no significant effect on the solution.

Figure 4.19 Temperature profiles for I=200 Amps, predicted by models with and without Boussinesq buoyancy forces. Note: Normalised temperature scale, melting point equivalent to 0.37

4.5.4 Conclusions

In agreement with the literature and scale analysis, the computational model has predicted that buoyancy forces are not important when modelling flow within a GMAW pool. This means that the buoyancy term can be eliminated from the governing equations and therefore provide a more robust solution.

4.6 INFLUENCE OF THE ARC PLASMA

4.6.1 Introduction

Choo & Szekely (1991) have shown that for GTAW, that the arc force is significant when compared to surface tension forces for currents of greater than 300 Amps. Therefore the effect of plasma forces in GMAW should also be investigated. Although in GMAW the plasma forces are likely to be smaller than in GTAW, because the ratio of the size of the cathode spot to the size of the anode spot is smaller. This means that the electro-magnetic force driving the flow within the plasma will be less, and the force on the pool surface due to the impinging plasma stream will be less. To verify this assumption an experimental analysis has been performed by Jarvis (1995).

4.6.2 Experiment

The experiment consisted of measuring the total force on the plate due to the welding process. Pressure forces were measured for GTAW and GMAW under similar welding conditions and the measured forces were compared. The force measured in GMAW was corrected to account for the effect of metal deposition and droplet impact forces. This was done by subtracting the gravitational force due to the additional mass, and the inertia force due to droplet impact from the total force measured.

The total force was measured by a digital balance which generated a counteracting force to maintain the position of the work piece. The balance was shielded from the effects of the welding current by a wooden platform, on top of which was a steel plate for electrical

connection. Care was taken to minimise any earthing effects by making electrical connection to the work piece through a pool of gallium. The scales were connected to a data logger and the total force recorded during welding. As the weld was carried out the total force increased due to the metal deposition, and when the arc was extinguished the force dropped back to a base value because of the removal of the arc and droplet force. The difference between this base value and the value immediately prior to the termination of the weld, is obviously the force due to arc and droplets. Droplet forces were calculated from the known droplet transfer rates, and subtracted from this total force to give the arc force. The procedure for GTAW was the same except that no correction was needed for metal deposition or droplet transfer rates. Welds were performed on C-Mn steel, and in the case of GTAW pure argon shielding gas and a 3.2mm electrode were used. In GMAW a 1.2mm steel filler wire and 72% Argon /18% CO_2 shielding gas were used.

4.6.3 Results and Discussion

The pressure measurements are compared graphically in Figure 4.20. As can be seen in Figure 4.20 the arc pressure forces in GMAW are lower for all currents than those in GTAW. The final GMAW reading appears to be inconsistent with all other readings including those taken at the same time for pulsed GMAW. The reason for this is not known, but may be due to incorrect compensation for the weight of filler metal addition. This could occur if the arc did not extinguish immediately.

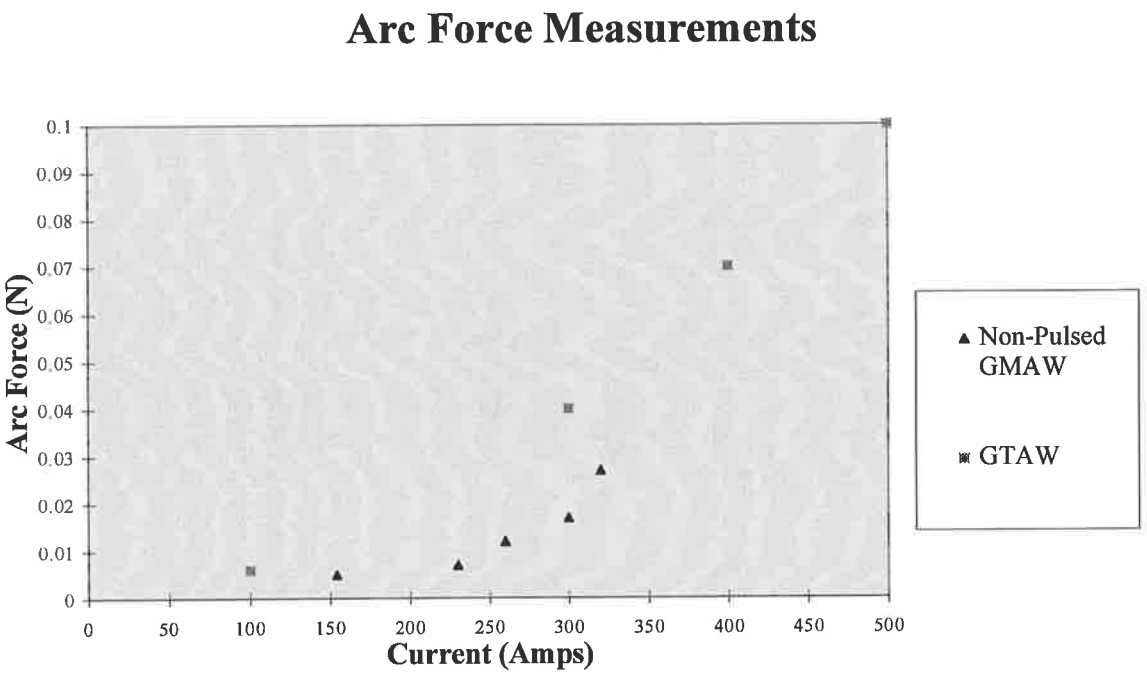

Figure 4.20 Comparison of GTAW and GMAW arc force measurements.

4.6.4 Conclusions

Choo & Szekely (1991) have shown that arc forces can be safely ignored when modelling GTAW pool flow at currents of less 300 Amps. The experimental work detailed above indicates that arc forces are smaller in GMAW than in GTAW. Therefore, it is safe to assume that forces due to the impinging arc plasma can be ignored when modelling GMAW pool flow at currents of less than 300 Amps.

Although the plasma pressure forces do not influence the flow directly, the interface between the arc and the pool does affect our ability to predict the heat flow into the pool. Models of the weld pool flow show a marked dependency on the form of the heat source assumed for the arc. In the literature to date, most models have assumed that the arc energy has a

Gaussian distribution determined only by the input current and voltage and some empirical tuning factor. It has been suggested in the literature (Mundra *et al.* 1992) that this approach is not satisfactory. This assumption is reasonable at low currents where the weld pool is flat, but at higher currents where the weld pool is deformed this model does not account for the effect of the deformation on the heat transfer to the pool surface. Work by Choo *et al.* (1992) has shown that there is a significant effect on the form of the heat transfer to the pool. Given the sensitivity of the weld pool shape to this assumed heat source, it may be necessary to develop a better heat source for the arc plasma for situations that involve significant pool deformation. However this is beyond the scope of this investigation.

4.7 CONCLUSIONS

Axi-symmetric numerical models have been developed and used to compare the effect of surface tension forces, electro-magnetic forces and buoyancy forces with droplet inertia forces. The results of these numerical models indicate that:

1) At very low currents both the numerical models and experiment have indicated that surface tension forces may have an effect on the flow within the pool, possibly influencing the depth of penetration. However, at currents above approximately 150 Amps, surface tension effects are negligible compared to the effects due to droplet impact.

2) In agreement with the scale analysis of Chapter 2, the axi-symmetric numerical models developed in this chapter indicate that at currents over approximately 150 Amps, the electro-magnetic force is the only force of any significance when compared to the droplet impact forces. However even the electro-magnetic effects are relatively small when compared to the momentum of the droplet.

3) Given that the droplet momentum is the dominant force within the weld pool (and that surface tension effects due to individual droplets is insignificant) the effect of the individual droplets may be ignored and the droplet treated as a momentum source term. This has a significant effect on the form of computational model that may be used, as it enables the use of much larger time steps in the case of transient solutions

and allows the use of quasi steady state assumptions.

4) Experimental results have confirmed the results within the literature, i.e. that plasma pressure forces can be safely ignored when modelling weld pool flow.

Therefore a full model of the convection within the weld pool must include droplet inertia forces if the flow is to be accurately modelled. However it appears that the individual droplets do have a very limited effect, and may be successfully modelled as a total momentum source. Electro-magnetic effects should also be included (especially at high currents), however given the relatively small effect it is probable that they can be modelled as an effective force rather than solve Maxwells equations. All of these models have used the turbulence model of Choo *et al.* (1992). The effect of turbulence within the pool and the best way to include it in the numerical models must be investigated. This is the focus of the next chapter. Once the turbulence can be effectively modelled, full models of weld pool convection can be developed (including droplet inertia and electromagnetic forces as demonstrated in the last two chapters).

Chapter 5

DROPLET IMPACT AND TURBULENCE

5.1 INTRODUCTION

In the previous chapters the relative magnitudes of the forces responsible for driving the flow within the weld pool were examined in order to verify the scale analysis of Chapter 2. This analysis treated the droplet as a slug of fluid, and has been verified by comparing predictions with the experimental results of Choo *et al.* (1992). However as the droplet impact velocity is increased, this approximation is complicated by the generation of turbulence. This turbulence can have a significant effect on the flow and heat transfer mechanisms within the pool, therefore there is a need to incorporate turbulence modelling in the weld pool models. The generation of turbulence is a complex phenomena which is influenced by the droplet impacting on the surface of the pool. Droplet surface interactions and their influence on the turbulence within the weld pool is analysed in this Chapter and the most suitable methods available to incorporate these effects into the numerical models are investigated.

5.2 DROPLET IMPACT

5.2.1 Introduction

When a liquid drop impinges on a free liquid surface, two types of behaviour can occur. In the first case the drop may deform the pool surface producing a cavity in the pool, which then fills rapidly producing a rebound column (Fig 5.1.a). Alternatively the drop may enter into the pool with negligible splashing and produce a vortex ring within the pool, which then travels down through the pool, often with a considerably larger velocity than the original drop (Fig 5.1.b).

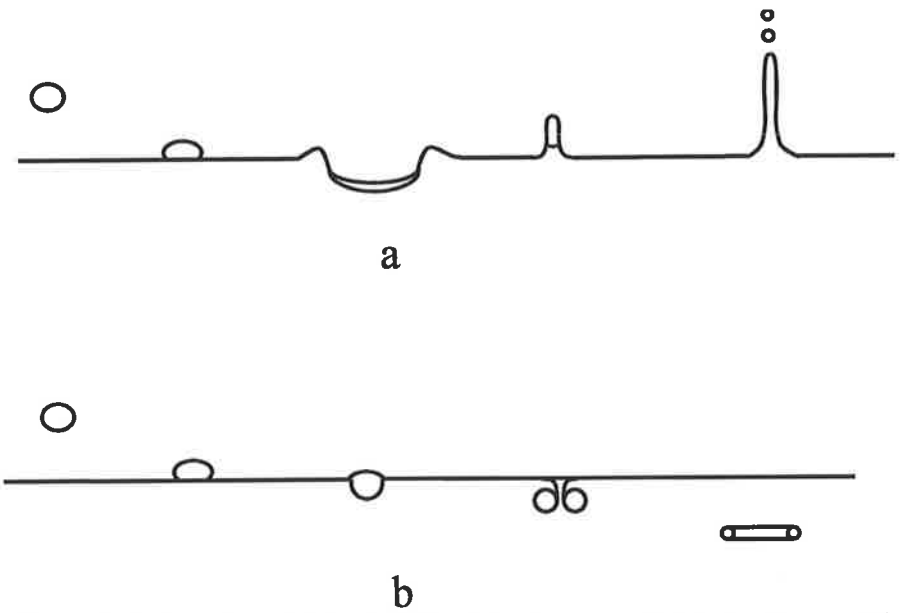

Figure 5.1 Droplet splash modes showing droplet behaviour with time.

If present in a weld pool this behaviour may be responsible for enhanced heat transfer and penetration. The use of vortex rings for underwater drilling (Chanine & Genoux, 1983) is evidence of their erosive power.

Before striking the surface of the liquid, a falling droplet contains free surface energy as well as kinetic energy due to both its translation and internal circulation. It has been shown that the kinetic energy due to internal circulation within the droplet, is generally small compared to the free surface energy and translational kinetic energy (Clift *et al.*, 1978). The energy that is used to create a vortex ring or a splash can originate from the translational kinetic energy of the drop and the free surface energy. The ratio of these is the Weber number: $W_e = \frac{\rho V^2 L}{\sigma}$.

For $W_e >> 1$, the kinetic energy of the droplet is significantly larger than the free surface energy, and it can be expected that if the surface tension forces do not contribute significantly to the deformation of the drop, a splash or rebound column will be formed. However, for $W_e << 1$ the free surface energy will contribute to the droplet deformation. The forces produced by surface tension in the region of high curvature between the drop and the pool, will help to drive the droplet into the pool creating a vortex ring. Therefore it can be estimated that there will be a critical Weber number of order 1 that will separate rebound column and vortex ring formation. Experimental work by Hsiao *et al.* (1988) has shown that the critical Weber number is 8 for a semi-infinite pool. As the Weber number increases even further, a crown will form on initial droplet entry as well as the rebound column some time after droplet impact.

The mode of impact is not determined by the Weber number alone. The depth of the pool and the relative time between droplet impacts also has an effect on the droplet mode. For relatively shallow pools (depth less than 1.5 x droplet diameter), a rebound column will not

form even for Weber numbers significantly greater than 8 (Hobbs & Osheroff, 1967 and Macklin & Hobbs, 1969). This is because there is not enough fluid in the pool to form a crater large enough to generate a rebound column. In a shallow pool the drop generally forms a crown at Weber numbers much larger than 8. At low Weber numbers the behaviour has not been thoroughly investigated in the literature. However some experimental flow work has indicated that a vortex ring still forms although it rapidly distorts on contact with the wall. Interaction of a vortex ring with a wall has been studied extensively in the literature, (see for example Walsh, 1987), and in general the result of such interactions is the formation of three or four counter rotating vortices (Figure 5.2).

The time between droplet impacts also has some bearing on the formation of the rebound column. As the time between droplet impact grows shorter, the formation of the rebound column is suppressed because the next droplet strikes the pool before the rebound column of the previous droplet has had time to form. The experimental work of Ching *et al.* (1984), shows that the critical frequency for low (8-300) Weber numbers is determined by a Strouhal number of approximately 0.2. What happens for Weber numbers of less than 8 has not been investigated, although some preliminary experimental studies carried out in this work does indicate that the vortex ring still forms. However, it rapidly interacts with the wall and the following vortex ring to form a very complicated chaotic motion. The interactions of two closely spaced vortex rings has been extensively studied in the literature, see for example Sharif & Leonard (1992) (Figure 5.3).

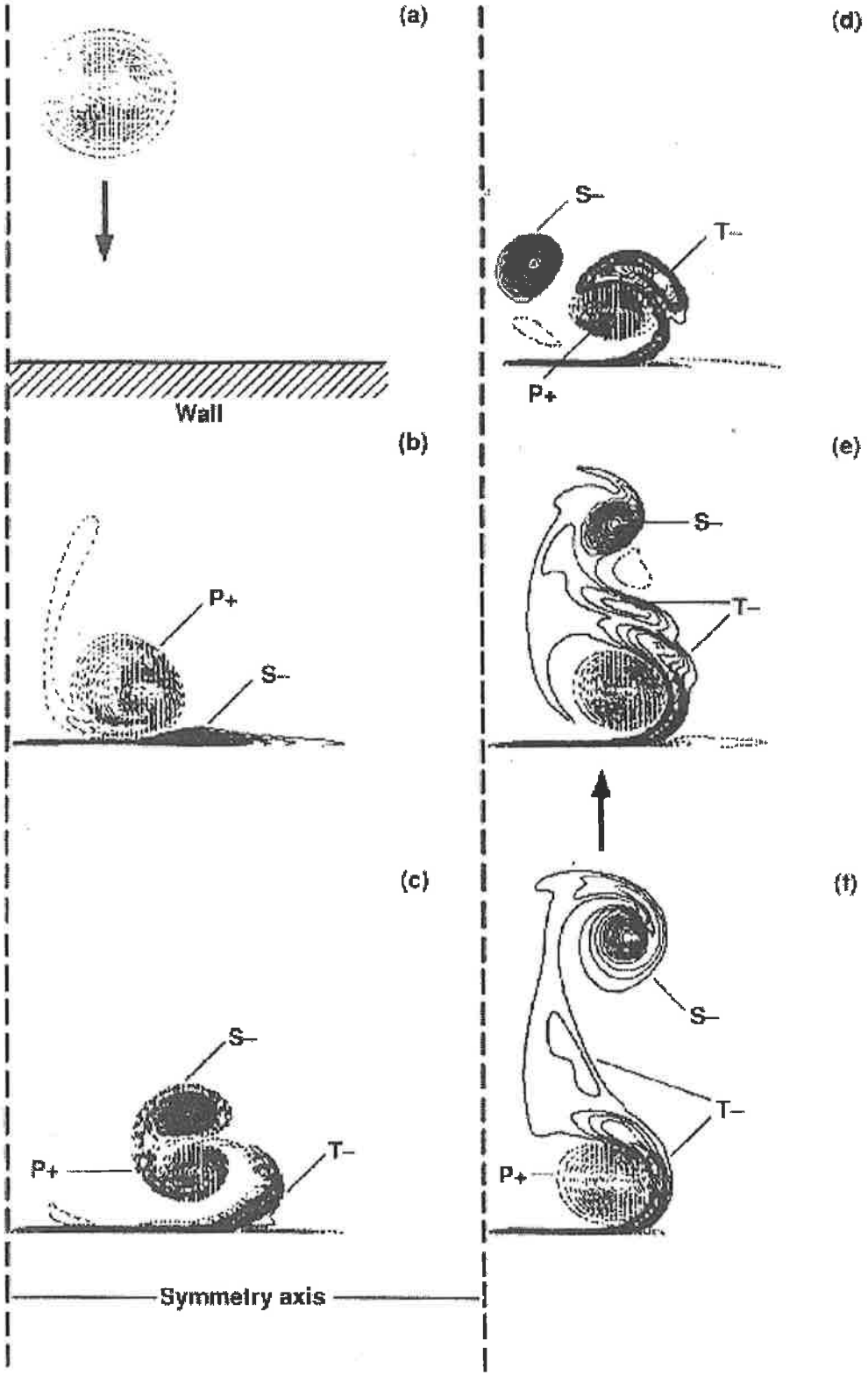

Figure 5.2 Vorticity Contours for Impingement of a Vortex ring on a no slip wall, (Sharif & Leonard, 1992)

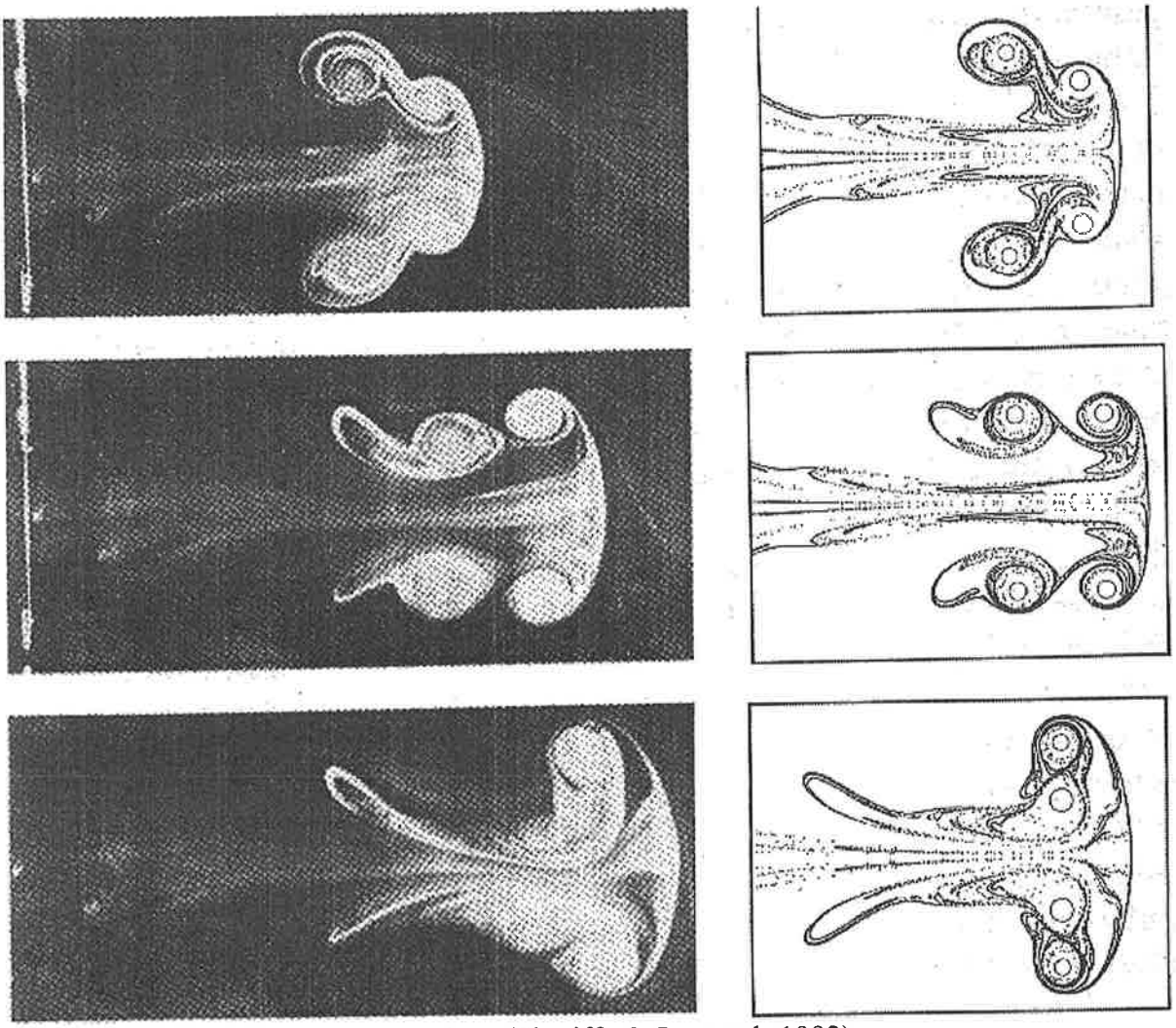

Figure 5.3 Interaction of two vortices (Shariff & Leonard, 1992)

Again, using the experimental data presented by Lancaster for argon rich electrode positive GMAW, the critical Weber number occurs at an arc current of approximately 150 Amps and the critical Strouhal number at approximately 140 Amps. This suggests that for currents of less than 150 amps, vortex ring formation could play a role in the flow within the weld pool. Even though, given the depth of the pool, the ring would not last for long but would rapidly interact with the wall forming complex vortical structures (see for example Walker *et al.*, 1987). Although at currents of greater than 150 amps the Weber number is above the critical

value, the rebound column would not form because the time between droplet impacts is too short. This means that above 150 amps, the droplet can be considered as a pulsatile momentum source with some remnant vorticity due to the free surface energy that has been destroyed. This observation further supports the scale analysis of Chapter 3 which predicted that surface tension forces could be important at low currents, with their effect diminishing with increasing current.

Previous attempts to model droplet impacts have ignored the effects of surface tension (Harlow & Shannon, 1967a,b) or viscosity (Prosperetti & Oguz, 1993). Therefore these results have not successfully predicted the formation of a vortex ring.

It is very difficult to simulate droplet impact directly using a traditional free surface algorithm, because with any standard approach the curvature is determined from the second derivative of function that determines the free surface. For example, for a three dimensional case where the surface is defined by $z = f(x,y)$, the curvature can be given by:

$$2C = \frac{f_{yy}(1+f_x^2) + f_{xx}(1+f_y^2) - 2f_{xy}f_xf_y}{(1+f_x^2+f_y^2)^{\frac{3}{2}}} \qquad (5.1)$$

where f_x represents the partial derivative of the surface in the x direction, and f_{yy} the second partial derivative in the y direction, etc. This means that prediction of the surface tension forces is extraordinarily sensitive to errors in the prediction of the surface position. Therefore a very fine mesh is required to accurately capture the surface position. This explains why no vortex ring formation was reported in the study of Nystrum (1986), who

used what appears to be a relatively coarse mesh which would be unable to accurately predict the surface curvature. Furthermore the time-scale of the droplet surface interaction (order of 10^{-3}s for the whole interaction), is so small that very small time-steps (order of 10^{-6}s), are required to capture the behaviour. The combination of a very fine mesh and very small time steps make a direct simulation beyond readily available computational resources. Therefore a simplified model of a droplet surface interaction has been developed to aid in the understanding the effect of vortex ring formation on the weld pool flow.

5.2.2 Source Term Model for Droplet Surface Interactions

The fundamental concept behind the model is to substitute the normal stress induced by surface tension with an equivalent force acting at an appropriate position and direction. This is indicated schematically in Figure 5.4.

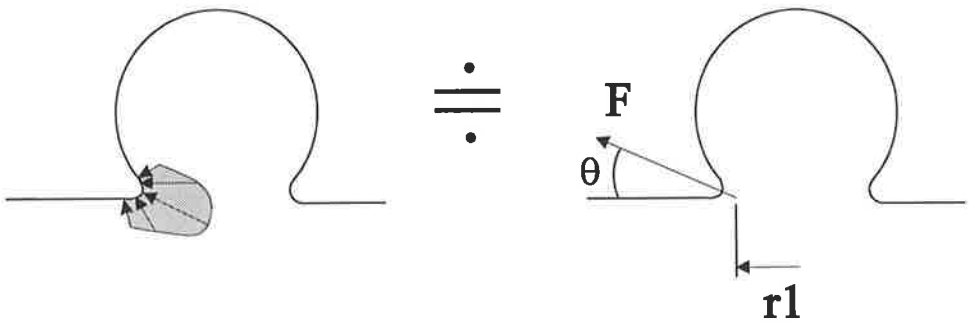

Figure 5.4 Fundamental concept for source term model for droplet surface interactions.

The stresses applied by surface tension to an interface can be described by the following equations, (Batchelor, 1967). In a 2-D or axi-symmetric case:

$$\sigma_n = 2\gamma C - p_a \tag{5.2}$$

$$\sigma_t = t_j \gamma_j \tag{5.3}$$

where γ is the coefficient of surface tension, C the mean Gaussian curvature, p_a the ambient pressure σ_t is the stress tangential to the surface and σ_n is the stress normal to the surface, t_j is the unit tangential vector and γ_j is the surface tension gradient. As can be seen from equation 5.3 the tangential component of the surface tension force is not dependent on curvature, only on the local variation in surface tension. Therefore assuming a constant surface tension, only the normal component of force is influenced by the region of high curvature between the drop.

Assuming that the pool surface at the point of impact can be taken to be horizontal, a simple geometric model can be constructed (Figure 5.5). From this model the angle at which the normal force acts can be approximated to be half way between the surface and the tangent at the point of contact.

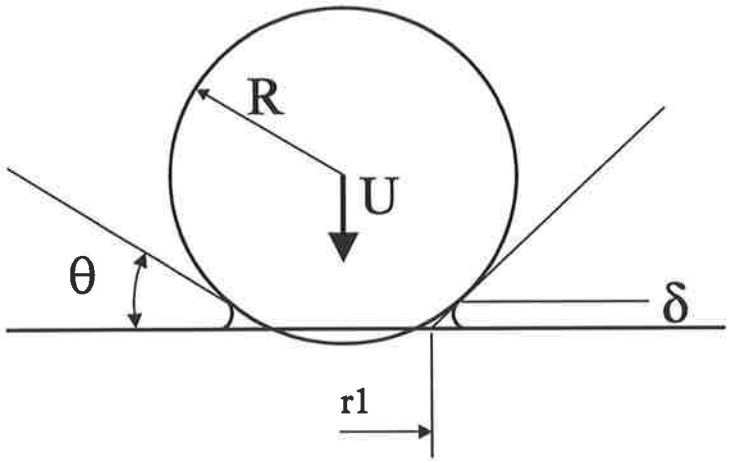

Figure 5.5 Geometric model defining the terms used in the simplified source term model for droplet surface interactions, for exact definitions refer to text.

Assuming that the fluid displaced by the droplet forms the bridge between the drop and the pool, Oguz & Prospetti (1993) have shown that the surface curvature, C can be estimated to be:

$$C \cong \frac{1}{aUt}\left(1 - \frac{a}{2+a}\left(\frac{2Ut}{R}\right)^{\frac{1}{2}}\right) \qquad (5.4)$$

where a = a numerical constant = 0.908, U is the droplet impact velocity, t is the time after droplet impact and R is the droplet radius. The height of the liquid bridge, δ can be estimated to be:

$$\delta = aUt \tag{5.5}$$

It is assumed that normal stress, which acts on the region of high curvature, can be replaced by a point force at the a radius *r1*. (This seems to be a reasonable approximation because the bridge has a relatively small area compared to the bulk of the drop during the period of interest). The force due to surface tension acting at the contact point can be given by:

$$F = (2\gamma C - p_a).2\pi.(2RUt - (Ut)^2)^{\frac{1}{2}}.\delta \tag{5.6}$$

acting at an angle of:

$$\theta = \arccos(1 - \frac{(Ut + \delta)}{R}) \tag{5.7}$$

where θ is the angle from the horizontal at which the effective force acts. The velocity due to the translational kinetic energy of the drop can be given by:

$$V = U \quad for \quad r < r1 \tag{5.8}$$

$$V = 0 \quad for \quad r > r1 \tag{5.9}$$

where *r1* is radius of the point of action of the equivalent force. The radius *r1* can be determined from the intersections of the tangent at the point of contact with the horizontal, and is given by:

$$r1 = (2RUt - (Ut)^2)^{\frac{1}{2}} - \delta\arctan(\frac{\pi}{2} - \theta) \tag{5.10}$$

At $t = 0$ the equation for the curvature (and hence force) is undefined, and it is necessary to

start the model some small but finite time after impact. This does not appear to be a significant problem and is quite representative of the physical behaviour. Furthermore, some of the geometric assumptions made by Oguz & Prospetti (1989) to derive the local curvature are not suited as $\delta/R <<< 1$. This may affect the accuracy of prediction as the forces due to surface tension effects are significant only for $\delta/R < 1$.

These equations (5.6 to 5.10) can then be applied to a computational model incorporating a free surface as velocity boundary conditions for the upper surface, and force or stress boundary conditions at the effective point of action. The accuracy of this approach was examined by comparing the predicted results to flow visualisation experiments, the experimental investigations are outlined in the following sections.

5.2.3 Experimental Investigations

Experimental investigations were undertaken in order to determine how accurately the model predicted the magnitude of the vorticity generated. The experimental arrangement is shown diagrammatically in Figure 5.6. The droplet was coloured with a dilute milk solution for initial investigations and a suspension of fine aluminium powder for filming. The suspension of fine aluminium powder was obtained by diluting a water based aluminium paint. Fine glass beads were also evaluated but did not provide the same image quality as the suspended aluminium. The experiment was illuminated using a 10 mV He-Ne laser which had been split into a sheet using a cylindrical lens. This provided a sheet of light of the order of 1mm thick. The droplet impact conditions used for comparison to the computational model gave a Weber number of 3 and a Reynolds number of 900. This is typical of a relatively low

current GMAW (of the order of 120 Amps), and this was chosen as a test case because the scale analysis has demonstrated that surface tension effects are more significant at low currents in GMAW pools.

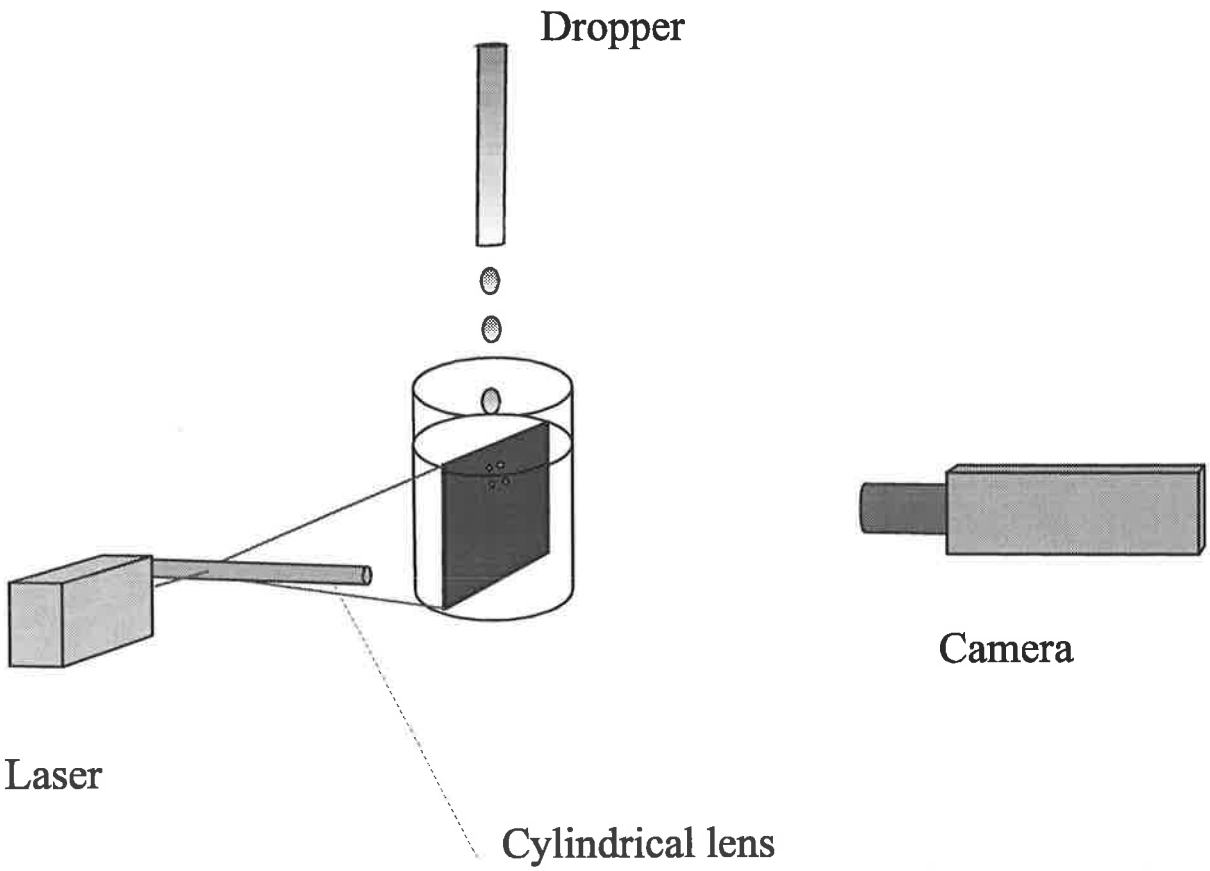

Figure 5.6 Experimental apparatus used to validate droplet impact and turbulence models.

The predicted ring formation appears similar to that observed in flow visualisation experiments. However this is somewhat of a qualitative comparison. It is difficult to get an accurate quantitative measure of the flow due to the low velocities and small scale which are characteristic of this phenomena. This means that the only comparison that can be made is

with the position and velocity of the vortex ring, not the internal velocities.

5.2.3 Results

Some examples of the results produced by the model can be seen in Figure 5.7 for a Weber number of 6. The examples shown have been run using FIDAP Computational Fluid Dynamics Code which relies on the method of spines (Satio & Scriven, 1981) to model the free surface. This code solves the full Navier Stokes equations using a finite element method. For these examples a fully coupled Newton scheme was used to solve the system

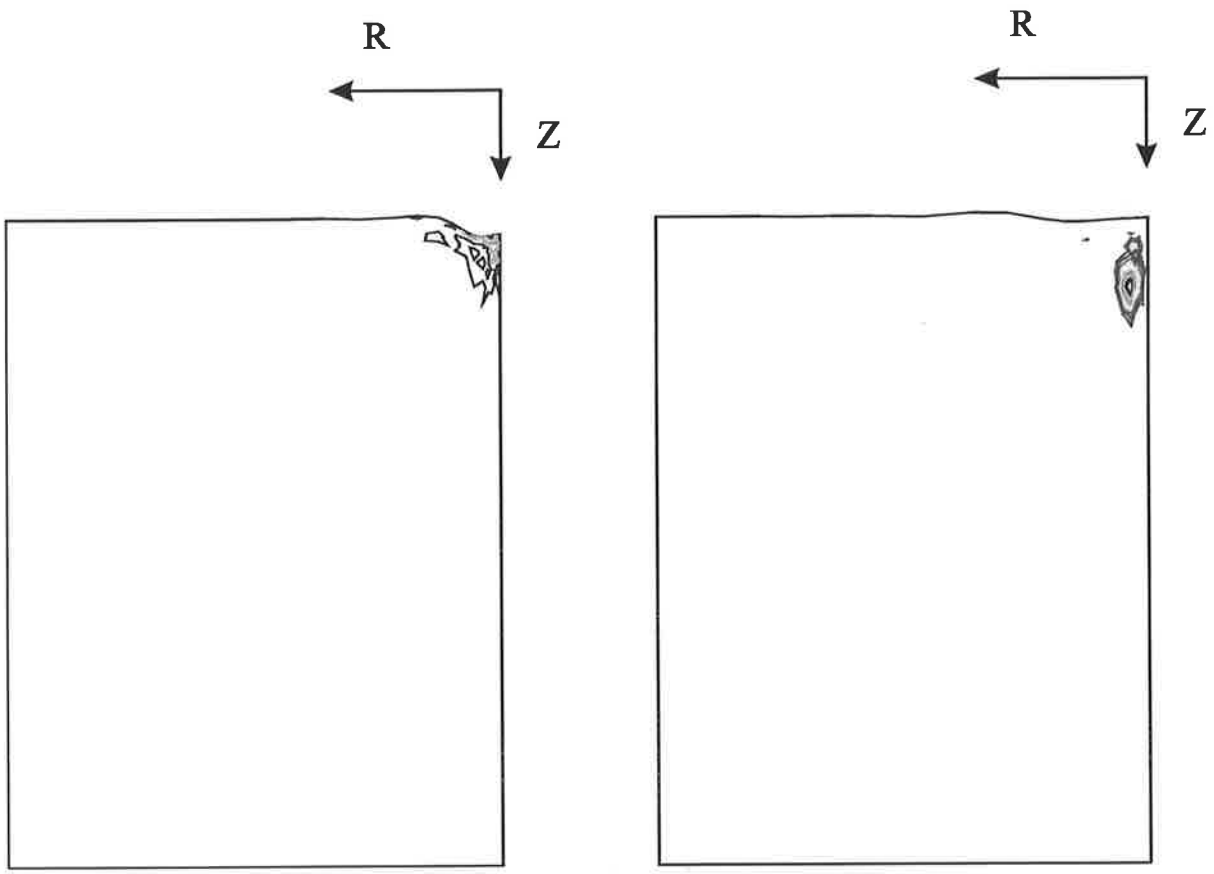

Figure 5.7 Model predictions W_e = 6, R_e =1000
(Vorticity contour plots 0 ⇒-1000)
Left t = 7.5ms, right t = 20 ms

of non linear equations as discussed in Appendix A.

In this implementation the model predicted vortex ring formation below a Weber numbers of approximately 9, which compares favourably with the experimental value of 8 obtained by Hsiao et al (1988).

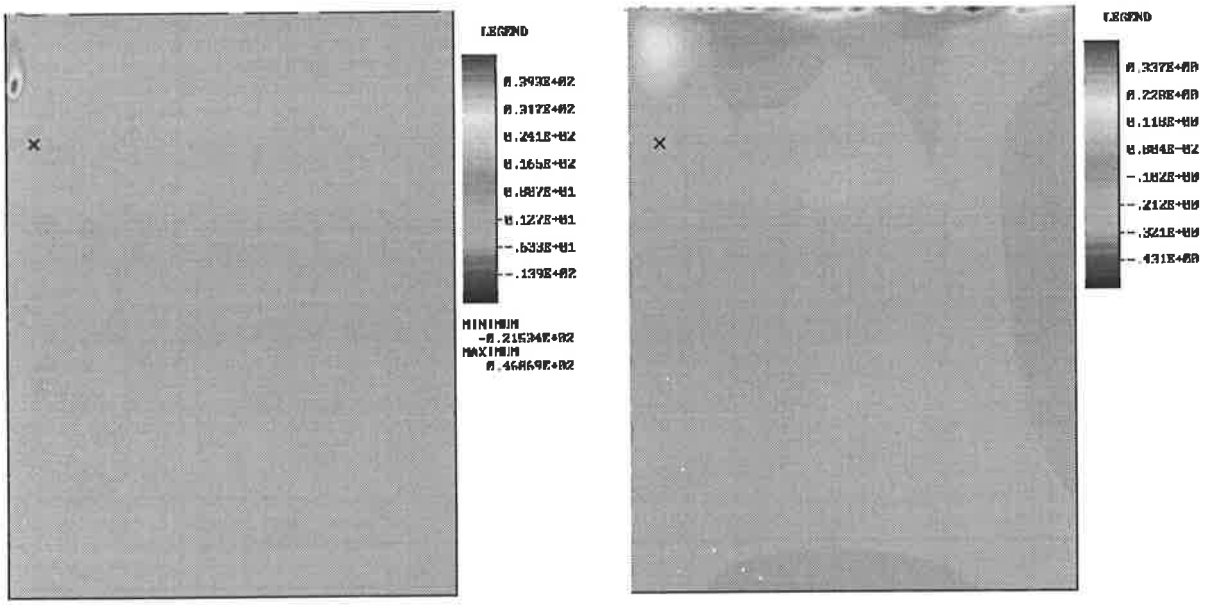

Figure 5.8 Left: source term model. Right: slug flow models. x experimentally measured vortex ring centre (We = 3, Re = 900). Note 2 orders of magnitude difference in the scale.

The experimental results are compared to the computed results in Figure 5.8 and 5.9. (Note that the magnitude of vorticity predicted with the present model is two orders of magnitude greater than that predicted by a slug flow representation in Figure 5.8). As can be seen from the results, the computer model under predicts the depth of penetration and velocity of the vortex ring at any given time (Figure 5.9).

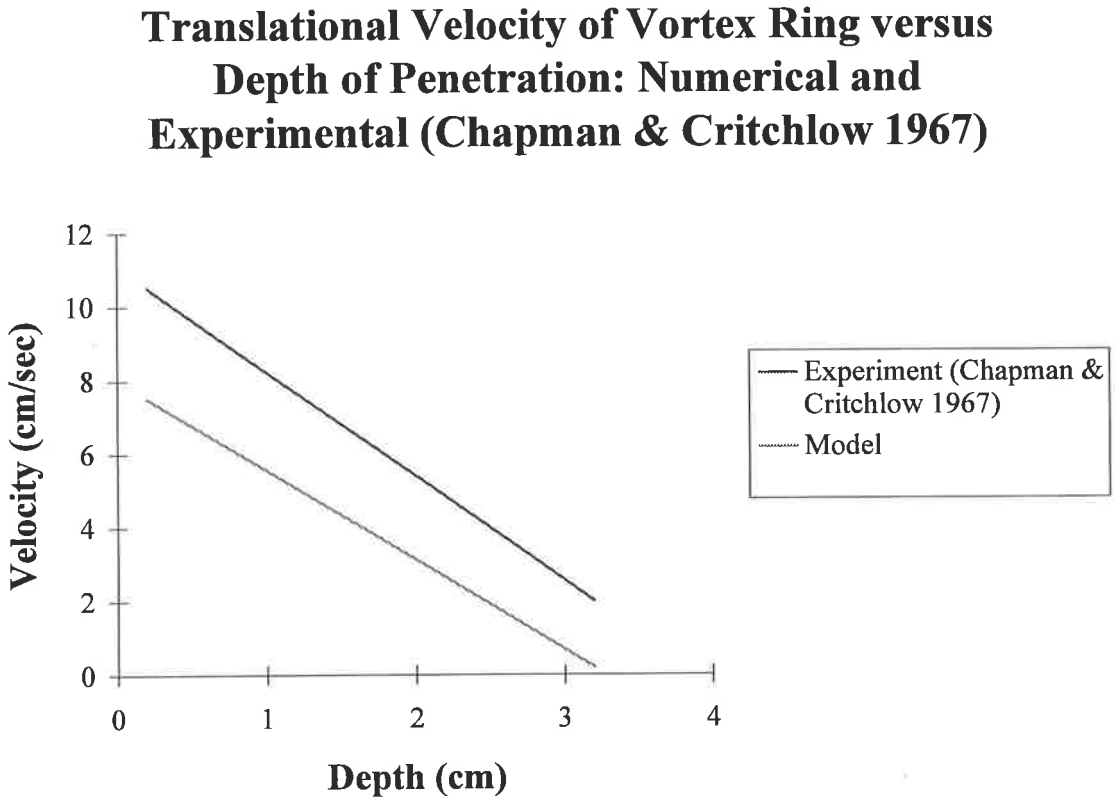

Figure 5.9 Vortex ring translational velocity: Numerical vs. experimental.

5.2.4 Discussion

By comparing the experimental and the computed velocities, it is apparent that the computed results exhibit the similar decay in velocity as the experimental. It appears that the only flaw in the computational model is the under-prediction of the initial velocity. This occurs because the estimate of curvature, as given by is not accurate at very small time. At very small time ($t < R/8U.a$) the curvature given by equation is approximately half the real value. If this estimate could be improved, it is the author's belief that the above method would provide satisfactory prediction of the vortex ring behaviour. This has not been done at this stage, because the method is still too slow for use in a welding model even though it is far less computationally expensive than direct simulation. For example, simulation of two seconds of real time immediately after one droplet impact required three weeks of computer time on a "Sun 4 workstation". This is because the problem still requires the use of very short time-steps and a relatively fine grid to capture the vortex ring behaviour.

This model can be used with a variety of free surface algorithms, including those that allow for the folding and breaking of surfaces (eg. Volume of Fluid, VOF) and those that don't (eg. method of spines and Height of Liquid, HOL). It should be noted that the model only attempts to model the effect of the original droplet impact. Any drops that may be formed by the break-up of the rebound column will not naturally be modelled correctly, and will need to be included explicitly when they strike the surface. Furthermore, methods which do not allow for the breaking of surfaces cannot be used if the rebound column breaks up. Neither of these factors present a problem when modelling GMAW pools as a rebound

column is never formed, because as the Weber number decreases the Strouhal number increases suppressing any column formation. While this model may be useful as an engineering tool, it will not replace direct simulation for the investigation of fundamental behaviour such as the effect of droplet oscillation on vortex penetration. Although changes can be made to account for the changing droplet shape, it is possible that they would not capture the detail necessary to accurately predict the changes in the vortex ring behaviour.

5.2.6 Conclusions

A simple geometric model has been used to develop a source term which can be used to model the formation of vortex rings by a liquid droplet impacting on a liquid surface. It satisfactorily predicts vortex ring formation but it does under-predict the initial velocity of the ring due to its relatively poor estimate of the surface curvature for very small time. Even with this relatively simple model, the prediction of vortex ring formation is still too computationally expensive to be useful in predicting the flow within a weld pool, particularly if one wishes to predict the effect of ring-ring or ring-wall interactions. Therefore for successful modelling of the flow within a GMAW weld, the vortex ring needs to be considered in such a way that the detail of the ring is not fully resolved.

In computational fluid mechanics, turbulence is "all the phenomena due to the irregular motion that occurs at scales below those resolvable on the grid employed for computational purposes" (M.B. Abott & D.R. Basco, 1989). Therefore if we cannot resolve the vortex motion on the given mesh, it appears that the best approach is to include the vortex ring behaviour in the turbulence effects. The method for doing this will be discussed in the next section.

In the case of GMAW, most interactions have a Weber number lower than the critical number, and a vortex ring can be expected. Due to the fine computational mesh, and resulting significant expense necessary to capture this ring to date, it has been included with the so called "turbulence" and its effects approximated for by the use of turbulence models. This approximation has been verified by comparing the results of the computational model

to the physical model in the literature.

Walker *et al.* (1987) conclude that even the interaction of a low Reynolds number laminar vortex ring with a wall leads to complex "turbulent" flow as the vortex ring deteriorates. Therefore in the case of multiple vortex ring impacts, the flow within the pool will certainly be turbulent. Based on these results, the flow within a GMAW pool is highly likely to be turbulent at quite low currents, with the droplet surface interactions responsible for driving the turbulence. Given that the flow within the pool is turbulent (due to the impact of the droplets) effective modelling techniques need to be developed to represent it. This will be discussed in the following section.

5.3 TURBULENCE

5.3.1 Introduction

As stated in Chapter 1, there has been discussion in the open literature on the role of turbulence in the flow in a GTA weld pool. There appears to be some evidence that the velocity fields within a GTAW pool are turbulent, or at the very least transitional. Due to the size and scale of the weld pool, as well as the presence of an intense arc plasma, there is no known direct measurement of turbulent velocity fluctuations. Visual observation of surface flow does indicate that there is some unsteady chaotic variation which is probably associated with the presence of turbulence. Choo *et al.* (1992 & 1994) have done numerical studies that include both the turbulent and the laminar assumption for weld pool flow. Their work demonstrates that weld pool shape predicted by a turbulent flow model is far closer to the experimental shape than that predicted using the laminar flow assumption. Malinowski & Bronicka *et al.* (1990) measured the velocity of marker particles on the pool surface, and determined that the pool Reynold's number was of the order of $3x10^3$ and therefore the flow was turbulent. They also explained that the pool shape was most likely due to turbulent heat transfer within the pool. These results call into question the results of many early modelling studies which all assume laminar flow.

If the flow in a GTAW pool is most likely turbulent or transitional, the flow within a GMAW pool (although not investigated in the literature) is almost certainly turbulent. The addition of the molten droplet at high velocity, as well as the significant surface tension

forces arising during droplet coalescence together with the larger pool shape, can only increase the level of turbulence in comparison to GTAW. As discussed in the previous section, the formation and destruction of vortex rings will force the flow to be turbulent even from relatively low Reynolds numbers. In addition, the natural variation in droplet size shape, impact position etc. of the metal transfer into the pool will increase the level turbulence within the pool.

The flow caused by the vortex structures (created by the droplet surface interactions) interacting with each other and the pool boundaries creates eddies several orders of magnitude smaller than the droplet itself. If the scale of droplet is one to two orders of magnitude less than the pool, and the eddies resulting from vortex interactions are three orders of magnitude less than the droplet, at least 10^9 grid-points are required (Landahl & Mollo-Christensen, 1992). A grid of this resolution is well beyond readily available computational resources. Indeed using the definition of Abbot & Basco (1990), that in computational fluid dynamics turbulence is the phenomena arising from flow which cannot be adequately resolved with the given mesh, these motions must be considered as turbulence. These small scale motions play an important role in the dissipation of heat and momentum and cannot be ignored, hence they must be incorporated into some form of turbulence model.

Electro-magnetic forces can affect turbulence, sometimes damping and sometimes amplifying the turbulence (see for example Kirko, 1965). However for low values of the magnetic field and high values of the Reynolds number (ie. $M/Re \leq 10^{-3}$ where M is the Hartman number and is defined as $M=B_o l_o \sqrt{[\sigma_e/\mu]}$ where B_o is the reference magnetic field density, l_o is the

length scale, σ_e is the electrical conductivity and μ is the permeability), the electro-magnetic force can act only as a body force, having negligible effect on the turbulent motion (Kirko, 1965). In a GMA weld pool M/Re is of the order of 10^{-3}, therefore the electro-magnetic forces can be considered as body forces with no impact on the turbulence, and regular turbulence models can be used. It should be noted that at higher currents (I > 275 Amps), the Magnetic number does exceed 10^{-3} and therefore the effects of the electro-magnetic force on the turbulence may need to be considered, if one is to model weld pool flow under these conditions.

Whilst it is apparent that some form of turbulence modelling is required, choosing the appropriate turbulence model and turbulence boundary conditions for accurate prediction is far less obvious. Therefore this section shall concentrate on the evaluation of several common turbulence models and methods for the application of the boundary conditions.

5.3.2 Accuracy Evaluation of Applicable Turbulence Models

As discussed in Chapter 2 there is a wide variety of available turbulence models, all with varying amounts of accuracy and computational cost, ranging from simple zero equation schemes to complex differential second moment closure schemes and large eddy simulations. The K-ε two equation turbulence model is the most commonly used for engineering modelling, and most likely to be applicable to weld pool flow because of its relatively low computational cost and relatively broad applicability. Therefore in this section the simple eddy viscosity model of Choo *et al.* (1994) and three versions of the K-ε model are investigated to determine their accuracy when modelling weld pool flow. The three versions

of the model include the standard K-ε model (Launder & Spalding, 1974), the extended version of Chen & Kim (1987), which includes modifications to incorporate the effect of streamline curvature, and the Re-normalisation group (RNG model), which was developed by Yakhot & Orszag (1986) by the application of re-normalisation theory to the governing equations. The suitability of these models for modelling weld pool flow has been evaluated by modelling an impinging turbulent jet. The impinging turbulent jet has been chosen as a test case because the physics of the flow is similar to the weld pool, and a database of experimental information exists within the open literature for the flow field generated by an impinging turbulent jet. The experimental results chosen in this test are those of Cooper *et al.* (1993). The Reynolds number of the tests (Re = 23000) is higher than that of the weld pool (Re = 2000 - 10000), however the tests still provide valuable information about the relative value of the different turbulence models.

5.3.2.1 Numerical models

The computational model is shown in the Figure 5.10 and the computational mesh in Figure 5.11.

The boundary and initial conditions can be described as follows:

1) A fully developed turbulent profile was prescribed for the inlet condition.

2) Boundary conditions for the turbulence variables were taken from Cooper *et al.* (1993).

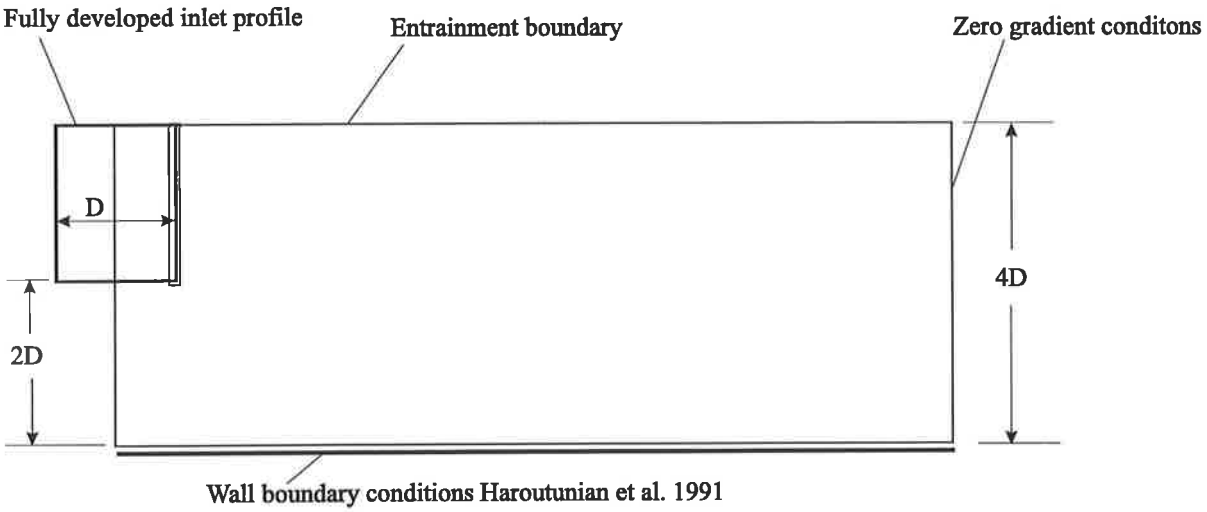

Figure 5.10 Boundary conditions for turbulence model evaluation.

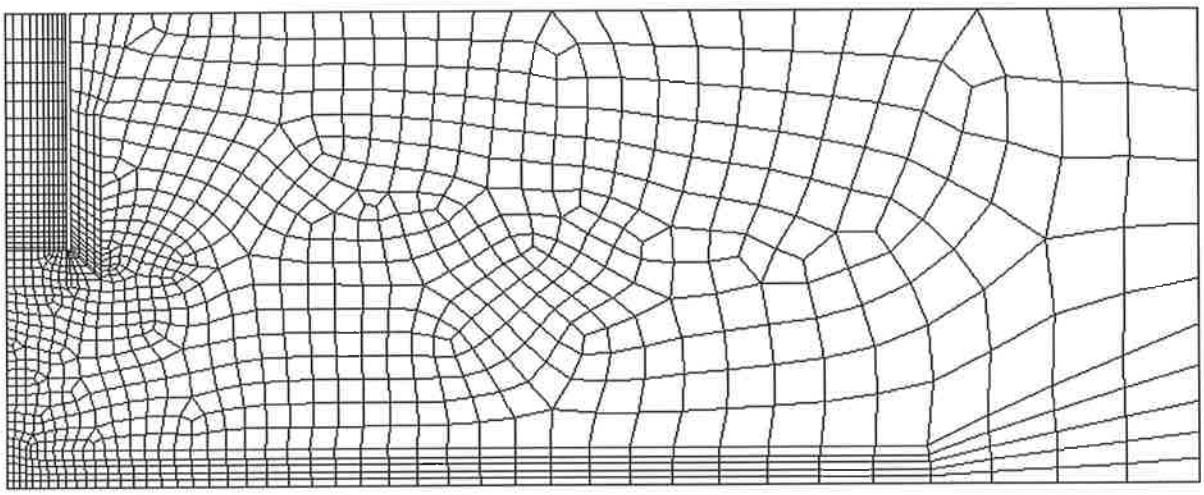

Figure 5.11 Typical computational mesh used for turbulence model evaluation.

3) Along the upper entrainment boundary, zero turbulence boundary conditions were applied to any entrained fluid and zero gradient velocity conditions.

4) Along the external boundary, zero gradient conditions were applied to all variables.

5) Along the wall boundary the boundary element approach of Haroutunian *et al.*

(1991) has been used.

5.3.2.2 Results

Figure 5.13 and Figure 5.14 show typical results for the velocity vectors and the turbulent viscosity plots, however in order to compare the models to experiment a more quantitative approach is required. In this case the standard test is to compare the radial velocity profile at certain points in the domain. Figure 5.12 compares the radial component of velocity from at a radius (r), of 2.5 pipe diameters (D). The profile is given at a distance y from the wall, where y varies from 0.05D to 0.4D with the velocity(U) normalised using the impinging jet velocity (Ui).

5.3.2.3 Discussion

It appears from the above results that all of the two equation models perform similarly well, however the standard K-ε is slightly better than the others. The zero equation model of Choo *et al.* (1992d) performs far worse than the two equation models at predicting the flow behaviour. This is because the zero equation model enhances the viscosity throughout the entire domain. Where as, the two equation models solve transport equations for the turbulence values throughout the domain and enhance the viscosity locally according to the results. A typical viscosity enhancement for a two equation model can be seen in Figure 5.14. Although the zero equation model does not enable the accurate prediction of the velocity field it does however provide an accurate indication of the enhancement of thermal

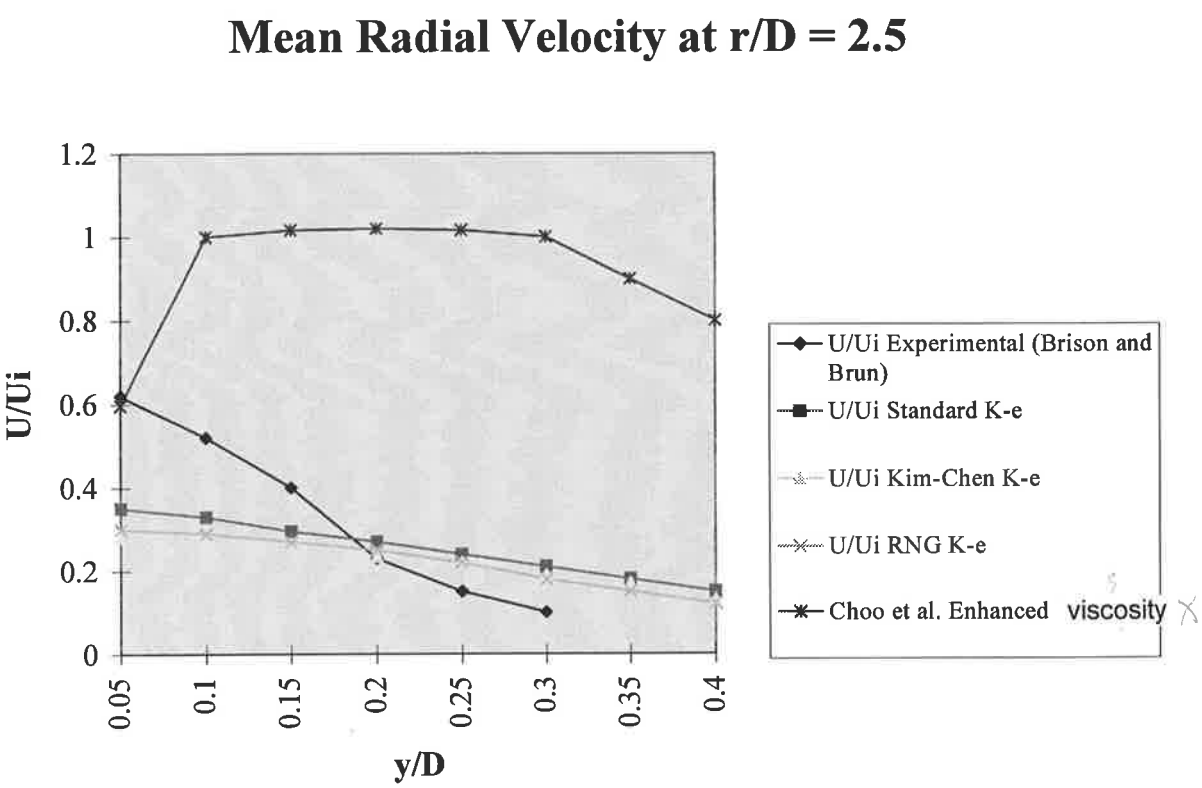

Figure 5.12 Turbulence model evaluation.

diffusion due to turbulence. This is because it has been empirically calibrated using temperature profiles rather than velocity fields.

Although the zero equation of Choo *et al.* (1994) does not appear to model the details of the flow well, it is however at least two orders of magnitude faster than all of the K-ε models, and it does model the enhancement of thermal diffusion within the pool due to turbulence relatively well due to its empirical tuning, it is therefore useful for turbulence modelling where computational resources prohibit the use of one of the more accurate two equation schemes.

Even though the two equation models were more accurate than the zero equation model they under-predicted the maximum velocity in the near wall region and over-predict the width of the wall jet (see Figure 5.12). This is because they over-estimate the amount of turbulent kinetic energy in the compressive region immediately under the jet exit, and therefore entrain too much ambient fluid within the wall jet. This example highlights the problem of using standard models to predict turbulence generated by complex flows. Most K-ε turbulence models have been developed for shear flows and do not account for generation of turbulence by other sources, e.g. strain, buoyancy, streamline curvature etc and therefore do not perform as well in a weld pool environment. However they are still the most accurate of the readily applicable turbulence models. Although the choice of turbulence models is relatively clear, accurate values for the turbulence boundary conditions are required if accurate predictions are to be made. Therefore determining the appropriate turbulence boundary conditions to represent droplet impact is the focus of the next section.

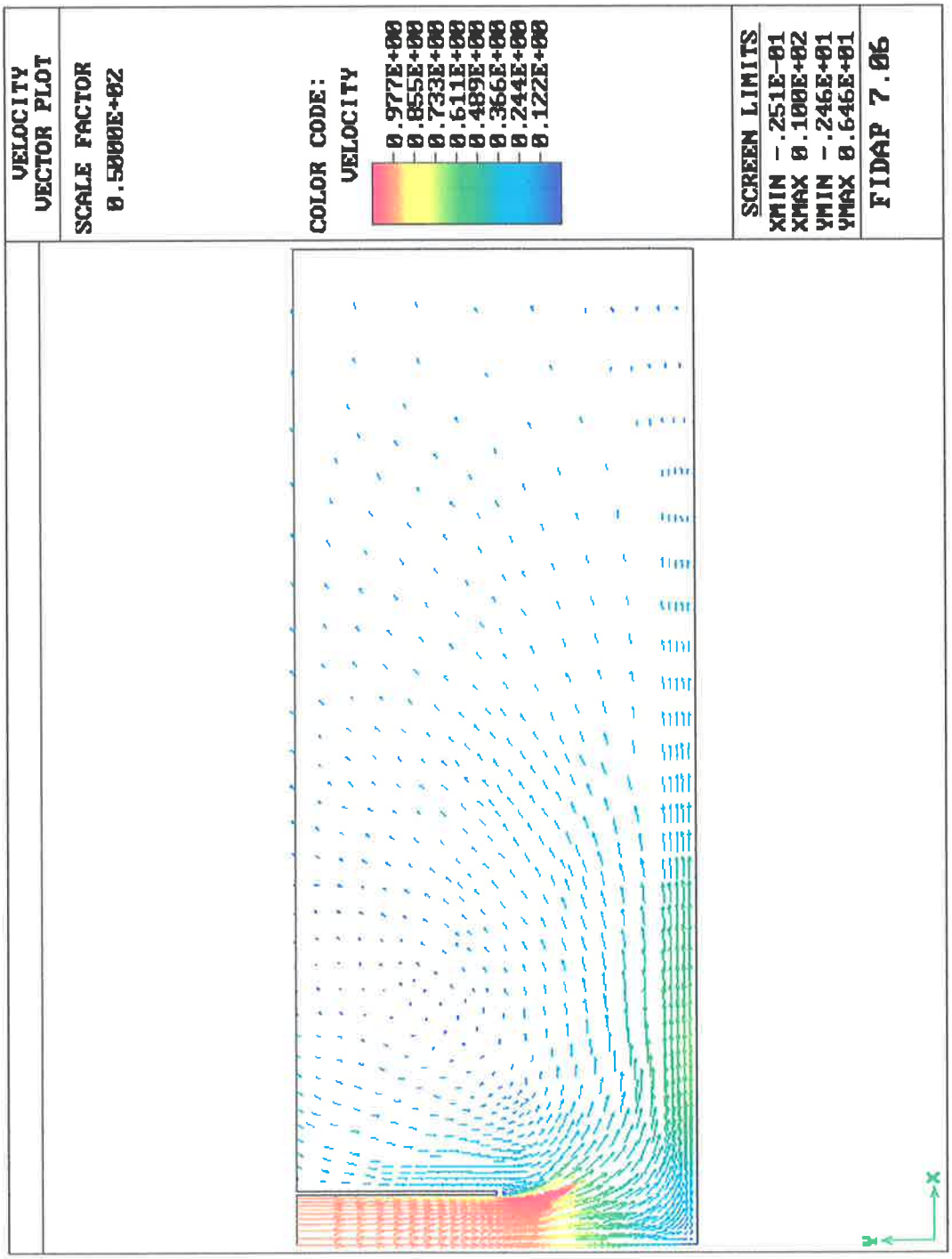

Figure 5.13 Turbulence model evaluation: typical velocity vector plot, standard K-e turbulence model.

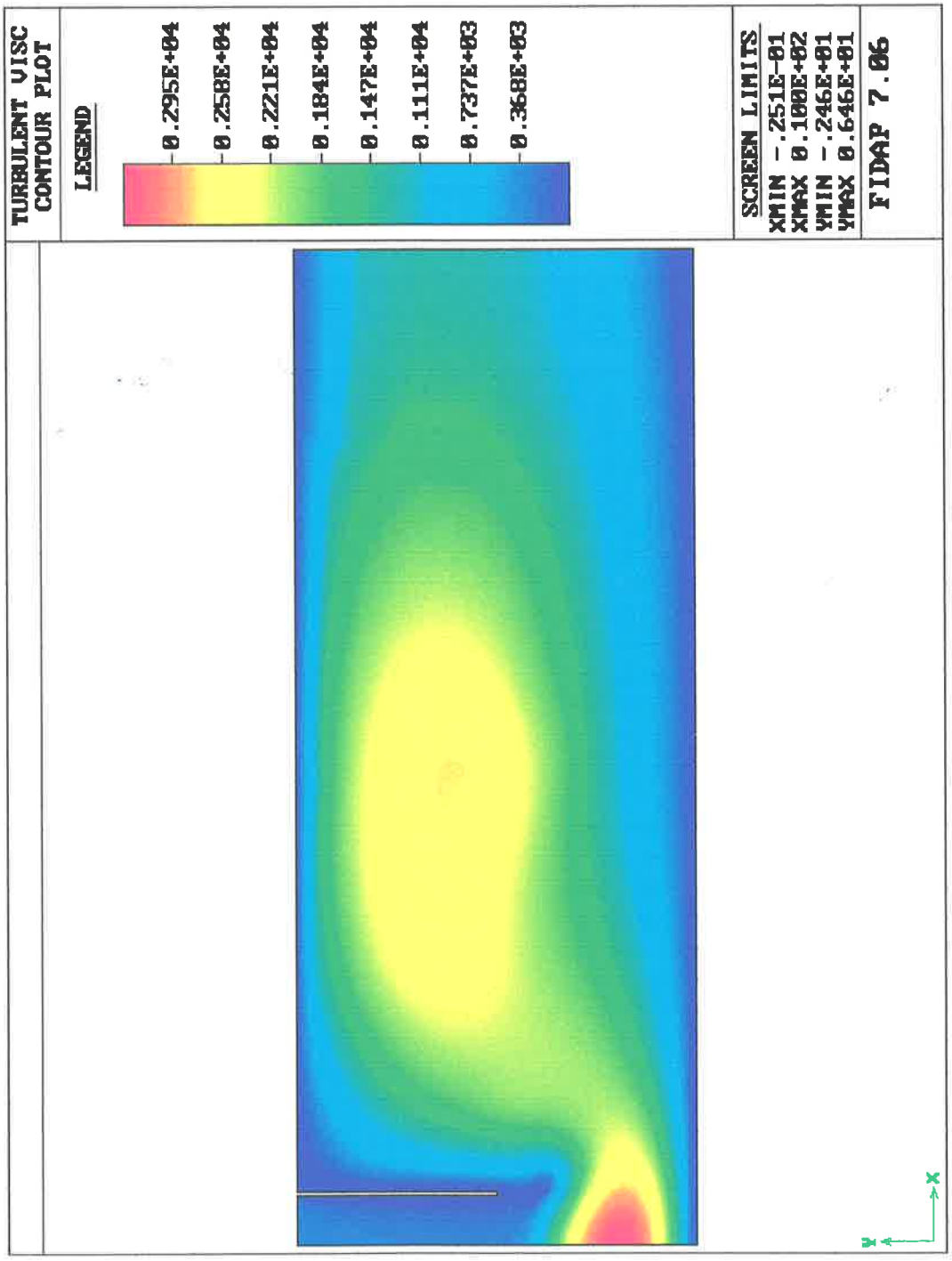

Figure 5.14 Turbulence model evaluation: typical turbulent viscocity contours, standard K-e turbulence model.

5.3.3 Turbulence Boundary Conditions

5.3.3.1 Introduction

The second problem with modelling turbulence in a GMAW pool, is the choice of boundary conditions for the turbulence variables. Normally, experimentally measured values for the turbulent kinetic energy and the dissipation length are used whenever possible, where the turbulent kinetic energy is defined by:

$$k = \frac{1}{2}\overline{u_i u_i} \tag{5.11}$$

where u_i is the velocity fluctuation about the mean in the i direction and the dissipation length, ε is defined by:

$$\epsilon = \frac{\mu}{\rho}\overline{\frac{\partial u_i'}{\partial x_j}\frac{\partial u_i'}{\partial x_j}} \tag{5.12}$$

When experimental values are not readily available the following scheme is used:

i) For internal flows the characteristic value of the turbulent kinetic energy, k, can be obtained from the following equation:

$$k = c_\mu^{\frac{1}{2}}\left(l_m\frac{du}{dy}\right)^2 \tag{5.13}$$

where c_μ is an empirical constant equal to 0.09, u is the stream-wise velocity component at the inlet plane, l_m is a typical length scale for the turbulent motions and y is the normal distance to the nearest wall.

ii) The turbulent dissipation length ε can then be obtained from:

$$\epsilon = c_\mu k^2 \left(l_m^2 \left| \frac{du}{dy} \right| \right)^{-1} \tag{5.14}$$

In the case of a weld pool, experimental determination of K and ε is not possible as it is velocity fluctuations within the molten pool have not been experimentally measured. In addition, following the standard technique is unlikely to give an accurate estimate given the fluctuating nature of the droplet impact and the effect of surface tension forces.

If the turbulent kinetic energy is defined as in equation 5.11 (where u_i is the fluctuation about some mean velocity), then in the case of droplet impingement, most of the fluctuation about the mean is due to the vorticity created by the droplet surface interactions and the interactions of this vorticity with that from successive droplets and the walls. Generation of this vorticity is primarily due to surface tension forces. It therefore seems reasonable from a conservation of energy viewpoint, to equate the amount of turbulent kinetic energy at the point of droplet impact to the amount of free surface energy destroyed by the impacting droplet. To examine the validity of this assumption, a flow visualisation experiment has been carried out and compared to numerical models using this approach.

5.3.3.2 Experiment

The experiment consisted of a continuous stream of water droplets falling under gravity into a cylindrical test vessel of clear water. The test vessel was illuminated by a thin sheet of light produced by passing a beam from a 10 mV He-Ne laser through a cylindrical lens. The flow patterns were then filmed using a video camera, and the measurements of the position

of the centres of the recirculation regions were taken directly from the screen (see Figure 5.6). Due to the fact that low velocities were involved, direct measurements of the velocities were not possible. Therefore, the centres of the recirculation regions were chosen to provide qualitative information on the accuracy of the scheme. Given the relatively crude level of turbulence modelling possible in weld pool modelling (see previous section), this level of validation is sufficient. The droplet impacts were observed at a Reynolds number of 1500, a Weber number of 5, and a Strouhal number of approximately 0.5 (where the Reynolds and Weber numbers are based on the droplet diameter and velocity, and the Strouhal is based on the droplet impact frequency). This compares to welding conditions where the Reynolds number varies from 1000 to 10000, the Weber number from 1 to 100 and the Strouhal number from 0.2 to 5. This is as close to real welding conditions as can be achieved with natural droplet formation. With natural water droplet formation it is very difficult to get high frequency droplets with a low Reynolds number, because the droplets are formed by instabilities acting on the liquid column. Therefore the longer the liquid column, the higher the frequency of droplet formation and the velocity of the droplet.

5.3.3.3 Computational model

Details of the computational model are as follows:

1) The model consisted of an axi-symmetric representation of the test vessel.

2) The impinging droplets were represented as a momentum source acting at the point of impact. Boundary conditions for the turbulence variables were applied at the same point. Comparison was made between models that applied boundary conditions

for the turbulent kinetic in a standard way (i.e. following equations 5.13 and 5.14) and those which equated the turbulent kinetic energy to the free surface energy of the drop. In both cases the turbulent dissipation length was calculated from equation 5.14.

3) Turbulence boundary conditions on the walls were applied using the boundary element approach of Haroutunian *et al.* (1991).

5.3.3.4 Results

Figure 5.13 shows the experimentally observed flow. Whilst the flow behaviour is obvious on the display monitor, it is far harder to see on a single frame. Therefore the observed flow behaviour has been superimposed over the image to aid in interpretation. The flow in the right hand side of the tank is more clearly revealed in the image because the laser was placed nearest to the right hand side of the tank (see Figure 5.6). Figure 5.14 compares the predictions of the standard approach to one equating the free surface energy destroyed by the turbulent kinetic energy. It is obvious that the modified technique does predict the two recirculation regions observed in practice. The centre of the lower recirculation region was measured directly on the display monitor and the results superimposed on the predicted flow pattern. As can be seen, the modified model does not exactly match experiment but it is a significant improvement on the standard approach.

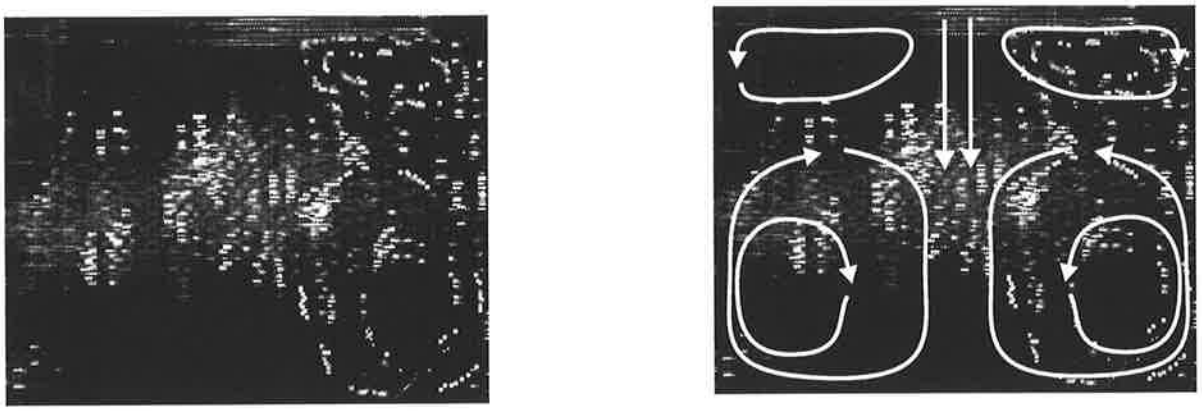

Figure 5.13 Experimental results:
i) Left - Raw image.
ii) Right - Raw image with observed motion superimposed.

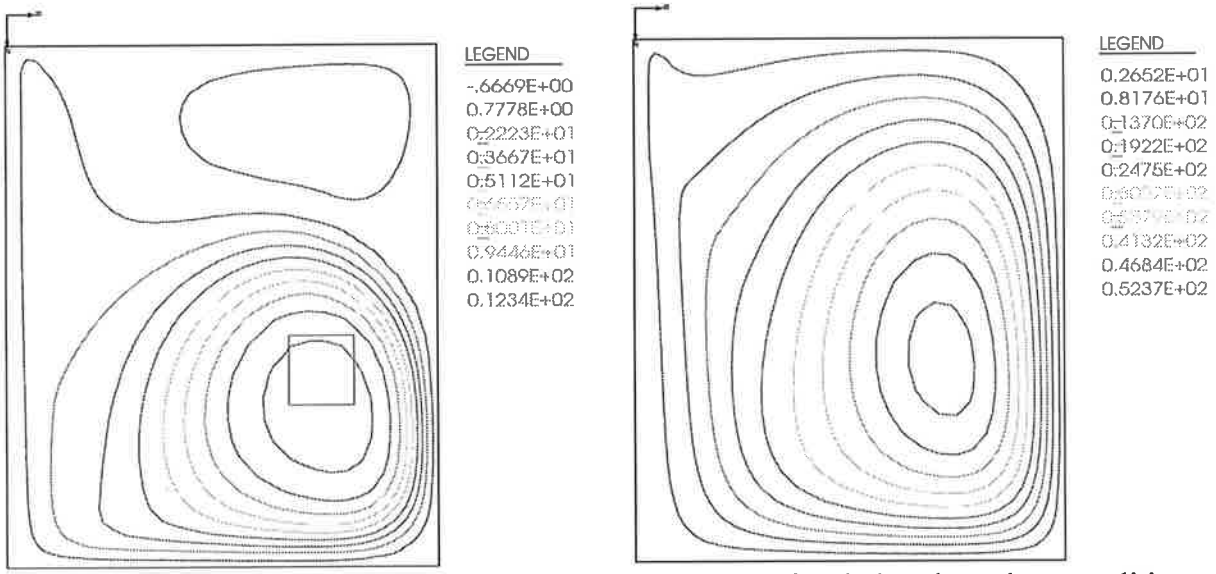

Figure 5.14 Streamline contour plots for the comparison of turbulent boundary conditions:
i) Left K from free surface energy destroyed, ε from geometry.
ii) Right standard K and ε boundary conditions.

5.3.3.5 Discussion

Traditional methods for the calculation of the turbulent kinetic energy do not give accurate prediction of the flow behaviour generated by impinging droplets. Equating the turbulent kinetic energy to the free surface energy destroyed by droplet impact does seem to be more

appropriate than traditional methods used to calculate the turbulent kinetic energy boundary conditions. The increased turbulent kinetic energy at the input boundary predicted by this technique gives a more accurate prediction of the flow behaviour. Therefore if the turbulent GMAW pool flow is to be modelled accurately, turbulence generation due to the impinging droplet needs to be incorporated. If two equation K-ε models are used, this can be done by equating the free surface energy destroyed to the turbulent kinetic energy created.

5.3.4 Conclusions

The flow within a GMAW pool is almost turbulent for most welding conditions, and this turbulence must be modelled if accurate predictions are to be made. The standard K-ε model appears to be best readily available two equation turbulence model. Equating the turbulent kinetic energy created and the free surface energy destroyed appears to be a suitable boundary condition for this variable. It appears that the combination of the standard K-ε and appropriate boundary conditions can provide a reasonable model of the flow driven by droplet impact.

5.4 SUMMARY AND CONCLUSIONS

Analysis has indicated that at low currents (I < 150 Amps), the interaction of the molten droplet with the weld pool surface results in the formation of a vortex ring. This vortex ring interacts with the walls of the pool and the vortex rings from the following droplets producing complex chaotic behaviour. At higher currents (I > 150 Amps), the vortex ring will not form but the flow will still be turbulent due to the high velocities. This behaviour occurs at scale well below that resolvable with the available computational meshes, therefore the pragmatic approach is to incorporate these effects into some form of turbulence models.

None of the readily available turbulence models are particularly suited for modelling complex impinging flow, however the standard K-ε two equation method is the best available choice. Application of the standard K and ε boundary conditions is not appropriate in the case of droplet surface interactions. Equating the surface energy of the droplet destroyed on impact with the generation of turbulent kinetic energy, provides a better prediction of the flow generated by droplets impinging on the pool surface. Turbulence boundary conditions for the free surface itself are poorly understood in the literature. The best available representation seems to assume Neumann or zero flux boundary conditions for this surface.

Therefore, given the current state of the art in modelling turbulence and the currently available computational resources, the best approach for the development of full 3D weld

pool models is to use the standard K-ε turbulence model and equate the turbulent kinetic energy generated to the free surface of the droplet.

Chapter 6

THREE DIMENSIONAL NAVIER STOKES SOLUTIONS

6.1 INTRODUCTION

In Chapters 3 and 4 the importance of the forces responsible for driving GMAW pool flow have been established. In Chapter 5 the importance of turbulence and the most appropriate way to model its effects have been determined. Using these results effective models of the flow within a GMAW pool have been developed.

As discussed in Chapter 1, in order to model the flow within the pool and the near weld thermal behaviour, it is necessary to solve for the Navier-Stokes equations, the thermal energy equation within the molten pool, and the thermal energy equation with appropriate boundary conditions within the solid plate. It is necessary to model the flow within the pool in three dimensions. Two-dimensional approximations, whilst useful for examining the interactions of the various driving forces, cannot predict thermal histories accurately without the use of correction factors. This is because they must ignore flow perpendicular to the plane being modelled. Inspection of experimentally measured pool shapes (see for example Figure 6.1), indicates that there is no one direction in which the flow is negligible compared to the other two directions. The weld pool shape shown in Figure 6.1 has been determined using a weld pool ejection device. This is discussed in more detail in section 6.2.6.3.

Essentially this device very rapidly removes the molten metal from the weld pool, giving an instantaneous 3D picture of the shape of the weld pool. From observation of the pool shape (and the obvious erosion patterns), the flow behaviour can be estimated. The inferred flow behaviour for a 214 Amp electrode positive, argon rich GMAW pool is shown in Figure 6.1. It is obvious in this figure that the flow has significant z and y components at the front of the pool, and a significant x component in the rear of the pool.

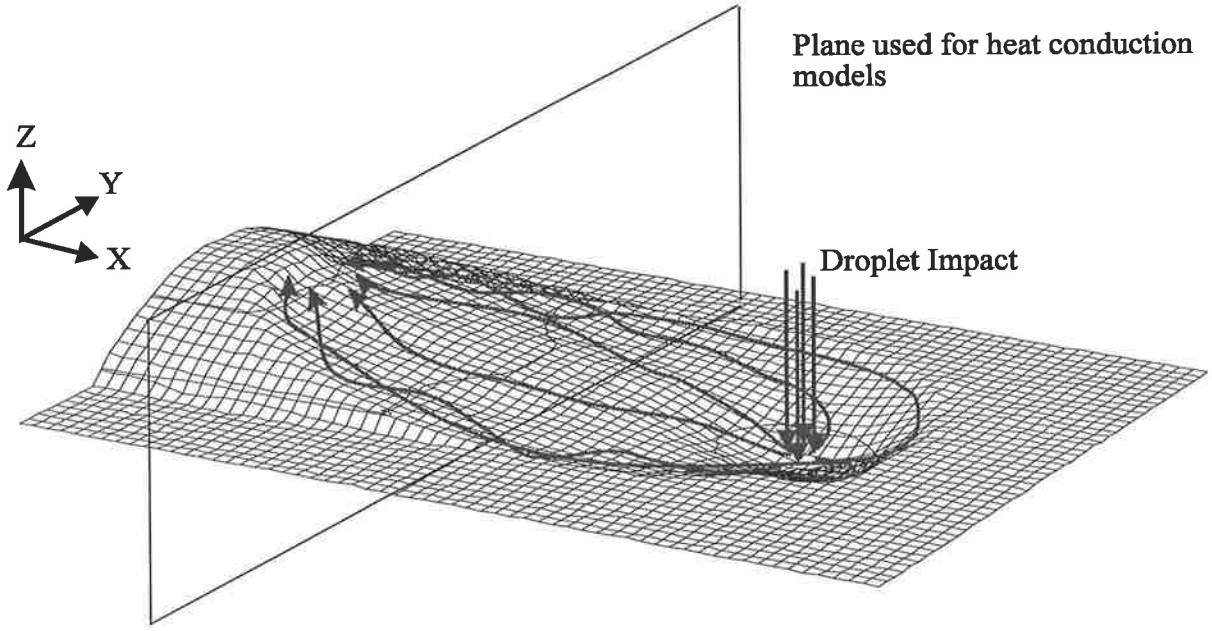

Figure 6.1 Fluid flow inferred from experimentally measured weld pool profile, Q = 1kJ/mm, v = 300mm/min, argon rich gas.

Heat conduction solutions have been able to successfully assume two dimensionality using a plane normal to the weld direction, because temperature gradients in the direction normal to the plane are small compared to that in the plane (see Figure 6.2). Although this is not entirely valid for a small region in front of the arc, it appears to give reasonable results when used with the appropriate empirical tuning factors. This approximation does not hold when

modelling weld pool flow, since majority of the fluid flow is normal to the (YZ) plane being modelled (as illustrated in Figure 6.1). Similar arguments also mean, one can not assume two dimensionality in the direction of the weld (plane ZX) as a majority of the heat flow is normal to this plane, (as illustrated in Figure 6.2).

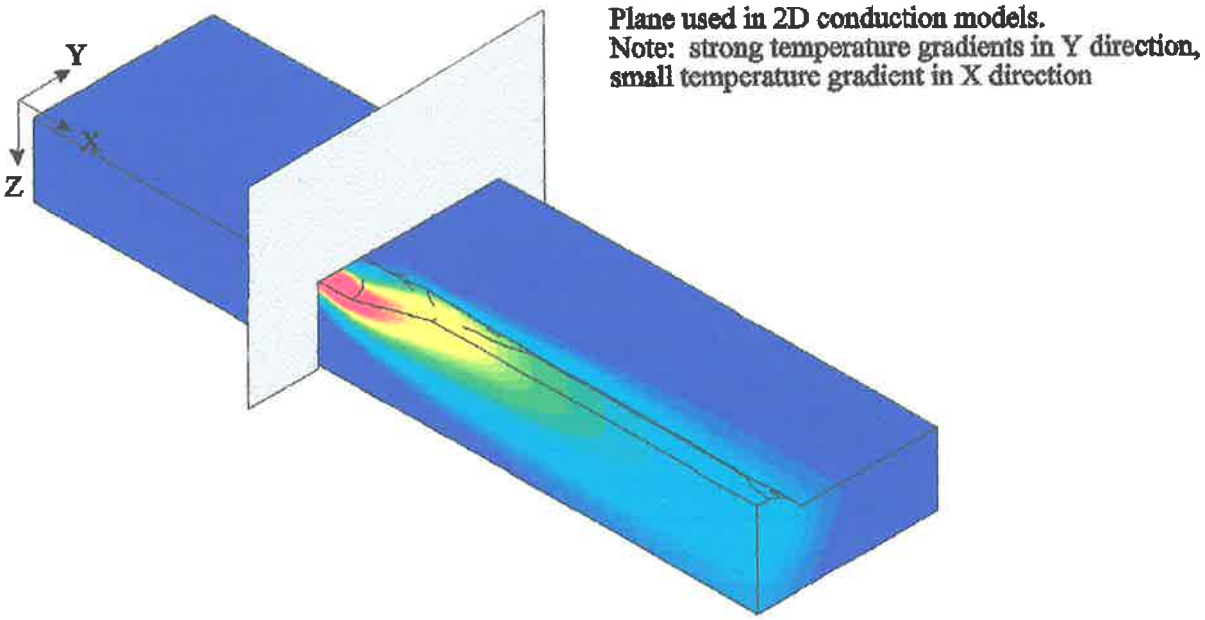

Figure 6.2 Calculated temperature profile illustrating heat flow, Q = 1kJ/mm, V= 300mm/min, argon rich gas.

6.2 THE EFFECT OF WELD POOL CONVECTION ON WELD POOL SHAPE AND NEAR WELD THERMAL HISTORY

6.2.1 Introduction

Heat conduction models cannot accurately predict near weld thermal histories or weld pool shapes without using significant empirical tuning. This has been extensively documented in the literature (see section 1.3). Much of this empirical tuning has been used to try to incorporate the effect of convection within the weld pool. In this section, predictions of near weld thermal histories from models incorporating convection within the pool have been compared to those from conduction-only models. This will help to quantify the effect of weld pool convection on near weld thermal histories, and should indicate how much of the inaccuracies of conduction models is due to poor incorporation of convective effects, and how much is due to other factors. The models that include convection incorporate the driving forces that have been shown to be significant in the analysis of Chapters 3 and 4, and turbulence as indicated by Chapter 5.

Three dimensional conduction and convection models incorporating electro-magnetic and phase change effects, require significant computational resources because of the significant number of unknowns, and the fine mesh needed to capture the melt boundary. With the currently available computational resources it is not possible to solve for the free surface position as well, because this adds another unknown and makes the solution significantly less stable. Therefore two different convection models with different boundary conditions

representing the free surface have been evaluated. These models have been compared to three different conduction models; one three dimensional, one two dimensional with a surface heat source, and one two dimensional with a complex multi part volumetric source. This will indicate the relative strengths of the various modelling approaches as well as help quantify the effect of convection within the weld pool.

6.2.2 Computational Model With Droplet Represented as Mass Flow

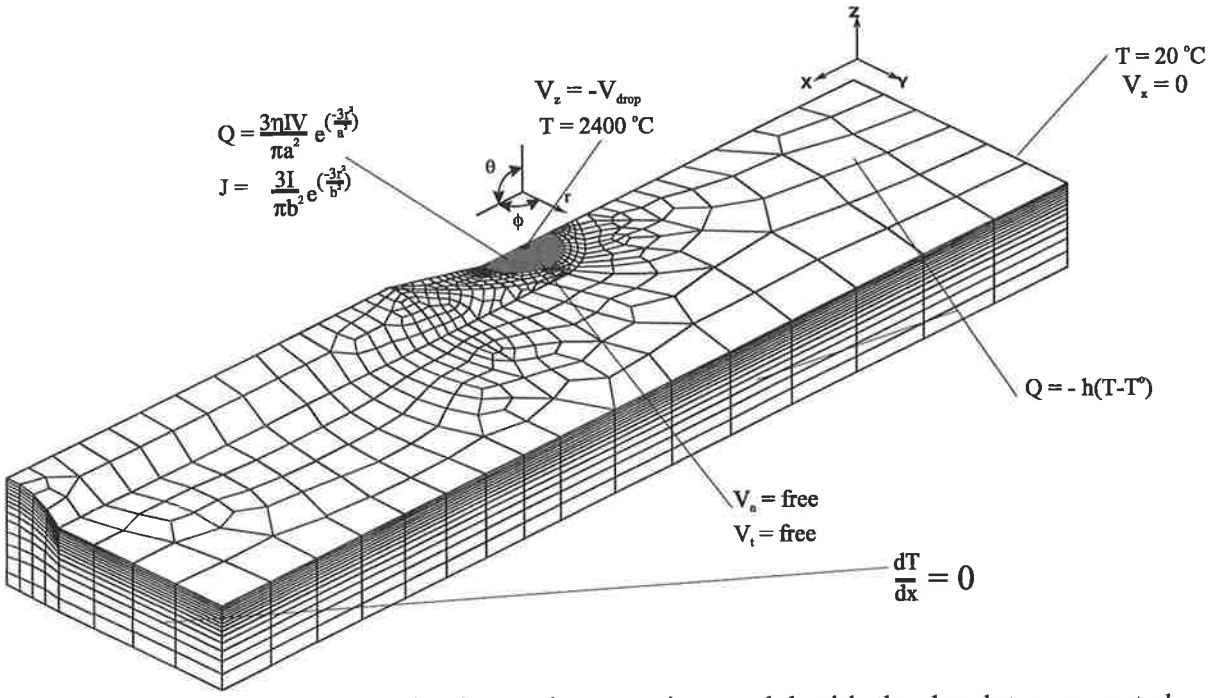

Figure 6.3 3 dimensional conduction and convection model with the droplet represented as a mass flow.

In this work, the flow within the pool has been modelled by solving the full Navier Stokes equations and the thermal energy equation, while the heat transfer within the plate is modelled by solving for the thermal energy equation with a prescribed plate velocity. Losses due to convection and radiation at the surface are included. This set of equations has been solved using the commercial Computational Fluid Dynamics (CFD) package FIDAP, which

is based on the finite element discretisation method. This approach is particularly useful for modelling weld pool flow because it allows non structured grids that are good at capturing the irregular shapes and the localised solutions that are inherent to the welding problem.

For this work the problem has been non-dimensionalised. This gives significant benefit in helping to understand the importance of various effects driving the weld pool. It also reduces the large differences in the magnitudes of the solution variables that naturally occur in melting problems, and therefore reduces numerical error and encourages solution stability. Non-dimensionalisation has been carried following the approach described in Chapter 3.

A quasi-steady state solution is assumed, this leads to significant savings in computational cost, because it effectively reduces the dimension of the problem from four to three. Furthermore it enables the use of only one mesh, rather than having to adapt the mesh at every time step to take into account the movement of the arc and the growth of the bead.

Boundary conditions have been applied to the model using two different coordinate systems. The first is a standard Cartesian system (x,y,z), with origin at the bottom front corner, and the second is a spherical coordinate system (r,θ,ϕ), with origin on the surface of the plate at the point of droplet impact. These coordinate systems are illustrated previously in Figure 6.3.

Details of the model are as follows:

(1) The model only considers the flow induced by the droplet impact and its electro-magnetic forces within the pool. Arc pressure and plasma shear forces, surface tension effects and buoyancy forces are not included. The analysis presented in Chapter 2 and Chapter 3 demonstrates that these forces are negligible compared to droplet impact forces, and can therefore be ignored without significantly sacrificing accuracy.

(2) The size, impact velocity and transfer frequency of weld droplets has been taken from previously published experimental work (Lancaster, 1984). The droplet was represented as a mass inflow with velocity equal to the root mean squared droplet impact velocity. The effective droplet radius over which this velocity acts is that required to give the correct mass flow rate.

(3) The top surface of the pool was not free to deform, and was assumed to be horizontal. A fixed pressure boundary condition was placed on the top surface of the pool allowed for continuity by letting mass flow out of the system. This is a common CFD technique for representing free surfaces (Rodi, 1980). However in this case it may not be accurate, as the fluid is free to leave the pool at any point on the surface. In reality the fluid is constrained by surface tension and arc pressure forces at the surface, and is forced to flow back along the pool. The accuracy of this assumption will be evaluated by comparing the predicted weld pool shape to an experimental one and one predicted from a model representing droplet impact as a momentum source which does not allow flow across the free surface.

(4) Along the bottom edges of the pool 'no-slip' conditions for a viscous fluid were assumed.

(5) The flow was taken to be Newtonian. This assumption has been experimentally verified by a previous researcher (Atthey, 1980).

(6) The flow within the pool was considered to be turbulent, and an enhanced viscosity model as used by Choo *et al.* (1992d, 1994) was used to account for the effect of turbulent dissipation and to encourage numerical stability. Although it was demonstrated in Chapter 5 that the standard K-ε model with appropriate boundary conditions was the best readily available turbulence model, the enhanced viscosity model is used in this section. This is because the complexity of a full three dimensional model incorporating melting and solidification, meant that computational resources were simply not available to solve another two transport equations for K and ε. However the enhanced viscosity model does incorporate the enhancement of thermal diffusion due to turbulence and should enable reasonable predictions of the near weld thermal history.

(7) The previous work in modelling flow in GTA weld pools (Zacharia, April 1992), has shown that it is important to consider the effect of temperature-dependent, thermo-physical properties. A fundamental difficulty in any calculation of the flow within the weld pool, is the lack of dynamic fluid physical properties for molten steel at high temperatures. In the present model the material properties are taken from

Zacharia *et al.* (1991). The latent heat of fusion is incorporated by calculating the specific heat capacity from the slope of the enthalpy temperature curve. As this does not involve a step in the specific heat temperature curve, this also improves the stability and accuracy of the solution. The material properties used the same scales as those presented in section 4.3.

8) Along the top surface of the pool there is a Gaussian heat distribution,

i.e. for $r < R_{arc}$: $Q^* = 3VI\acute{\eta} / (\pi R_{arc}^2)^* \exp (-3r^2/R_{arc}^{2)}$

9) Arc current is assumed to be distributed in a Gaussian manner and an effective electro-magnetic force is then calculated using equations 4.9 to 4.12.

10) Within the droplet impact zone the temperature is constrained to 2400°C in line with the experimental work from Jelmorinio *et al.* (1977).

11) Convective losses from all external surfaces are included, and symmetry about the axis is assumed.

12) The thermal boundary conditions for the model are summarised below:

At x = 0 mm: T* = ambient temperature = To/ΔT

At x = 100 mm: No temperature flux across the surface, i.e. dT/dx = 0

The discretised system of equations are solved by using a modified segregated solution technique. A segregated technique is adopted because fully coupled direct solvers require

far too much memory for a problem of this complexity. In a traditional segregated solution technique, each variable is solved for in turn; once for each iteration. In this modified version each variable is solved in turn, but pressure and the temperature are solved for repeatedly in each iteration. This acts to stabilise the pressure and temperature fields at each iteration.

6.2.3 Computational Model With Droplet Represented as a Momentum Source

In the previous section, the model represented the droplet as a mass inflow. This necessitates free velocity boundary conditions on the pool surface. This may not accurately represent the flow constraints at the surface of a real pool. Creating the need for a more appropriate free surface boundary condition. To do this the droplet has been represented as a momentum source rather than a mass flow. This enables more accurate free slip boundary conditions to be imposed on the upper surface without violating continuity requirements.

As in section 6.2.2 the model represents a quasi-steady state bead on plate weld. For numerical solution the model has been non-dimensionalised using the procedure found in Chapter 2.

As in section 6.2.2, the boundary conditions are applied using two separate co-ordinate systems. These, as well as the boundary conditions, are summarised in Figure 6.4. The model is exactly the same as that presented in section 6.2.2 except for the following points:

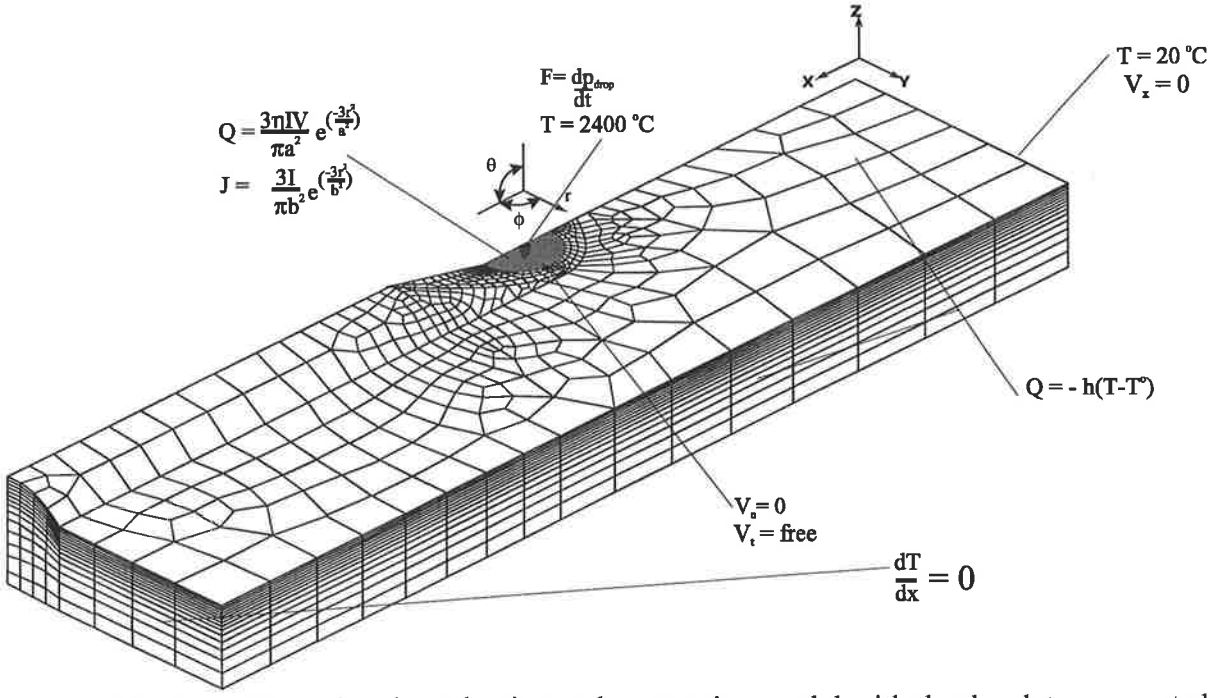

Figure 6.4 Three dimensional conduction and convection model with the droplet represented as a momentum source.

(1) The size, impact velocity and transfer frequency of weld droplets has been taken from previously published experimental work (Lancaster, 1984). The total momentum flow into the pool per unit time has been calculated as the droplet velocity multiplied by the droplet mass and the transfer frequency. This is equivalent to the total force acting on the weld pool due to droplet impact. This force is then applied as a volumetric body force to a volume with a radius equivalent to that of the drop with its top on the surface of the pool.

(2) The top surface of the pool was not free to deform, and was assumed to be horizontal. A free slip boundary was assumed at this surface and flow was not allowed across the boundary, ie. the tangential component of velocity was free and

the normal component of velocity was constrained to be zero.

The discretised system of equations are solved by using a segregated solution technique. A segregated technique is adopted because fully coupled direct solvers require far too much memory for a problem of this complexity. An incremental solution strategy has been used. This involves solving the problem repeatedly, gradually increasing the driving force each time and using the previous solution as the initial guess, until the actual driving force is reached. As the initial guess is close to the final solution, it is within the radius of convergence of the segregated solver.

6.2.4 Three Dimensional Conduction Only Solutions

In order to help quantify the effect of convection on the heat transfer within the pool, a conduction only models (incorporating exactly the same thermal boundary conditions and mesh) was used without solving for convection within the pool. This should enable direct evaluation of the effect of convection on near weld thermal histories and weld pool shape.

All model details are exactly the same as those in sections 6.2.2 and 6.2.3, except that convective flow is not considered in the molten pool.

The thermal boundary conditions are exactly the same as those presented in section 6.2.2, and are shown in Figure 6.5.

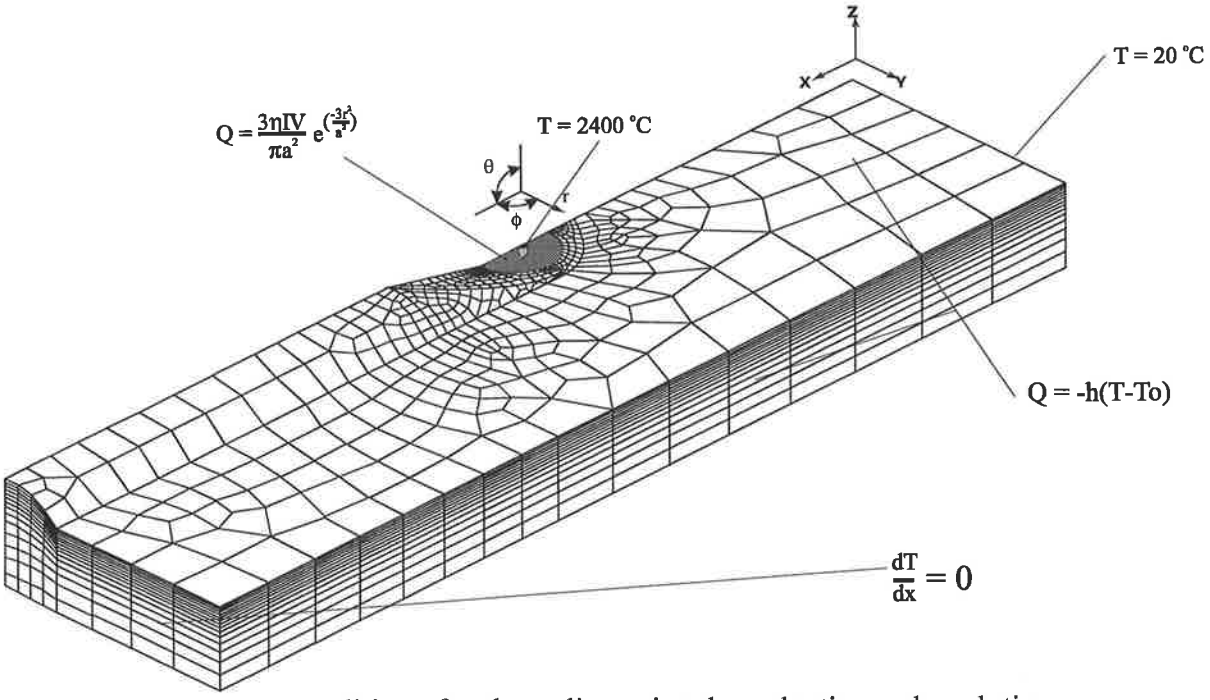

Figure 6.5 Boundary conditions for three dimensional conduction only solutions.

6.2.5 Two Dimensional Conduction Only Solutions

Often traditional conduction models are often based on two dimensional transient solutions. Hence it is also useful to compare results from these models to ones from the more complex three dimensional quasi-steady state models. Comparison will be made to models incorporating two different heat sources with the first having a Gaussian surface source identical to the three dimensional models of sections 6.2.4, 6.2.3 and 6.2.5. The second model incorporates a complex two part volumetric heat source, as used by Painter (1994).

6.2.5.1 Surface source

The three dimensional convection models represent the arc as a Gaussian heat source at the surface in line with experimentally indicated arc current distribution. This is appropriate as they allow for the redistribution of this heat due to convection, by solving for the convection within the pool. Whilst early conduction models used surface heat sources, more recent models have used volumetric heat sources because surface sources do not give accurate predictions. In this case we wish to evaluate the inclusion of convection and so must compare models with identical boundary conditions, therefore a surface Gaussian source has been used, considering this to be the "true" condition..

6.2.5.2 Volumetric source

In recent times researchers have developed complex distributed heat sources for conduction only models, (see section 1.3). A model of this nature is included in this comparison to evaluate the effectiveness of using modified source distributions to account for convective flow in two dimensional conduction-only solutions. The model used in this case uses a double Gaussian volumetric heat source to represent the heat from the arc, as well as a point heat source located at some distance below the surface to represent the heat contained within the droplet (see Figure 6.7). This form of source definition gives rise to empirical tuning factors which must be derived from comparison with experiment. The empirical tuning factors used in this model are those of Liew (1992).

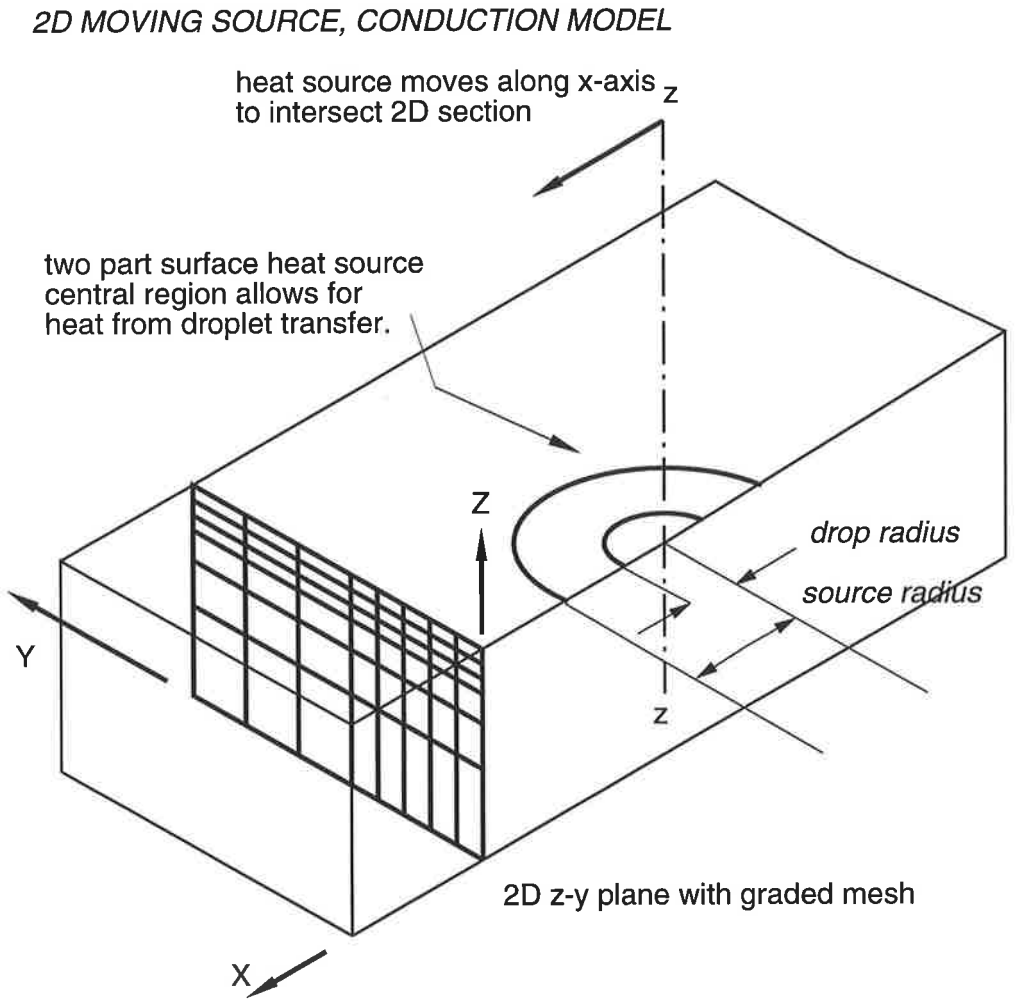

Figure 6.6 Two dimensional conduction only model with surface source.

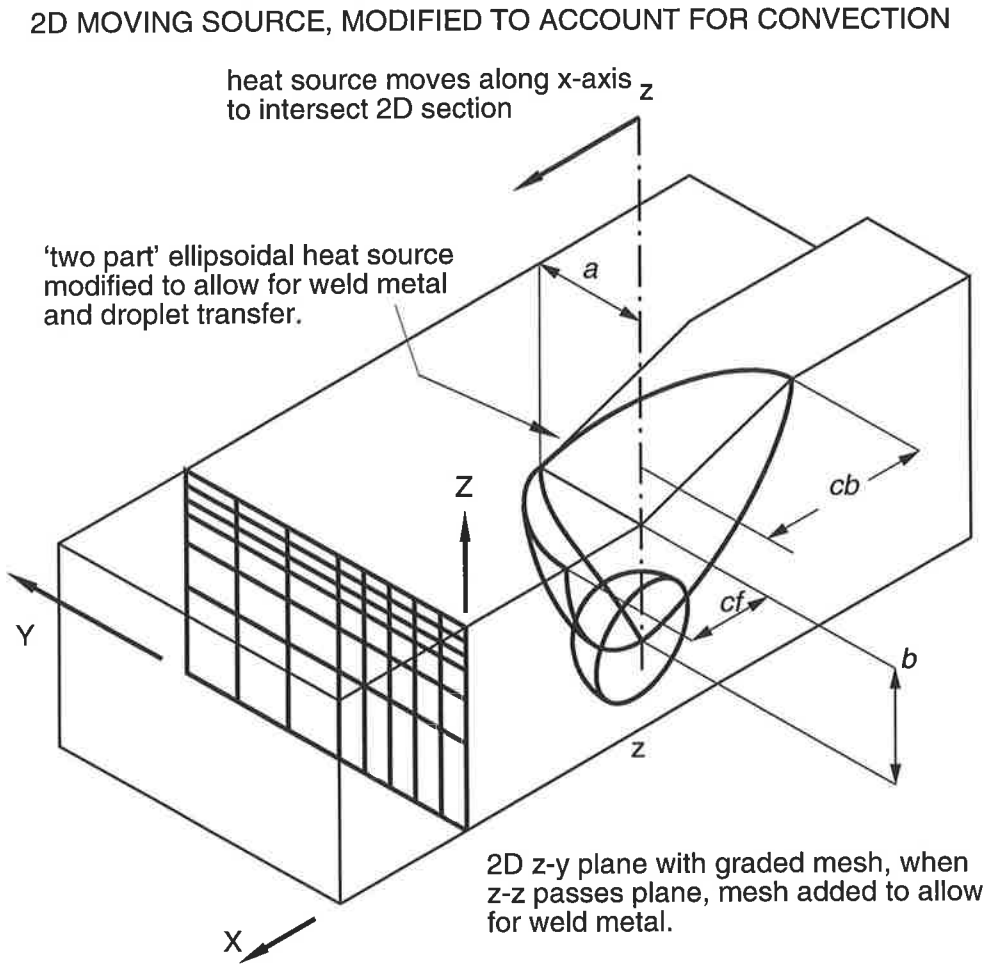

Figure 6.7 Two dimensional conduction only model with volumetric source.

6.2.6 Experimental Validation

6.2.6.1 Introduction

In order to provide confidence in the predictions of the computational model, some form of experimental validation is required. Various techniques that have been used to verify the

results of the above models are outlined in the following sections.

6.2.6.2 Weld Pool Filming

While it is not possible to observe the flow within the weld pool, it may be possible to observe the surface behaviour. This would act as a valuable validation for the predicted surface velocities. A fundamental problem with filming processes that include an arc, is that the intense light created by the arc renders the viewing of everything else impossible. Obviously if surface behaviour is to be observed the effect of the arc must be eliminated in some way. A pulsed laser camera has been used to examine the weld pool behaviour. This device uses several lasers firing in series with the camera shutter. The laser light is more intense than that of the arc, allowing viewing of the pool surface.

To examine the validity of the computational model experimental welds with the same input conditions as those modelled, were filmed with pulsed laser camera. Unfortunately this did not provide much significant information. The lasers, although removing the arc, did not provide a diffuse source so the image was very shadowy and it was impossible to observe the form of the pool surface. There was also a problem with the reflection of the laser from the smooth weld pool surface, further obscuring the view of the pool. Finally, the camera was only able to film at 30 frames per second, which is inadequate given that the droplet transfer is in the order of 300 Hz and the resonant frequency of the weld pool of the order of 10 Hz. This frame rate was so low that much important information was missing or indecipherable due to aliasing effects.

Further attempts have been made to observe the surface behaviour using a sodium lamp to illuminate the weld pool. The pool was then filmed through a monochromatic filter. The sodium lamp is stronger at the filter frequency than the arc and it should therefore swamp out the arc allowing viewing of the pool surface. As the sodium lamp is a diffuse source, the problems due to shadows and reflections that occurred with the laser source should be reduced. However, light reflecting in the fumes produced by the welding process made viewing the pool surface impossible.

At this stage all attempts to film the pool have been unsuccessful, therefore model validation has focused on validating temperature prediction by comparing the predicted weld pool shapes and near weld thermal histories with experiment.

6.2.6.3 Weld Pool Ejection Device

A weld pool ejection technique has been used to examine the shape of the weld pool using a weld pool tipping device which has been developed in the CSIRO-Division of Manufacturing Technology Adelaide laboratories and provides similar information to weld pool sections. Instead of a 2-D slice the full 3-D picture of the weld pool is available. This has the significant advantage in that the shape of the pool in front of and behind the point of droplet impact can be examined, rather than just the depth of maximum penetration.

The weld pool ejecting device holds the base metal in position while the weld is being performed, and then rapidly pulls it away and inverts it. This breaks the arc and ejects the molten metal giving an instantaneous picture of the weld pool shape. This device has been

of significant use for evaluation of predicted weld pool shapes. A wide array of different welding conditions have been investigated and profiles digitised by Gunter & Sparrow (1993). The measured length, depth and width have been compared to that predicted by the computational models.

6.2.6.4 Temperature Measurements

It is relatively common practice to embed thermal-couples near the weld pool and use the thermal histories from them to determine the thermal behaviour within the plate. Liew (1992) has performed such experiments for bead on plate welds under a variety of welding conditions. His results have been used to provide experimental information on the maximum and minimum $T_{8/5}$'s for a given weld. This has also been used to validate the predictions provided by the computational models.

6.2.6.5 Summary

Whilst it is not possible to gain experimental information on the flow behaviour within a GMAW weld pool, it is possible to gain information on the weld pool shape and near weld thermal histories. As these are the primary variables of interest when predicting weld pool flow, it is appropriate to use them to confirm the predictions of the numerical models. Therefore the weld pool length, depth, width and the maximum and minimum $T_{8/5}$s predicted by the numerical models will be compared to those determined experimentally.

4.2.7 Comparison of Numerical Models

Bead on plate (electrode positive, 1.2mm diameter solid electrode, Argon rich gas, 300mm/min) welds, carried out at three heat inputs of 0.5, 1.0 and 1.5 kJ/mm. Weld pool shapes were measured experimentally using the weld pool tipping device and the near weld thermal histories measured using thermo-couples. The different models are compared to experiment and to one another in Figures 6.15 to 6.17, with the results are expressed as percentage of the measured experimental values. Typical flow patterns, weld pool shapes and temperature profiles as predicted by the convection models are shown in Figures 6.8 to 6.13.

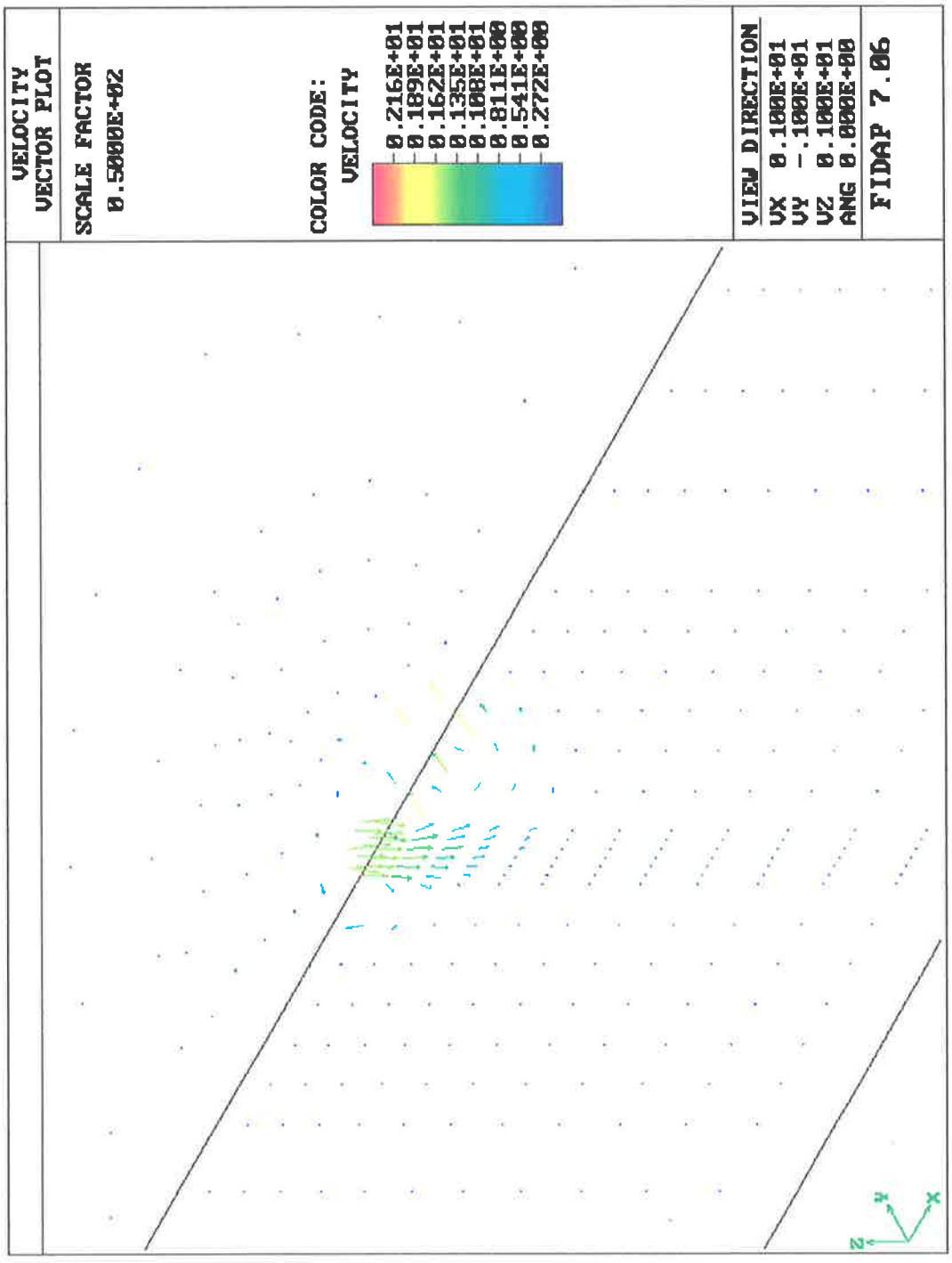

Figure 6.8 Vector velocity plot: Mass flow source, Q = 1.5 kJ/mm, V = 300mm/min, Argon rich gas.

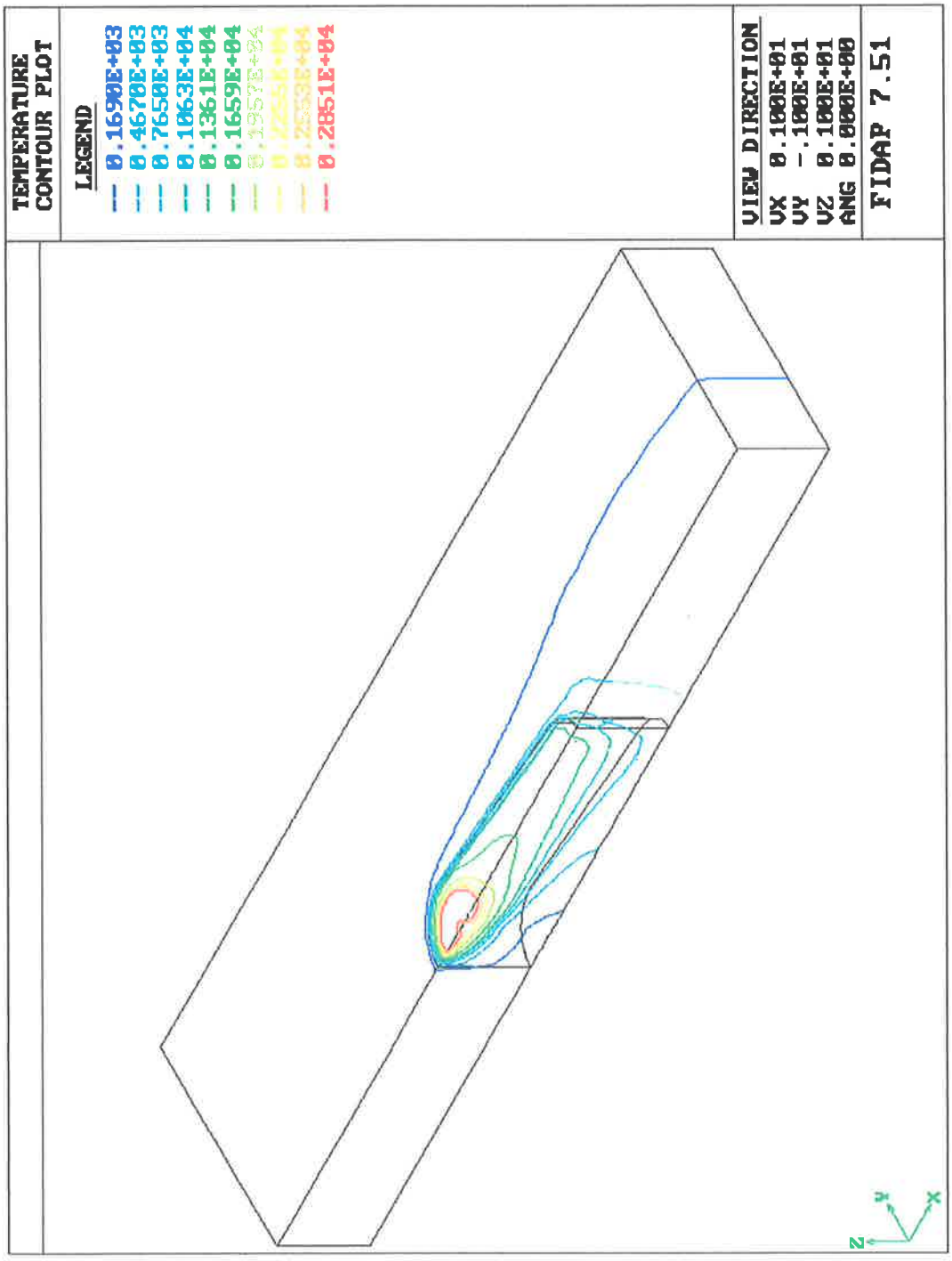

Figure 6.9 Temperature contour plot: Mass flow source, Q = 1.5 kJ/mm, V = 300mm/min, Argon rich gas.

Figure 6.10 Predicted pool shape: Mass flow sourceQ = 1.5 kJ/mm, V = 300mm/min, Argon rich gas.

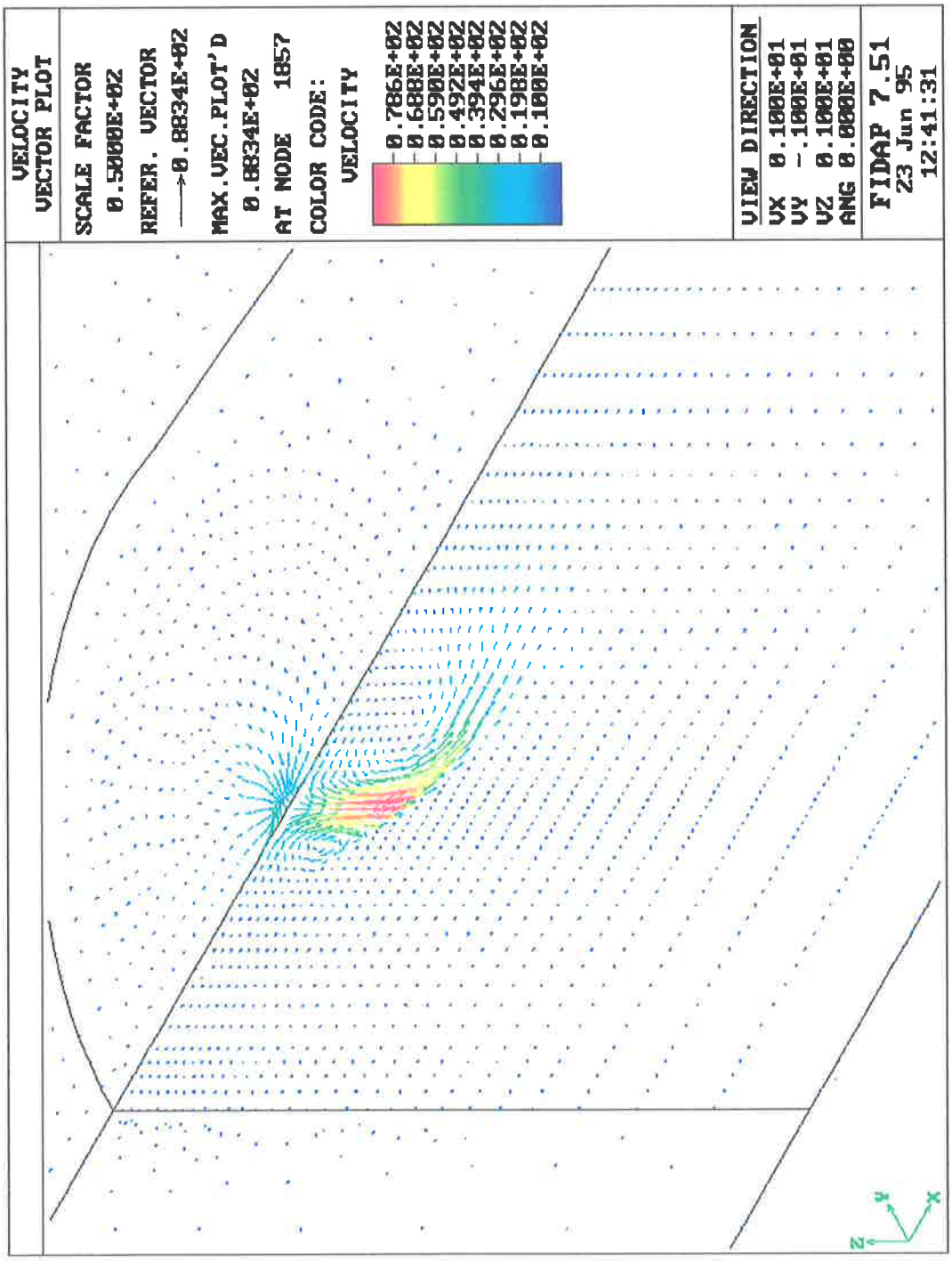

Figure 6.11 Vector velocity plot: Momentum source, Q = 1.5 kJ/mm, V = 300mm/min, Argon rich gas.

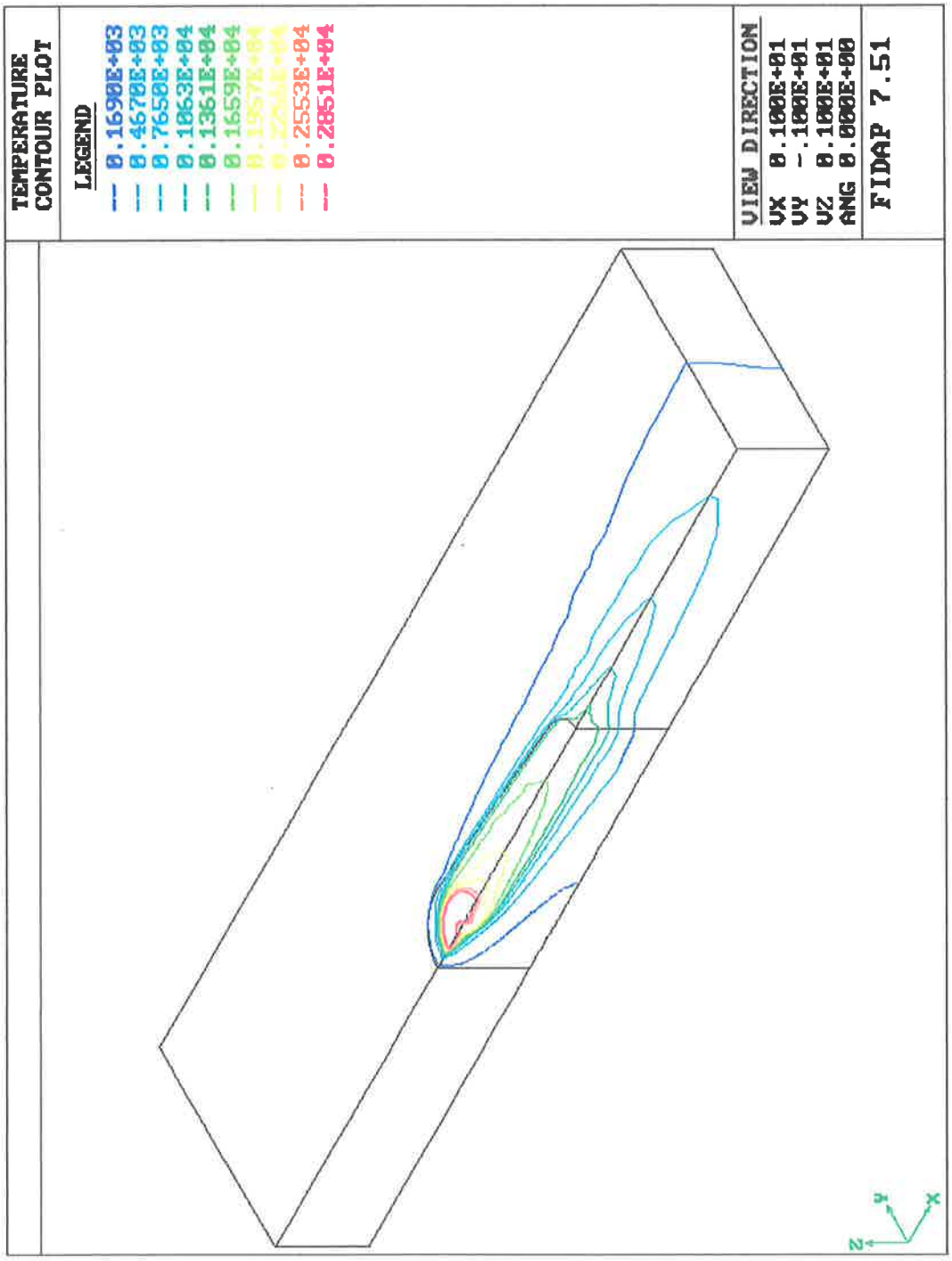

Figure 6.12 Temperature contour plot: Momentum source, Q = 1.5 kJ/mm, V = 300mm/min, Argon rich gas.

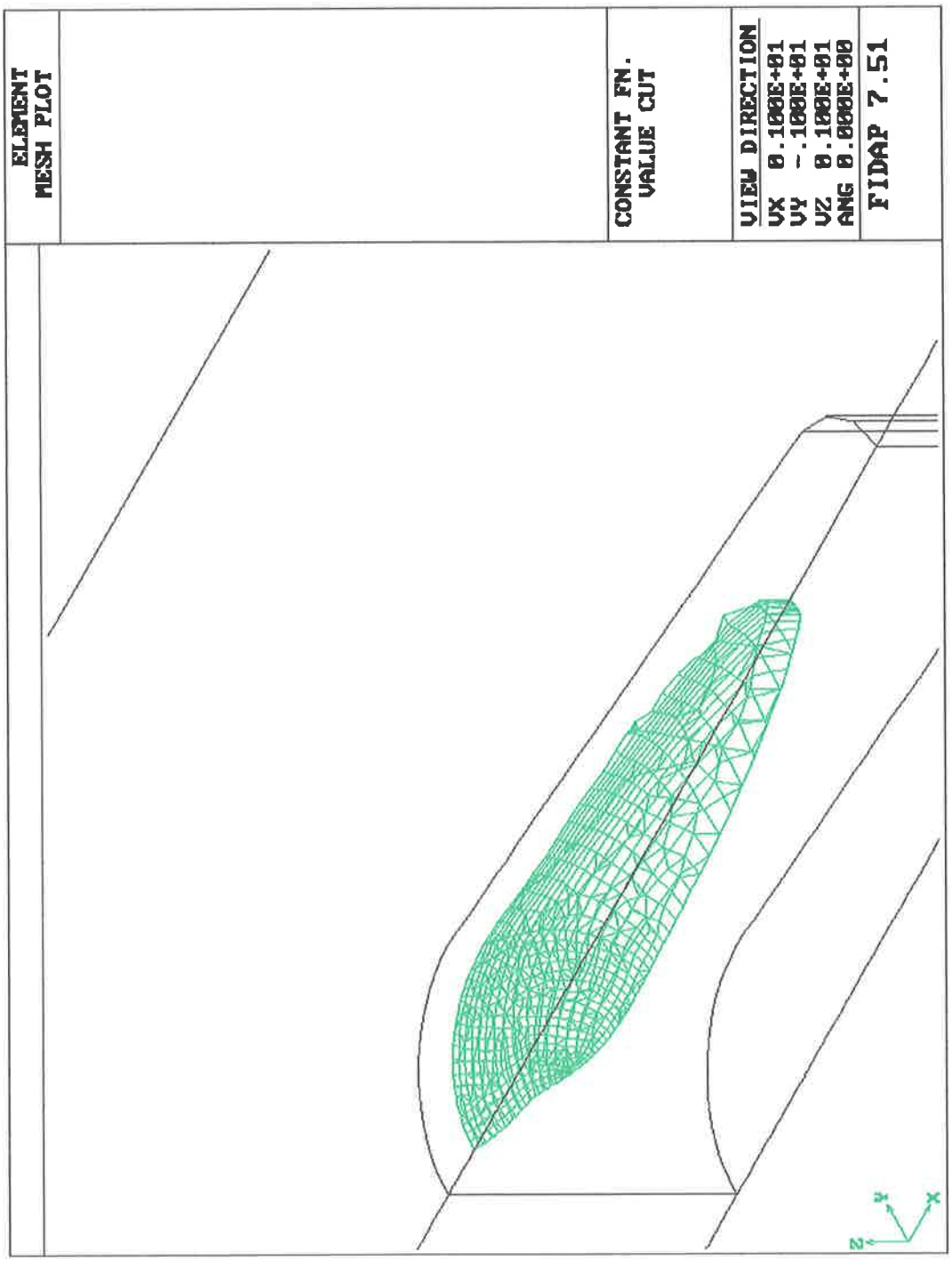

Figure 6.13 Predicted pool shape: Momentum source, Q = 1.5 kJ/mm, V = 300mm/min, Argon rich gas.

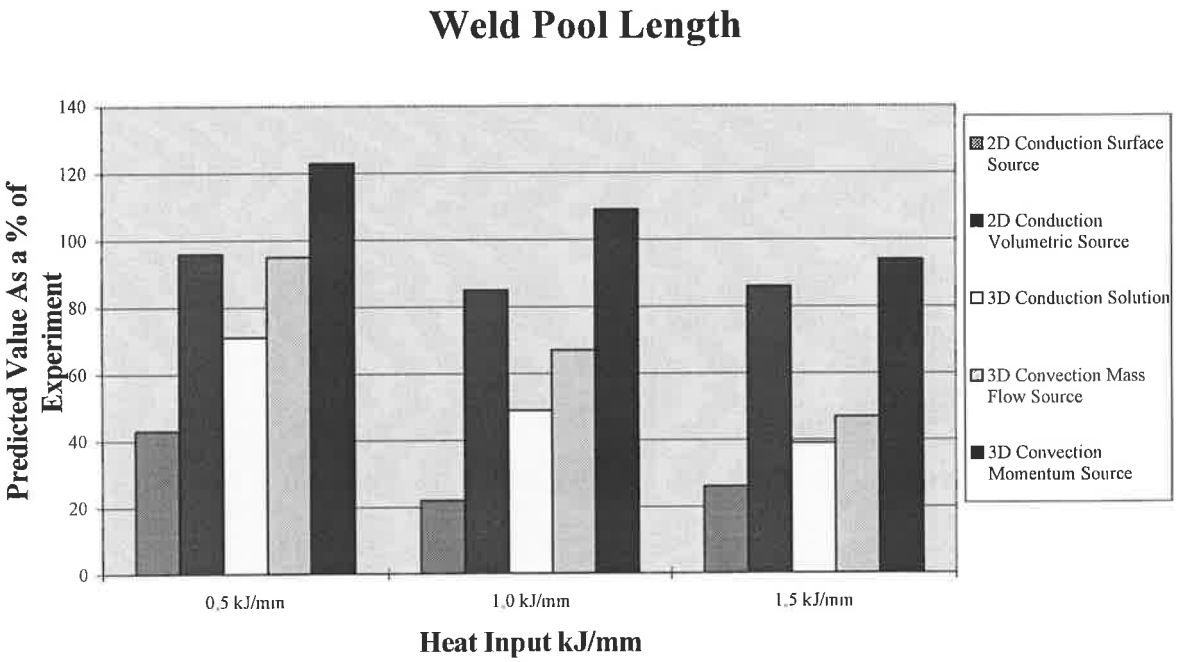

Figure 6.15 Model comparison: Weld pool length.

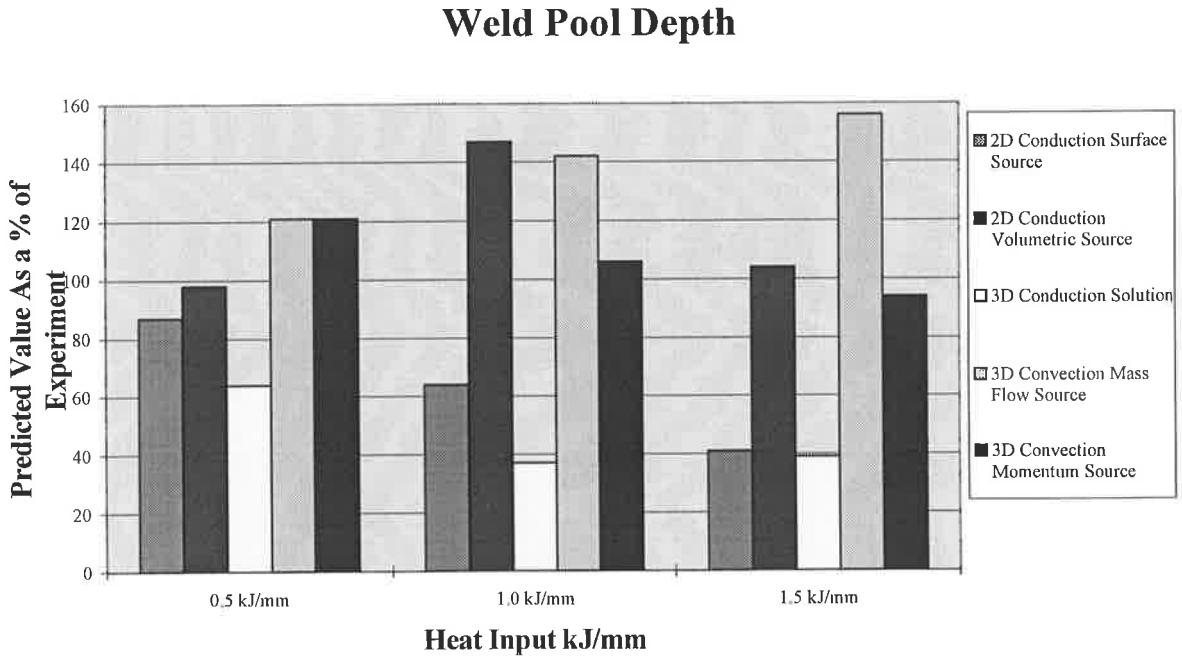

Figure 6.14 Model comparison: Weld pool depth.

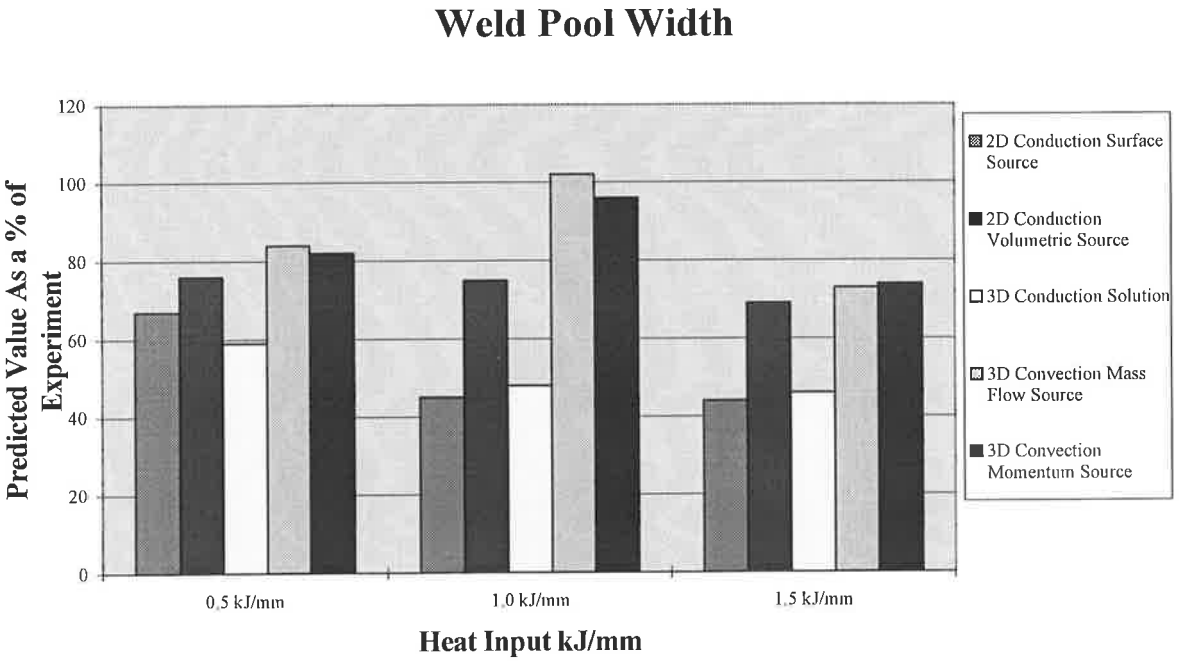

Figure 6.16 Model comparison: Weld pool width.

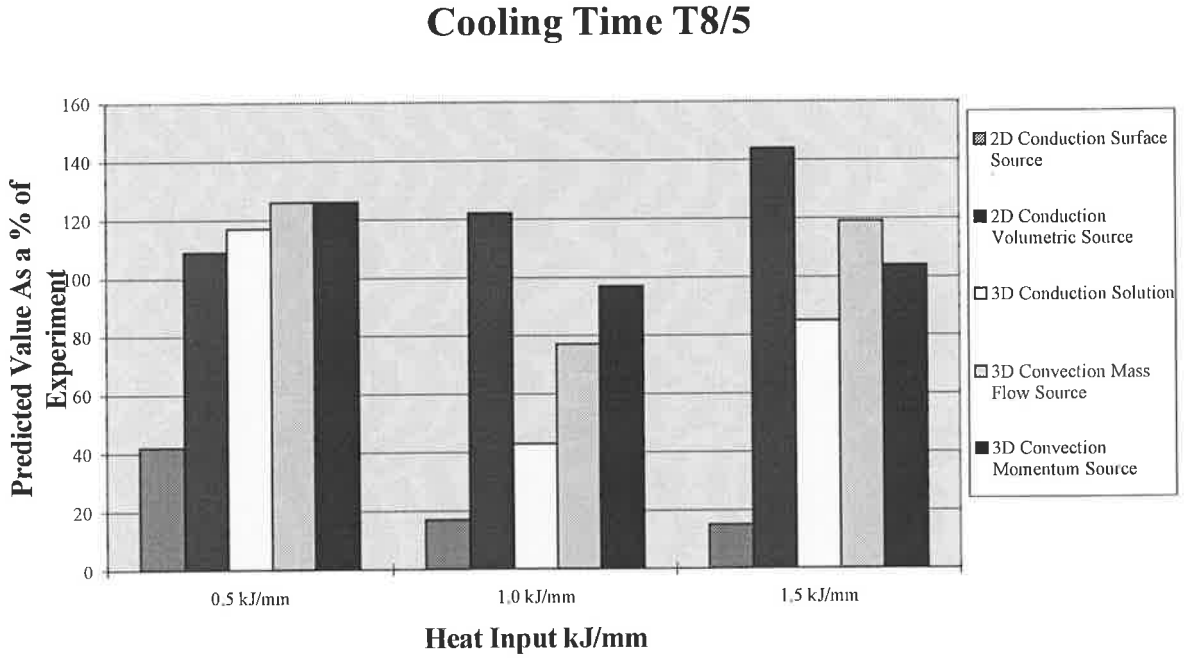

Figure 6.17 Model comparison: T8/5 cooling times.

6.2.8 Conclusions of Model Comparison

It is apparent from Figures 6.15 to 6.18 that the models incorporating convection within the pool are more accurate than the unmodified conduction alone solutions. Both the two and three dimensional models using the surface source were far less accurate than the either of the convection models or the modified conductivity model. Even though the heat distribution from a welding arc has been experimentally measured to be a surface Gaussian, it is obvious that unless convection in the pool is taken into account this is very poor representation of the GMAW process. It is apparent that convection must be incorporated either into the heat source formulation as in the modified conduction source or directly solved for as in the convection models.

Of the two convection models, the one using the momentum source with the free slip upper surface boundary conditions is much more accurate than the one using the mass flow source and the fixed pressure free surface boundary condition. This clearly demonstrates the importance of accurately representing the upper free surface. It is probable that if computational resources allowed for the position of the upper free surface to be solved for, even more accurate solutions could be obtained. It is clear from Figures 6.10 and 6.13 that the characteristic "finger and crater" profile, whilst being present, is not as intense as that observed experimentally. This is due to the relatively crude enhanced viscosity turbulence model used. If a more accurate turbulence model could be used a more intense finger and crater would be formed. This is because in the current model the viscosity is enhanced throughout the entire pool, smoothing out the flow behaviour and temperature profiles. In a more advanced model the viscosity is dependent on the flow behaviour and therefore varies

locally; this allows for more rapid variation in the dependent variables.

The modified two dimensional conduction only solution is of a similar accuracy to the most accurate convection solution. However a good comparison is to be expected in this case due to the empirically tuned volumetric nature of the heat source. The heat source has effectively been tuned by adjustment of the defining parameters in order to get agreement with experimental results. This heat source requires up to 7 empirical tuning factors only 1 of which can be directly empirically linked to arc current. Such models cannot be used outside the tightly constrained conditions in which it has been experimentally verified. In contrast the convection solution requires only 3 empirical inputs, the droplet momentum the arc efficiency and the effective arc radius. Furthermore the droplet momentum can be linked to the process parameters. However the 3 dimensional convection solutions do require vast computational resources; approximately 3 weeks of CPU time on a Sun 10/30 workstation. An ideal solution would combine speed and efficiency of the modified conduction solution with the accuracy and reduced empirical input required for the convective solution.

6.3 CONCLUSIONS

The results demonstrate that the inclusion of convective flow within the weld pool does significantly improve the accuracy of the predicted weld pool shape and near weld thermal histories. Three dimensional convection models require significant computational resources; approximately 100-1000 times that required for the three dimensional conduction-alone models. Therefore, there would be significant benefit if conduction-only models could be modified to accurately include the effect of conduction within the weld pool. Traditional heat source modifications do this through almost arbitrary empirical tuning. The amount of empirical tuning required needs to be reduced and reflect the effect of process parameters if such a technique is to be useful in a practical environment. The development of a model that includes reduced empirical input (required by the convection models), with the computational efficiency of the conduction solution, is the focus of the next chapter.

It should be noted that the use of the K-ε turbulence models and modified K-ε boundary conditions, as recommended in Chapter 5, have not been used in the models presented in this chapter as originally intended due to the significant computational cost. Chapter 5 has been included in the thesis as it provides information on the importance of turbulence in modelling weld pool flow and suggests appropriate ways to model its effect. As such Chapter 5 gives important insight into nature of the flow within the pool and methodology for future modelling efforts.

Chapter 7

MODIFIED THREE DIMENSIONAL CONDUCTION SOLUTIONS

7.1 INTRODUCTION

The previous chapter has demonstrated that convective heat transfer must be included if accurate predictions of near weld thermal histories are to be made. It has also demonstrated that flow within a GMA weld pool is highly complicated with many different influences, not all of which can be incorporated into the numerical models given currently available theoretical and computational resources. Even with the rapid increase in computational power, the solution of a fully coupled set of equations which accurately couple the arc to the weld pool and to the base metal are still a long way from being solved in a research environment, let alone an everyday industrial setting. Therefore there would be significant benefit in being able to incorporate convective affects without solving the full Navier-Stokes equations.

Previous attempts to model weld pool convection both within this thesis and the open literature, have had to make many assumptions to reduce the problem to a size that can be solved with current computational resources. These assumptions include:

i) The coupling between the arc and the pool: All models to date, including those within this thesis, have assumed Gaussian heat and current distributions. This has been shown to be questionable by Choo *et al.* (1992) when the pool surface is distorted. Furthermore the coupling between the arc and the pool may lead to a significant increase in the importance of electro-magnetic driving forces at very high currents (I >> 250 Amps).

ii) Free surface effects: To date nobody has accurately modelled the free surfaces including the effects of the arc, metal transfer and the flow within the pool. In the previous chapter, solution for the free surface position was attempted. However when combined with all other demands (including emf and melting/solidification) the task was beyond the available computational resources. Kim & Na (1994) have tried to incorporate free surface effects but their solution did not include the effects of weld pool flow which was shown to be important by Lin & Eagar (1985), or metal transfer (which was shown to be much larger than arc pressure force in Chapter 4). Therefore the validity of their results must be questioned. The location of the free surface is important in terms of the point of application for the arc and droplet heat sources. If the point of application of the heat source is wrong, then inclusion of convective effects will not remove this error.

iii) Turbulence: The transitional to turbulent flow found in the GMA weld pool has not been accurately included in three dimensional models. The axi-symmetric GTA models of Choo *et al.* (1992) have incorporated turbulence via simple enhanced viscosity thermal conductivity and a more complex K-ε model. The results of Chapter 5 showed that both of these approaches did not model impinging flow well.

In the previous chapter the cost of implementing the K-ε model was prohibitive, let alone the more complex second order schemes that would be needed to accurately model the turbulence. Furthermore, these complex differential stress models require knowledge of the distance from the boundary and the boundary conditions for the individual stress components. Techniques for determining this essential information for all but the simplest cases do not exist and these models are some way off practical application. In addition researchers within the field do not have a clear understanding of the effect of a free surface on turbulence (Miyata, 1994). There are no available turbulence models that can accurately accommodate the effect of the free surface on turbulence (Miyata, 1994); in particular the effect of breaking, folding and connecting surfaces on the turbulence within the fluid is poorly understood. Turbulence models that incorporate these effects are required if accurate predictions of the flow induced by droplet coalescence is to be achieved. Even with the rapid increase in computing power accurate models of weld pool convection will not be possible until suitable turbulence modelling schemes can be practically implemented.

Turbulence can have a significant effect on heat and fluid flow, therefore the crudity of the assumptions needed to model it may have a significant effect on the predicted weld pool shape. With currently available computational resources, only crude zero equation turbulence models can be used in full three dimensional weld pool models. Chapter 5 shows that this technique does not accurately capture the detail of the flow behaviour. Although Chapter 6 reveals that even with this limitation, models that incorporate the effect of convection provide significantly better results than those

without convection.

Given the relative crudity of the assumptions needed to allow a tractable solution to the full convection problem, it is probable that further simplification of the problem to eliminate the need to solve the full Navier Stokes equations will not significantly reduce the accuracy of the solution. Although it is apparent that convection must be included, it is likely that an analytical or order of magnitude technique will provide a solution of a similar accuracy to the full solution, with a significant reduction in the computational cost. The following section will develop an analytical technique that models the effect of convection using enhanced thermal conductivity within the weld pool.

7.2 EFFECTIVE THERMAL CONDUCTIVITY SOLUTIONS.

7.2.1 Introduction

Convection within the pool significantly enhances the heat transfer in the direction of the flow over that provided by conduction alone. Traditional heat transfer solutions have used modified heat distributions, or modified the thermal conductivity of the molten metal in an attempt to simulate the effect of fluid flow (see Chapter 2 for examples). However this has been done on a relatively ad hoc basis, effectively using the distribution form and the conductivity as tuning factors to improve the accuracy of the solution.

The most commonly used approach within the literature is to model the weld pool as a modified Gaussian volumetric heat source. The volume over which the heat is distributed is prescribed by empirical constants, (see Chapter 2). Because of the volumetric nature of this source the effect of the fluid flow is included within its formulation, (for example see Figure 6.7). Unfortunately, in order to accurately predict near weld temperatures the correct empirical tuning factors are required, and determining these parameters for every combination of process input conditions and work-piece geometry is impractical. The distribution of heat flow across the pool boundary can not be directly measured, and will undoubtedly vary significantly with variation in operating parameters. Therefore it is impossible to see how closely the assumed distribution matches reality. However, the form of the heat distribution from the arc to the pool surface is commonly assumed to be Gaussian following experimentally measured current distributions and the heat from the droplets can be represented as a point source. Therefore if it were possible to accurately predict how the

flow within the pool redistributes this heat, a more accurate and broadly applicable heat source should result, (see figure 7.1 for diagrammatic representation). Convection within the pool locally enhances the transport of heat within the pool effectively increasing the local thermal conductivity. If it were possible to systematically link the directional conductivity with the parameters driving weld pool flow, so as to model the effect of the convection, a significantly more accurate model should result.

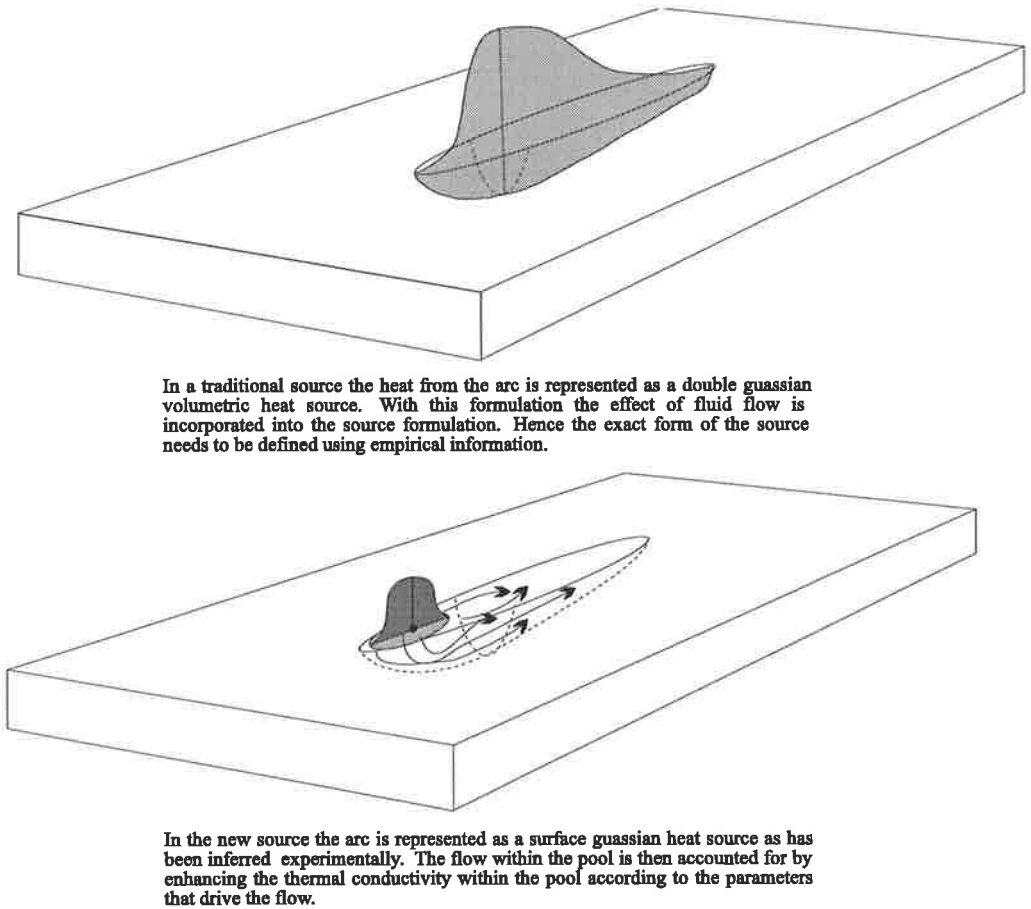

Figure 7.1 Comparison of the traditional volumetric heat source with the enhanced thermal conductivity solution.

7.2.2 Calculation of Effective Thermal Conductivity

Obviously some analysis is required to link the thermal conductivity to the flow conditions. This is extraordinarily difficult analytically as there are very few known solutions to the Navier-Stokes equations, and all of these are for relatively simple geometries and boundary conditions. A full regression analysis of experimental data is also very difficult because of the vast number of variations in process parameters and work-piece geometry. However an analytical solution combined with a scale analysis using empirical data provides a relatively simple technique for providing relatively accurate answers with a minimum of empirical tuning.

It should be noted that changing the effective thermal conductivity of the liquid metal affects the weld pool shape relatively slowly. Simple tests have shown that a large change in the effective thermal conductivity changes the pool depth only slightly. Given that this effect is so small, the calculation of effective conductivity need not be highly accurate and an order of magnitude analysis should be satisfactory.

Convective heat transfer is measured non-dimensionally by the Nusselt number: $N = \frac{hL}{k}$, where h is the convective heat transfer coefficient, L is a typical length scale and k is the thermal conductivity. When calculating the heat flow between two surfaces across a liquid layer, Grober (1961) has shown that the Nusselt number represent the ratio of effective conductivity to real conductivity. This means that the Nusselt number represents the ratio of the apparent conductivity, $k_e = hL$ to the true conductivity k, and directly represents a measure of the increase of heat transfer due to convection over that by pure conduction

through a layer of stagnant fluid.

$$N = \frac{k_e}{k} \tag{4.1}$$

Therefore if we can calculate the Nusselt number of weld pool flow we can calculate the effective thermal conductivity. Following Choo *et al.* (1992), let us assume that the effect of turbulence within the pool can be represented by an increase in the viscosity and the thermal conductivity. Therefore the flow within the pool is considered as a laminar flow with an effective viscosity and an effective conductivity. Semi-analytical techniques are available to calculate the Nusselt number for various flow situations. In the case of the weld pool let us consider an idealised pool, as two dimensional flow into a wedge. Using the similarity analysis and the Falkner Scan (Cebeci & Bradshaw 1984) transformation, the governing partial differential equations can be reduced to ordinary differential equations and some simple solutions for given situations determined. For details of this procedure see Cebeci and Bradshaw 1984. This analysis gives the following equations for the Nusselt number:

$$N_u = 0.564\sqrt{(m+1)}\ \ Pr^{\frac{1}{2}} Re^{\frac{1}{2}} \tag{4.2}$$

for a Prandtl number < 1, where m is defined by $\beta = \frac{2m}{m+1}$ and $\frac{\pi}{2}\beta$ is the wedge angle as defined in Figure 7.2.

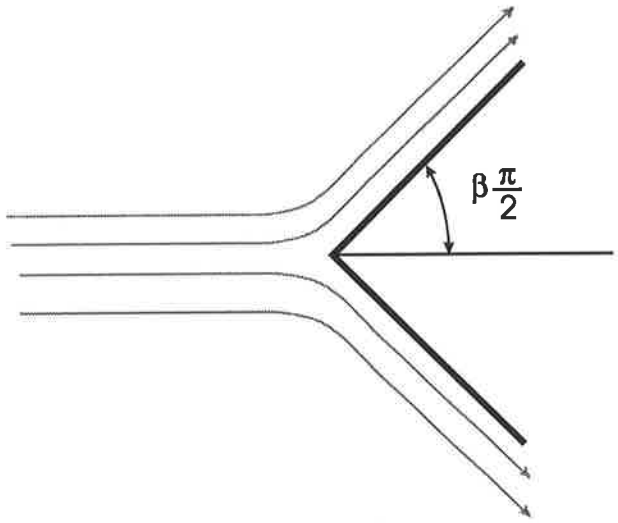

Figure 7.2 Flow past a wedge

Taking β equal to 1, (ie. m equal to 1) represents flow impinging on a plate held normal to the flow. This can be considered as a first approximation to the flow within the weld pool. Defining the Reynolds number (using the droplet impact velocity and wire diameter), taking droplet impact velocity from the literature (Lancaster, 1981) and substituting it into the equation, gives the following plot of effective thermal conductivity multiplying factor versus current.

As can be seen in figure 7.3, this analysis leads to effective thermal conductivity multiplying factors ranging between 6 and 28. These values are somewhat larger than the 6-10 enhancement factors quoted in the literature, however the effective thermal conductivity values used within the literature are for use with volumetric heat sources. In that case the effective thermal conductivity effectively approaches infinity as the heat is added directly to every point within the volume.

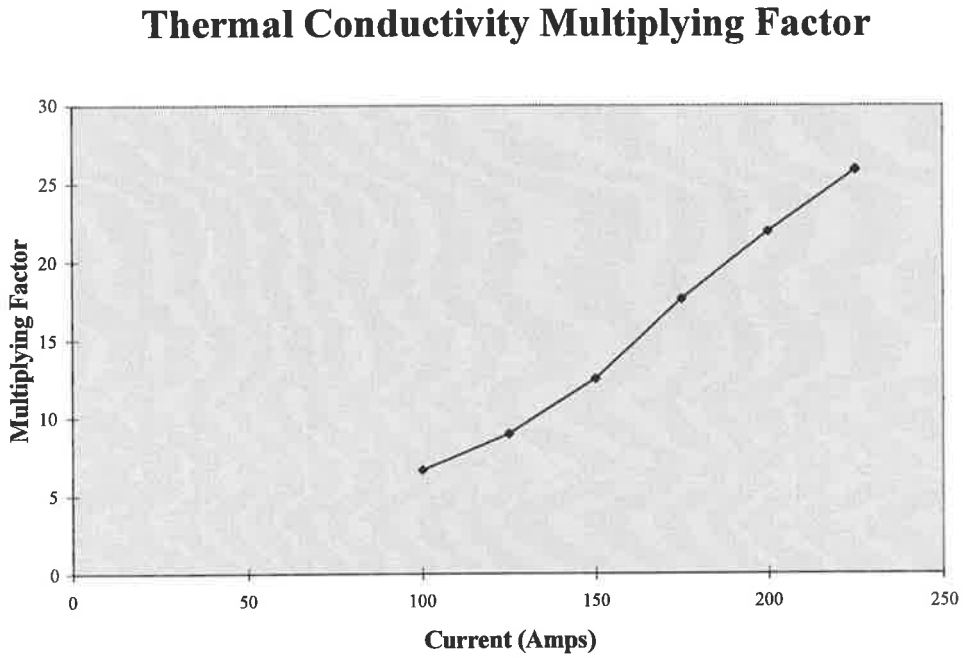

Figure 7.3 Variation of thermal conductivity multiplying factor

7.2.3 Computational Model

The effective thermal conductivity approach outlined above, has been tested by using it to predict weld pool shape and thermal histories and comparing the results to experiment and full convective solutions. The thermal boundary conditions and solution technique were identical to those for the three dimensional conduction-only solution presented in section 6.2.4 and Figure 6.5, and are not repeated here.

7.2.4 Results and discussion

Typical temperature profiles and weld pool shapes are presented in Figure 7.9 and Figure 7.10. The predicted weld pool depth, length, width and $T_{8/5}$'s are compared to the momentum source convective model from the previous chapter in Figures 7.4 to 7.7. The results are expressed as a percentage of the experimentally measured values.

As can be seen the prediction is very good, with the effective thermal conductivity model having similar accuracy to the full convection solution using the momentum source for droplet representation. It is not as accurate as the full convection solutions for low currents, where it appears to over estimate the effect of convection, however it is as accurate as the modified volumetric source presented in the previous chapter and requires far less empirical information. The model presented in this chapter only requires information on the droplet transfer velocity, the arc efficiency factor and effective radius rather than the many almost arbitrary numerical tuning factors required by a modified volumetric source. Therefore it is likely that this model will be more broadly applicable than the traditional modified source solution.

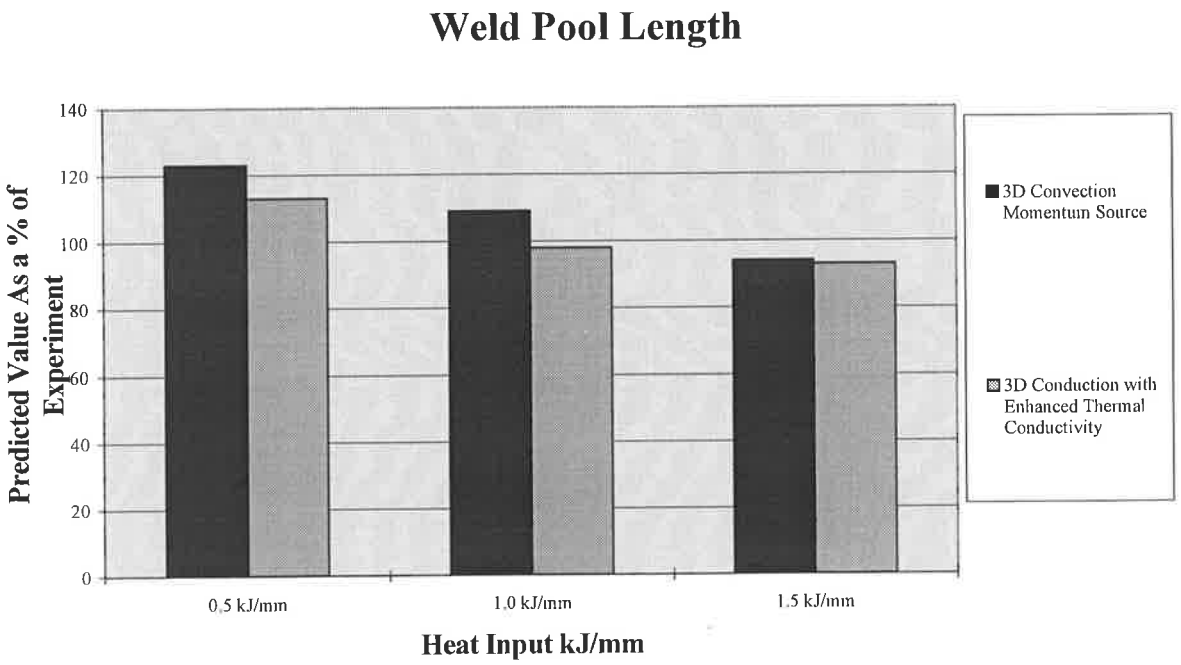

Figure 7.4 Model comparison: Weld pool length.

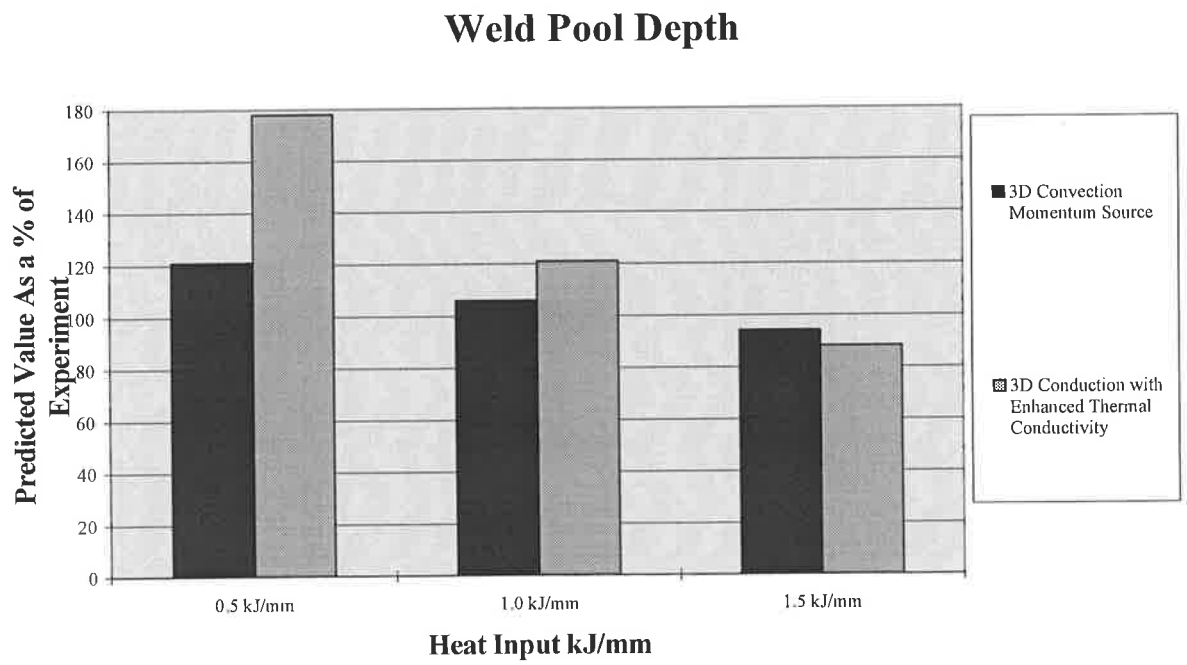

Figure 7.5 Model comparison: Weld pool depth.

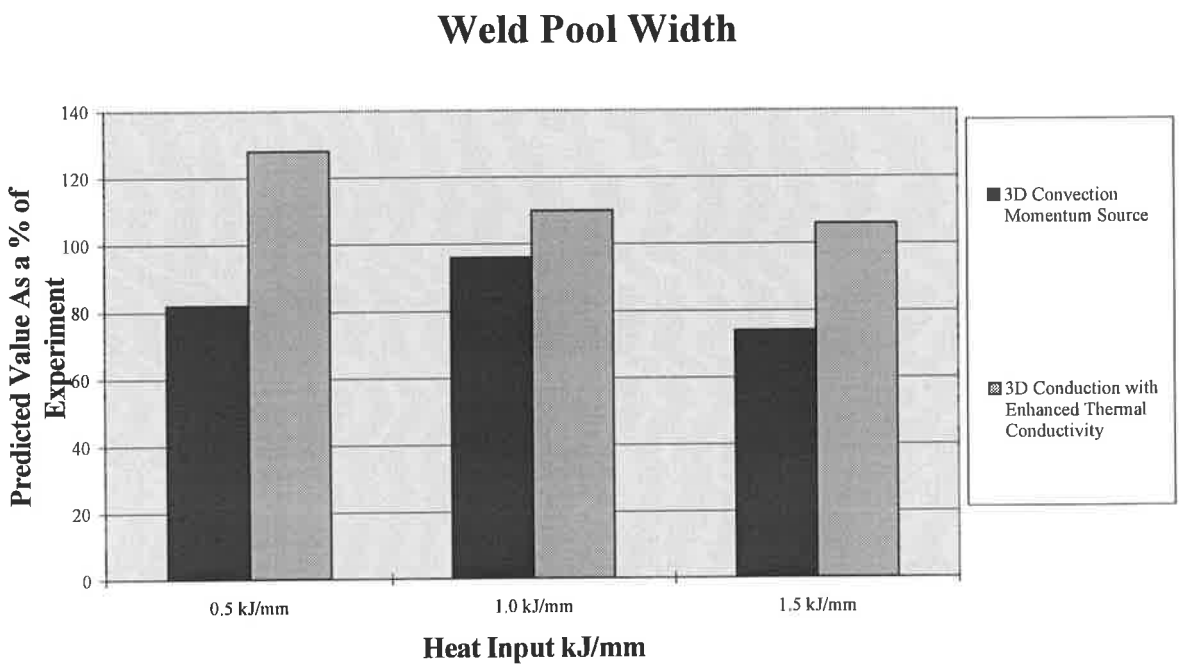

Figure 7.6 Model comparison: Weld pool width.

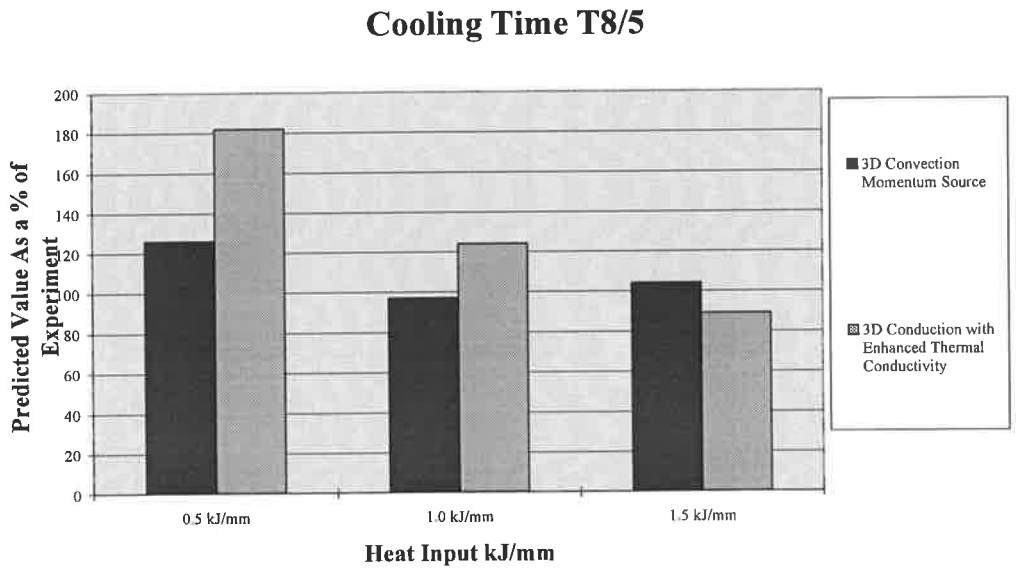

Figure 7.7 Model comparison: T8/5 cooling time.

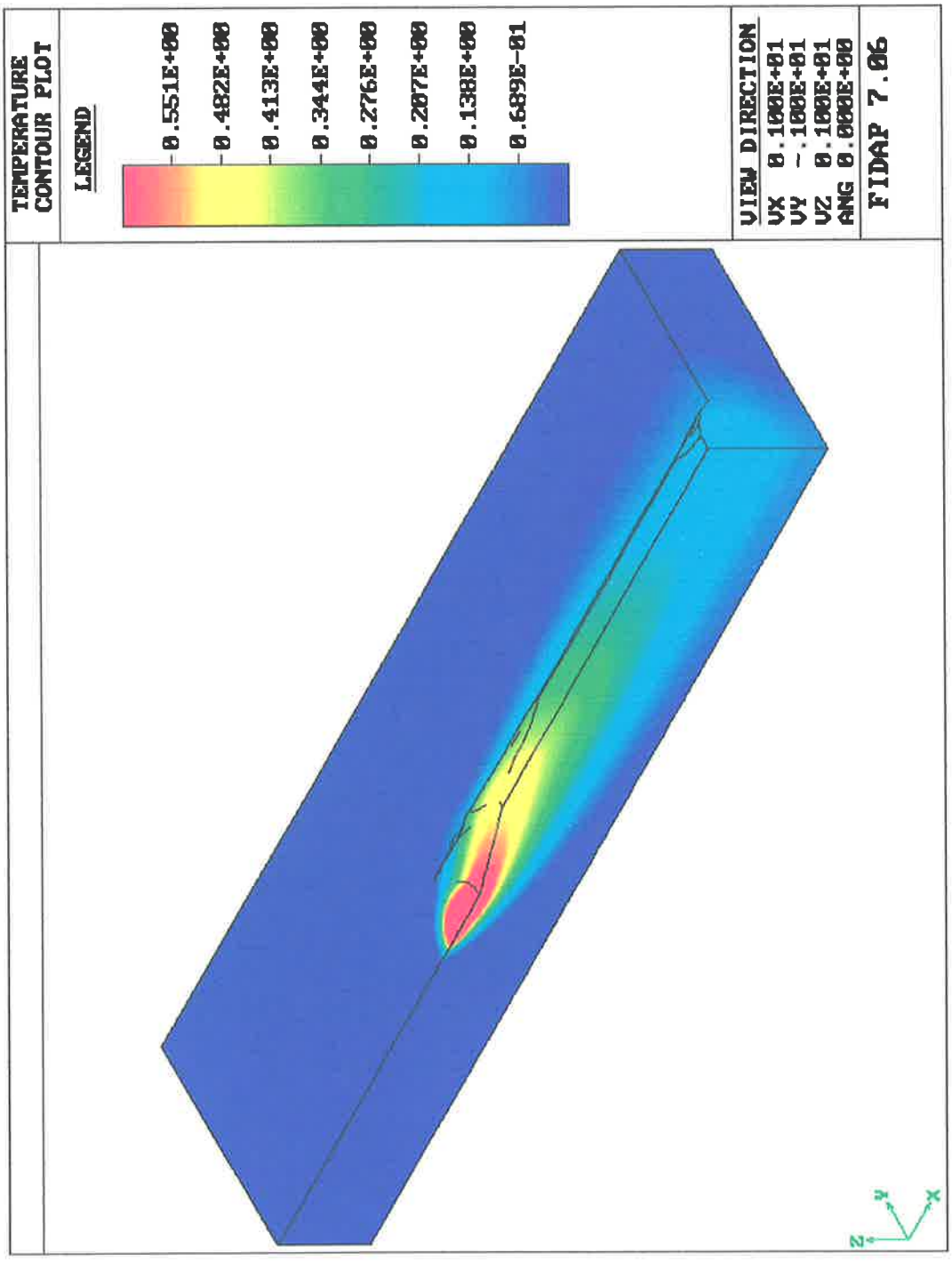

Figure 7.9 Temperature plot: Modified thermal conductivity, Q = 1.5 kJ/mm, V = 300mm/min, Argon rich gas.

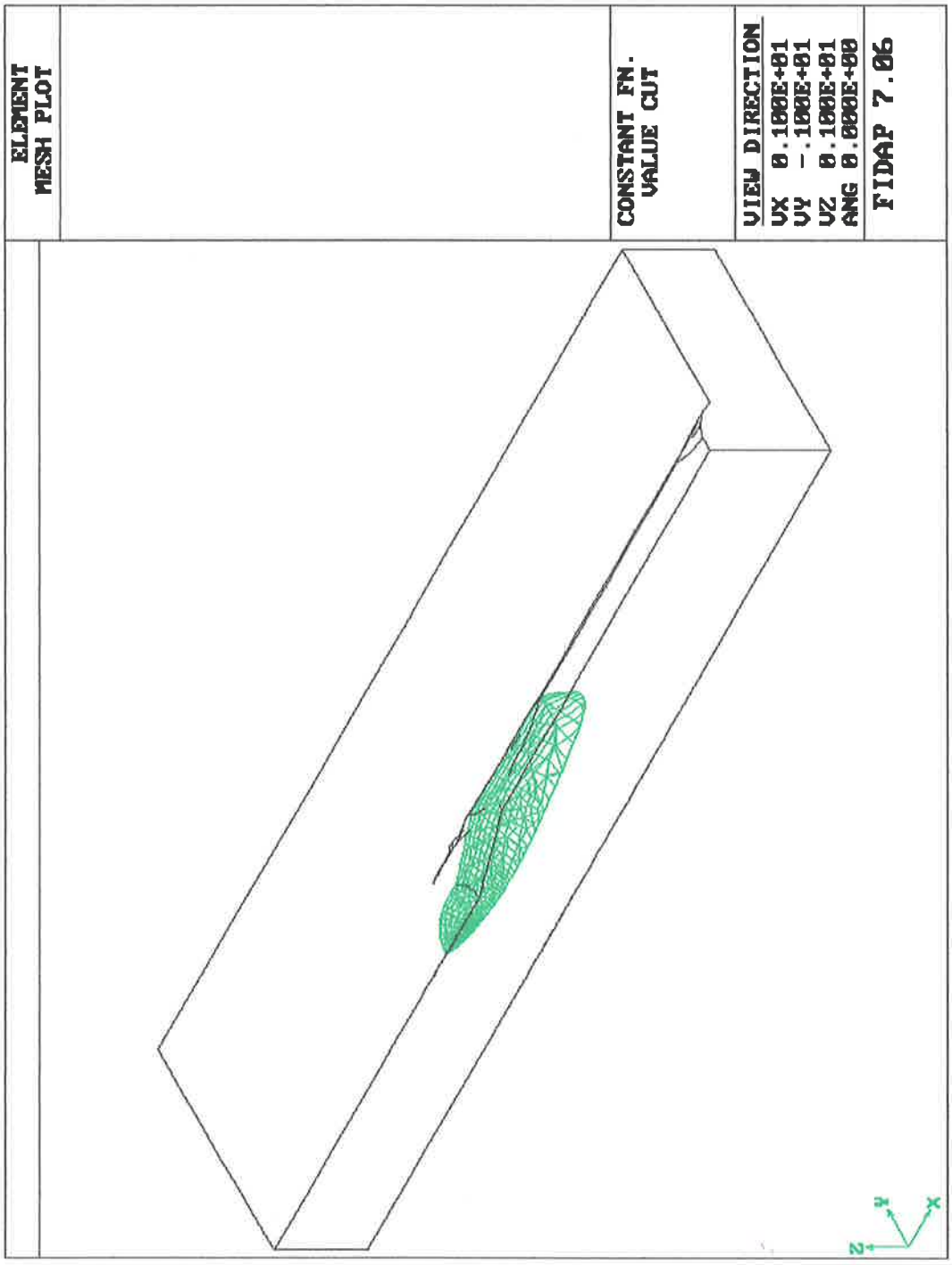

Figure 7.10 Pool shape: Modified thermal conductivity, Q = 1.5 kJ/mm, V = 300mm/min, Argon rich gas.

7.3 CONCLUSIONS

A modified thermal conductivity model based on the most important driving forces within the weld pool has been developed. The model is far closer to reality than traditional conduction-based solutions. Instead of relying on an arbitrary source form empirically "tuned" to give the right answers, this model uses a source based on a "realistic" source form and incorporates the distribution of this heat by convection. Convective transfer is accounted for by enhancing the thermal conductivity based on a dimensionless form of the droplet momentum forces, (which have been shown in Chapters 2 and 3 to be the dominant force in driving weld pool flow). The model predictions are significantly improved over standard conduction based modelling techniques and it is significantly faster than full conduction and convection solutions. Furthermore the model requires far less empirical information than traditional conduction solutions as the only empirical information fed into the model is the droplet momentum forces.

The model should be applicable for any welding condition in which the momentum flux into the pool is known. This is a significant improvement over the traditional heat source which can only be used for the welding conditions it has been calibrated for. It should be noted that where the free surface and the point of droplet entry is not approximately level to the top of the plate, (for example V groove welding), allowance will need to be made or else inaccurate answers will result because of the inaccurate location of the arc and droplet heat sources.

Chapter 8

SUMMARY AND CONCLUSIONS

8.1 SUMMARY AND CONCLUSIONS

The ultimate aim of this thesis was to develop a numerical model of convective flow within a GMA weld pool that models the physical behaviour as accurately as possible given the available time and resources. A detailed investigation of the effect of convection on the weld pool shape and near weld thermal history has been carried out, as well as the development and investigation of the most appropriate form of modelling weld pool convection. Models have been developed to enhance our understanding of weld pool flow and increase our ability to predict near weld thermal histories. Initial axi-symmetric models were developed to further the understanding of weld pool convection in GMA weld pools and this was then used to develop full convection models of the weld pool. Using the knowledge gained from these convection models, a conduction model that enables relatively quick accurate prediction of weld pool shape has been developed. It is envisaged that this relatively simple model will be useful for the prediction of real world thermal histories.

Initial work concentrated on determining the relative importance of the different driving forces within the weld pool. Analysis of the governing equations and appropriate boundary conditions, using approximation theory, has indicated that the droplet impact force is by far

the most important force present within the weld pool. It is approximately an order of magnitude larger than electromagnetic forces (which are the next most significant). Surface tension forces are of a similar importance to electro-magnetic forces at low currents and several orders of magnitude smaller at high currents. Buoyancy forces are negligible for all currents.

Due to the approximate nature of scale analysis these results have been further investigated using computational fluid dynamics models. The numerical models used to investigate the relative magnitude of driving forces were all based on axi-symmetric approximations. Although these approximations cannot be used to accurately predict weld pool shape and thermal history, because the flow is inherently three dimensional, they are the next logical step in developing full 3-D convection models. Their use is valid for determining the importance of the different driving forces, and from a pragmatic viewpoint they require significantly less computational power than full three dimensional models. In agreement with the scale analysis of Chapter 2, models of both normal and tangential surface tension only directly affect the flow within the pool at currents of less than about 150 Amps. Numerical models also indicate that compared to inertia forces, buoyancy forces have no measurable effect on weld pool flow and are negligible when modelling the weld pool. The computational modelling indicates that electromagnetic forces do have a measurable effect on the shape of the weld pool. Inclusion of electro-magnetic forces cause approximately 5% variation in depth to width ratio at 100 amps and 10% at 200 amps. In particular, the electro-magnetic forces seem to concentrate the flow to the central region of the pool. Therefore, although electromagnetic effects should be included when modelling weld pool

convection, given such a relatively small effect, it is possible to use a simpler, more efficient technique for including electromagnetic forces than fully solving Maxwell's equations.

Both the scale and computational analysis have been carried out for electrode positive, argon rich gas, and free flight transfer GMAW. Consequently, conclusions may not hold for variations from this mode of welding. In particular the relative importance of driving forces for "dip transfer" may be different to that determined by the analysis in this thesis. Therefore, the simple model developed in this thesis is not applicable to non free flight transfer without some form of modification.

From the results of Chapters 2 and three it is apparent that under free flight transfer conditions the droplet impact forces are the most significant forces in driving weld pool flow, with electro-magnetic forces a distant second. Therefore if control of the weld pool shape and near weld thermal history is desired, the most effective parameter to manipulate is the droplet inertia. Surface tension gradient forces, and therefore minor element effects, will not have any effect except possibly at very low currents (of the order of 100 amps). It therefore appears that droplet transfer into a GMA weld pool can be suitably modelled by considering it as a heat and momentum source; and incorporating the electromagnetic force within the pool.

Chapter 5 demonstrates that surface tension forces generated during droplet impact have an effect on the generation of turbulence within the pool and in this way affect the heat transfer within the pool. Appropriate methods to model this effect were investigated and appropriate

turbulence models and turbulence boundary conditions suggested. Given our limited knowledge of material properties in the high temperature plasma environment, the approach developed in Chapter 5 is suitable for the modelling of turbulence within the weld pool. However due to the complexities of three dimensional modelling with finite computational resources, this approach could not be incorporated into the full three dimensional convection models. The accuracy of any predictions of convective flow within the weld pool environment is limited by the accuracy of the turbulence model used.

Having determined what forces to include and the effect of turbulence within the pool, efficient three dimensional models of the GMAW process were constructed. Due to limitations in the available computational resources and the enormous demands of three dimensional modelling, these models could not include the free surface. Furthermore they could only include relatively simple turbulence models which were unlikely to completely model the effects of the complex turbulence that occurs within the weld pool. In order to incorporate the effect of a free surface without actually solving for the free surface position, two different models with different boundary conditions representing the free surface were tried. Both models demonstrated that the inclusion of convective flow within the weld pool improved the prediction of weld pool shape and near weld thermal history over models including conduction alone. Comparison of the model predictions also demonstrated that the accuracy of such models depends on accurate boundary conditions on the free surface. Both models were very expensive computationally, with the most accurate model needing 200 hours of CPU time on a Sun 10/30 workstation. Clearly these models are a long way from practical applicability. Furthermore, given the relative crudities imposed by the available

computational resources in modelling the turbulence and the free surface, the accuracy of a full convection solution the results is not worth the computational cost. Simple turbulence models such as those used Chapter 4, enhance the local viscosity and thermal conductivity according to some semi-empirical rule. Given the inherent inaccuracies in the readily available turbulence models for complex impinging and swirling flows with melting and solidification, and the limitations placed on the accessible turbulence models by the available computational resources. It is probable that a simple scheme to allow for convective flow by enhancing the local thermal conductivity will not significantly reduce the accuracy of prediction.

Given the cost and limitations of a full solution, a model that incorporates the effect of convection without solving for the Navier Stokes equations was developed. This model is three or four orders of magnitude quicker than full convection solutions, and is more accurate than traditional conduction solutions that either ignore convection or include it within the formulation of the heat source. Unlike the traditional double Gaussian heat source it does not require empirical tuning for every possible variation in welding process parameters. It is only dependent on the magnitude of the forces driving weld pool flow, and for free flight transfer modes it only requires information on the magnitude of the droplet inertia forces and arc form. This seems far more realistic as the heat distribution is only dependent on the arc and flow within the pool rather than some arbitrarily defined parameters. The model accounts for the flow within the pool, however it does require knowledge of the position of the pool surface so that the heat flux (due to the arc and the droplet) can be applied at the correct position. This means that the model only accounts for the effect of convection within

the pool, not variations in the point of action of the arc and droplets. Therefore a method to predict the surface position is required in those cases where this cannot be predicted a-priori. When the surface position can be predicted the model developed in Chapter 5 represents a relatively quick and accurate way of predicting the near weld thermal histories.

8.2 FUTURE WORK

8.2.1 Introduction

As mentioned in the previous section there are obviously some limitations to the work presented in this thesis due to the time, resources and knowledge base available. This section contains a summary of work that could be undertaken to clarify and extend this work.

8.2.2 Pool Surface

As it stands, the model developed in Chapter 7 is able to account for the effect of convection when modelling thermal behaviour in GMAW. This is quite useful where a relatively simple efficient prediction of thermal histories is required. Although the predicted weld pool dimensions agree favourably with experiment, the model does not predict the characteristic finger and crater weld pool profile. This may be because the current model uses a fixed, flat pool surface, if the weld pool surface position and the form of the heat source was accurately modelled, this may result in a more accurate pool shape prediction. Therefore, a method is required to predict the surface profile given the welding parameters and work-piece geometry. There are several examples within the literature on attempts to predict the surface position. Lancaster (1979) presents an analytical method for a two dimensional axi-symmetric pool. Here, the surface position is determined by a force balance between the pressure due to the arc plasma, and the forces due to hydrostatic pressure as well as surface tension forces within the pool. However this approach does assume an axi-symmetric pool. Modification of this model to incorporate the more realistic weld pool shape and to estimate the pool volume a-priori is required if it is to be used in conjunction with the conduction model presented in

Chapter 7. Kim & Na (1994) solve the surface position for a three dimensional GMA weld pool numerically, also based on a balance between the arc pressure and the hydrostatic and surface tension. They ignore the effect of metal transfer which is questionable in the light of the results of this thesis which clearly demonstrated that for GMAW metal transfer forces are larger than those due arc pressure. Their approach seems reasonable for GTAW but is unsuitable for GMAW. However both of the above techniques would appear to be capable of modification to include the effect of metal transfer.

Furthermore, the development of filming techniques to film the surface of the pool would be a useful research development. Until now, most attempts at filming the weld pool surface have been unsuccessful due to viewing problems associated with the presence of the arc and the fumes produced by the process. It is envisaged that successful filming of the pool would help our understanding of the flow mechanisms, as well as provide experimental validation for surface position and models. It may also help quantify the effect of plasma pressure on the pool surface position and fluid flow. Furthermore if an effective filming technique is developed it may be possible to place marker particles on the surface and track fluid flow. This would enhance our understanding, as well as provide useful validation for computational and scale analysis fluid dynamics models.

8.2.3 Droplet Characteristics

If a truly predictive model of the GMAW process is to be developed (where the weld pool shape and the thermal history is predicted for any combination of input parameters, weld geometry and shielding gas) a model capable of predicting the droplet characteristics from these parameters is necessary. In particular, prediction of the total inertia forces and heat

content is required.

8.2.4 Different Transfer Modes

The implications of different transfer modes would need to be investigated if a more broadly applicable model is to be developed. The analyses in this thesis has focussed on free flight droplet transfer modes. Clearly for, short circuiting transfer modes, the relative importance of the driving forces will be affected, in particular, electro-magnetic forces are likely to be more significant and droplet inertia force less significant than in free flight transfer. Analysis of the relative importance of different driving forces within a dip transfer pool is required if the effect of convection within the pool is to be understood and modelled. If the enhanced thermal conductivity model developed in Chapter 5 is to be used for dip transfer, a modified version which takes into account the important driving forces in a dip transfer pool will need to be developed. The most appropriate way to do this would be through the use of a modified Reynolds number based on the important driving forces within the weld pool. This could be done using an estimate of the maximum velocity in the pool, which since the droplet impact velocity tends to zero in the case of dip transfer would be related to surface tension and electro-magnetic forces.

8.2.5 Computational Fluid Dynamics of Turbulence and Free Surface Flow

Even with the current rapid increase in computer power, there will still be some difficulty in developing detailed models of the flow within a GMAW pool in the immediate future. With the rapid increase in computer power complex three dimensional models (including free surface and complex turbulence models) will become practical in the not too distant future,

however there are still some aspects of the flow which are not fully understood. In particular, our understanding of the effect of a free surface on turbulence is an area of ongoing research. The generation of turbulence by the interaction or collision of two surfaces is generally poorly understood. The model developed in Chapter 5 is relatively inexact, but is more than satisfactory given the constraints of the available turbulence models and material properties.

In general, practical two equation turbulence models perform poorly in the presence of stagnation regions and strong streamline curvature. Whilst more complex differential stress models are better at predicting the effects of turbulence within these regions, the application of these models to a complex practical geometry is not yet possible. Generally, these models require some form of measure to the moving pool boundaries, to take into account wall and surface effects. The development of models that incorporate this effect for practical application is an important area of research within the computational fluid dynamics community, however it is still some way from fruition.

Both turbulence modelling and the effect of the free surface on turbulence, are areas of active research within the fluid and computational fluid mechanics communities. Even if the computational resources were available to solve a transient three dimensional turbulent free surface problem (with electro-magnetic and phase change effects), until these issues are resolved detailed modelling of weld pool flow is unlikely to provide highly accurate descriptions of the flow field.

Appendix 1

FINITE ELEMENT COMPUTATIONAL FLUID DYNAMICS

A1.1 INTRODUCTION

There are many numerical techniques available for the modelling of fluid flow. Most of the computational modelling of fluid flow carried out within this thesis has been done using the "FIDAP" finite element computational fluid dynamics code. Some initial work was done in developing an in house code based on Patankar's "SIMPLE" (Semi Implicit Pressure Linked Equations) family of algorithms (a finite volume staggered grid technique). This approach was impractical, as the development of such a code for effective use in a welding environment would be a major undertaking, and would not have allowed time for investigation of the physics of the convective heat transfer which is the fundamental area of investigation in this study. The finite element technique has been used as it readily allows for the inclusion of complex geometries often found within a welding environment. A commercial code was chosen because the fundamental solution algorithms are well proven and advanced pre and post processing capabilities are provided. Modelling efforts are not limited by FIDAP, since this code allows the linking of user coded FORTRAN subroutines, providing almost limitless functionality. A brief summary of the application of the finite

elements to fluid mechanics may be found in the following section.

A1.2 APPLICATION OF THE FINITE ELEMENT METHOD TO FLUID DYNAMICS

Convective heat transfer is described by the following equations:

Continuity Equation:

$$\frac{\delta u}{\delta x} + \frac{\delta v}{\delta y} + \frac{\delta w}{\delta z} = 0 \qquad \textbf{(A1.1)}$$

The Navier Stokes equations:

$$\rho\left[\left(\frac{\partial u}{\partial t}\right) + u\left(\frac{\partial u}{\partial x}\right) + v\left(\frac{\partial u}{\partial y}\right) + w\left(\frac{\partial u}{\partial z}\right)\right] = \frac{\partial p}{\partial x} + \rho F_x + \mu\left(\frac{\partial^2 u}{\partial x^2} + \frac{\partial^2 u}{\partial y^2} + \frac{\partial^2 u}{\partial z^2}\right) \qquad \textbf{(A1.2)}$$

$$\rho\left[\left(\frac{\partial v}{\partial t}\right) + u\left(\frac{\partial v}{\partial x}\right) + v\left(\frac{\partial v}{\partial y}\right) + w\left(\frac{\partial v}{\partial z}\right)\right] = \frac{\partial p}{\partial x} + \rho F_y + \mu\left(\frac{\partial^2 v}{\partial x^2} + \frac{\partial^2 v}{\partial y^2} + \frac{\partial^2 v}{\partial z^2}\right) \qquad \textbf{(A1.3)}$$

$$\rho\left[\left(\frac{\partial w}{\partial t}\right) + u\left(\frac{\partial w}{\partial x}\right) + v\left(\frac{\partial w}{\partial y}\right) + w\left(\frac{\partial w}{\partial z}\right)\right] = \frac{\partial p}{\partial x} + \rho F_z + \mu\left(\frac{\partial^2 w}{\partial x^2} + \frac{\partial^2 w}{\partial y^2} + \frac{\partial^2 w}{\partial z^2}\right) \quad \textbf{(A1.4)}$$

and the energy equation,

$$\rho C_p \frac{dT}{dt} = \frac{\partial}{\partial x}(k\frac{\partial T}{\partial x}) + \frac{\partial}{\partial y}(k\frac{\partial T}{\partial y}) + \frac{\partial}{\partial z}(k\frac{\partial T}{\partial z}) + Q_s \quad \textbf{(A1.5)}$$

The finite element analysis reduces these equations to discrete form by breaking up the domain into a number of simply shaped regions called finite elements, and then approximating the solution for the unknown variables as some function across the elements.

A1.3 DISCRETISATION

Within each element the dependent variables u,v,w,p,T are interpolated in terms of the values to be determined at a set of nodal points. Within each element the velocity, pressure and temperature fields are approximated by,

$$u_i(x,t) = \phi^T \mathbf{U}_i(t) \quad \textbf{(A1.6)}$$

$$p(x,t) = \psi^T \mathbf{P}(t) \quad \textbf{(A1.7)}$$

$$T(x,t) = \upsilon^T \mathbf{T}(t) \quad \textbf{(A1.8)}$$

where **U**, **P**, and **T** are column vectors of nodal point unknowns, and Φ, Ψ and υ are column

vectors of the interpolation functions. Inserting into the governing equations with appropriate boundary conditions gives the following set of equations.

$$f_1(\phi,\psi,\upsilon,\mathbf{U_i},\mathbf{P},\mathbf{T}) = \mathbf{R_1} \qquad \text{Momentum} \qquad \textbf{(A1.9)}$$

$$f_2(\phi,\mathbf{U_i}) = \mathbf{R_2} \qquad \text{Mass Conservation} \qquad \textbf{(A1.10)}$$

$$f_3(\phi,\upsilon,\mathbf{u_i},\mathbf{T}) = \mathbf{R_3} \qquad \text{Energy Conservation} \qquad \textbf{(A1.11)}$$

$\mathbf{R_i}$ are the residuals or errors resulting from approximating with the interpolation functions. The Galerkin method aims to reduce these errors to zero in a weighted sense by making the residuals orthogonal to the interpolation functions.

The details of this procedure can be found in the literature, see for example Zienkiewicz (1991). The results of these manipulations lead to the following system of equations:

$$\begin{pmatrix} \mathbf{M} & \mathbf{0} & \mathbf{0} \\ \mathbf{0} & \mathbf{N} & \mathbf{0} \\ \mathbf{0} & \mathbf{0} & \mathbf{0} \end{pmatrix} \begin{pmatrix} \dot{\mathbf{U}} \\ \dot{\mathbf{T}} \\ \dot{\mathbf{P}} \end{pmatrix} + \begin{pmatrix} \mathbf{A(U)} + \mathbf{K(U,T)} & \mathbf{B(T)} & -\mathbf{C} \\ \mathbf{0} & \mathbf{D(U)} & \mathbf{0} \\ -\mathbf{C}^{\mathbf{T}} & \mathbf{0} & \mathbf{0} \end{pmatrix} \begin{pmatrix} \mathbf{U} \\ \mathbf{T} \\ \mathbf{P} \end{pmatrix} = \begin{pmatrix} \mathbf{F(T} \\ \mathbf{G(U,T)} \\ \mathbf{0} \end{pmatrix} \qquad \textbf{(A1.12)}$$

where **A** and **D** represent the convection, and **K** and **L** the diffusion of momentum and energy respectively. **M** and **N** represent the mass and terms in the governing equations. **F** and **G** represent the forcing functions in terms of the body and surface forces, while **B** represents the buoyancy term. Once the continuous system of equations has been reduced to a discrete system we can use numerical techniques to solve it.

A1.4 LINEARISATION SCHEME

The solution of the non-linear set of equations is the most time-consuming part of the algorithm, and therefore choice of the solution strategy is critical. As shown above, the Galerkin Finite Element method (when applied to the Navier Stokes equations) results in a set of non-linear algebraic equations which can be represented as:

$$\mathbf{K(u)\,u} = \mathbf{F} \qquad \textbf{(A1.13)}$$

In this thesis two different approaches have been used to solve this set of equations. For two dimensional problems, a fully coupled approach in which all equations are solved simultaneously has been used. For large two dimensional and three dimensional problems, a segregated solver has been adopted in which all variables are solved in a sequential and uncoupled manner. This technique requires far more iterations than a fully coupled technique, however it has lower memory and CPU demands for each iteration. As the size of the problem grows, the cost of each iteration of the segregated approach becomes increasingly less costly than a fully coupled approach. In fact as the problem size increases, the memory and disk requirements of the fully coupled approach rapidly exceed the available limits making a segregated solution the only possible approach.

For the modelling of GMA weld pools carried out in this thesis, two different fully coupled schemes have been used to model two dimensional models. The successive substitution scheme, or fixed point iteration scheme, has been used to solve for problems where there is no free upper surface. This scheme has a relatively large radius of convergence and is

therefore very useful when the solution is significantly different to the initial guess. It is particularly useful for solving flows involving turbulence modelling. For flows with free surfaces Newton based schemes are better because of the highly coupled nature of the solution.

A1.5 LINEAR EQUATION SOLVER

All of the above techniques require the solution of a system of linear equations. This can be done either by direct Gaussian elimination or by iterative methods. For the coupled schemes this has been done using a direct Gaussian elimination. This method has the advantage that after a finite number of operations, a solution is always obtained. Furthermore iterative methods perform very poorly on the form of matrix produced by these methods. However for large scale problems the computational cost becomes prohibitive, hence the use of segregated solution schemes with iterative linear equation solvers is preferred. Iterative methods start with some initial guess and compute a series of solutions that converge to the exact solution. In this thesis iterative methods have been used with a segregated solution algorithm to solve large three dimensional problems. The particular iterative solver used depends on the form of the matrix to be solved. With the segregated solution algorithm both non-symmetric and symmetric linear systems are encountered. The iterative methods used for both matrix forms are detailed below.

i) Symmetric coefficient matrix: In this case the matrix is both symmetric and positive. Haroutunian *et al.* (1993) have shown that the conjugate residual method is the most

appropriate for the solution of the symmetric system of equations. For details of this technique see Haroutunian *et al.* (1993).

ii) Non- symmetric coefficient matrix: Haroutunian *et al.* (1993) have also shown that the conjugate gradient squared method is the most efficient algorithm for solving the non-symmetric set of equations formed by the segregated solution algorithm. For details of this technique see Haroutunian *et al.* (1993).

PUBLICATIONS ARISING FROM THIS THESIS

i) Davies M.H, Painter M.J, Wahab M.A.

Investigation of the Interaction of a Molten Droplet with a Liquid Weld-pool Surface: A Computational and Experimental Approach

Submitted to the International Welding Journal, Jan 1995.

ii) Davies M.H, Painter M.J, Wahab M.A.

Computational Modelling of the Interaction of a Molten Droplet with a Liquid Weld Pool Surface

WTIA Fabcon/Fabfair, Wollongong. September 1993.

iii) Wahab M.A, Painter M.J, Davies M.H, Battersby S.

Temperature Modelling, Weld Pool Geometry and Interaction of Molten Droplets with a Liquid Weld Pool Surface

Australasian Heat and Mass Transfer Conference, Brisbane, December 1993.

iv) Davies M.H, Painter M.J, Wahab M.A.

The Numerical Modelling of Weld Pool Convection in Gas Metal Arc Welding

Compumod's 7th Australasian Users Conference, Sydney, October 1993.

v) Davies M.H, Painter M.J, Wahab M.A.

A Source Term for the Computational Modelling of the Flow Generated by a Liquid Droplet Impinging on a Liquid Surface

Computational Fluid Dynamics '94, Stuttgart Germany, September 1994.

vi) Davies M.H, Painter M.J, Wahab M.A.

A Comparison of Weld Pool Shapes Predicted form Models Incorporating Conduction And Convection"

WTIA Conference, Melbourne, November 1994.

vii) Wahab M.A., Painter M.J., Davies M.H.

The Prediction of Temperature Distribution and Weld Pool Geometry in Gas Metal Arc Welding Process

Advances in Materials and Processing Technologies (AMPT '95), Dublin, 7-11 August 1995.

REFERENCES

Abbot M.B. & Basco D.R.

Computational Fluid Dynamics : An Introduction for Engineers

Longman Scientific and Technical 1989

Adams C.M.

Cooling Rates and Peak Temperatures in Fusion Welding

Welding Journal, v37, n5, May 1958, pp210-215

Andersson B.A.B.

Thermal Stresses in Submerged Arc Welded Joints Considering Phase Transformations.

Trans. ASME. v100, Oct. 1978 pp356-362

Ando K. & Nishiguchi K.

Mechanism of Formation of SG-212-156-68 Pencil-point Wire Tip in MIG Arc Welding

IIW Document , 1968

Apps R.L. & Milner E.R.

Heat Flow in Argon Arc Welding

British Welding Journal, v2, n10, 1955, pp475-485

Atthey D.R.

A Mathematical Model for Fluid Flow in a Weld Pool at High Currents

J. Fluid Mechanics, 1980, v98, pt4, pp787-801

Batchelor J.K.

An Introduction to Fluid Mechanics

Cambridge University Press, 1967

Battersby S., Painter M.J. & Wahab M.A.

A New Modelling Method Applied to Aspects of Metal Transfer in GMAW

Proceedings: Fabcon/Fabfair '93 - Towards a Competitive Edge, pub. Welding

Technology Institute of Australia, 1993, pp306-310

Bish R.L.

The Melting Rate of a Single Phase Welding Wire

Welding Journal v71, n7, July 1992, pp243s-245s

Block-Bolten A. & Eagar T.W.

Metal Vaporisation from Weld Pools

Metallurgical Transactions B, v15B, n9, Sept. 1984, pp461-469

Brackbill J.U., Koethe D.B. & Zemach C.,

A Continuum Method for Modelling Surface Tension

J. Comp. Phys. Vol 100, 1992, pp335-354

Bradstreet B.J.

Effect of Surface Tension & Metal Flow on Weld Bead Formation

IIW Document 212-138-68, 1986

Brown, R.H.

Jet Cutting Technology : A Review and Bibliography.

BHRA Fluid Engineering 1981.

Brown S. & Song H.

Finite Element Simulation of Welding of Large Structures

Journal of Engineering for Industry, v114, November 1992, pp441-451

Brown S. & Song H.

Implications of Three Dimensional Numerical Simulations for Welding of Large Structures.

Welding Journal Research Supplement, v71, n2, 1992, pp55s-62s

Buchmayr B.

PC-Based Software in Welding Technology

Mathematical Modelling of Weld Phenomena, ed. H.Cerjak & K.E.Easterling, pub. Institute of Materials, 1993, pp315-345

Carroll K. & Mesler R

Splashing Liquid Drops Form Vortex Rings and Not Jets at Low Froude Numbers

J. Appl. Phys. 52(1), January 1981, pp507

Chakravarti A.P., Thibau R. & Bala S.R.

Cooling Characteristics of Bead-on-plate Welds

Metal Construction, v17, n3, 1985 pp178R-183R

Chandel R.S.

Mathematical Modelling of Gas Metal Arc Features

Proceedings: Modelling of Casting & Welding Processes IV

ed A.F.Giamei & G.J.Abbaschian, pub. Minerals, Metals & Materials Soc. USA 1988, pp109-120

Chanine G.L., Genoux P.F.

Collapse of a Cavitating Vortex Ring.

Journal of Fluids Engineering, 1983, Vol. 105, pp400-405

Chapman D.S. & Critchlow P.R.

Formation of Vortex Rings from Falling Drops

J. Fluid Mech. 1967, Vol 29, part 1, pp177-185

Chen Y.S. & Kim S.W.

Computation of Turbulent Flows using an Extended K-ε Turbulence Closure Model

NASA CR-179204, 1987

Chen W.H., Banjerjee P. & Chin B.A.

Study of Penetration Variations in GTAW

Proceedings: Recent Trends in Welding Science and Technology, May 1989

ed. S.A.David & J.M.Vitek, pub. ASM International, 1990, pp517-522

Ching B., Golay M.W. & Johnson T.J.

Droplet Impacts Upon Liquid Surfaces

Science, Vol. 226, No. 4674, 2 Nov. 1984, pp535-537

Choo R.T.C., Skezley J. & Westhoff R.C.

Modelling of High Current Arcs with Emphasis on Free Surface Phenomena in the Weld Pool

Welding Journal v69, n9, Sept. 1990, pp346s-361s

Choo R.T.C, Szekely J. & Westhoff R.C

Modelling of High Current Arcs with Emphasis on Free Surface Phenomena in the Weld Pool

Welding Journal v69, n9, Sept 1990, pp346s-361s

Choo R.T.C. & Skezely J.

The Effect of Gas Shear on Marangoni Flows in Arc Welding

Welding Journal v70, n9, Sept. 1991, pp223s-233s

Choo R.T.C. & Skezely J.

Vaporisation Kinetics & Surface Temperatures in a Mutually Coupled Spot Gas Tungsten Arc Weld and Weld Pool

Welding Journal v71, n3, March 1992, pp77s-92s

Choo R.T.C., Skezely J. & Westhoff R.C.

On the Calculation of the Free Surface Temperature of Gas Tungsten Arc Weld Pools from First Principles: Part 2 Modelling the Weld Pool and Comparison with Experiment

Metallurgical Transactions B, v23B, June 1992, pp371-384

Choo R.T.C., Skezely J. & Westhoff R.C.

On the Calculation of the Free Surface Temperature of Gas Tungsten Arc Weld Pools from First Principles: Part 1 Modelling the Welding Arc

Metallurgical Transactions B, v23B, June 1992, pp357-369

Choo R.T., Mukai K. & Toguri J.M.

Marangoni Interaction of a Liquid Droplet Falling onto a Liquid Pool

Welding Journal v72, n4, April 1992, pp139s-146s

Choo R.T.C. & Skezely J.

The Possible Role of Turbulence in GTA Weld Pool Behaviour

Welding Journal, Feb 1994, pp25-31s

Christensen N., Davies V de L. & Gjermudsen K.

The Distribution of Temperature in Arc Welding

British Welding Journal v12, n2, Feb. 1965, pp54-75

Classification of Metal Transfer

IIW Document XII-636-76, 1976

Clift R., Grace J.R, & Weber M.E.

Bubbles, Drops, and Particles, Academic Press, 1978

Cooper D., Jackson D.C., Launder B.E. & Liao G.X.

Impinging Jet Studies for Turbulence Model Assessment - Flow-Field Experiments

International Journal of Heat and Mass Transfer, Vol 36, No. 10, pp2675-2684

Deam R.T.

Weld Pool Frequency: A New way to Define a Weld Procedure

Proceedings: Recent Trends in Welding Science and Technology, May 1989

ed. S.A.David & J.M.Vitek, pub. ASM International, 1990, pp967-973

Debroy T.

Weld Pool Surface Phenomena - A Perspective

Mathematical Modelling of Weld Phenomena, ed. H. Cerjak & K.E. Easterling, pub. Institute of Materials UK., 1993, pp24-38

Dillenbeck V.R. & Castagno L.

The Effects of Various Shielding Gases and Associated Mixtures in GMA Welding of Mild Steels

Welding Journal v66, n9, 1987 pp45-49

Dunn G.J. & Eagar T.W.

Metal Vapours in Gas Tungsten Arcs: Part II, Theoretical Calculations of Transport Properties.

Metallurgical Transactions A, v17A, Oct.1986, pp1865-1871

Eagar T.W.

An Iconoclast's View of the Physics of Welding - Rethinking Old Ideas

Proceedings: Recent Trends in Welding Science and Technology, May 1989

ed. S.A.David & J.M.Vitek, pub. ASM International, 1990, pp341-347

Eager T.W & Tsai N.S.

Temperature fields Produced by Travelling Distributed Heat Sources

Welding Journal v62, n12, Dec. 1983, pp346s-355s

Easterling K.E.

Keynote address: Predicting Heat Affected Zone Microstructures and Properties in Fusion Welds

Proceedings: Recent Trends in Welding Science & Technology, May 1989, ed. S.A.David & J.M.Vitek, pub. ASM International 1990, pp177-189

Essers W.G. & Walter R.

Heat Transfer and Penetration Mechanisms with GMA & Plasma GMA Welding

Welding Journal v60, n2, Feb. 1981, pp37s-42s

Essers W.G. & Walter R.

Some Aspects of the Penetration Mechanisms in Metal-inert-gas (MIG) Welding

Proceedings: Arc Physics & Weld Pool Behaviour, published by Welding Institute, Cambridge, May 1989, pp289-301

FIDAP Users Manual, Fluid Dynamics International.

Friedman E.

Thermo-mechanical Analysis of the Welding Process Using the Finite Element Method

Trans. ASME J Pressure Vessel Technology v97, n3. Aug. 1975 pp206-213

Friedman E. & Glickstein S.S.

Effect of Weld Pool Configuration on Heat Affected Zone Shape

Welding Journal, v60 n6 June 1981, pp110s-112s

Friedman E. & Glickstien S.S.

An Investigation of the Thermal Response of Stationary Gas Tungsten Arc Welds

Welding Journal, v55, n12, Dec. 1976, pp408s-420s

Friedman E.

On the Calculation of Temperature Due to Arc Welding

Computer Simulation for Materials Application: Nuclear Metallurgy v20 n2 April 1976

pp1160-1170

Friedman E.

Numerical Simulation of the Gas Tungsten Arc Welding Process

Numerical Modelling of Manufacturing Processes, ASME Winter Annual Meeting Dec

1977. ASME pub. NY10071 pp35-47

Friedman E.

Finite Element Analysis of Arc Welding

WAPD-TM-1430 Bettis Atomic Power Laboratory, Jan 1980.

Friedman E.

Analysis of Weld Puddle Distortion and Its Effect on Penetration

Welding Journal, v57, n6, June 1978, pp161s-166s

Giedt W.H.

Weld Penetration and the Effects of Deviations in Machine Variables

Report SAND-87-8221, Sandia National Labs USA, July 1987.

Giedt W.H., Tallerico L.N. & Fuerschbach P.W.

GTA Welding Efficiency: Calorimetric & Temperature Field Measurement

Welding Journal v68, n1, 1989, pp28s-32s

Glickstein, S.S.

Basic Studies of the Arc Welding Process

Proceedings; Trends in Welding Research in United States, ed. S.A.David, pub. ASM,

Metals Park, November 1981, pp3-53

Goldak J.A., McDill M., Oddy A., House R., Chi X. & Bibby M.J.

Computational Heat Transfer for Weld Mechanics

Proceedings: Advances in Welding Science & Technology, TWR'86, ed. S.A.David, pub. ASM International , May 1986, pp15-21

Goldak J.A, Bibby M.J., Moore J., House R. & Patel B.

Computer Modelling of Heat Flow in Welds

Trans AIME vol17B, September 1986, pp587-600

Goldak J.A., Chakravarti A. & Bibby M.J.

A Double Ellipsoid Finite Element Model for Welding Heat Sources

IIW Doc 212-603-85, Jan. 1985

Goldak J.A., Chakravarti A. & Bibby M.J.

A New Finite Element Model for Welding Heat Sources

Metallurgical Trans B, v15B, June 1984 pp299-305

Goldak J.

Keynote Address: Modelling Thermal Stresses and Distortions in Welds.

Proceedings: Recent Trends in Welding Science and Technology TWR'89, ed. S.A.David & J.M.Vitek, May 1989, pp71-83

Goldak, J. & Bibby, M.

Computational Thermal Analysis of Welds: Current Status and Future Directions

Proceedings; Modelling and Control of Castings and Welding Processes IV, ed.

A.F.Giamei & G.J.Abbaschian, pub. Minerals, Metals & Materials Soc. May 1988, pp153-167

Govardhan S.M. & Chin B.A.

Monitoring GTAW using Measured Surface Temperature Gradients

Proceedings: Recent Trends in Welding Science and Technology, May 1989

ed. S.A.David & J.M.Vitek, pub. ASM International, 1990, pp383-396

Greene W.J.

An Analysis of Transfer in Gas Shielded Welding Arcs

AIEE Transactions, Part II: Applications & Industry v79, 1960, pp194-203

Grober H., Erk S., Grigull U.

Fundamentals of Heat Transfer

McGraw Hill, New York, 1961.

Grosh R.J. & Trabant E.A.

Arc Welding Temperatures

Welding Journal, v35, n8, August 1956, pp396s-400s

Halmoy E.

Wire Melting Rate, Droplet Temperature & Effective Anode Melting Potential

Proceedings: Arc Physics & Weld Pool Behaviour, pub. Welding Institute, Cambridge

May 1979, pp49-57

Harlow F.H. & Shannon J.P.

Distortion of a Splashing Liquid Drop

Science, Vol 157, 4 August 1967, pp547-550

Harlow F.H. & Shannon J.P.

The Splash of a Liquid Drop

Journal Of Applied Physics Vol. 38, No. 10, Sept 1967, pp.3855-3866

Harlow F.H. & Welch J.E.

Numerical Calculation of Time-Dependent Viscous Incompressible Flow of Fluid with a Free Surface

Phys. of Fluids, Vol 8, 12 December 1963, pp2182-2189

Haroutunian V, Engleman, M.S.

Two Equation Simulations of Turbulent Flows:

A Commentary on Physical and Numerical Aspects

Advances in Finite Element Analysis in Fluid Dynamics, FED-Vol. 171

ASME Winter Annual Meeting New Orleans , Louisiana, Nov 28 - Dec 3, 1993

He Q.L. & Standish N.,

A Model Study of Residence Time of Metal Droplets in the Slag in BOF Steelmaking,

ISIJ International, Vol 30, 1990, No. 5, pp356-361

Heiple C.R. & Burgardt P.

Penetration in GTA Welding

Proceedings: Weldability in Materials Symposium

ed. R.A.Patterson & K.W.Mahin, pub. ASM International, Oct.1990, pp73-80

Heiple C.R. & Roper J.R.

Effects of Minor Elements on GTAW Fusion Zone Shape

Proceedings: Trends in Welding Research in the United States, Nov. 1981

ed S.A.David, pub. ASM 1982, pp489-522

Heiple C.R. & Burgardt P.

Effect of SO_2 Shielding Gas Additions on GTA Weld Shape????

Welding Journal, v64, n6, June 1986, pp159s-162s

Hibbet H. & Marcel P.

A Numerical Thermomechanical Model for the Welding and Subsequent Loading of a Fabricated Structure

Computers and Structures v3, 1973, pp1145-1174

Hirt C.W. & Nichols B.D.

Volume of Fluid method for the Dynamics of Free Boundaries

J. Comp. Phys. Vol 39, 1981, pp201-225

Hobbs P.V. & Osheroff T.

Splashing of Drops on Shallow Liquids

Science, Vol. 155, 1 Dec 1967, pp. 1184-1186

Hsaio M., Lichter S. & Quintero Q.S.

The Critical Weber Number for Vortex and Jet Formation for Drops Impinging on a Liquid Pool

Phys. Fluids, 31 (12), December 1988, pp3560-3562

Huang P.G.

The Computation of Elliptic Turbulent Flows with Second Moment Closure Models

Phd Thesis , Faculty of Technology, University of Manchester, 1986

Ion J.C

Modelling the Microstructural Changes in Steels Due to Fusion Welding

University of Lulea, Sweden, Thesis 1984:36D 1984

Jarvis L.

Arc Pressure Forces in GTAW and GMAW

Private Communications 1995

Jelmorini G., Tichelaar G.W. & Van den Heuvel G.J.P.M.

Droplet Temperature Measurement in Arc Welding

IIW Document 212-411-77, 1977

Jhaveri P., Moffatt W.G. & Adams C.M.

The Effect of Plate Thickness on Heat Flow In Welding and Cutting

Welding Journal v41 , n1, Jan 1962, pp12-16

Christensen N., Davies V de L. & Gjermudsen K.

The Distribution of Temperature in Arc Welding

British Welding Journal v12, n2, Feb. 1965, pp54-75

Johnson J.A., Carlson N.M., Smartt H.B. & Clark D.E.

Process Control of GMAW: Sensing of Metal Transfer Mode

Welding Journal, v70, n4, April 1991, pp91s-98s

Kamala V. & Goldak J.A.

Error due to Two Dimensional Approximation in Heat Transfer Analysis of Welds

Welding Journal, v72, n9, September 1993, pp440s-446s

Kannatey-Asibu E., Kikuchi N., Jallad A.R.

Experimental Finite Element Analysis of Temperature Distribution During Arc Welding.

Trans. ASME. Journal of Engineering Materials Technology, v111, n1, Jan. 1989 pp9-18

Kasuya T. & Yurioka N.

Prediction of Welding Thermal History by a Comprehensive Solution

Welding Journal v72, n4, March 1993, pp107s-115s

Kim S.D. & Na S.J.

Effect of Weld Pool Deformation on Weld Penetration in Stationary Gas Tungsten Arc Welding

Welding Journal v71, n5, May 1992, pp179s-193s

Kim Y.S. & Eagar T.W.

Analysis of Metal Transfer in Gas Metal Arc Welding

Welding Journal v71, n6, June 1993, pp269s-277s

Kim Y.S., McEligot D.M. & Eagar T.W.

Analysis of Electrode Heat Transfer in Gas Metal Arc Welding

Welding Journal v70, n1, Jan. 1991, pp20s-31s

Kim Y.S.

Metal Transfer in Gas Metal Arc Welding

PhD Thesis MIT, Cambridge Mass. USA 1989

Kim Y.S. & Eagar T.W.

Temperature Distribution & Energy Balance in Electrode During GMAW

Proceedings: Recent Trends in Welding Science & Technology, May 1989,

ed. S.A.David & J.M.Vitek, pub. ASM International, 1990, pp13-19

Kirko I.M.

Magnetohydrodynamics of Liquid Metals

Consultants Bureau 1965.

Kohira K., Yataka T. & Yurioka N.

A Numerical Analysis of the Diffusion and Trapping of Hydrogen in Steels and Steel Weldments.

IIW Doc. 1X-951-76, 1976

Kou S. & Wang Y.H.

Three Dimensional Convection in Laser Melted Pools

Metallurgical Transactions A, v17A, Dec. 1986, pp1986-2265

Kou S. & Le Y.

Three Dimensional Heat Flow and Solidification during Autogenous GTA Welding of Aluminium Plates

Metallurgical Transactions A, v14A, Nov.1983, pp2245-2253

Kou S. & Wang Y.H.

Computer Simulation of Moving Arc Weld Pools

Metallurgical Transactions A, v17A, Dec. 1986, pp2271-2277

Kou S. & Wang Y.H.

Weld Pool Convection and its Effect

Welding Journal, v65, n3, March 1986, pp63s-70s

Kraus H.G.

Experimental Measurement of Thin Plate 304 Stainless Steel GTA Weld Pool Surface Temperatures.

Welding Journal, v66, n12, Dec 1987, pp353s-359s

Kraus H.G.

Experimental Measurement of Stationary SS304, SS3161 & 8603 GTA Weld Pool Surface Temperatures.

Welding Journal, v68, n7, July 1989, pp269s-279s

Krutz G.W. & Segerlind L.J.

Finite Element Analysis of Welded Structures

Welding Journal v57, n7, 1978, pp211s-216s

Kumar B.V., Mohanty O.N. & Biswas A.

Welding of Thin Steel Plates: A New model for Thermal Analysis

Journal of Materials Science 27, 1992, pp203-209

Lambert J.A.

Cast-to-cast Variability in Stainless Steel Mechanised GTA Welds

Welding Journal v70, n5, May 1991, pp41-52

Lancaster, J.F.

The Physics of Welding

IIW Publication, Pergamon Press, 1984.

Lancaster J.F.

Metal Transfer in Fusion Welding

Proceedings: Arc Physics & Weld Pool Behaviour, pub. The Welding Institute,

Cambridge, May 1979, pp135-146

Lancaster J.

The Physics of Fusion Welding: Part 1: The Electric Arc in Welding

&

The Physics of Fusion Welding: Part 2: Mass Transfer & Heat Flow

IEE Proceedings v134, pt. B, n5, Sept.1987, pp233-254

Launder B.E. and Spalding D.B.

The Numerical Computation of Turbulent Flows

Computers in Applied Mechanics and Engineering, Vol. 3,1 974, pp269-289

Landahl M.T. & Mollo-Christensen E.

Turbulence and Random Processes in Fluid Mechanics

Cambridge University Press 1987

Leschinzer M.A.

Refined Turbulence Modelling for Engineering Flows.

Computational Fluid Dynamics '94, Proceedings 2nd European Computational Fluid Dynamics Conference, 5-8 September 1994, Stuttgart Germany, John Wiley and Son, Invited Speakers, pp.33-46

Leschinzer M.A. & Rodi W.

Calculation of Annular and Twin Parallel Jets Using Various Discretization Schemes and Turbulence Model Variations

Journal of Fluids Engineering, v103, June 1981, pp352-360

Lesiur M.

Turbulence in Fluids

ed Kluwer, Academic Publishers, 1990

Lesnewich A

Control of Melting Rate & Metal Transfer in Gas Shielded Metal Arc Welding. Part 2

Control of Metal Transfer

Welding Journal v37, n9, Sept. 1958, pp418s-425s

Lesnewich A

Control of Melting Rate & Metal Transfer in Gas Shielded Metal Arc Welding. Part 1

Control of Melting Rate

Welding Journal v37, n8, Aug. 1958, pp343s-353s

Leung C.K., Pick R.J. & Mok D.H.B.

Finite Element Modelling of a Single Pass Weld

WRC Bulletin 356, August 1990

Leung C.K. & Pick R.J.

Finite Element Analysis of Multi-Pass Welds

WRC Bulletin 356, August 1990

Lienonen J.I. & Karjalainen

Unexpected weld profiles in GTA with Oxidising Shielding Gas

Proceedings: Recent Trends in Welding Science and Technology, May 1989

ed. S.A.David & J.M.Vitek, pub. ASM International, 1990, pp387-390

Lin M.L. & Eagar T.W.

Influence of Surface Depression and Convection in Gas Tungsten Arc Welding

Transport Phenomena in Materials Processing, SME PED-Vol 10, Nov. 1983, pp63-69

Lin M.L. & Eagar T.W.

Influence of Arc Pressure on Weld Pool Geometry

Welding Journal v64, n6, June 1985, pp163s-169s

Liu S. & Siewert T.A.

Metal Transfer in Gas Metal Arc Welding: Droplet Rate

Welding Journal v68, n2, Feb.1989, pp52s-58s

Liu S., Siewert T.A. & Lan H.

Metal Transfer Mode in Gas Metal Arc Welding

Proceedings: Recent Trends in Welding Science & Technology, TWR'89

ed S.A.David & J.M.Vitek, pub ASM International, May 1989, pp475-479

Ludwig H.C.

Current Density and Anode Spot Size in GTA Welding

Welding Journal v47, n5, May 1968, pp234s-240s

Ludwig H.

Metal Transfer Characteristics in Gas Shielded Arc Welding

Welding Journal v36, n1, Jan. 1957, pp23s-26s

Macklin W.C, & Hobbs P.V.

Subsurface Phenomena and the Splashing of Drops on Shallow Liquids

Science, Vol. 166, Oct 1969, pp. 107-108

Mahin K.W., Shapiro A.B. & Hallquist J.

Assessment of Boundary Condition Limitations on the Development of a General

Computer Model for Fusion Welding.

Proceedings: Advances in Welding Science and Technology. ed S.A.David, pub. ASM

International, pp215-223

Makara A.M., Savitskii M.M.,Kushnirenko B.N., Varenko N.I., Melnik A.D., Ganelin D. & Toshchev A.M.

The Effect of Refining on the Penetration of Metal in Arc Welding

Automatic Welding v30, n9, Sept. 1977, pp1-3

Malmuth N.D., Hall W.F., Davies B.I. & Rosen C.D.

Transient Thermal Phenomena and Weld Geometry in GTAW

Welding Journal, v53, n9, Sept. 1974, pp388s-400s

Mangonon P.L. & Mahimkar M.A

A Three Dimensional Heat Transfer Finite Element Model of the SAW of HSLA Steels

Proceedings: Advances in Welding Science & Technology,

ed. S.A.David, pub ASM International, May 1986, pp35-47

Masubushi K.

Analysis of Welded Structures,

International Series on Materials Science and Technology,

v33, pub. Pergamon Press UK. 1980

Matsunawa A. & Nishiguchi K.

Arc Characteristics in High Pressure Argon Atmospheres

Proceedings: Arc Physics and Weld Pool Behaviour, pub. Welding Institute Abington,

Cambridge, May 1979, pp123-133

McGlone, J.C. & Grant I.A.

Weld HAZ Cooling Prediction: A Review

Joining Sciences, v1, n2, Jan. 1992, pp62-67

McLay R. & Carey G.F.

Coupled Heat Transfer, Viscous Flow and Magnetic Effects in Weld Pool Analysis

International Journal of Numerical Methods in Fluids v9, 1989, pp713-730

McNallan M.J. & Debroy T.

Effect Of Temperature and Composition on Surface Tension in Fe-Ni-Cr Alloys

Containing Sulphur

Metallurgical Transactions B, v22B, August 1991, pp557-560

Mills G.S.

Fundamental Mechanisms of Penetration in GTA Welding

Welding Journal, v58, n1 Jan 1979 pp21s-24s

Mills G.S.

Fundamental Mechanisms of Penetration in GTA Welding

Welding Journal v58, n1, Jan.1979 pp21s-24s

Moore J.E., Bibby M.J. & Goldak J.A.

The Significance of the Point Source Model Assumptions on Weld Cooling Times

IIW Doc 212-604-85, Jan. 1985

Morton B.R. & Cresswell R.W.

Raindrops in the Sea 1 - Generation of Vorticity and Vortex Ring Production,

11th Australasian Fluid Mechanics Conference, University of Tasmania, Hobart, Australia,

14-18 December, 1992, pp611-618

Morton B.R. & Cresswell R.W.

Raindrops in the Sea 2 - Experimental Studies of Vortex Ring Generation,

11th Australasian Fluid Mechanics Conference, University of Tasmania, Hobart, Australia,

14-18 December, 1992, pp611-618

Mundra K., Debroy T., Zacharia T. & David S.A.

Role of Thermo-physical Properties on Weld Pool Modelling

Welding Journal v71, n9, Sept. 1992, pp313s-320s

Myers P.S., Uyehara O.A. & Borman G.L.

Fundamentals of Heat Flow in Welding.

Welding Research Council Bulletin, n123, New York, 1967.

Needham J.C. & Carter A.W.

Material Transfer Characteristics with Pulsed Current

British Welding Journal v12, n5, 1965, pp229-241

Needham J., Cooksey C. & Milner D.

The Transfer of Metal in Inert Gas Shielded Arc Welding

British Welding Journal v7, n5, 1966, pp101-114

Nied H.A.

Weld Pool Geometry Predictions Using a 2D Heat Flow Model

Proceedings; Advances in Welding Science & Technology, TWR'86, ed. S.A.David, pub. ASM, May 1986, pp21-27

Nunes A.C.

An Extended Rosenthal Weld Model

Welding Journal v62, n6, June 1983, pp165s-170s

Nystrum S.

Rainfall Measurements using Underwater Ambient Noise

J. Acoustic. Soc. Am. 79 (4), April 1986, pp972-982

Oddy A.S, Goldak J.A & McDill J.M.

Transformation Effects in the 3D Finite Element Analysis of Welds

Proceedings; Recent Trends in Welding Research and Technology, TWR'89

ed S.A.David & J.M.Vitek, pub. ASM International, May 1989, pp97-103

Ohji T., Nishiguchi K. & Kometani Y.

Optimisation of Welding Parameters by a Numerical Model of Thin Plate TIG Arc Welding

Technology Report of Osaka University, v36, n1826, March 1986, pp47-53

Ohji T., Miyake A., Tamura M., Inque H. & Nishiguchi K.

Minor Element Effects on Weld Penetration

Welding International v4, n12, 1990, pp959-963

Oreper G.M., Eagar T.W., & Skezely J.

Convection in Arc Weld Pools

Welding Journal v62, n11, Nov. 1983, pp307s-312s

Oreper G.M. & Skezely J.

Heat and Fluid Flow Phenomena in Weld Pools

J. Fluid Mechanics v147, 1984, pp53-79

Painter M.J.

Private Communications

1995

Paley Z.

Heat Flow in Welding Heavy Steel Plate

Welding Journal, v43, n1, Jan. 1964, pp71s-79s

Paley Z. & Hibbet P.

Computation of Temperature in Actual Weld Designs

Welding Journal, v54, n10, Nov. 1975, pp385s-392s

Paley Z. & Barry J.M. & Adams C.M.

Heat Conduction from Moving Arcs

Welding Journal, v42, n3, March 1963, pp97s-102s

Pardo E. & Weckman D.

A Numerical Model of the GMA Welding Process

Proceedings; Modelling and Control of Castings and Welding Processes IV, ed.

A.F.Giamei & G.J.Abbaschian, pub. Minerals, Metals & Materials Soc. May 1988, pp187-197

Pardo E. & Weckman D.C.

The Interaction Between Process Variables and Bead Shape in GMA Welding: A Finite Element Analysis

Proceedings: Recent Trends in Welding Science & Technology, May 1989, ed. S.A.David & J.M.Vitek, pub. ASM International 1990, pp391-397

Patankar S.V.

Numerical Heat Transfer & Fluid Flow

Hemisphere Publishing Corporation, 1980

Pavelic R., Tanbakuchi R., Ujehara O. & Myers P.

Experimental and Computed Thermal Histories in GTA welding of Thin Plates

Welding Journal v48, n7, July 1969, pp295s-305s

Pavelic V.

Weld Puddle Shape and Size Correlation in Metal Plates Welded by GTA Process

Proceedings: Arc Physics and Weld Pool Behaviour Conference, Welding Institute, London, May 1971, pp251-258

Persson K.A. & Stenbacka N.

The Significance of Different Welding Parameters to Penetration and Weld Metal Cross-sectional Area in Short-arc GMAW

Sveiseteknikk v44, n4, 1989, pp59-63

Pintard J.

Formation et Croissance des Gouttes, Force Auxquelles Elles Sont Surmises Avant et Pendant le Transfer

IIW Document 212-89-66, 1966

Prosperetti A. & Oguz H.N

The Impact of Drops on Liquid Surfaces and the Underwater Noise of Rain

Annual. Rev. Fluid Mech. 1993, Vol 25, pp577-602

Rhee S. & Kannatey-Asibu J.R.

Observation of Metal Transfer during Gas Metal Arc Welding

Welding Journal v71, n10, October 1992, pp381s-386s

Roberts D.K. & Wells A.A.

A Mathematical Examination of the Effect of Bounding Planes on the Temperature Distribution due to Welding

British Welding Journal, 1 (12) 1954, pp553-560

Rodi W.

Turbulence Models and their Application in Hydraulics

IAHR 1980

Rodriguez F. & Mesler R.

The Penetration of Drop-Formed Vortex Rings into Pools of Liquid

Journal of Colloid and Interface Science, Vol 121, No 1 January 1988. pp121-129

Rosenthal, D.

Mathematical Theory of Heat Distribution During Welding and Cutting

Welding Journal Research Supplement v20, n5, 1941, pp220s-234s

Rykalin N.N. & Bekelov A.J.

Calculating the Thermal Cycle in the Heat Affected Zone from 2D Outline of Molten Weld Pool

Welding Production, v14, 1967, pp42-42

Rykalin N.N. & Nikolaev A.V.

Welding Arc Heat Flow

Welding in the World, 93/94, 1971 pp112-132

Satio H. & Scriven L.E.

Study of Coating Flow by the Finite Element Method,

J. Comp. Phys. 42, 1981, pp53

Shariff K, Leonard A.

Vortex Ring

Annual Review of Fluid Mechanics, 1992, Vol. 24, pp.235-279

Shinoda T., Suguira S., Takeuchi Y., Nagata M. & Shimzu T.

Effect of Surface Tension on Weldability

Proceedings: Advanced Technology in Welding, Materials Processing & Evaluation, 5th. JWS International Symposium, Tokyo, April 1990, v2, pp791-796

Shirali A.A.

Effect of Trace Elements on Weld Penetrations of GTA Welds

Joining Sciences v1, n33, 1992, pp167-175

Simpson S.W., Peiyuan Zhu & Rados M.

Study of a Consumable Anode in An Electric Welding Arc

Proceedings: Fabcon/Fabfair '93 - Towards a Competitive Edge, pub. Welding Technology Institute of Australia, 1993, pp285-290

Smartt H.B. & Einerson C.J.

A Model for Heat & Mass Input Control in GMAW

Welding Journal v72, n5, May 1993, pp217s-229s

Solomon H.D. & Levy S.

HAZ Temperatures and Cooling Rates as Determined by a Simple Computer Program.

Proceedings; Trends in Welding Research in United States, ed. S.A.David, pub. ASM,

Metals Park, November 1981, pp173-205

Spencer J.P.

Penetration Effects of the Compound Vortex in Gas Metal Arc Welding

Thesis: Naval Postgraduate School Montroy, CA 93943.

Spicer R.A., Baeslack W.A., Kelly T.J.

Elemental effects on GTA Spot Weld Penetration in Cast Alloy.

Welding Journal v69, n8, Aug.1990, pp285s-288s

Sudnik V.A. & Rybakov A.S.

Calculation and Experimental Models of the Moving Arc of a Non-Consumable Electrode in Argon

Welding International v6, n4, 1992, pp301-303

Sudo S., Hashimoto H. & Ikeda A.

Measurements of the Surface Tension of a Magnetic Fluid and Interfacial Phenomena

JSME International Journal, Series II, Vol. 32, No. 1, 1989, pp.47-51

Szekely J

The Mathematical Modelling of Arc Welding Operations

Proceedings; Advances in Welding Science & Technology, TWR'86, ed. S.A.David, pub. ASM, May 1986, pp3-15

Tanaka S.

untitled

J. Japan Welding Society, v13, pp347-356, 1943

Tekriwal P. & Mazumder J.

3D Finite Element Analysis of Multi-pass GMAW

Proceedings; Modelling and Control of Castings and Welding Processes IV, ed. A.F.Giamei & G.J.Abbaschian, pub. Minerals, Metals & Materials Soc. May 1988, pp167-177

Tekriwal P. & Mazumder J.

Effect of Torch Angle and Shielding Gas Flow on TIG Welding - A Mathematical Model

Met. Construction June 1988 v20, n6, pp275R-279R

Tekriwal P. & Mazumder J.

Finite Element Modelling of Arc Welding Processes

Proceedings: Advances in Welding Science and Technology. ed S.A.David, pub. ASM International, pp71-80

Thomsan J.J. & Newall H.F.

On the Formation of Vortex Rings by Drops Falling into Liquids, and some Related Phenomena

Proceedings of the Royal Society of London, Vol 39, 1885, pp417

Tsai C.L.

Finite Source Theory

Proceedings: Modelling of Casting & Welding Processes,

New England College, Henniker N.E., 1983.

Tsai M.C. & Kou.S.

Marangoni Convection in Weld Pools with a Free Surface

International Journal for Numerical Methods in Fluids, v9, 1989, pp1305-1316

Tsai M.C. & Kou S.

Electromagnetic-Force-Induced Convection in Weld Pools with Free Surfaces

Welding Journal, v69, n6, June 1990, pp241s-245s

Tsao K.C. & Wu C.S.

Fluid Flow and Heat Transfer in GMA Weld Pools

Welding Journal v67, n3, March 1988, pp70s-75s

Ueguri S., Hara K. & Komura H.

A Study of Metal Transfer in Pulsed GMA Welding

Welding Journal v64, n8, Aug.1985, pp242s-248s

Ushio M.

Mathematical Modelling of Flow in the Weld Pool

Welding International v5, n9, 1991, pp679-683

Walker J.D.A., Smith C.R., Cerra A.W. & Doligalski T.L.

Impact of a Vortex Ring on a Wall

Journal of Fluid Mechanics 1987, vol. 181, pp99-140

Walsh W.D. & Dickinson C.

A Low Temperature Analog for the VPPA Process

Proceedings: Recent Trends in Welding Science and Technology, May 1989

ed. S.A.David & J.M.Vitek, pub. ASM International, 1990, pp507-510

Waszink J.H. & Piena M.J.

Experimental Investigation of Drop Detachment & Drop Velocity in GMAW

Welding Journal v65, n11, Nov.1986, pp289s-298s

Waszink J.H. & Graat L.H.J.

Experimental Investigation of the Forces Acting on a Drop of Weld Metal

Welding Journal v62, n4, April 1983, pp108s-116s

Waszink J.H. & Van den Heuvel G.J.P.M.

Heat Generation & Heat Flow in the Filler Metal During GMA Welding

Welding Journal v61, n8, Aug.1982, pp269s-282s

Watkins A.D., Smartt H.B. & Einerson C.J.

Heat Transfer in Gas Metal Arc Welding

Proceedings: Recent Trends in Welding Science & Technology

ed. S.A.David & J.M.Vitek, pub. ASM International, 1990 pp19-23

Weckman D.C., Mallory L.C. & Kerr H.W.

A Technique for the Prediction of Average weld Pool Width and Depth for GTA welds on Stainless Steels

Zeitschrift fur Metallkunde v80, n7, July 1989, pp459-468

WELDPLAN: Software from Danish Welding Institute

Wells A.A.

Heat Flow in Welding

Welding Journal v31, n5, May 1952, pp263s-267s

Westby 0.

Temperature Distribution in the Workpiece by Welding.

Department of Metallurgy and Metal Working, Technical University Trondheim, Norway

1968

Xiao Y.H., Ouden G.

A Study of GTA Weld Pool Oscillation

Welding Journal v69, n8, Aug. 1990, pp289s-293s

Yakhot V. & Orszag S.A.

Renormalization Group Analysis of Turbulence. 1. Basic Theory

Journal of Scientific Computing, Vol. 1, No. 1, 1986, pp3-51

Zacharia T., David S.A. & Vitek J.M.

Effect of Evaporation and Temperature Dependent Material Properties on Weld Pool Development

Metallurgical Transactions B, v22B, April 1991, pp233-241

Zacharia T. & David S.A.

Heat & Fluid Flow in Welding

Mathematical Modelling of Weld Phenomena

ed. H. Cerjak & K.E. Easterling, pub. Institute of Materials 1993, pp3-23

Zacharia T., Eraslan A.H. & Aidun D.K.

Modelling of Non-autogenous Welding

Welding Journal v67, n1, Jan.1988, pp18s-27s

Zacharia T., David S.A., Vitek J.M. & Kraus H.G.

Computational Modelling of Stationary Gas-Tungsten-Arc Weld Pools and Comparison to Stainless Steel 304 Experimental Results

Metallurgical Transactions B, v22B, April 1991, pp243-257

Zacharia T., Eraslan A.H., Aidun D.K. & David S.A.

Three Dimensional Transient Model for Arc Processes

Metallurgical transactions B, v20B, April 1989, pp645-659

Zacharia T., David S.A., Vitek J.M. & Debroy T.

Weld Pool Development during GTA and Laser Beam Welding of Type 304 Stainless Steels; Part 1 Theoretical Analysis

Welding Journal v68, n12, Dec. 1989, pp499s-509s

Zacharia T., David S.A., Vitek J.M. & Debroy T.

Weld Pool Development during GTA and Laser Beam Welding of Type 304 Stainless Steels; Part 2 Experimental Correlation

Welding Journal v68, n12, Dec. 1989, pp510s-519s

Zienkiewicz, O. C.

The finite element method

McGraw-Hill, New York, 1977